Microplastics in agricultural soils – effects on physical, chemical, and microbiological processes

DISSERTATION

submitted to attain the degree of Doctor of Natural Sciences
(Dr. rer. nat.)
at the Faculty of Biology, Chemistry, and Earth Sciences
of the University of Bayreuth

by
Ryan Bartnick
born in Broken Arrow, OK, USA

Bayreuth, 2025

This doctoral thesis was prepared at the department of Soil Ecology at the University of Bayreuth from October 2020 until June 2025 and was supervised by Prof. Dr. Eva Lehndorff.

This is a full reprint of the thesis submitted to obtain the academic degree of Doctor of Natural Sciences (Dr. rer. nat.) and approved by the Faculty of Biology, Chemistry and Geosciences of the University of Bayreuth.

Form of the thesis: cumulative dissertation

Date of submission: 04.06.2025

Date of defense: 14.10.2025

Acting dean: Prof. Dr. Markus Retsch

Doctoral committee:

Prof. Dr. Eva Lehndorff (reviewer)
Prof. Dr. Johanna Pausch (reviewer)
Prof. Dr. Efstathios Diamantopoulos (chair)
Dr. Magdalena Mair

To Mom & Dad

Summary

Microplastics (MPs) affect key soil properties relevant to agriculture: physical structure, chemical properties, and microbial processes, with their specific functions. This thesis examines how pristine and degraded conventional MPs (CMPs: polyethylene, PE, and polyethylene terephthalate, PET) and biodegradable MPs (BMPs: polybutylene adipate terephthalate, PBAT) affect different soil types. It integrates five studies that combined greenhouse and laboratory experiments to assess MPs impacts on soil physical aggregation and water holding capacity (WHC), carbon storage, respiration, nutrient cycling, and microbial community shifts.

As the basis for studying combined physical (aggregation and WHC), chemical (pH, C, N, nutrients), and microbial (abundance and diversity) properties among differing soil types (silty loam and sandy loam), a greenhouse experiment was conducted (Study 1, Greenhouse Experiment) with maize and MPs amendments (types: PBAT, PE, and PET; concentrations: 0.1 and 1% w/w; size ranges: 75–400, 200–400, 75–200, and <75 µm) over 18 weeks. A ^{15}N-labeled ammonium-nitrate fertilizer traced nutrient fate. Further complimentary studies were conducted: a respiration experiment assessed CO_2 emissions, microbial biomass and community shifts (Study 2, Soil Respiration); a UV-weathering experiment evaluated accelerated photodegradation of PE and PET for size fragmentation and surface reactivity (Study 3, Plastic Reactivity); a method development for quantification of MPs in soil with thermal desorption-gas chromatography-tandem mass spectrometry (TD-GC-MS/MS) (Study 4, Method); and a conceptual viewpoint reconsidering the size definition of MPs in soil (Study 5, Viewpoint).

Soil physical functions, aggregation and water retention, were minimally affected by CMPs. In contrast, BMPs enhanced microaggregate stability and WHC, but only under plant growth. This suggests soil structural improvement was mediated by biological functions, such as microbial activity and root exudations, which are more active in arable soils such as the silty loam. Sandy loam, with poor inherent structure, remained unaffected by MPs. As for chemical functions, MPs contributed to soil total carbon in proportion to their polymer carbon content. However, BMPs triggered microbial priming effects, as evidenced by increased CO_2 emissions and nitrogen immobilization. These effects were amplified in the nutrient-poor, unstructured sandy soil, where microbial communities likely responded more rapidly to the BMP-carbon

inputs. CMPs, however, showed limited chemical influence unless degraded, as plant growth appeared to mask their effect on nutrient cycling. Microbial activity and community composition varied between soil and polymer types. BMPs stimulated microbial biomass and significantly altered prokaryotic community composition, particularly in sandy loam, which showed enrichment of microbial genera associated with plastic degradation and nitrogen cycling. This suggested that lower quality soils may be more microbially responsive to MPs inputs due to resource limitations.

To evaluate potential long-term risks associated to increase in MPs surface reactivity, CMPs were artificially weathered to simulate environmental degradation. UV-weathered PE increased surface oxidation, hydrophilicity, negative surface charge, and cation exchange capacity (CEC), indicating increased environmental reactivity. In contrast, PET remained chemically stable under the same conditions. These findings demonstrate that degradation state critically alters CMP functions in soil, with PE potentially causing long-term risks to soil CEC and contaminant mobility.

Methodological advances included the development of a mass-based method for polymer quantification in soils without cleanup. Here again, the role of soil type differentiation in MPs detection and interpretation became clear with the developed method, as it discovered plastics quantification requires correction for humic substance interference in organic-rich soils.

As plastic size was critical to previous findings, a viewpoint emerged that challenges the established <5 mm definition of MPs as overly broad for soil systems. As most soil processes operate at the micro- to nanoscale, the thesis proposes a revised classification aligned with the SI: microplastics as 1–1000 µm and nanoplastics as 1–1000 nm. This refined framework would better align MP research with ecologically relevant soil process scales.

In conclusion, BMPs demonstrated a dual role: enhancing physical structure in structured soils (silty loam) but disrupting chemical and microbial processes in vulnerable soils (sandy loam) due to its rapid biodegradability and microbial stimulation. CMPs, in contrast, showed longer-term risks primarily after degradation, with PE exhibiting high environmental reactivity after weathering. Collectively, these findings highlight that plastic effects in the environment are not universal but depend on polymer properties and soil-specific conditions. For agroecosystem risk assessments, it is essential to consider soil type, degradation state, and particle size when evaluating the sustainability of conventional or biodegradable plastic use in agricultural soils of varying quality.

Zusammenfassung

Mikroplastik (MPs) beeinträchtigt wichtige Bodeneigenschaften, die für die Landwirtschaft relevant sind: physikalische Struktur, chemische Eigenschaften und mikrobielle Prozesse mit ihren spezifischen Funktionen. Diese Arbeit untersucht, wie frisches und degradiertes konventionelles Mikroplastik (CMPs: Polyethylen, PE, und Polyethylenterephthalat, PET) sowie biologisch abbaubares Mikroplastik (BMPs: Polybutylenadipatterephthalat, PBAT) verschiedene Bodentypen beeinflussen. Sie umfasst fünf Studien, in denen Gewächshaus- und Laborexperimente kombiniert wurden, um die Auswirkungen von MP auf die physikalische Aggregierung und Wasserhaltekapazität (WHC) des Bodens, die Kohlenstoffspeicherung, den Nährstoffkreislauf, die mikrobielle Atmung und Veränderungen in der mikrobiellen Gemeinschaft zu bewerten.

Als Grundlage für die Untersuchung der kombinierten physikalischen (Aggregation und WHC), chemischen (pH-Wert, C, N, Nährstoffe) und mikrobiellen (Häufigkeit und Vielfalt) Eigenschaften verschiedener Bodentypen (schluffiger Lehm und sandiger Lehm) wurde ein Gewächshausversuch (Studie 1, Gewächshausversuch) mit Mais und MP-Zusätzen (Typen: PBAT, PE und PET; Konzentrationen: 0,1 und 1 % w/w; Größenbereiche: 75–400, 200–400, 75–200 und <75 µm) über 18 Wochen durchgeführt. Ein mit ^{15}N markierter Ammoniumnitratdünger erlaubte den Nährstoffverbleib zu verfolgen. Weitere ergänzende Studien wurden durchgeführt: Ein Bodenatmungsexperiment betrachtete CO_2-Emissionen, mikrobielle Biomasse und Veränderungen in der mikrobiellen Lebensgemeinschaft (Studie 2, Bodenatmung); ein UV-Verwitterungsversuch befasste sich mit der Größenfragmentierung und Zunahme der Oberflächenreaktivität von PE und PET nach photochemischer Verwitterung (Studie 3, Kunststoffabbau). Es wurde weiter eine Methodenentwicklung zur Quantifizierung von MP im Boden mittels thermischer Desorption-Gaschromatographie-Tandem-Massenspektrometrie (TD-GC-MS/MS) durchgeführt (Studie 4, Methode) und eine konzeptionelle Betrachtung, die die Definition der Größe von MP im Boden überdenkt, angeschlossen (Studie 5, Standpunkt).

Die physikalischen Funktionen der Böden, Aggregation und Wasserrückhaltung, wurden durch CMPs nur minimal beeinflusst. Im Gegensatz dazu verbesserten BMPs die Stabilität der Mikroaggregate und die WHC, jedoch nur unter Pflanzenwachstum. Ich konnte zeigen, dass die Verbesserung der Bodenstruktur durch die Anregung biologischer Funktionen wie mikrobielle Aktivität und Wurzelausscheidungen bedingt wurde und insbesondere durch MP-

Zugabe in Ackerböden mit schluffigem Lehm effektiv war. Sandiger Lehm mit seiner, von Natur aus, schlechten Struktur blieb in dieser Perspektive von MPs unbeeinträchtigt. Was die chemischen Funktionen betrifft, trugen MPs proportional zu ihrem Polymerkohlenstoffgehalt zum Gesamtkohlenstoffgehalt des Bodens bei. BMPs lösten jedoch zusätzlich mikrobielle Priming-Effekte aus, was sich in erhöhten CO_2-Emissionen und Stickstoffimmobilisierung zeigte. Diese Effekte wurden in nährstoffarmen, unstrukturierten Sandböden verstärkt, wo mikrobielle Gemeinschaften wahrscheinlich schneller auf die Kohlenstoffeinträge durch BMPs reagierten. CMPs zeigten jedoch nur einen begrenzten chemischen Einfluss, sofern sie nicht abgebaut wurden, da das Pflanzenwachstum ihre Wirkung auf den Nährstoffkreislauf offenbar maskierte. Die Auswirkung von MPs auf mikrobielle Aktivitäten und Zusammensetzung variierten zwischen Boden- und Polymertypen. BMPs stimulierten die mikrobielle Biomasse und veränderten die Zusammensetzung der prokaryotischen Gemeinschaft erheblich, insbesondere in sandigem Lehm, der eine Anreicherung von Mikroorganismen aufwies, die mit dem Abbau von Kunststoff und dem Stickstoffkreislauf in Verbindung gesetzt werden. Dies deutete darauf hin, dass Böden von geringerer Qualität aufgrund begrenzter Ressourcen möglicherweise mikrobiell stärker auf MP-Einträge reagieren.

Um potenzielle Langzeitrisiken zu bewerten, wurden CMPs künstlich verwittert, um eine Aktivierung der Oberfläche und damit einhergehende Umwelteffekte zu simulieren. UV-verwittertes PE erhöhte die Oberflächenoxidation, Hydrophilie, negative Oberflächenladung und Kationenaustauschkapazität (KAK), was auf eine erhöhte Umweltreaktivität hindeutet. Im Gegensatz dazu blieb PET unter den gleichen Bedingungen chemisch stabil. Diese Ergebnisse deuten darauf hin, dass Plastikdegradation die Funktionen von CMPs im Boden entscheidend verändert, wobei PE potenziell langfristige Risiken für die KAK des Bodens und die Mobilität von Schadstoffen mit sich bringt.

Zu den methodischen Fortschritten dieser Arbeit gehörte die Entwicklung einer massenbasierten Methode zur Polymerquantifizierung in Böden ohne Reinigung. Hier wurde erneut klar, welche Bedeutung Bodeneigenschaften für die Analyse und Umweltbewertung von MP haben, insbesondere wurde hier erstmals gezeigt, dass in organikreichen Böden eine Korrektur der PE-Quantifizierung notwendig ist.

Da in dieser Studie gezeigt werden konnte, dass die Größe der Plastiksorten für die Auswirkung auf Bodenfunktionen entscheidend ist, wird vorgeschlagen die etablierte Definition von MP als <5 mm für Bodensysteme zu verwerfen. Da die meisten Bodenprozesse im Mikro- bis Nanobereich ablaufen, schlägt diese Arbeit eine überarbeitete Klassifizierung vor, die sich an das SI-System anlehnt: Mikroplastik soll als 1–1000 µm und Nanoplastik als

1–1000 nm definiert werden. Diese optimierte Definition erlaubt die experimentelle MP-Forschung in Zukunft besser an ökologisch relevante Bodenprozessskalen anzupassen.

Zusammenfassend lässt sich sagen, dass vor allem bioabbaubares Plastik, die BMPs, eine Rolle im Boden spielen: Sie verbessern die physikalische Struktur in strukturierten Böden (schluffiger Lehm), stören jedoch aufgrund ihrer schnellen biologischen Abbaubarkeit und mikrobiellen Stimulation chemische und mikrobielle Prozesse in empfindlicheren Böden (sandiger Lehm). Konventionelles Plastik, die CMPs, hingegen zeigten vor allem durch oberflächliche Abbauprozesse längerfristige Risiken, da PE nach der Verwitterung eine erhöhte Umweltreaktivität aufwies. Insgesamt unterstreichen diese Ergebnisse, dass die Auswirkungen von Kunststoffen auf die Umwelt nicht universell sind, sondern von den Eigenschaften der Polymere und bodenspezifischen Bedingungen abhängen. Für die Risikobewertung in Agrarökosystemen ist es unerlässlich, den Bodentyp und den Abbauzustand und die Partikelgröße der Plastiksorten zu berücksichtigen, um die Folgen der Verwendung von konventionellen oder biologisch abbaubaren Kunststoffen in landwirtschaftlichen Böden abschätzen zu können.

Acknowledgements

I would like to thank, first and foremost, Prof. Dr. Eva Lehndorff for the great opportunity to participate in this project. I have learned so much and always felt such great support from her. I express my gratitude for always having faith in me to work through problems and I am very appreciative of the entire Soil Ecology department at the BayCEER for their always open and continued support. Thanks to Prof. Dr. Werner Borken, Prof. Dr. Martin Obst, Dr. Andrea Scheibe, Nicola Braun, and Mirza Becevic for their expertise and assistance in these studies.

A special thanks to Karin Söllner for her unwavering support and love for science and students. Thanks to Uwe Hell for his super technical expertise and problem-solving skills. I would also like to thank Dr. Nele Meyer for her support, ideas, and advice to help me start this project. I want to thank Prof. Dr. Gerhard Gebauer, Prof. Dr. Alexander Frank, and technician Christine Tiroch at the Isotope Biogeochemistry Laboratory at the BayCEER for analyzing numerous isotopic samples.

Immense gratitude to owed to the late Prof. Dr. Britta Planer-Friedrich and the Environmental Chemistry program of the University of Bayreuth for giving me this opportunity to learn and inspiring me to keep pushing forward.

Table of Contents

List of Figures

List of Tables

Abbreviations

ANCOM	analysis of composition of microbiomes
BMPs	biodegradable microplastics
CAL	calcium-acetate-lactate
CEC	cation exchange capacity
CMPs	conventional microplastics
ESEM	environmental scanning electron microscopy
FTIR	Fourier-transform infrared spectroscopy
HA	humic acid
MBC	microbial biomass carbon
MPs	microplastics
NPs	nanoplastics
OM	organic matter
PA	polyamide
PBAT	polybutylene adipate terephthalate
PE	polyethylene
PET	polyethylene terephthalate
PLA	polylactic acid
PP	polypropylene
PS	polystyrene
PVC	polyvinyl chloride
SEM	scanning electron microscopy
SOC	soil organic carbon
SOM	soil organic matter
TD-GC-MS/MS	thermal desorption-gas chromatography-tandem mass spectrometry
WHC	water holding capacity
XPS	X-ray photoelectron spectroscopy

EXTENDED SUMMARY

1. Introduction

1.1 Rationale

Despite the growing body of research on microplastics (MPs), significant gaps remain in our understanding of their effects on soil functions. Current knowledge on MPs primarily focuses on their presence, distribution, and potential toxic effects, but there is limited understanding of how different polymer types, sizes, and degradation states influence soil functions: physical soil properties such as water retention, aggregation, and soil structure stability; chemical properties of soil altered by the presence or interactions between MPs, carbon (C), and soil nutrients; and the influence of MPs on soil microbial communities and diversity. MPs can possibly alter the physical structure of soils by their hydrophobic surfaces to reduce water holding capacity (WHC) and disrupt aggregate formation and stability. Soil chemistry is potentially influenced by MPs to change pH, nutrient cycling, carbon storage, and interact with non-polar and charged species in soils. Additionally, soil microbiology is potentially altered by microorganisms interacting with MP surfaces, potentially degrading them as an energy source, leading to shifts in microbial community composition and preferential abundance. As MPs transform and degrade into soils, are inhabited by microbes, and mixed into soil organo-mineral complexes, these interactions can become more complex and difficult to elucidate. Soil health is critical for plant production and food security, which are threatened by the incorporation of MPs in agroecosystems. Therefore, this study focuses on surveying soil functions affected by MPs of decreasing sizes (<500 µm) and polymer type in two soil types (silty loam and sandy loam) to reveal which functions are most relevant to certain soil systems. Additionally, quantification methods were developed to detect MPs in soil at environmentally relevant concentrations. As the current accepted definition of MPs in soils is quite broad (<5 mm), a viewpoint was given to urge future MPs research to emphasize the most relevant sizes which modify soil functions. These findings will direct future studies to appropriate experimental designs and to consider the most relevant soil confounders which interplay with polymer type and size of MPs incorporated into soils.

1.2 State of the research

With the extensive use of plastics from a variety of polymer types, sources, and applications, the terrestrial environment is now experiencing a new foreign object for the first

time in human history: a mixture of plasticized polymers with a variety of shapes and sizes in increasing localized quantities. Early plastic production was praised for its innovation, with little concern for its long-term persistence, only gaining attention once plastic pollution became visible in marine ecosystems (Barnes et al., 2009). The degradation rates of plastics depend on many factors and estimates show conventional MPs (CMPs), such as polyethylene (PE), polyethylene terephthalate (PET), and polypropylene (PP), can persist for hundreds of years (Chamas et al., 2020; Laforsch et al., 2020). Additionally, the imbalance between production and degradation continues to drive plastic accumulation (Machado et al., 2018), increasing interesting in biodegradable alternatives.

Plastics offer substantial material benefits, and have improved many aspects of quality of life, but this comes at the cost of widespread pollution with little insight into future consequences and their fate in the environment (Rillig, 2012; W. Shi et al., 2024; Villarrubia-Gómez et al., 2024). Much of plastic production on land has transported to streams and oceans, an estimated 80% (Richard et al., 2024). Initial observations of large collections of plastics on beach fronts and huge areas of floating debris were found in the ocean, but much remains as MPs which are harder to observe (Arthur et al., 2009; Browne et al., 2011; Thompson et al., 2004). While research on plastic pollution has primarily focused on marine systems, terrestrial plastic studies is at an early stage and often adapt marine studies to soil research.

The global spread of plastics remains poorly quantified, though recent evidence confirms their ubiquitous presence (Zhou et al., 2020). Around 79% of plastics are estimated to end up in landfills and natural environments (Geyer et al., 2017), including ~12.5 tonnes used in agriculture (Hofmann et al., 2023). The majority of plastics are introduced to terrestrial environments (Geyer et al., 2017; Rillig & Lehmann, 2020), and current production is about half a billion of tonnes of plastics annually and growing (Dokl et al., 2024), but estimating global soil concentrations is difficult due to inadequate methods and high variability. Larger plastics (>1 mm, defined in this thesis as macroplastics) degrade to form MPs which are often incorporated into soils via agricultural inputs, e.g. mulch films or compost, or runoff from roads, landfills, or urban areas (Figure 1), accumulating locally or transporting until deposition conditions are met (Barnes et al., 2009; Rillig et al., 2017).

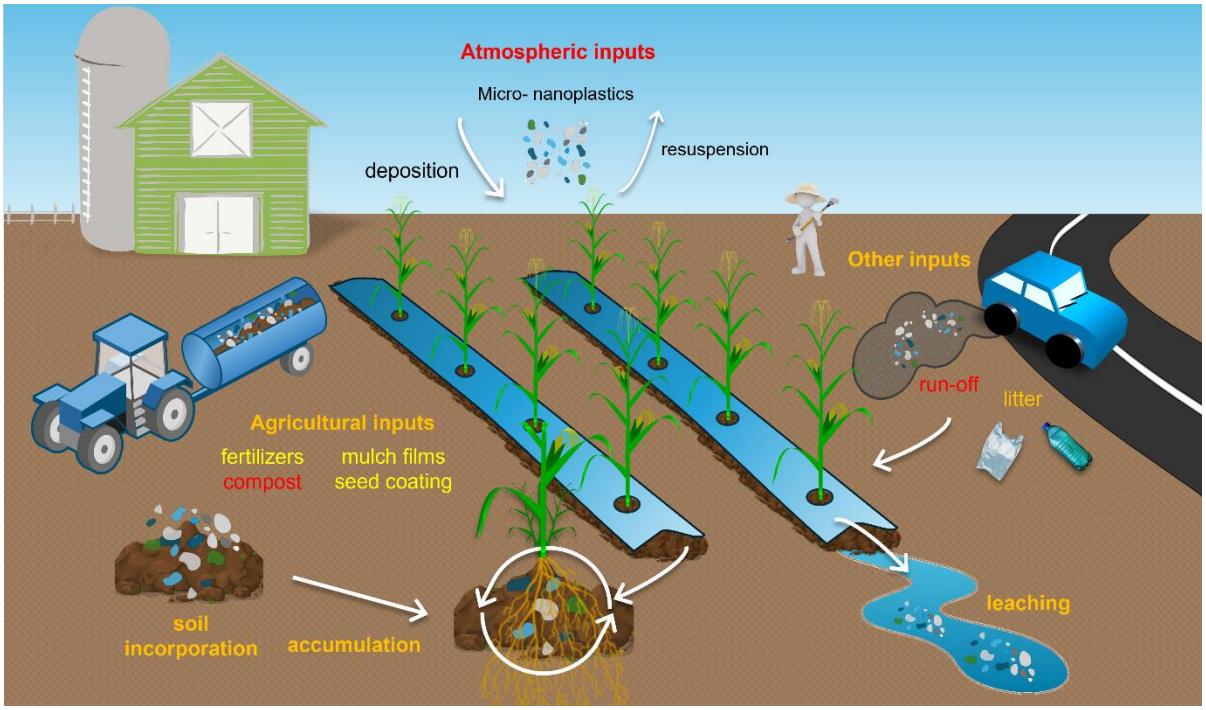

Figure 1. Proposed cycle of plastics in agricultural landscapes, with primary (yellow) and secondary (red) sources resulting in a mixture (orange) of various sources, sizes, and degradation states of plastics and their potential fate in a soil system.

MPs enter agricultural soils through various routes and forms. Some studies distinguish primary and secondary nanoplastics (NPs, <1 µm) by source, which are often mixed in agricultural systems. Primary sources include mulch films and coatings for fertilizers, seeds, and pesticides. Secondary sources of plastics include run-off, atmospheric deposition, compost/sludge application, and wastewater (Figure 1). However, this does not take into account the size and the degradation state of plastics, which are more relevant to soil functions. While pristine plastics (unweathered) pose risks, they will eventually degrade, fragment, and likely to cause further disruptions (Chamas et al., 2020; Steinmetz et al., 2016). Additionally, biodegradable MPs (BMPs) such as polybutylene adipate terephthalate (PBAT) and polylactic acid (PLA) degrade faster than non-degradable CMPs, but may produce harmful effects to ecosystems (Hu et al., 2023; Martínez et al., 2024).

In the actual environment, MPs introduced into agriculture are a mixture of primary and secondary resources, with various degradation states (degrees of weathering), shapes, sizes, roughness, and polymer chemistry. The size of plastics in agricultural soil depends on its source, and whether primary or secondary, most MPs result from the breakdown of larger plastics, such as litter or mulch films (Steinmetz et al., 2022), or direct input of smaller plastics through compost, fertilizers, and wastewater (Corradini et al., 2019; Sa'adu & Farsang, 2023).

Additional plastic inputs unrelated to farming come from atmospheric deposition, run-off from roads or landfills, and nearby urban or industrial activity. Roads contribute MPs from vehicle brake dust and tire wear (Eisentraut et al., 2018). Atmospheric plastic deposition is also understudied, partly because air sampling methods are limited to filter size, but studies confirm MPs and NPs are common in the atmosphere from source emissions (Kernchen et al., 2024). Therefore, plastics are ubiquitous, even in remote areas, and agricultural MPs inputs may be underestimated, depending on local pollution intensity and practices (Jia et al., 2024; Yang et al., 2021).

In summary, more research and methodology are needed estimating agricultural soil inputs and outputs, and major gaps are missing to understand the effect of MPs on ecosystem functions (Figure 1). It is unclear how much MPs accumulate in soil, and which soil systems are prone to MPs leaching, incorporation in aggregates, taken up by plants, or mineralized by microbes. The fate of plastics incorporated into soil is still unknown, whether they fully degrade to CO_2 and other gaseous byproducts or become stabilized in soil as a potential carbon sink. Concentrations of plastic inputs into agriculture are not well estimated or region specific, and influenced by multiple sources that are understudied (atmospheric, run-off, and local source pollution).

To assess the relevance of MPs in agriculture and plant production, a comprehensive view of soil processes is necessary. MPs comprise a variety of polymer chemistry, shapes, sizes, densities, roughness, color, and additives. Identifying the most relevant attributes will reduce the dimensionality of plastics for agricultural studies. Therefore, this thesis examines how MPs affect soil functions, categorized into three interacting domains: physical (e.g., pore space, aggregate stability, and hydrodynamics), chemical (e.g., nutrient and ion exchange), and microbial (e.g., changes in community diversity, abundance, and preferential colonization) (Figure 2). These processes interact and influence, either directly or indirectly, soil health and plant productivity, which is the central focus of this thesis.

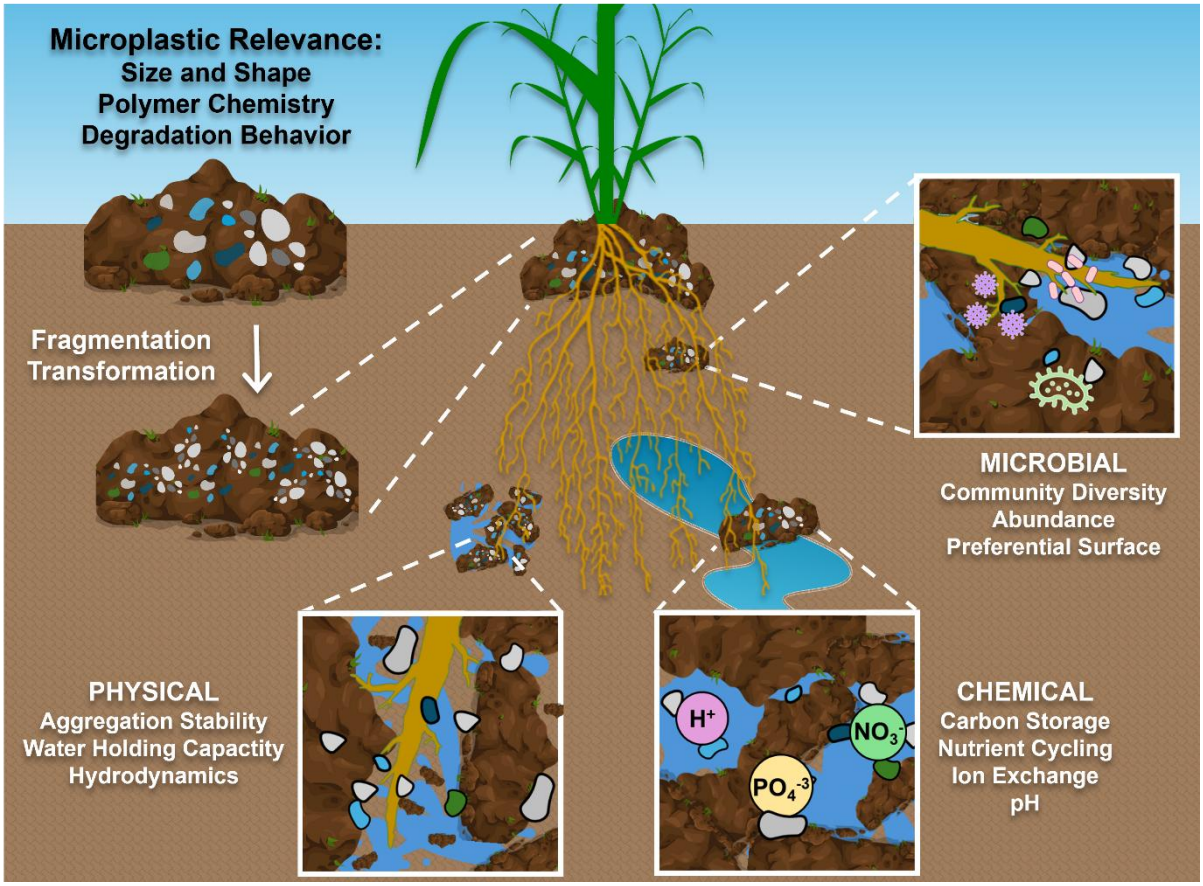

Figure 2. Incorporated microplastics undergo fragmentation and transformation in soil with crops and exhibit compound interactions with soil physical, chemical, and microbial properties.

1.3 Microplastic effect on soil physical structure

Concerning physical soil structure, the aggregation behavior of different soil types is related to functions of carbon and water storage (Amelung et al., 2024; Totsche et al., 2018). Stable aggregate formation involves the interaction between pore structure, which shapes the physical framework of air, water, roots, and soil particles; water retention, which supports microbial activity and binding processes; and mineral-associated organic matter, which chemically stabilizes particle associations over time (Huang et al., 2005; Yudina & Kuzyakov, 2023). For plastic size to be relevant in soil, it must be small enough to enter aggregates and persist long enough to participate in aggregation processes (Y. Liu et al., 2023). Larger macroplastics (>1 mm) will likely be transported laterally along the the topsoil until further reduction in size or directly mixed in by animals or farming practices (Steinmetz et al., 2022; Zhang & Liu, 2018). Therefore, microplastics (<1 mm) pose greater concern to soil health as they are more likely to be incorporated and mixed with other soil components (Z. Jia et al.,

2024). With high inputs from mulch films and composting, most plastics in soil exist as MPs and further as NPs, which are largely understudied but gaining attention (Gigault et al., 2018; Pérez-Reverón et al., 2023).

As plastics in their pristine form are almost always hydrophobic and less dense than soil particles, concerns were raised that their input disturbs soil aggregate stability and WHC (Wan et al., 2019). MPs are often found within macro- and microaggregate formation, relative to their shape and size (Zhang & Liu, 2018). Soil aggregate formation and stability may be negatively affected by the presence of MPs as a hydrophobic surface, or a replacement of mineral components in aggregates (Machado et al., 2018). MPs in soil increase hydrophobic surfaces and are also shown to reduce the capillary flow to plants (Cramer et al., 2023). The incorporation of small MP (<500 µm) in soil micro-aggregates leads to their instability and thus to a deterioration of the humus content, water storage and nutrient supply of the soil (Lehmann et al., 2021; Souza Machado et al., 2018). Therefore in this thesis, MPs specifically <500 µm were selected and produced for experimentation in soils, as this represents the most relevant size to interact with many specific soil processes and organisms (Mondellini et al., 2024; Pérez-Reverón et al., 2023). Studies investigating BMPs effect on soil aggregation are limited (L. Han et al., 2024; Lehmann et al., 2021); therefore, biodegradable PBAT was included in experimentation to observe if biodegradation and microbial exudates influence aggregation. Effects likely vary between soils of different textures (sand, silt, clay), which show distinct natural aggregation. Therefore, for experimentation, two distinct soil types were tested, silty loam and sandy loam, to reveal how MPs behavior may differ in certain soil textures.

In Study #1 (Greenhouse Experiment) – *Physicochemical Responses of Agricultural Soils to Biodegradable and Conventional Microplastics* – aggregation stability was evaluated in two soil types (silty loam and sandy loam) introduced with CMPs, PE and PET, and biodegradable PBAT at differing concentrations (0.1%, 1% *w/w*) and size ranges (200–400, 75–200, and <75 µm). Soil treatments were also separately planted with maize over one harvest (18 weeks) to see if MPs disrupt aggregate formation and if plant growth mitigates or alters these effects. It is hypothesized that MPs reduce formation of macroaggregates due to their hydrophobicity, while BMPs alter aggregation differently through the increased release of exudates during degradation. Soil hydrodynamics was tested by evaluating WHC in the treatment groups, as it is hypothesized that MPs reduce WHC due to their hydrophobic surface.

1.4 Microplastic effect on soil chemistry

As most plastics are primarily composed of carbon (C) and considered organic carbon, this implies that MPs function in soil organic matter (SOM), and humus and other associated forms of soil derived carbon can be mistaken for plastic carbon (Rillig, 2018; Rillig et al., 2021). MP carbon is bound in stable polymers which are fundamentally different than the diverse, reactive, and biodegradable forms of native organic carbon found in soil (Kopecký et al., 2022; Stevenson, 1994). For CMPs, their carbon is more inert and not part of soil biological carbon turnover, however their presence has still shown to affect C storage through increasing microbial activity, which subsequently increases native C turnover and soil CO_2 emissions (S. Zhao et al., 2024). CMPs, such as PE, can increase CO_2 emissions, although through changes in soil structure and not through direct degradation (Nguyen et al., 2025; Yu et al., 2021). However BMPs form CO_2 and other greenhouse gases due to their fast degradation and quick change in soil microbial nutrient cycling, resulting in increased soil emissions compared to CMPs (Sander, 2019; Xue et al., 2023). This implies that MPs can affect carbon sequestration and disrupt the natural C cycling in soil.

MPs often enter agricultural soils through organic fertilizers and solid waste, becoming incorporated with soil components (Watteau et al., 2018; Weithmann et al., 2018). This results in a mixture of plastics that have potential for complex interaction in soil chemistry, related to both microbiological activity and physical soil conditions. As MPs increase in degradation state, their chemical functionality may be altered from hydrophobic to hydrophilic behavior. Multiple forces are therefore at interaction on the surface of plastics in a complex soil environment, not only electrostatic interactions but non-polar adsorption as well, e.g. van der Waals and hydrophobic adsorption (Strawn et al., 2020). The presence of MPs could therefore alter the native chemical state of soils, but effects are likely complex and dependent on polymer chemistry and their respective degradation behavior. Even pristine MPs may carry negative surface charges capable of adsorbing positively charged soil nutrients (Meng et al., 2022). Alternatively, hydrophobic properties of MPs may disrupt organic matter (OM) association to minerals, which alters the nutrient retention of soils. Additionally, the pH of differing soils may also be affected by MPs or influence how MPs behave in a soil system (Ding et al., 2023; Zhao et al., 2021). PET and BMPs release acidic species through degradation. This results in potentially complex interactions between non-polar and polar functions in soils and MPs surface chemistry, especially after degradation and transformation.

For agricultural practices where high plastic use is deemed necessary for its benefits, i.e. mulching and fertilizer applications, there is a hopeful transition from utilizing CMPs to BMPs. However, this shift may bring unforeseen consequences, as biodegradation by microbes is the primary catalyst for most BMPs decomposition in soils (Priya et al., 2022; Zumstein et al., 2018). BMPs have shown to alter C storage and induce priming effects (K. Jia et al., 2024; Xue et al., 2023). As microbial communities shift toward plastic-degrading taxa, a priming effect may increase soil carbon and nutrient turnover (Miao et al., 2019; Zhang et al., 2022), consequently furthering soil CO_2 emissions (W. Zhao et al., 2024). The goal was to assess if MPs alter soil chemistry, focusing on nutrient cycling, microbial carbon dynamics, and the role of degraded plastics in chemical interactions. It was hypothesized that MPs would disrupt and inhibit soil nutrient cycling to plants, increase soil CO_2 emissions through microbial stimulation, and that BMPs or degraded CMPs would amplify these effects. Responses were expected to vary by soil type, with sandy loam being more sensitive than silty loam due to lower organic matter content and structural stability.

In Study #1 (Greenhouse Experiment) – *Physicochemical Responses of Agricultural Soils to Biodegradable and Conventional Microplastics* – nutrient cycling between soil treatments with and without MPs was traced with a ^{15}N-labeled ammonium nitrate fertilizer added in localized, labeled soil bags, and with additional testing of available phosphate and potassium. Nitrate label was traced throughout bulk soil, labeled soil bags, and plant root and leaves to evaluate distribution of added fertilizer; as it was hypothesized that MPs, and further with BMPs, interrupt nutrient cycling to plants through disruption of OM adsorption complexes or immobilize nutrients through microbial biodegradation.

Study #2 (Soil Respiration) – *Biodegradable Microplastic Increases CO_2 Emission and Alters Microbial Biomass and Bacterial Community Composition in Different Soil Types* – investigated the effects of two soil types, sandy loam and loam, introduced with different concentrations (0.1%, 1% *w/w*) and sizes (50–200, 200–500, and 630–1200 µm) of PE and PBAT on carbon storage and cycling by measuring soil CO_2 emissions and substrate-induced microbial respiration over four weeks. In this study, it was hypothesized that biodegradable PBAT will increase soil CO_2 emissions more than conventional PE; that smaller biodegradable particles will be degraded faster due to their larger surface area; and MPs influence will be dependent on soil type, that loamy soil will release more CO_2 than sandy loam, due to their physical impact on soil structure.

In Study #3 (Plastic Reactivity) – *UV-Degraded Polyethylene Exhibits Variable Charge and Enhanced Cation Adsorption* – PE and PET (200–400 µm) were degraded in an accelerated

UV-weathering chamber to assess changes in functional group formation as a results of plastic degradation dependent on polymer chemistry. Since pristine MPs were used for greenhouse studies for prior experimentation before further field studies (due to time restraints), degraded MPs were produced separately and tested for their change in surface chemistry, functional group formation, change in roughness, hydrophobicity, and potential for altered cation exchange capacity (CEC) in soils. It was hypothesized that the degradation of MPs which are occurring in the environment have transformed surfaces that exhibit varying behavior from pristine MPs, which implicate complex behavior in actual soil systems.

1.5 Microplastic effect on soil biology

It is common knowledge now that MPs in the environment, and especially soils, are quickly colonized by microorganisms for their stable surface and possible energy source when degraded (Miao et al., 2019; Rillig et al., 2024). This leads to biofilm formation on MP surfaces by preferential microbial communities. Some researchers have proposed soil now contains a microbial "plastisphere", where a complex network of bacteria, fungi, organic, and mineral constituents form a distinct ecosystem in soil which was not previously there before plastic production (Rillig et al., 2024; Zhou et al., 2021). This results in shifts in the soil microbial community and enzyme activity often seen in MPs research (Feng et al., 2022; Q. Wang et al., 2022). Microbes that can utilize MPs surfaces in soil will be in better competition than microbes that cannot, therefore creating an imbalance after MPs incorporation in soil.

Additionally, the transformed surfaces of MPs may be a vector for pathogenic organisms or harmful substances, resulting in toxic effects to soil organisms (Huerta Lwanga et al., 2016; Mueller et al., 2020), which often co-occur with plastic waste (Kirstein et al., 2016; Li et al., 2024; Wu et al., 2019). This can lead to proliferation of specific pathogenic or antibiotic-resistant microbes that have been found associated to MPs (Li et al., 2018). The introduction of BMPs to soil are likely to further disrupt soil microbial communities, resulting in accumulation of polymer degraded byproducts or microbial residues, affecting the previously established soil system (Xue et al., 2023; Zhou et al., 2021). It is expected that biodegradation favors microbial taxa most efficient at degrading MPs, thereby reducing overall biodiversity.

These shifts accompany loss in microbial environmental resilience and biodiversity; potentially causing a decline in plant-growth promoting bacteria and other mutually beneficial microbial interactions with plants (Tanunchai et al., 2022; Jie Wang et al., 2024). MPs

incorporated into soil can therefore affect microbiology in soil and subsequently larger biota in soils, such as plants (Rillig et al., 2019). Primary plant production has been shown to be influenced by a combination of factors related to the microbiological community and its nutrient cycling which are altered with the presence of MPs (Z. Jia et al., 2024; F. Wang et al., 2022). Both positive and negative plant production has been observed in the presence of both CMPs and BMPs (Cao et al., 2024; K. Jia et al., 2024; Xue et al., 2023). Therefore, in this thesis it was examined whether CMPs and BMPs stimulated specific microbes and shifted microbial communities, with the expectation that BMPs would drive greater microbial activity and community changes. Further, it was hypothesized that these changes would alter primary plant production, resulting in reduced plant biomass, and that effects would vary between soil types.

In Study #1 (Greenhouse Experiment) – *Physicochemical Responses of Agricultural Soils to Biodegradable and Conventional Microplastics* – microbial community composition and biodiversity were assessed in micro- and macroaggregate fractions of the greenhouse experiment to determine community shifts or diversity reduction in the presence of PE or PBAT in two soil types (silty loam and sandy loam). After experimentation, plant root and shoot biomass were measured to determine the overall influence of MPs to plant production. This study tested the hypothesis that the presence of MPs disturbs the microbial community, especially with BMPs, which alter nutrient availability (immobilization) to plants via a priming effect, hindering plant biomass production.

In Study #2 (Soil Respiration) – *Biodegradable Microplastic Increases CO_2 Emission and Alters Microbial Biomass and Bacterial Community Composition in Different Soil Types* –shifts in soil microbial biomass and bacterial community composition were investigated in the respiration experiment. Using substrate-induced respiration determined microbial biomass carbon (MBC) and growth, it was hypothesized that BMPs will alter the soil microbial community more than CMPs, favoring taxa associated with MPs degradation and C mineralization. It was additionally hypothesized that smaller sizes of PBAT would further increase microbial biomass and decrease diversity by degrading faster than coarser particles.

1.6 Quantification of microplastics in soil and viewpoint to future studies

There is currently a lack of adequate methods for detecting and determining MP concentrations in soil. However, mass spectrometry (MS) techniques combined with pyrolysis

and gas chromatography (GC) have proven to be a reliable direction for quantification (Albignac et al., 2023; Fischer & Scholz-Böttcher, 2017; Steinmetz et al., 2020; Stock et al., 2022). There is further potential in developing thermal desorption (TD) methods targeting at surveying soil samples in a quick and economic way (David et al., 2018; Dümichen et al., 2017; Duemichen et al., 2019; Seeley & Lynch, 2023). In the past, particle counts were a common method to account for the plastic content in soils, however, this is only qualitative when considering toxicology and regulation. Fourier-Transform Infrared (FTIR) and other similar microscopic methods have offered quantitative data to evaluate MPs concentration in soils (Piehl et al., 2018), but often require extensive and time-consuming clean-up steps (Möller et al., 2021); however, a direct mass-based approach has been sought after (Albignac et al., 2023; Primpke et al., 2020). Large-volume offline pyrolysis of soil was utilized with non-polar sorbents to avoid clean-up steps entirely, and then investigate remaining sources of interference, such as from SOM. As polymers differ in chemistry, many MS methods have been researched to identify the most relevant pyrolytic species from many polymer types, highlighting common interferences and limitations (Dierkes et al., 2022; Okoffo et al., 2020; Rødland et al., 2022). Therefore, a new and focused TD-GC-MS/MS was developed, and the simultaneous detection of multiple MPs polymer types was tested to assess quantification performance without sample clean-up and to evaluate the major interferences affecting MPs detection in soils.

In addition to the challenges of quantifying MPs, there are inconsistencies surrounding the discussion of MPs size classification and their relevance to soil functions (Z. Chen et al., 2024; Hartmann et al., 2019). MPs research initially focused on marine environments (Arthur et al., 2009; Thompson et al., 2004), but growing concerns highlight soils as significant accumulators of plastic pollution. However, it seemed that the widely accepted definition of microplastics (<5 mm) that originates from marine research is rather unsuitable for soil studies, as most soil processes and biotic interactions occur at much smaller scales. The current classification fails to reflect the physical constraints and ecological relevance of MPs and further degradation into NPs in soil ecosystems (Gigault et al., 2018; Pérez-Reverón et al., 2023). A further reclassification of MPs and NPs would recommend researchers align experimental designs to the most relevant soil functions affected by realistic MPs sizes. Therefore, as a conclusion to this thesis, a viewpoint was established highlighting the need to focus on adequate plastic sizes in soil system studies.

In Study #4 (Method) – *Plastic Quantification and Polyethylene Overestimation in Agricultural Soil Using Large-Volume Pyrolysis and TD-GC-MS/MS* – a new quantification

method for MPs in soil was developed by combining large-volume pyrolysis with thermal desorption-gas chromatography-tandem mass spectrometry (TD-GC-MS/MS). This study analyzed MPs, fresh and diagenetically altered OM, and lab blanks, and quantified PE, PET, and polystyrene (PS) in the two agricultural soils (sandy loam and silty loam). This study aimed to (1) simplify quantification for MPs at environmentally relevant concentrations in direct soil matrices, (2) enhance sensitivity and selectivity by utilizing tandem MS to further differentiate MPs from other carbon sources in soils, and (3) observe interferences of soil components with MPs and provide an estimation for SOM interferences for consideration of future studies. This method development is meant to serve as a base for further application in soil science and other environmental research areas dealing with plastic detection in complex matrices.

Study #5 (Viewpoint) – *From Sea to Land: Setting the Size Definition of Plastics for Soil Studies* – criticized the current marine-derived definition of microplastics (<5 mm) as rather unsuitable for soil ecosystems, as soil processes (e.g., water retention, carbon storage, nutrient cycling, and microbial interactions) predominantly occur at micro- to nanoscales. The viewpoint highlights the need to align experimental plastic particle sizes to the respective soil system scales in which plastics are incorporated and influence soil functions. Further, a refined classification of microplastics (1–1000 µm) and nanoplastics (1–1000 nm) would better reflect their interactions with the relevant size of soil biota and physicochemical. By utilizing standardized, soil-relevant size definitions, research can more accurately assess plastic impacts on soil health and bridge disciplinary gaps in environmental plastic pollution studies.

1.7 Objectives

The main research question of concern was: How do microplastics affect critical soil functions—physical, chemical, and biological—related to agricultural soil processes and plant production?

To analyze the interrelatedness of MPs influence on soil functions, key objectives were answered by relating findings of multiple studies as the following:

(1) Investigate if microplastics affect physical properties of soil by reducing the formation of soil aggregates and their stability in the rhizosphere, affecting soil physical structure and its functions such as carbon, water, and nutrient storage.

Study #1 (Greenhouse Experiment) – *Physicochemical Responses of Agricultural Soils to Biodegradable and Conventional Microplastics*

(2) Assess whether microplastics alter chemical properties of soil by interacting with mechanisms of soil aggregation, natural nutrient storage in the soil, i.e. cation exchange, and if differing plastic types and their weathered products have transformed surfaces with functional groups that further alter soil chemistry.

Study #1 (Greenhouse Experiment) – *Physicochemical Responses of Agricultural Soils to Biodegradable and Conventional Microplastics*

Study #2 (Soil Respiration) – *Biodegradable Microplastic Increases CO_2 Emission and Alters Microbial Biomass and Bacterial Community Composition in Different Soil Types*

Study #3 (Plastic Reactivity) – *UV-Degraded Polyethylene Exhibits Variable Charge and Enhanced Cation Adsorption*

(3) Identify if microplastics shift soil microbial communities and reduce species abundance and diversity, further enhanced by biodegradable plastic.

Study #1 (Greenhouse Experiment) – *Physicochemical Responses of Agricultural Soils to Biodegradable and Conventional Microplastics*

Study #2 (Soil Respiration) – *Biodegradable Microplastic Increases CO_2 Emission and Alters Microbial Biomass and Bacterial Community Composition in Different Soil Types*

(4) Quantify microplastics in soils with improved spectrometric methods aimed at targeting a variety of polymer types simultaneously at environmentally relevant concentrations.

Study #4 (Method) – *Plastic Quantification and Polyethylene Overestimation in Agricultural Soil Using Large-Volume Pyrolysis and TD-GC-MS/MS*

(5) Further develop and refine methodology of experimental studies focused on plastics in soil to consider the relevant size of plastics for soil processes.

Study #5 (Viewpoint) – *From Sea to Land: Setting the Size Definition of Plastics for Soil Studies*

This thesis provides a comprehensive assessment of MPs impact on critical soil physical, chemical, and biological functions in an agricultural context. These findings should integrate the various mechanisms by which different plastic types, degradation states, and sizes affect soil processes, which have complex interactions in differing soil types. This multi-faceted approach is preferable for understanding MPs interactions in soils which have potential for contrasting effects dependent on various soil conditions. Further development of MPs quantification in soil and views on best research practices should guide future researchers to more comprehensive and focused experiments.

2. Synopsis

2.1 Experimental design

For this thesis, the focus was on the impact of CMPs (PE, PET) and BMPs (PBAT) on agricultural soils and a typical crop plant (maize) which was tested in a main greenhouse experiment (achieve objectives 1-3 related to soil physical, chemical, and biological functions). An extended summary of the greenhouse experimental design can be found in Study 1 (Greenhouse Experiment) supporting information (SI, pages S2-3). As this experiment would take at least one year until completion, short-term experiments were conducted during this time to answer specific respective questions: (1) method development to detect simultaneous MPs in soil at environmentally relevant concentrations without sample clean-up, and to evaluate key contributors of soil interferences and overestimations in MPs quantification; (2) a soil respiration experiment of soil amended with conventional PE and biodegradable PBAT to evaluate MPs contribution to CO_2 production, substrate-induced biomass growth, and changes to microbial community composition; (3) production and characterization of degraded CMPs (PE and PET) via UV-degradation with multiple analyses of their change in particle size reduction, increased surface roughness, hydrophobic tendencies, surface area functional group formation, and relevant cation exchange sorption. An additional viewpoint was established with the total knowledge to direct future researchers studying MPs in soil to consider the size of MPs incorporated in soil, commonly <1 mm, in accordance with the respective sizes of soil functions, instead of the currently accepted definition of MPs as <5 mm.

2.2 Plastic preparation and degradation

In order to fulfill a 1% concentration of MPs in the greenhouse experiment with many replicates and treatments, several kgs of MPs were prepared in the first step via cryomilling to fractionate initial plastic beads into MPs, then subsequent airjet sieving to the specific particle size fractions used in experimentation. The plastic polymers used were low density-polyethylene (PE, Lupolen 1800 P-1 – LyondellBasell, Rotterdam, NL), polyethylene terephthalate (PET, CleanPET WF – Veolia Umweltservice, Hamburg, Germany), and polybutylene adipate terephthalate (PBAT, M·VERA® B5026 – BIO-FED, Cologne, Germany). The resulting MPs were irregularly shaped, and surfaces initially roughened by the mechanical milling process, which can represent the variety of fragmented plastics found in

the environment. For treatments comparing MPs concentrations (0.1% and 1% w/w) and not specific size ranges, a plastic "size mix" (75–400 µm) was produced by combining size fractions in a ratio 6:1 (200–400:75–200 µm). Particle size distribution was confirmed with a particle size and shape analyzer (Microtrac FlowSync, Retsch, Haan, Germany).

Degraded plastics were produced to better represent plastics particles found in the environment after transformation on the soil surface. Using a UV-weathering chamber Q-SUN XE-3 (Q-LAB, Westlake, OH) equipped with three xenon lamps and a Daylight-Q filter, PE and PET with initial size range distribution of 200–400 µm were continuously stirred in deionized water (38°C) for 400 and 2000 hours to simulate degradation (Meides et al., 2021, 2022). Specifically, solar radiation (UVA), 60 W/m^2 (at 300–400 nm) and 50% relative humidity, corresponding to a total irradiance of 594 W/m^2, comparable to natural sunlight. MPs were degraded an estimated 5x faster than in the environment, corresponding to around 3 months (400 h) and 14 months (2000 h) of degradation for the MPs in this experiment (Menzel et al., 2022). As chemical surface characterization of degraded plastics had not been performed yet, a sorption experiment was conducted to compare multiple instrumental measurements of degraded plastics to form a complete picture of its degradation behavior based on polymer type. This information can extrapolate better what might be happening at the surface of natural degraded plastic particles, where functional groups formed from UV photo-oxidation and hydrolysis are likely to interact with soil mineral and nutrient components (see section 2.3.4).

2.3 Results and Discussion

The focus of this thesis is on the alteration of quality of typical agricultural soils due to threats of plastic inputs and their properties that degrade soil quality. It was expected that main soil functions such as WHC, aggregation, organic carbon and nutrient storage are challenged by the increasing amount of plastics entering soil, which differs widely depending on the properties of the plastics and in particular higher quality (e.g. silty loam) and lower quality (e.g. sandy loam) soils. It was hypothesized that MPs would alter key soil functions in ways dependent on both plastic and soil properties. This thesis shows that especially the combination of biodegradable plastic and high quality, loamy soil, led to changes in soil properties: the aggregation was significantly improved in loamy soil, however, at the cost of nitrogen reduction. Further, this thesis found that even conventional plastics, such as PE, become increasingly more surface active over time that affect cation exchange when exposed to

weathering conditions. This altogether challenges the view of plastics as being chemically inert and instead presents a differentiated picture in which various plastic types exhibit very specific and environmentally relevant functions. Overall, this thesis demonstrates that MP impacts are soil and polymer specific, influencing interconnected physical, chemical, and biological functions, which is essential for detangling interactions and assessing the risks of MP contamination in agriculture.

2.3.1 Biodegradable plastic (PBAT) as mediator of soil aggregation and soil water holding capacity (Study 1)

MPs have been shown to alter soil structure by interfering with aggregate formation and stabilization (Jiaxin Wang et al., 2024); therefore, this study hypothesized that MPs, especially at smaller sizes, would disrupt soil aggregation, with more pronounced effects in silty loam soil due to its finer texture and higher structural development. In Study 1, the silty loam contained more silt and organic matter which supported greater aggregate formation and WHC than sandy loam and was thus expected to be greater disturbed by the hydrophobic presence of MPs. MPs were introduced at environmentally realistic concentrations of (1% w/w), and considering the experiment was conducted for one growth cycle in "fresh" (sieved and unstructured) prepared soil, effects between soil aggregation treatments were low and not statistically significant ($p > 0.05$, Tukey's HSD). Although MPs did not disturb aggregation as hypothesized, this is in accordance with other studies showing minimal effects at environmentally concentrations around 1% (Yu et al., 2023).

In sandy loam soil, aggregation formation was minimal even with plant growth and was unchanged by the presence of MPs. However, in the silty loam, trends were observed especially among the biodegradable PBAT treatments (Study 1, Figure 2). PBAT combined with plant growth enhanced aggregate occlusion and WHC, particularly under plant growth, likely via microbial degradation byproducts and polymeric residues acting as "gluing agents" (Figure 3). These byproducts are associated with microbial degradation and formation of dissolvable polymers and oligomers (Li et al., 2025; Jiaxin Wang et al., 2024; Zumstein et al., 2018), and combined with microbial biomass formation, simulates support for aggregation formation. In sandy loam, high soil porosity and large proportion of coarse sand particles prevent OM retention and microbial exudates, particularly extracellular polymeric substances (EPS), from forming substantial amounts of aggregates. Consequently, these microbial residues associated with microbial turnover and nitrogen (N) cycling of fertilizer were found to be more diffused

into the bulk soil (see Section 2.3.2). MPs size treatments without maize showed only minor early, trends in silty loam (4 weeks) but by end of experimentation (18 weeks) resembled controls. The hypothesis that smaller sized MPs would further disturb aggregation was not observable, and effects between size treatments were weak. Considering these observations were based on a single bulk replicate, further studies are needed to confirm effects.

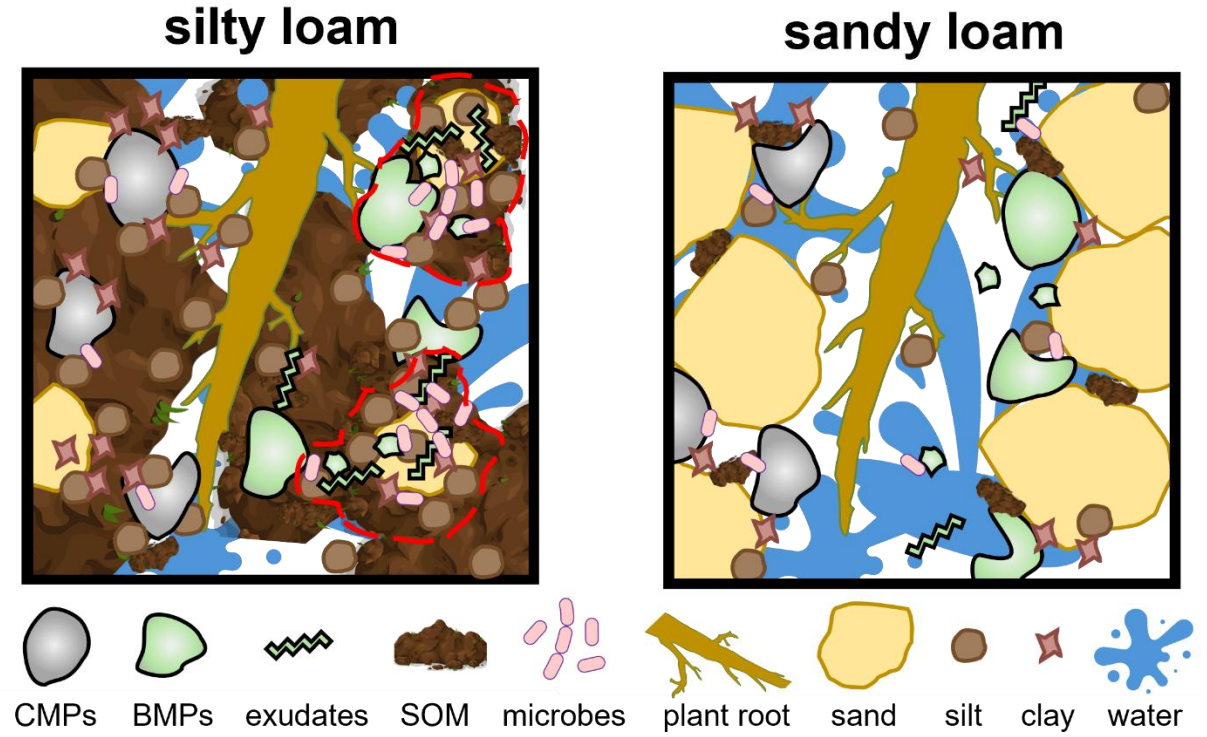

Figure 3. Conceptual distribution of conventional (CMPs) and biodegradable (BMPs) microplastics within soil aggregation materials (based on Six et al., 2004; Totsche et al., 2018). Red outline shows enhanced aggregate formation and water holding capacity in silty loam with BMPs via stimulation of microbial exudates and residues, whereas sandy loam has insufficient structure to retain substantial aggregates.

Soil water retention and WHC were hypothesized to decrease due to MPs hydrophobic surface properties, as previous studies have shown mixed effects dependent on polymer type and shape (Shafea et al., 2023; Wan et al., 2019; Xie et al., 2023). In Study 1, WHC in silty loam followed aggregation trends: CMPs had minimal impact, while PBAT slightly increased WHC (Study 1, Figure S4, SI), likely due to the same biodegradation process that also increased microaggregate formation and stability. However, even pure sand control treatments showed increased WHC, indicating results may be related to increased porosity with addition of micro-sized particles. This is contrary to the hypothesis that MPs would reduce water retention, and

further studies are now showing that soil moisture actually increases in mulching practices over long-term use (Ding et al., 2023), demonstrating that MPs effects are tied to land use as well. Soil physical structure is central to carbon storage, water regulation, and plant growth, although the results in this study show that pristine CMPs at environmentally realistic concentrations have limited impact. BMPs improved soil aggregation and WHC, but these benefits are outweighed by potential subsequent nutrient immobilization (Section 2.3.3) and did not increase plant production. Overall, the impact of MPs on soil physical structure depends on polymer type: plant growth can mitigate negative effects of CMPs (Krehl et al., 2022), whereas BMPs degradation and formation of microbial residues accelerate aggregate formation. Higher quality agricultural soils, such as silty loams, may experience improved aggregation and water retention due to BMP-induced microbial activity, while lower-quality soils, i.e. sandy loams, often lack the structural support to benefit similarly. Soil type is a major confounding factor influencing how MPs affect soil properties and plant growth, and land use practices, such as long-term plastic mulching, can modulate these effects. Therefore, reviews should strongly consider these confounders when analyzing studies on MPs effects in soil systems.

2.3.2 Biodegradable plastics (PBAT) enhance C mineralization and N-cycling in soil through microbial activation (Studies 1-2)

MPs were hypothesized to disrupt soil nutrient cycling and enhance soil CO_2 emissions through microbial stimulation (Yu et al., 2021; W. Zhao et al., 2024), with effects varying by polymer and soil type. BMPs may further impact soil fertility due to their degradability and influence on microbial soil priming (K. Jia et al., 2024; Xue et al., 2023). Low quality soils, such as sandy loams, were expected to be more sensitive than structured, silty loams. In Study 1 (Greenhouse Experiment), soil chemical parameters were analyzed: pH, total carbon and nitrogen, and available nutrients (ammonium, nitrate, phosphate, and potassium). Additionally, a ^{15}N-labeled ammonium nitrate tracer was locally applied to track distribution in soil and plant uptake (Study 1, Figure S1, SI). A principal component analysis (Study 1, Figure 2) showed that MPs treatments clustered toward more strongly by polymer type than size. Silty loam had more distinct groupings than in sandy loam, particularly for PBAT, as silty loam had a greater soil structure which allowed for more interactions.

Overall, total C was raised in both soil types proportional to the C content of each plastic polymer type; indicating plastic can act as a replacement for organic carbon, potentially misrepresenting native C stocks (Rillig, 2018). Given the lower C content of sandy loam (0.5%)

compared to silty loam (1.6%), the influence of MPs on total C stock was more pronounced in sandy loam. Potential priming effects (changes in OM decomposition and nutrient mineralization due to the addition of external substrates) were reflected in reduced fertilizer-N retention (Section 2.3.3) and also evidenced by Study 2 (Soil Respiration), which measured CO_2 dynamics and microbial activity with MPs amendments. No effects on C dynamics were observed with PE in any size range. However, PBAT amendments led to increased microbial biomass carbon (MBC) and CO_2 emissions (Study 2, Figures 1-2), with smaller PBAT particles further enhancing these effects. Furthermore, sandy loam was more sensitive than silty loam, likely due to lower SOM and structural stability. PBAT biodegradation is therefore likely to initiate SOM priming effects, which can be more intensive in poor quality soils (Guliyev et al., 2023; Zumstein et al., 2018), and can accelerate both soil organic carbon (SOC) turnover and immobilize other nutrient pools such as nitrogen (K. Jia et al., 2024; Meng et al., 2022). These short-term carbon turnovers pose risks to long-term carbon storage in agricultural soils, where repeated PBAT inputs could exacerbate carbon loss rather than promote sequestration.

In agricultural soils, maintaining optimal N availability is crucial for plant productivity, and MPs have been shown to influence N dynamics through interactions with soil quality and microbial activity (Rillig et al., 2019; Weithmann et al., 2018). It was hypothesized CMPs would affect N by altering soil structure, while BMPs would influence N-cycling by immobilizing available N (ammonium and nitrate) when priming effects are initiated via biodegradation. In Study 1 (Greenhouse Experiment), soil N was altered early between MP treatments and controls, which stabilized over time similar to other plant-available nutrients. PBAT decreased soil total N in silty loam, the higher-quality arable soil, but slightly increased N in sandy loam, the lower-quality soil (Table 1). In silty loam, N reduction by PBAT was still prevalent at the end of experiment with maize growth, whereas sandy loam showed increased N with PBAT without plant growth, possibly as residual PBAT-derived OM from changed microbial dynamics (Tanunchai et al., 2022). This was even significant for treatments with 0.1% concentration of PBAT, indicating strong interactions between N-cycling and PBAT biodegradation even at low concentrations. Subtle size-dependent effects were observed in silty loam with PBAT and maize growth, as decreasing particle size further decreased soil N. This aligns with the previously observed increased MBC and CO_2 emissions with BMPs (Rauscher et al., 2023; Jiaxin Wang et al., 2024). These findings suggest PBAT altered N-cycling differently by soil type: sandy loam enhanced fertilizer-N retention via increased microbial activity and N-cycling communities, while in silty loam apparent priming effects were

indicated by reduction of soil intrinsic N and fertilizer-N, coinciding with increased microbial respiration and abundance (see Section 2.3.5).

Table 1. Microplastics effects in differing soil types (silty loam and sandy loam) with plant growth on key physical, chemical, and biological functions, with contrasting effects between conventional (CMPs) and biodegradable (BMPs) microplastics.

Category	parameter	**silty loam**		**sandy loam**	
		CMPs	BMPs	CMPs	BMPs
Physical	aggregate formation	↓	↑	↭	↭
	aggregate stability	↓	↑	↭	↭
	water holding capacity	↭	↑	↭	↭
Chemical	pH	↭	↭	↭	↭
	CO_2 emissions	↭	⇧	↭	⇧
	total nitrogen	↓	⇩	↭	↑
	plant-available nutrients (N_{min}, P_{CAL}, K_{CAL})	↭	↭	↭	↭
	priming effect	↭	⇧	↭	↭
	fertilizer-N retention	↭	⇩	↭	⇧
	plant fertilizer-N uptake	↭	↭	↭	⇧
Biological	plant production	↓	↓	↑	↭
	root N allocation	↭	⇧	↭	↭
	microbial abundance	↭	⇧	↭	⇧
	microbial diversity	↭	↭	↭	↭
	microbial community shift	↭	⇧	↭	⇧
	microbial N-cycling community	↭	↭	↭	⇧

⇧⇩ = significant effect, ↓↑ = minor effect, ↭ = no effect

N_{min} = mineral nitrogen, CAL = Calcium-acetate-lactate extraction

2.3.3 PBAT biodegradation reduces soil pH and nutrient storage function in soil (Study 1)

MPs can increase or decrease soil pH dependent on polymer type and soil conditions (Ding et al., 2023; Zhao et al., 2021). Over experimentation time, pH shifted naturally without plants: silty loam decreased (6.5 to 6.1), whereas sandy loam increased (6.7 to 7.2), driven by wet-dry cycles and microbial turnover. Plant growth mediated pH in both soil types, regardless of MPs, in line with previous studies (Z. Chen et al., 2024; Krehl et al., 2022). Without plants, PBAT in the smallest size (<75 µm) significantly reduced pH in sandy loam (Study 1, Figure S6, SI). This is due to faster biodegradation of smaller particles and release of organic acids (Rauscher et al., 2023). Therefore, divergent pH trends with plastic type were shown to be also soil type dependent.

Plant-available nutrients (ammonium, nitrate, phosphate, and potassium) were mostly depleted by the end of experimentation due to maize growth, regardless of MPs presence. Early effects (4 weeks) of MPs were different in each soil type: ammonium declined in silty loam but sometimes increased in sandy loam (Study 1, Figure S10, SI), and available nitrate increased in both soils (Study 1, Figure S11-12, SI), contrary to the hypothesis that MPs reduce soil available nutrients. Phosphate and potassium showed scattered increases in some MPs treatments, without a distinct pattern. Thus, MPs at 1% w/w did not consistently alter nutrient cycling in planted systems. Short-term (<1 month) MPs experiments show temporary nutrient increases not reflective of long-term MP impacts, which often show net negative nutrient depletion with repeated plastic contamination (Ding et al., 2023; Meng et al., 2022). Furthermore, CMPs will likely acquire specific sorption capabilities after sufficient degradation in the environment (Section 2.3.4), transforming CMPs ability to sorb available nutrients, related to multiple soil properties, polymer type and size.

The applied ^{15}N-labeled ammonium-nitrate fertilizer allowed further tracing of plant-available N in soil. In silty loam, PBAT reduced ^{15}N-fertilizer recovery compared to controls in both the bulk soil and inside the labeled fertilizer bags, suggesting lower available N retention (Study 1, Figure 3). However, opposite in sandy loam, PBAT caused a higher retention of ^{15}N-fertilizer within the isotopic bags, possibly indicating N immobilization as increased microbial activity and N-cycling communities were observed here (see Section 2.3.5). Across both soil types, the smallest size of PBAT (<75 µm) again showed the largest impact (Study 1, Figure S13, SI). PBAT degradation in sandy loam promoted retention and redistribution of the ^{15}N-fertilizer; whereas in silty loam, soil-derived N sources were available

and PBAT led to degradation of the available N pool, consistent with priming effects (Huang et al., 2023; Inubushi et al., 2022). The increased porosity of sandy loam and N-dependent microbial biodegradation of PBAT, likely distributed the ^{15}N-fertilizer further throughout the bulk soil and retention in the labeled-bags, which was not seen within the silty loam which contained more native, soil-derived N sources. Early microbial degradation of PBAT consumed available N from both native soil N and the applied fertilizer to support microbial biomass growth, especially within the sandy loam, effectively immobilizing fertilizer-N before plant uptake. Although CMPs had no significant effects on soil nutrient availability in their pristine state, environmental weathering after longer exposure is expected to alter their surfaces, increasing chemical functionality and reactivity over time.

2.3.4 Alteration of plastics in the environment and increase in environmental reactivity (Study 3)

Plastic was once considered inert in soils. However, it was hypothesized that environmental degradation transforms MP surfaces (Chamas et al., 2020), increasing reactivity that differs from pristine MPs and results in complex interactions in soils (Menzel et al., 2022). Study 3 (Plastic Reactivity) investigated the surface change and sorption behavior of artificially degraded CMPs, as pristine CMPs were not expected to strongly affect soils initially, but impacts could increase with longer exposure and repeated inputs. In order to isolate these complex interactions plastics exhibit in the soil environment (Bläsing & Amelung, 2018), both chemical and physical properties were studied specific to polymer types PE and PET.

After MP particles (initially 200–400 µm) were exposed to accelerated UV-weathering and continuous stirring in water, scanning electron microscopy (SEM) revealed significant fragmentation and surface alteration occurred in PE particles, whereas PET showed minor surface alterations (Study 3, Figure 2). After 2000 hours of UV exposure, PE particles decreased in size by an average factor of 46 (Study 3, Figure 1, Table 1), fragmenting into many smaller, roughened particles and that formed an estimated ~2.5% of NPs (Study 3, Figure S3, SI). This finding aligned with previous studies linking low crystallinity to surface driven fragmentation, microcrack formation, and sub-particle release (Menzel et al., 2022; Zhang et al., 2024). In contrast, PET after 2000 degradation hours showed only minor flaky detachment from the outermost surface layers and slight size reduction. UV-penetration of the PET surface is limited to ~15–50 µm surface depths, forming an oxidized barrier that resists photo-oxidation to deeper layers (Day & Wiles, 1972; Grossetête et al., 2000; Lewandowski et al., 2013);

therefore PET likely fragments slowly and persists longer in soils (Chamas et al., 2020). Thus, PE fragments extensively and rapidly when exposed to UV, while PET remains stable and potentially accumulates over time.

Chemically, PE surfaces developed abundant oxygen-containing functional groups (carboxyls, hydroxyls, alcohols, peroxides) through photo-oxidation during UV-exposure (Study 3, Figures 4-5, Table 2), increasing surface polarity (Study 3, Figure 6) and reactivity with cations under alkaline conditions (Study 3, Figure 7). Fourier-transform infrared spectroscopy (FTIR) and X-ray photoelectron spectroscopy (XPS) measured formation of C-O and C=O bonds corresponding to alcohols, ketones, and carboxylic acids, demonstrating progressive oxidation and chain scission (Z. Lin et al., 2022; Moulder et al., 1995; Suresh et al., 2011). This fragmentation increased surface area and roughness, and increased new functional group formation likely to enhance the environmental reactivity of PE (Mauel et al., 2022). Environmental SEM (ESEM) showed PE transitioned from hydrophobic to hydrophilic behavior with 2000 hours of degradation (Study 3, Figure 3); consistent with recent studies (Shang et al., 2022; Zhang et al., 2024). These oxidized, smaller PE particles exhibited higher negative zeta potentials (Study 3, Figure 6), indicating increased negative surface charge and potential swelling in alkaline conditions. Furthermore, CEC measurements on degraded PE exhibited pH-dependent charges which could potentially contribute to soil CEC. This indicated, for example, that degraded PE at 1% w/w in soil would contribute ~0.075 $cmol_c\ kg^{-1}$ in alkaline conditions (pH = 9), comparable to one-tenth the sorption power of a reactive clay (Study 3, Figure 7). Although soils typically contain more clay (dependent on type), MPs could compete with clay binding sites (Li et al., 2021), especially where MPs accumulation is high or CEC is initially low (Büks & Kaupenjohann, 2020; Z. Jia et al., 2024). Therefore, degraded PE should be monitored in context to soils vulnerable to changes in CEC.

PET has inherent ester and aromatic structures that remained largely resistant to photo-oxidation, showing only minor shifts in surface chemistry detectable in either FTIR or XPS. ESEM detected mixed surfaces of hydrophobic and hydrophilic patches on PET over degradation time, without increased hydrophilicity. Negative zeta potential of PET increased with increasing degradation time similar to PE, mainly due to increased surface area and roughness rather than chemical modification (Mauel et al., 2022; Meides et al., 2022). After 2000 degradation hours, CEC of PET was slightly increased under alkaline conditions, but only around one-seventieth that of the reference clay (Study 3, Figure 7). Slower fragmentation and photo-oxidative resistance suggests PET may persist longer in soils, likely influencing soil properties through increased surface roughness rather than charge effects (Chamas et al., 2020).

These transformations imply weathered PE, with high surface area and polar groups, could substantially affect soil CEC in alkaline or MP-rich micro-sites, while PET effects are subtler but persistent (Figure 4). However, further natural degradation by UV-light, hydrolysis, and microbes will continue altering plastic surfaces, resulting in complex and largely unknown soil interactions (Wang et al., 2023). Furthermore, changes in MP sorption mechanics also increases the risk of soil contaminants being distributed and bioaccumulated (Tourinho et al., 2019). The degradation behavior of MPs is specific to each polymer type, and their environmental fate as agricultural inputs remain largely unknown.

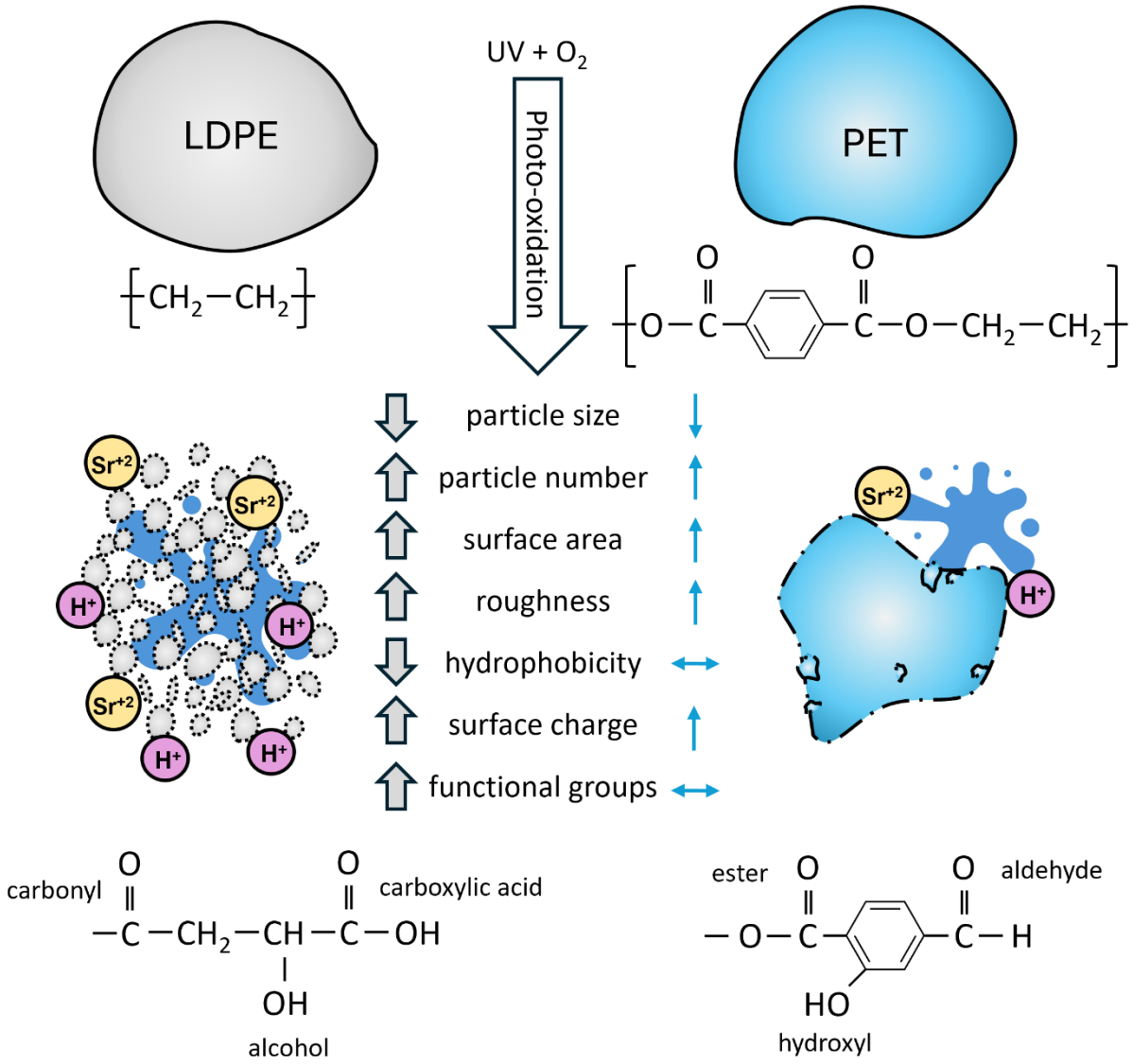

Figure 4. Plastic degradation state influences physicochemical properties resulting in functional group formation and transformed size and surfaces which can further react with chemical soil components (protons and cations). Polyethylene (PE) degradation after 2000

hours results in significantly transformed particles, whereas polyethylene terephthalate (PET) is resistant to photo-oxidation.

2.3.5 Biodegradable microplastics affect plant nutrient uptake and shift soil microbiological communities (Studies 1-2)

It is expected that CMPs and especially BMPs can affect soil microbial communities, and key taxa have been identified associated to plastics degradation (L. Han et al., 2024; Rillig et al., 2024). This thesis hypothesized that BMPs shift microbial communities to favor bioplastic degraders, impacting biodiversity and stimulating specific taxa. Due to the combined effects that BMPs may have on microbial communities favoring degraders and thereby altering plant nutrient acquisition, it was further hypothesized that these changes would negatively affect plant growth and biomass production. In Study 1 (Greenhouse Experiment), neither CMPs nor BMPs significantly affected plant growth, likely due to the single growth cycle and low plastic concentration (1% w/w). Plants may mitigate most negative effects of MPs depending on environmental conditions and plant species (Z. Chen et al., 2024; Krehl et al., 2022). However, contrasting effects appeared between soil types: MPs reduced plant growth in silty loam but increased it in sandy loam (Study 1, Figure 5).

PBAT influenced the uptake of ^{15}N-fertilizer with different responses dependent on soil type. In silty loam, maize ^{15}N uptake increased in roots with PBAT (Study 1, Figure 3), coinciding with higher root N content (Study 1, Table S3, SI) and reduced shoot biomass (Study 1, Figure 5). In sandy loam, maize ^{15}N uptake was increased in roots and shoots with PBAT, with no difference in biomass compared to controls. Therefore, plant responses to changes in the nutrient pool via PBAT degradation are soil type dependent. Reduced growth may result from plants avoiding microbially immobilized N due to toxic byproducts from PBAT degradation (Martínez et al., 2024; Qi et al., 2020; Zumstein et al., 2018). In silty loam, maize potentially utilized soil-derived N sources and allocated more N to roots, possibly via fungal symbiosis to secure mineral N (Tanunchai et al., 2022), but at the cost of reduced shoot growth. In sandy loam, where total N was limited, plants appeared to access microbially immobilized N-fertilizer, but this did not increase plant biomass, indicating PBAT byproducts or altered N cycling may impair plant growth. During initial PBAT degradation before plant growth, microbes likely sequestered fertilizer-N into their biomass (immobilization), thereby reducing the amount of fertilizer available to plants. As microbial turnover progressed during plant growth, part of this immobilized N was released back into the soil and became available for

plant uptake. However, this delayed release appeared to disturb plant N acquisition, as the eventual plant uptake of previously immobilized fertilizer-N had no growth benefits. Other factors such as nutrient limitation and plant species (Lozano & Rillig, 2020), and soil drought or flooded conditions (Jie Wang et al., 2024) also influence MPs effects on agricultural systems.

PBAT addition (1% w/w, 75–400 µm) altered microbial communities within macro- and microaggregates, with variations observed between sandy and silty loams. As expected, maize presence significantly affected microbial composition across treatments. PBAT treatments in both soil types, especially with plants, caused distinct community shifts versus controls and PE treatments (Study 1, Figure 4A). This is consistent with BMPs research showing short-term changes microbial community and enzyme activity (Huang et al., 2023; Xue et al., 2023; Zhou et al., 2021). In sandy loam soils, aggregate size influenced microbial community structure, with notable differences between micro- and macroaggregates (Study 1, Figure 4B), but aggregate size had no additional effect in silty loam, indicating soil type influences the impact of PBAT on microbial distribution.

Differential abundance identified by Analysis of Composition of Microbiomes (ANCOM) showed that PBAT treatments, especially in sandy loam, enriched certain bacterial genera, *Xylophilus* had the highest differential abundance, while substantially reducing *Azospirillum*, among other genera (Study 1, Figure 4C). Predictive metagenomic analysis indicated an increased abundance of genes related to denitrification and nitrification pathways in sandy loam PBAT treatments (Study 1, Figure 4D), suggesting PBAT biodegradation may enhance microbial functions involved in nitrogen transformations associated with N-cycling processes (Tanunchai et al., 2022).

As previously mentioned (Section 2.3.2), PBAT (1% w/w) significantly increased microbial biomass and CO_2 emissions in both soil types, while pristine PE had no effect (Study 2, Figures 1-2), suggesting microbes actively utilized PBAT as a carbon source, stimulating growth. PBAT also shifted soil prokaryotic community composition, whereas PE did not (Study 2, Figures 4-6). Enrichment of *Caulobacteraceae* was found in both soil types with PBAT amendments, which have been previously identified with BMPs degradation (Rüthi et al., 2020). Both Studies 1-2 found *Comamonadaceae* enriched in sandy loam with PBAT, which are known to be primary degraders of polyesters (Nguyen et al., 2021; Weig et al., 2021; Yoshida et al., 2016).

In Study 2 (Soil Respiration), smaller PBAT particles in sandy loam led to greater microbial activity, matching Study 1 which found that specific aggregate sizes promote

biodegradation communities. This is attributed to greater microbial access to PBAT in sandy loam soils due to lower aggregate occlusion, and reduced protection from microbial degradation (Totsche et al., 2018). Overall, these findings highlight that lower quality, sandy loams may be more responsive and vulnerable to microbial shifts induced by BMPs, while silty loams may resist change but have potential impacts on plant nutrient dynamics and biomass production.

2.3.6 Method development for quantification of microplastics in soils (Study 4)

As plastic use and contamination is ubiquitous and present in every analytical lab, it is very difficult to find controlled soils without plastic, and even archived soil has been shown to have plastic contamination (Rotchell et al., 2024). A detection method was critical to establish for future field studies, and important implications for overestimation of PE was found (Figure 5). This thesis developed a robust method for quantifying microplastics (PE, PET, and PS) in agricultural soils without pre-cleanup while maintaining low concentrations, sample representativeness, and identified common interferences from OM (Bartnick et al., 2024). Large-volume pyrolysis allowed larger samples (up to 1 g) on homogenized (milled) soil samples, allowing for better sample representation. Utilizing precisely sized standard plastic particles (125 × 125 × 20 μm^3) assisted in improving accuracy for calibration (Oster et al., 2024) and essential for identifying low quantification limits. Tandem mass spectrometry allowed for better selectivity of ions, especially PET, and further enhanced separation of PE from OM interferences. In order to rectify contributions from OM to PE signals, a mathematical calculation was suggested to correct PE overestimation caused by diagenetically altered OM, such as found with humic acid (HA). HA was found OM contributed up to 72% of PE signals, meaning recalcitrant OM in soils may consist of the same hydrocarbon chains found in PE pyrolysis. A correction factor (mathematical calculation, Study 4, SI) was derived to adjust PE quantification in soils with <1.5% organic carbon; as soils with higher OM content require cleanup for accurate PE representation.

Tandem MS is not well established for plastic detection but is a very promising method for soil compared to using scan modes common in MS applications for plastic quantification (Albignac et al., 2023), so this thesis can be used as starting point to simultaneously detect many plastic types in soil which are of interest to researchers (Table 2). Further polymer types can be included, given retention times do not overlap. This method is recommended for simultaneous quantification of MPs in soils down to 1 mg/kg, however this can be improved

with further estimation on specific interferences of OM to PE, such as recalcitrant OM forms (Kopecký et al., 2022). Considerations of co-pyrolysis effects of pyrolyzing plastic polymers simultaneously and additional matrix effects that may be present in soils. Additionally, considerations should be given to interferences such as co-pyrolysis of plastics together forming secondary products (see PET interferences, Table 2). Coralli et al. (2022) discovered co-pyrolysis effects with PET, specifically with polyamides (PA6 and PA6,6) and polyvinyl chloride (PVC). They show that N from PA interact with PET during pyrolysis to form aromatic nitriles, and chloroethyl ester formation from terephthalic acid of PET and vinyl groups of PVC (Coralli et al., 2022). This indicates secondary pyrolysis products that should be monitored in future mass-based analytics, especially PET, which was shown to influence the pyrolysis of PBAT in this thesis.

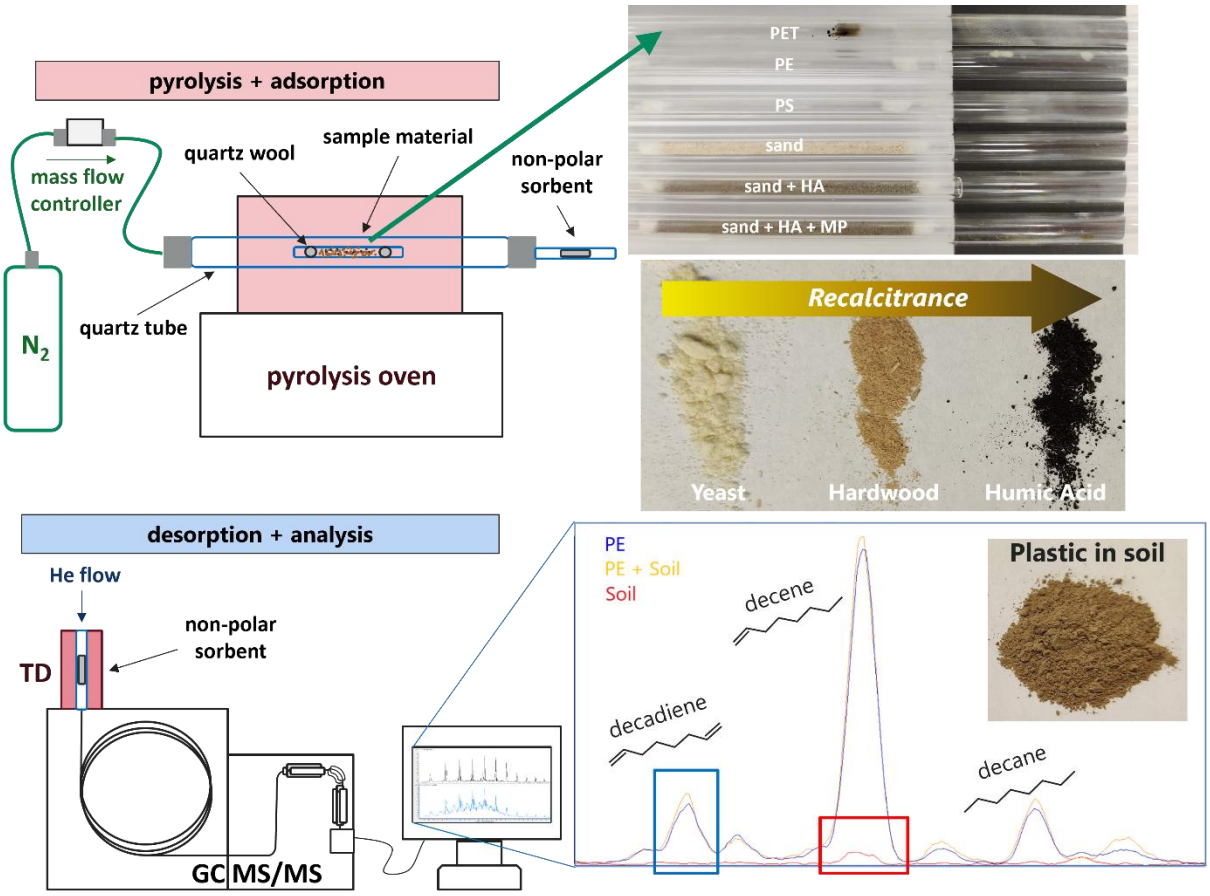

Figure 5. Method procedure of TD-GC-MS/MS, highlighting interference of specific hydrocarbon chains of polyethylene (blue) with recalcitrant soil organic matter (red); adapted from Bartnick et al. (2024).

Fortunately, no co-pyrolysis between polyolefins (PE and PP) and PS with other plastic types are observed (Albignac et al., 2023; Coralli et al., 2022). However, they have the largest

potential for overestimation by OM interference (Bartnick et al., 2024; Kittner et al., 2022). Polyolefins contain long-chained hydrocarbons that can overlap with each other and SOM (Figure 5), so considerations should be taken when using scan mode. Therefore, this study concluded that conventional pyrolysis-GC/MS methods for quantifying MPs in soils are prone to PE overestimation due to interference from natural OM. This methodological advancement could provide more accurate plastic quantification, critical for assessing contamination levels and ecological risks in agricultural soils. Separate analysis of each polymer is ideal but costly, so knowing specific interferences is beneficial. Additional polymers of interest that were not included: vinyl polymers such as PVC and polyvinyl acetate; polyurethanes which contain N; tire wear and transformed products (Klöckner et al., 2021); and fluoropolymers (Teflon) which are an understudied contributor to polyfluoroalkyl substances in soils (Lohmann et al., 2020).

Table 2. Plastic polymer compounds*, classification, and quantified pyrolysis products of TD-GC-MS/MS with known interferences.

polymer abbr.	polymer name	chemical classification	quantification compound (pyrolysis product)	molecular formula	t_R (min)	molar mass	SRM (*m/z*)		interferences
							Q1	Q3	
PA6	polyamide 6 (nylon 6)	polyamide	caprolactam	$C_6H_{11}NO$	14.5	113	113	85	co-pyrolysis PET
PA66	polyamide 66 (nylon 6,6)	polyamide	1,6-hexanediamine	$C_6H_{12}N_2$	11.2	116	87	56	co-pyrolysis PET
PBAT	polybutylene adipate terephthalate	aliphatic-aromatic polyester	terephthalic acid dibut-3-enyl-ester	$C_{16}H_{18}O_4$	27.5	274	203	149	co-pyrolysis PET
PE	polyethylene	polyolefin	1,13-tetradecadiene	$C_{14}H_{26}$	17.3	194	81	79	OM contribution
PET	polyethylene terephthalate	aromatic polyester	ethyl benzoate	$C_9H_{10}O_2$	12.8	150	150	122	co-pyrolysis PA, PBAT
PLA	polylactic acid	aliphatic polyester	lactide	$C_6H_8O_4$	11.9 – 12.8	144	56	28	OM contribution
PMMA	polymethyl methacrylate	vinyl / acrylic	methyl methacrylate	$C_5H_8O_2$	14.8	100	69	41	
PP	polypropylene	polyolefin	2,4,6,8-tetramethyl-10-undecene	$C_{15}H_{30}$	15.8 – 16.2	210	111	69	
PS	polystyrene	vinyl / aromatic	2,4-diphenyl-1-butene	$C_{16}H_{16}$	23.1	208	208	104	

*Compounds identified by specific retention time (t_R) and selected reaction monitoring (SRM) ions of interest (m/z) at quadrupole 1 (Q1) and quadrupole 3 (Q3) of MS/MS.

2.3.7 Viewpoint on future soil studies to consider microplastics size as 1–1000 µm (Study 5)

This thesis integrates findings from multiple studies to elucidate how MPs particle size influences soil physical structure, nutrient cycling, and microbial dynamics. Among the soil functions assessed, microbial community composition and nutrient cycling were particularly sensitive to smaller PBAT MPs (<200 µm), highlighting that plastic particle size is critical to determining interactions within soil systems. It has become common in soil science to define MPs as particles <5 mm, adopted from marine research (Arthur et al., 2009) and formalized by NOAA to include the broadest range of plastic debris. However, this conflicts with the standard soil particle size limit of <2 mm, which defines the start of soil formation (Brady & Weil, 2017). Most soil processes relevant to pollutant and soil fertility occur at the micron or sub-micron scale, such as interactions with mineral components, aggregation behavior, biological effects on microbes and fauna, and chemical sorption (Study 5, Figure 1). Larger plastics (>1 mm) typically only act as physical barriers until degraded into smaller MPs capable of more complex interactions (Arthur et al., 2009; Pérez-Reverón et al., 2023). As most soil functions are within the range of microplastic interaction (here defined as 1-1000 um), a larger definition of MPs up to 5 mm is outside relevant interaction scales, as MPs incorporation into soil aggregates and pores likely occurs at the micron or lower range (Z. Jia et al., 2024; Zhang & Liu, 2018).

MPs must be within a size range ingestible or biologically interactive to affect soil organisms. Nanoplastics (here defined at 1-1000 nm) pose the greatest biological risk due to their high sorption behavior to cells, additives, and pollutants at this scale (Pérez-Reverón et al., 2023; Richard et al., 2024; Rillig et al., 2024). The International System of Units (SI) defines the "micro-" prefix as 1–1000 µm (10^{-6} to 10^{-9} m), which is used by the overarching scientific community and would be more appropriate for defining MPs sizes relevant to their respective soil function (Bartnick & Lehndorff, 2025). MPs further degrade into NPs, which the definition of is also debated (Pérez-Reverón et al., 2023) but also could adhere to the SI (10^{-9} to 10^{-12} m). As there is high variability in plastic chemistry, size, shape, and additives, determining exact cause and effect remains challenging; nonetheless, standardized and precise definitions are essential for scientific and regulatory clarity. Further refinement of MPs into both defined size and chemical characteristics will likely occur when toxic effects are known to occur more commonly in certain soil systems with BMPs and degraded, reactive CMPs at the size range capable of soil incorporation (typically <1 mm). The further mixed effects by inputs of varieties of polymer mixtures and complex environments will take considerable research to disentangle the primary physicochemical interactions governing plastic behavior in soil systems.

2.4 Conclusion and Outlook

This thesis leads to the following conclusions:

1) BMPs biodegradation increased soil aggregation formation, stability, and WHC in silty loam through an interaction with maize plant growth and formation of microbial residues, whereas sandy loam lacked the structure for improvement. CMPs (PE and PET) in their pristine state had minimal influence on soil physical structure within one growth cycle.
2) BMPs induced an apparent priming effect via biodegradation in silty loam with reduction in soil total N and increased microbial activity, whereas in sandy loam, BMPs stimulated microbial retention of fertilizer-derived N in soil and its uptake by maize, but without benefits to plant growth. Although pristine CMPs had minimal effect, degradation such as by UV photo-oxidation transformed their surface to be more chemically reactive and hydrophilic, potentially influencing long-term soil chemistry.
3) BMPs shifted microbial communities through preferential colonization and degradation, leading to increased microbial abundance, CO_2 emissions, and selective increase in N-cycling microbial communities, which were most prevalent in sandy loam; whereas pristine CMPs had minimal effect.
4) MPs quantification in environmental soils benefited from large-volume pyrolysis and tandem MS spectrometry, which enabled quick sample throughput with no clean-up and targeted specific MPs pyrolysis products that distinguished them from SOM.
5) A redefinition of microplastics (1–1000 µm) and nanoplastics (1–1000 nm) would better align MPS research on relevant ecological impacts with soil-specific processes (e.g., aggregation, nutrient cycling, and microbial interactions) that predominantly occur at micro- and nanoscales, which then align with SI units and standardize research across multiple disciplines.

Future plastic studies would greatly benefit from the following suggestions:

- Focus research on soil confounders such as soil type and nutrient fertilization that exhibit complex interactions with MPs, modifying their impacts
- Increase experimentation using environmentally relevant plastic sizes and naturally degraded plastics to enhance the applicability of studies to real-world conditions
- As microplastics likely degrade and fractionate into nanoplastics, research should focus on the fate of transformed nanoplastics particles in soils
- Caution should be given to the alternative use of biodegradable plastics in agriculture due to the quick turnover of SOM, microbial interactions, and quickly induced priming effects

3. Contributions to the included manuscripts

This Ph.D. thesis consists of five manuscripts: three published, one submitted, and one completed. The co-authors listed on the manuscripts contributed the following:

Manuscript 1: Physicochemical Responses of Agricultural Soils to Biodegradable and Conventional Microplastics

Status: Manuscript completed, planned submission to *Soil Biology and Biochemistry*, 2025.

R. Bartnick: Writing – original draft, conceptualization, data curation, visualization, investigation, formal analysis, methodology

A. Jakobs: Writing – original draft, conceptualization, data curation, visualization, investigation, formal analysis, methodology

T. Lüders: Writing – review & editing, conceptualization, funding acquisition, project administration, resources, supervision

E. Lehndorff: Writing – review & editing, conceptualization, funding acquisition, project administration, resources, supervision

Manuscript 2: Biodegradable Microplastic Increases CO_2 Emission and Alters Microbial Biomass and Bacterial Community Composition in Different Soil Types

Status: Published in *Applied Soil Ecology*, *182*, 104714, 2023. https://doi.org/10.1016/j.apsoil.2022.104714

A. Rauscher: Writing – original draft, data curation, visualization, investigation, formal analysis, methodology

N. Meyer: Writing – review & editing, conceptualization, resources, supervision

A. Jakobs: Writing – review & editing, formal analysis, investigation, visualization

R. Bartnick: Writing – review & editing, conceptualization, resources

T. Lüders: Writing – review & editing, funding acquisition, project administration, resources, supervision

E. Lehndorff: Writing – review & editing, conceptualization, funding acquisition, project administration, resources, supervision

Manuscript 3: UV-degraded Polyethylene Exhibits Variable Charge and Enhanced Cation Adsorption

Status: Manuscript completed, submitted to *Geoderma*, June 2025.

R. Bartnick: Writing – original draft, conceptualization, data curation, formal analysis, investigation, visualization

S. Shahriari: Writing – original draft, data curation, formal analysis, investigation, methodology

G. Auernhammer: Writing – review & editing, data curation, formal analysis, investigation

U. Mansfeld: Writing – review & editing, data curation, investigation, methodology, visualization

W. Reichstein: Investigation, formal analysis, methodology

L. Hülsmann: Writing – review & editing, data curation, software, validation

E. Lehndorff: Writing – review & editing, conceptualization, funding acquisition, project administration, resources, supervision

Manuscript 4: Plastic Quantification and Polyethylene Overestimation in Agricultural Soil Using Large-Volume Pyrolysis and TD-GC-MS/MS

Status: Published in *Environmental Science & Technology*, *58*(29), 13047–13055. https://doi.org/10.1021/acs.est.3c10101

R. Bartnick: Writing – original draft, conceptualization, data curation, investigation, formal analysis, methodology, visualization

A. Rodionov: Writing – review & editing, resources, supervision, validation

S. D. J. Oster: Writing – review & editing, formal analysis, methodology, resources

M. G. J. Löder: Writing – review & editing, resources, supervision, project administration

E. Lehndorff: Writing – review & editing, conceptualization, funding acquisition, project administration, resources, supervision

Manuscript 5: From Sea to Land: Setting the Size Definition of Plastics for Soil Ecosystem Studies

Status: Published in *Journal of Plant Nutrition and Soil Science*, *188*(3), 373–375, 2025. https://doi.org/10.1002/jpln.12006

R. Bartnick: Writing – original draft, conceptualization, investigation, visualization

E. Lehndorff: Writing – review & editing, conceptualization, funding acquisition, project administration, supervision

4. References

Albignac, M., Oliveira, T., Landebrit, L., Miquel, S., Auguin, B., Leroy, E., Maria, E., Mingotaud, A. F., & Halle, A. (2023). Tandem mass spectrometry enhances the performances of pyrolysis-gas chromatography-mass spectrometry for microplastic quantification. *Journal of Analytical and Applied Pyrolysis*, *172*, 105993. https://doi.org/10.1016/j.jaap.2023.105993

Amelung, W., Tang, N., Siebers, N., Aehnelt, M., Eusterhues, K., Felde, V. J. M. N. L., Guggenberger, G., Kaiser, K., Kögel-Knabner, I., Klumpp, E., Knief, C., Kruse, J., Lehndorff, E., Mikutta, R., Peth, S., Ray, N., Prechtel, A., Ritschel, T., Schweizer, S. A., … Totsche, K. U. (2024). Architecture of soil microaggregates: Advanced methodologies to explore properties and functions. *Journal of Plant Nutrition and Soil Science*, *187*(1), 17–50. https://doi.org/10.1002/jpln.202300149

Arthur, C., Baker, J., & Bamford, H. (2009). Proceedings of the International Research Workshop on the Occurrence, Effects and Fate of Microplastic Marine Debris. *National Oceanic and Atmospheric Administration Technical Memorandum NOS-OR&R-30*.

Barnes, D. K. A., Galgani, F., Thompson, R. C., & Barlaz, M. (2009). Accumulation and fragmentation of plastic debris in global environments. *Philosophical Transactions of the Royal Society of London. Series B, Biological Sciences*, *364*(1526), 1985–1998. https://doi.org/10.1098/rstb.2008.0205

Bartnick, R., & Lehndorff, E. (2025). From Sea to Land: Setting a Size Definition of Plastics for Soil Ecosystem Studies. *Journal of Plant Nutrition and Soil Science*, *188*(3), 373–375. https://doi.org/10.1002/jpln.12006

Bartnick, R., Rodionov, A., Oster, S. D. J., Löder, M. G. J., & Lehndorff, E. (2024). Plastic Quantification and Polyethylene Overestimation in Agricultural Soil Using Large-Volume Pyrolysis and TD-GC-MS/MS. *Environmental Science & Technology*, *58*(29), 13047–13055. https://doi.org/10.1021/acs.est.3c10101

Bläsing, M., & Amelung, W. (2018). Plastics in soil: Analytical methods and possible sources. *The Science of the Total Environment*, *612*, 422–435. https://doi.org/10.1016/j.scitotenv.2017.08.086

Brady, N. C., & Weil, R. R. (2017). *The nature and properties of soils* (Global edition). Pearson.

Browne, M. A., Crump, P., Niven, S. J., Teuten, E., Tonkin, A., Galloway, T., & Thompson, R. (2011). Accumulation of microplastic on shorelines woldwide: Sources and sinks. *Environmental Science & Technology*, *45*(21), 9175–9179. https://doi.org/10.1021/es201811s

Büks, F., & Kaupenjohann, M. (2020). Global concentrations of microplastics in soils – a review. *SOIL*, *6*(2), 649–662. https://doi.org/10.5194/soil-6-649-2020

Cao, Z., Kim, C., Li, Z., & Jung, J. (2024). Comparing environmental fate and ecotoxicity of conventional and biodegradable plastics: A critical review. *The Science of the Total Environment*, *951*, 175735. https://doi.org/10.1016/j.scitotenv.2024.175735

Chamas, A., Moon, H., Zheng, J., Qiu, Y., Tabassum, T., Jang, J. H., Abu-Omar, M., Scott, S. L., & Suh, S. (2020). Degradation Rates of Plastics in the Environment. *ACS Sustainable Chemistry & Engineering*, *8*(9), 3494–3511. https://doi.org/10.1021/acssuschemeng.9b06635

Chen, Z., Carter, L. J., Banwart, S. A., Pramanik, D. D., & Kay, P. (2024). Multifaceted effects of microplastics on soil-plant systems: Exploring the role of particle type and plant species. *The Science of the Total Environment*, *954*, 176641. https://doi.org/10.1016/j.scitotenv.2024.176641

Coralli, I., Giorgi, V., Vassura, I., Rombolà, A. G., & Fabbri, D. (2022). Secondary reactions in the analysis of microplastics by analytical pyrolysis. *Journal of Analytical and Applied Pyrolysis*, *161*, 105377. https://doi.org/10.1016/j.jaap.2021.105377

Corradini, F., Meza, P., Eguiluz, R., Casado, F., Huerta-Lwanga, E., & Geissen, V. (2019). Evidence of microplastic accumulation in agricultural soils from sewage sludge disposal. *The Science of the Total Environment*, *671*, 411–420. https://doi.org/10.1016/j.scitotenv.2019.03.368

Cramer, A., Benard, P., Zarebanadkouki, M., Kaestner, A., & Carminati, A. (2023). Microplastic induces soil water repellency and limits capillary flow. *Vadose Zone Journal*, *22*(1). https://doi.org/10.1002/vzj2.20215

David, J., Steinmetz, Z., Kučerík, J., & Schaumann, G. E. (2018). Quantitative Analysis of Poly(ethylene terephthalate) Microplastics in Soil via Thermogravimetry-Mass Spectrometry. *Analytical Chemistry*, *90*(15), 8793–8799. https://doi.org/10.1021/acs.analchem.8b00355

Day, M., & Wiles, D. M. (1972). Photochemical degradation of poly(ethylene terephthalate). III. Determination of decomposition products and reaction mechanism. *Journal of Applied Polymer Science*, *16*(1), 203–215. https://doi.org/10.1002/app.1972.070160118

Dierkes, G., Lauschke, T., & Földi, C. (2022). Analytical Methods for Plastic (Microplastic) Determination in Environmental Samples. In F. Stock, G. Reifferscheid, N. Brennholt, & E. Kostianaia (Eds.), *Plastics in the Aquatic Environment—Part I* (pp. 43–67). Springer International Publishing. https://doi.org/10.1007/698_2021_744

Ding, F., Li, S., Lu, J., Penn, C. J., Wang, Q.-W., Lin, G., Sardans, J., Penuelas, J., Wang, J., & Rillig, M. C. (2023). Consequences of 33 Years of Plastic Film Mulching and Nitrogen Fertilization on Maize Growth and Soil Quality. *Environmental Science & Technology*, *57*(25), 9174–9183. https://doi.org/10.1021/acs.est.2c08878

Dokl, M., Copot, A., Krajnc, D., van Fan, Y., Vujanović, A., Aviso, K. B., Tan, R. R., Kravanja, Z., & Čuček, L. (2024). Global projections of plastic use, end-of-life fate and potential changes in consumption, reduction, recycling and replacement with bioplastics to 2050. *Sustainable Production and Consumption*, *51*, 498–518. https://doi.org/10.1016/j.spc.2024.09.025

Duemichen, E., Eisentraut, P., Celina, M., & Braun, U. (2019). Automated thermal extraction-desorption gas chromatography mass spectrometry: A multifunctional tool for comprehensive characterization of polymers and their degradation products. *Journal of Chromatography. A*, *1592*, 133–142. https://doi.org/10.1016/j.chroma.2019.01.033

Dümichen, E., Eisentraut, P., Bannick, C. G., Barthel, A.-K., Senz, R., & Braun, U. (2017). Fast identification of microplastics in complex environmental samples by a thermal degradation method. *Chemosphere*, *174*, 572–584. https://doi.org/10.1016/j.chemosphere.2017.02.010

Eisentraut, P., Dümichen, E., Ruhl, A. S., Jekel, M., Albrecht, M., Gehde, M., & Braun, U. (2018). Two Birds with One Stone—Fast and Simultaneous Analysis of Microplastics: Microparticles Derived from Thermoplastics and Tire Wear. *Environmental Science & Technology Letters*, *5*(10), 608–613. https://doi.org/10.1021/acs.estlett.8b00446

Feng, X., Wang, Q., Sun, Y., Zhang, S., & Wang, F. (2022). Microplastics change soil properties, heavy metal availability and bacterial community in a Pb-Zn-contaminated soil. *Journal of Hazardous Materials*, *424*(Pt A), 127364. https://doi.org/10.1016/j.jhazmat.2021.127364

Fischer, M., & Scholz-Böttcher, B. M. (2017). Simultaneous Trace Identification and Quantification of Common Types of Microplastics in Environmental Samples by Pyrolysis-Gas Chromatography-Mass Spectrometry. *Environmental Science & Technology*, *51*(9), 5052–5060. https://doi.org/10.1021/acs.est.6b06362

Geyer, R., Jambeck, J. R., & Law, K. L. (2017). Production, use, and fate of all plastics ever made. *Science Advances*, *3*(7), 1700782. https://doi.org/10.1126/sciadv.1700782

Gigault, J., Halle, A., Baudrimont, M., Pascal, P.-Y., Gauffre, F., Phi, T.-L., El Hadri, H., Grassl, B., & Reynaud, S. (2018). Current opinion: What is a nanoplastic? *Environmental Pollution (Barking, Essex : 1987)*, *235*, 1030–1034. https://doi.org/10.1016/j.envpol.2018.01.024

Grossetête, T., Rivaton, A., Gardette, J. L., Hoyle, C. E., Ziemer, M., Fagerburg, D. R., & Clauberg, H. (2000). Photochemical degradation of poly(ethylene terephthalate)-modified copolymer. *Polymer*, *41*(10), 3541–3554. https://doi.org/10.1016/S0032-3861(99)00580-7

Guliyev, V., Tanunchai, B., Udovenko, M., Menyailo, O., Glaser, B., Purahong, W., Buscot, F., & Blagodatskaya, E. (2023). Degradation of Bio-Based and Biodegradable Plastic and Its Contribution to Soil Organic Carbon Stock. *Polymers*, *15*(3). https://doi.org/10.3390/polym15030660

Han, L., Chen, L., Feng, Y., Kuzyakov, Y., Chen, Q., Zhang, S., Chao, L., Cai, Y., Ma, C., Sun, K., & Rillig, M. C. (2024). Microplastics alter soil structure and microbial community composition. *Environment International*, *185*, 108508. https://doi.org/10.1016/j.envint.2024.108508

Hartmann, N. B., Hüffer, T., Thompson, R. C., Hassellöv, M., Verschoor, A., Daugaard, A. E., Rist, S., Karlsson, T., Brennholt, N., Cole, M., Herrling, M. P., Hess, M. C., Ivleva, N. P., Lusher, A. L., & Wagner, M. (2019). Are We Speaking the Same Language? Recommendations for a Definition and Categorization Framework for Plastic Debris. *Environmental Science & Technology*, *53*(3), 1039–1047. https://doi.org/10.1021/acs.est.8b05297

Hofmann, T., Ghoshal, S., Tufenkji, N., Adamowski, J. F., Bayen, S., Chen, Q., Demokritou, P., Flury, M., Hüffer, T., Ivleva, N. P., Ji, R., Leask, R. L., Maric, M., Mitrano, D. M., Sander, M., Pahl, S., Rillig, M. C., Walker, T. R., White, J. C., & Wilkinson, K. J. (2023). Plastics can be used more sustainably in agriculture. *Communications Earth & Environment*, *4*(1). https://doi.org/10.1038/s43247-023-00982-4

Hu, L., Zhou, Y., Chen, Z., Zhang, D., & Pan, X. (2023). Oligomers and Monomers from Biodegradable Plastics: An Important but Neglected Threat to Ecosystems. *Environmental Science & Technology*, *57*(27), 9895–9897. https://doi.org/10.1021/acs.est.3c04423

Huang, F., Zhang, Q., Wang, L., Zhang, C., & Zhang, Y. (2023). Are biodegradable mulch films a sustainable solution to microplastic mulch film pollution? A biogeochemical perspective. *Journal of Hazardous Materials*, *459*, 132024. https://doi.org/10.1016/j.jhazmat.2023.132024

Huang, P.-M., Wang, M.-K., & Chiu, C.-Y. (2005). Soil mineral–organic matter–microbe interactions: Impacts on biogeochemical processes and biodiversity in soils. *Pedobiologia*, *49*(6), 609–635. https://doi.org/10.1016/j.pedobi.2005.06.006

Huerta Lwanga, E., Gertsen, H., Gooren, H., Peters, P., Salánki, T., van der Ploeg, M., Besseling, E., Koelmans, A. A., & Geissen, V. (2016). Microplastics in the Terrestrial Ecosystem: Implications for Lumbricus terrestris (Oligochaeta, Lumbricidae). *Environmental Science & Technology*, *50*(5), 2685–2691. https://doi.org/10.1021/acs.est.5b05478

Inubushi, K., Kakiuchi, Y., Suzuki, C., Sato, M., Ushiwata, S. Y., & Matsushima, M. Y. (2022). Effects of biodegradable plastics on soil properties and greenhouse gas production. *Soil Science and Plant Nutrition*, *68*(1), 183–188. https://doi.org/10.1080/00380768.2021.2022437

Jia, K., Nie, S., Tian, M., Sun, W., Gao, Y., Zhang, Y., Xie, X., Xu, Z., Zhao, C., & Li, C. (2024). Biodegradable microplastics can cause more serious loss of soil organic carbon by priming effect than conventional microplastics in farmland shelterbelts. *Functional Ecology*, *38*(11), 2447–2458. https://doi.org/10.1111/1365-2435.14662

Jia, Z., Wei, W., Wang, Y., Chang, Y., Lei, R., & Che, Y. (2024). Occurrence characteristics and risk assessment of microplastics in agricultural soils in the loess hilly gully area of Yan' an, China. *The Science of the Total Environment*, *912*, 169627. https://doi.org/10.1016/j.scitotenv.2023.169627.

Kernchen, S., Schmalz, H., Löder, M. G. J., Georgi, C., Einhorn, A., Greiner, A., Nölscher, A. C., Laforsch, C., & Held, A. (2024). Atmospheric deposition studies of microplastics in Central Germany. *Air Quality, Atmosphere & Health*, *17*(10), 2247–2261. https://doi.org/10.1007/s11869-024-01571-w

Kirstein, I. V., Kirmizi, S., Wichels, A., Garin-Fernandez, A., Erler, R., Löder, M., & Gerdts, G. (2016). Dangerous hitchhikers? Evidence for potentially pathogenic Vibrio spp. On microplastic particles. *Marine Environmental Research*, *120*, 1–8. https://doi.org/10.1016/j.marenvres.2016.07.004

Kittner, M., Kerndorff, A., Ricking, M., Bednarz, M., Obermaier, N., Lukas, M., Asenova, M., Bordós, G., Eisentraut, P., Hohenblum, P., Hudcova, H., Humer, F., István, T. G., Kirchner, M., Marushevska, O., Nemejcová, D., Oswald, P., Paunovic, M., Sengl, M., … Bannick, C. G. (2022). Microplastics in the Danube River Basin: A First Comprehensive Screening with a Harmonized Analytical Approach. *ACS ES&T Water*, *2*(7), 1174–1181. https://doi.org/10.1021/acsestwater.1c00439

Klöckner, P., Seiwert, B., Wagner, S., & Reemtsma, T. (2021). Organic Markers of Tire and Road Wear Particles in Sediments and Soils: Transformation Products of Major Antiozonants as Promising Candidates. *Environmental Science & Technology*, *55*(17), 11723–11732. https://doi.org/10.1021/acs.est.1c02723

Kopecký, M., Kolář, L., Perná, K., Váchalová, R., Mráz, P., Konvalina, P., Murindangabo, Y. T., Ghorbani, M., Menšík, L., & Dumbrovský, M. (2022). Fractionation of Soil Organic Matter into Labile and Stable Fractions. *Agronomy*, *12*(1), 73. https://doi.org/10.3390/agronomy12010073

Krehl, A., Schöllkopf, U., Májeková, M., Tielbörger, K., & Tomiolo, S. (2022). Effects of plastic fragments on plant performance are mediated by soil properties and drought. *Scientific Reports*, *12*(1), 17771. https://doi.org/10.1038/s41598-022-22270-5

Laforsch, C., Ramsperger, A. F. R. M., Mondellini, S., & Galloway, T. S. (2020). Microplastics: A Novel Suite of Environmental Contaminants but Present for Decades. In F.-X. Reichl & M. Schwenk (Eds.), *Regulatory Toxicology* (pp. 1–26). Springer Berlin Heidelberg. https://doi.org/10.1007/978-3-642-36206-4_138-1

Lehmann, A., Leifheit, E. F., Gerdawischke, M., & Rillig, M. C. (2021). Microplastics have shape- and polymer-dependent effects on soil aggregation and organic matter loss – an experimental and meta-analytical approach. *Microplastics and Nanoplastics*, *1*(1). https://doi.org/10.1186/s43591-021-00007-x

Lewandowski, S., Rejsek-Riba, V., Bernès, A., Perraud, S., & Lacabanne, C. (2013). Multilayer films ageing under ultraviolet radiations: Complementary study by dielectric spectroscopy. *Journal of Applied Polymer Science*, *129*(6), 3772–3781. https://doi.org/10.1002/app.38747

Li, C., Liu, J., Rillig, M. C., Bank, M. S., Fantke, P., Zhu, D., Zhu, Y.-G., & Jin, L. N. (2024). What harmful microbes are lurking in the world's 7 billion tonnes of plastic waste? *Nature*, *634*(8032), 30–32. https://doi.org/10.1038/d41586-024-03150-6

Li, J., Zhang, K., & Zhang, H. (2018). Adsorption of antibiotics on microplastics. *Environmental Pollution (Barking, Essex : 1987)*, *237*, 460–467. https://doi.org/10.1016/j.envpol.2018.02.050

Li, M., Zhang, X., Yi, K., He, L., Han, P., & Tong, M. (2021). Transport and deposition of microplastic particles in saturated porous media: Co-effects of clay particles and natural organic matter. *Environmental Pollution*, *287*, 117585. https://doi.org/10.1016/j.envpol.2021.117585

Li, Y., Yan, Q., Zou, C., Li, X., Wang, J., Shao, M., & Jia, H. (2025). Microplastic-Induced Alterations in Soil Aggregate-Associated Carbon Stabilization Pathways: Evidence from δ^{13} C Signature Analysis. *Environmental Science & Technology*, *59*(11), 5545–5555. https://doi.org/10.1021/acs.est.4c09242

Lin, Z., Jin, T., Zou, T., Xu, L., Xi, B., Xu, D., He, J., Xiong, L., Tang, C., Peng, J., Zhou, Y., & Fei, J. (2022). Current progress on plastic/microplastic degradation: Fact influences and mechanism. *Environmental Pollution (Barking, Essex : 1987)*, *304*, 119159. https://doi.org/10.1016/j.envpol.2022.119159

Liu, Y., Rillig, M. C., Liu, Q., Huang, J., Khan, M. A., Li, X., Liu, Q., Wang, Q., Su, X., Lin, L., Bai, Y., Guo, G., Huang, Y., Ok, Y. S., Hu, S., Wang, J., Ni, H., & Huang, Q. (2023). Factors

affecting the distribution of microplastics in soils of China. *Frontiers of Environmental Science & Engineering*, *17*(9). https://doi.org/10.1007/s11783-023-1710-4

Lohmann, R., Cousins, I. T., DeWitt, J. C., Glüge, J., Goldenman, G., Herzke, D., Lindstrom, A. B., Miller, M. F., Ng, C. A., Patton, S., Scheringer, M., Trier, X., & Wang, Z. (2020). Are Fluoropolymers Really of Low Concern for Human and Environmental Health and Separate from Other PFAS? *Environmental Science & Technology*, *54*(20), 12820–12828. https://doi.org/10.1021/acs.est.0c03244

Lozano, Y. M., & Rillig, M. C. (2020). Effects of Microplastic Fibers and Drought on Plant Communities. *Environmental Science & Technology*, *54*(10), 6166–6173. https://doi.org/10.1021/acs.est.0c01051

Machado, A. A. S., Kloas, W., Zarfl, C., Hempel, S., & Rillig, M. C. (2018). Microplastics as an emerging threat to terrestrial ecosystems. *Global Change Biology*, *24*(4), 1405–1416. https://doi.org/10.1111/gcb.14020

Martínez, A., Perez-Sanchez, E., Caballero, A., Ramírez, R., Quevedo, E., & Salvador-García, D. (2024). PBAT is biodegradable but what about the toxicity of its biodegradation products? *Journal of Molecular Modeling*, *30*(8), 273. https://doi.org/10.1007/s00894-024-06066-0

Mauel, A., Pötzschner, B., Meides, N., Siegel, R., Strohriegl, P., & Senker, J. (2022). Quantification of photooxidative defects in weathered microplastics using 13C multiCP NMR spectroscopy. *RSC Advances*, *12*(18), 10875–10885. https://doi.org/10.1039/d2ra00470d

Meides, N., Mauel, A., Menzel, T., Altstädt, V., Ruckdäschel, H., Senker, J., & Strohriegl, P. (2022). Quantifying the fragmentation of polypropylene upon exposure to accelerated weathering. *Microplastics and Nanoplastics*, *2*(1). https://doi.org/10.1186/s43591-022-00042-2

Meides, N., Menzel, T., Poetzschner, B., Löder, M. G. J., Mansfeld, U., Strohriegl, P., Altstaedt, V., & Senker, J. (2021). Reconstructing the Environmental Degradation of Polystyrene by Accelerated Weathering. *Environmental Science & Technology*, *55*(12), 7930–7938. https://doi.org/10.1021/acs.est.0c07718

Meng, F., Yang, X., Riksen, M., & Geissen, V. (2022). Effect of different polymers of microplastics on soil organic carbon and nitrogen—A mesocosm experiment. *Environmental Research*, *204*(Pt A), 111938. https://doi.org/10.1016/j.envres.2021.111938

Menzel, T., Meides, N., Mauel, A., Mansfeld, U., Kretschmer, W., Kuhn, M., Herzig, E. M., Altstädt, V., Strohriegl, P., Senker, J., & Ruckdäschel, H. (2022). Degradation of low-density polyethylene to nanoplastic particles by accelerated weathering. *The Science of the Total Environment*, *826*, 154035. https://doi.org/10.1016/j.scitotenv.2022.154035

Miao, L., Wang, P., Hou, J., Yao, Y., Liu, Z., Liu, S., & Li, T. (2019). Distinct community structure and microbial functions of biofilms colonizing microplastics. *The Science of the Total Environment*, *650*(Pt 2), 2395–2402. https://doi.org/10.1016/j.scitotenv.2018.09.378

Möller, J. N., Heisel, I., Satzger, A., Vizsolyi, E. C., Oster, S. D. J., Agarwal, S., Laforsch, C., & Löder, M. G. J. (2021). Tackling the Challenge of Extracting Microplastics from Soils: A Protocol to Purify Soil Samples for Spectroscopic Analysis. *Environmental Toxicology and Chemistry*, 844–857. https://doi.org/10.1002/etc.5024

Mondellini, S., Schwarzer, M., Völkl, M., Jasinski, J., Jérôme, V., Scheibel, T., Laforsch, C., & Freitag, R. (2024). Size dependent uptake and trophic transfer of polystyrene microplastics in unicellular freshwater eukaryotes. *The Science of the Total Environment*, *929*, 172470. https://doi.org/10.1016/j.scitotenv.2024.172470

Moulder, J. F., Stickle, W., Sobol, P., & Bomben, K. D. (1995). *Handbook of X-Ray Photoelectron Spectroscopy*. 84–85.

Mueller, M.-T., Fueser, H., Trac, L. N., Mayer, P., Traunspurger, W., & Höss, S. (2020). Surface-Related Toxicity of Polystyrene Beads to Nematodes and the Role of Food Availability.

Environmental Science & Technology, *54*(3), 1790–1798. https://doi.org/10.1021/acs.est.9b06583

Nguyen, M.-K., Rakib, Md. R. J., Hwangbo, M., & Kim, J. (2025). Microplastic accumulation in soils: Unlocking the mechanism and biodegradation pathway. *Journal of Hazardous Materials Advances*, *17*, 100629. https://doi.org/10.1016/j.hazadv.2025.100629

Nguyen, N. H. A., El-Temsah, Y. S., Cambier, S., Calusinska, M., Hrabak, P., Pouzar, M., Boruvka, M., Kejzlar, P., Bakalova, T., Gutleb, A. C., & Sevcu, A. (2021). Attached and planktonic bacterial communities on bio-based plastic granules and micro-debris in seawater and freshwater. *Science of The Total Environment*, *785*, 147413. https://doi.org/10.1016/j.scitotenv.2021.147413

Okoffo, E. D., Ribeiro, F., O'Brien, J. W., O'Brien, S., Tscharke, B. J., Gallen, M., Samanipour, S., Mueller, J. F., & Thomas, K. V. (2020). Identification and quantification of selected plastics in biosolids by pressurized liquid extraction combined with double-shot pyrolysis gas chromatography-mass spectrometry. *The Science of the Total Environment*, *715*, 136924. https://doi.org/10.1016/j.scitotenv.2020.136924

Oster, S. D. J., Bräumer, P. E., Wagner, D., Rösch, M., Fried, M., Narayana, V. K. B., Hausinger, E., Metko, H., Vizsolyi, E. C., Schott, M., Laforsch, C., & Löder, M. G. J. (2024). A novel proof of concept approach towards generating reference microplastic particles. *Microplastics and Nanoplastics*, *4*(1). https://doi.org/10.1186/s43591-024-00094-6

Pérez-Reverón, R., Álvarez-Méndez, S. J., González-Sálamo, J., Socas-Hernández, C., Díaz-Peña, F. J., Hernández-Sánchez, C., & Hernández-Borges, J. (2023). Nanoplastics in the soil environment: Analytical methods, occurrence, fate and ecological implications. *Environmental Pollution*, *317*, 120788. https://doi.org/10.1016/j.envpol.2022.120788

Piehl, S., Leibner, A., Löder, M. G. J., Dris, R., Bogner, C., & Laforsch, C. (2018). Identification and quantification of macro- and microplastics on an agricultural farmland. *Scientific Reports*, *8*(1), 17950. https://doi.org/10.1038/s41598-018-36172-y

Primpke, S., Fischer, M., Lorenz, C., Gerdts, G., & Scholz-Böttcher, B. M. (2020). Comparison of pyrolysis gas chromatography/mass spectrometry and hyperspectral FTIR imaging spectroscopy for the analysis of microplastics. *Analytical and Bioanalytical Chemistry*, *412*(30), 8283–8298. https://doi.org/10.1007/s00216-020-02979-w

Priya, A., Dutta, K., & Daverey, A. (2022). A comprehensive biotechnological and molecular insight into plastic degradation by microbial community. *Journal of Chemical Technology & Biotechnology*, *97*(2), 381–390. https://doi.org/10.1002/jctb.6675

Qi, Y., Ossowicki, A., Yang, X., Huerta Lwanga, E., Dini-Andreote, F., Geissen, V., & Garbeva, P. (2020). Effects of plastic mulch film residues on wheat rhizosphere and soil properties. *Journal of Hazardous Materials*, *387*, 121711. https://doi.org/10.1016/j.jhazmat.2019.121711

Rauscher, A., Meyer, N., Jakobs, A., Bartnick, R., Lueders, T., & Lehndorff, E. (2023). Biodegradable microplastic increases CO2 emission and alters microbial biomass and bacterial community composition in different soil types. *Applied Soil Ecology*, *182*, 104714. https://doi.org/10.1016/j.apsoil.2022.104714

Richard, C. M. C., Dejoie, E., Wiegand, C., Gouesbet, G., Colinet, H., Balzani, P., Siaussat, D., & Renault, D. (2024). Plastic pollution in terrestrial ecosystems: Current knowledge on impacts of micro and nano fragments on invertebrates. *Journal of Hazardous Materials*, *477*, 135299. https://doi.org/10.1016/j.jhazmat.2024.135299

Rillig, M. C. (2012). Microplastic in terrestrial ecosystems and the soil? *Environmental Science & Technology*, *46*(12), 6453–6454. https://doi.org/10.1021/es302011r

Rillig, M. C. (2018). Microplastic Disguising As Soil Carbon Storage. *Environmental Science & Technology*, *52*(11), 6079–6080. https://doi.org/10.1021/acs.est.8b02338

Rillig, M. C., Ingraffia, R., & Souza Machado, A. A. (2017). Microplastic Incorporation into Soil in Agroecosystems. *Frontiers in Plant Science*, *8*, 1805. https://doi.org/10.3389/fpls.2017.01805

Rillig, M. C., Kim, S. W., & Zhu, Y.-G. (2024). The soil plastisphere. *Nature Reviews. Microbiology*, *22*(2), 64–74. https://doi.org/10.1038/s41579-023-00967-2

Rillig, M. C., & Lehmann, A. (2020). Microplastic in terrestrial ecosystems. *Science (New York, N.Y.)*, *368*(6498), 1430–1431. https://doi.org/10.1126/science.abb5979

Rillig, M. C., Lehmann, A., Souza Machado, A. A., & Yang, G. (2019). Microplastic effects on plants. *The New Phytologist*, *223*(3), 1066–1070. https://doi.org/10.1111/nph.15794

Rillig, M. C., Leifheit, E., & Lehmann, J. (2021). Microplastic effects on carbon cycling processes in soils. *PLoS Biology*, *19*(3), 3001130. https://doi.org/10.1371/journal.pbio.3001130

Rødland, E. S., Samanipour, S., Rauert, C., Okoffo, E. D., Reid, M. J., Heier, L. S., Lind, O. C., Thomas, K. V., & Meland, S. (2022). A novel method for the quantification of tire and polymer-modified bitumen particles in environmental samples by pyrolysis gas chromatography mass spectroscopy. *Journal of Hazardous Materials*, *423*(Pt A), 127092. https://doi.org/10.1016/j.jhazmat.2021.127092

Rotchell, J. M., Mendrik, F., Chapman, E., Flintoft, P., Panter, I., Gallio, G., McDonnell, C., Liddle, C. R., Jennings, D., & Schofield, J. (2024). The contamination of in situ archaeological remains: A pilot analysis of microplastics in sediment samples using µFTIR. *The Science of the Total Environment*, *914*, 169941. https://doi.org/10.1016/j.scitotenv.2024.169941

Rüthi, J., Bölsterli, D., Pardi-Comensoli, L., Brunner, I., & Frey, B. (2020). The "Plastisphere" of Biodegradable Plastics Is Characterized by Specific Microbial Taxa of Alpine and Arctic Soils. *Frontiers in Environmental Science*, *8*. https://doi.org/10.3389/fenvs.2020.562263

Sa'adu, I., & Farsang, A. (2023). Plastic contamination in agricultural soils: A review. *Environmental Sciences Europe*, *35*(1). https://doi.org/10.1186/s12302-023-00720-9

Sander, M. (2019). Biodegradation of Polymeric Mulch Films in Agricultural Soils: Concepts, Knowledge Gaps, and Future Research Directions. *Environmental Science & Technology*, *53*(5), 2304–2315. https://doi.org/10.1021/acs.est.8b05208

Seeley, M. E., & Lynch, J. M. (2023). Previous successes and untapped potential of pyrolysis-GC/MS for the analysis of plastic pollution. *Analytical and Bioanalytical Chemistry*, 2873–2890. https://doi.org/10.1007/s00216-023-04671-1

Shafea, L., Felde, V. J. M. N. L., Woche, S. K., Bachmann, J., & Peth, S. (2023). Microplastics effects on wettability, pore sizes and saturated hydraulic conductivity of a loess topsoil. *Geoderma*, *437*, 116566. https://doi.org/10.1016/j.geoderma.2023.116566

Shang, C., Wang, B., Guo, W., Huang, J., Zhang, Q., Xie, H., Gao, H., & Feng, Y. (2022). The weathering process of polyethylene microplastics in the paddy soil system: Does the coexistence of pyrochar or hydrochar matter? *Environmental Pollution*, *315*, 120421. https://doi.org/10.1016/j.envpol.2022.120421

Shi, W., Wu, N., Zhang, Z., Liu, Y., Chen, J., & Li, J. (2024). A global review on the abundance and threats of microplastics in soils to terrestrial ecosystem and human health. *The Science of the Total Environment*, *912*, 169469. https://doi.org/10.1016/j.scitotenv.2023.169469

Six, J., Bossuyt, H., Degryze, S., & Denef, K. (2004). A history of research on the link between (micro)aggregates, soil biota, and soil organic matter dynamics. *Soil and Tillage Research*, *79*(1), 7–31. https://doi.org/10.1016/j.still.2004.03.008

Souza Machado, A. A., Lau, C. W., Till, J., Kloas, W., Lehmann, A., Becker, R., & Rillig, M. C. (2018). Impacts of Microplastics on the Soil Biophysical Environment. *Environmental Science & Technology*, *52*(17), 9656–9665. https://doi.org/10.1021/acs.est.8b02212

Steinmetz, Z., Kintzi, A., Muñoz, K., & Schaumann, G. E. (2020). A simple method for the selective quantification of polyethylene, polypropylene, and polystyrene plastic debris in soil by pyrolysis-gas chromatography/mass spectrometry. *Journal of Analytical and Applied Pyrolysis*, *147*, 104803. https://doi.org/10.1016/j.jaap.2020.104803

Steinmetz, Z., Löffler, P., Eichhöfer, S., David, J., Muñoz, K., & Schaumann, G. E. (2022). Are agricultural plastic covers a source of plastic debris in soil? A first screening study. *SOIL*, *8*(1), 31–47. https://doi.org/10.5194/soil-8-31-2022

Steinmetz, Z., Wollmann, C., Schaefer, M., Buchmann, C., David, J., Tröger, J., Muñoz, K., Frör, O., & Schaumann, G. E. (2016). Plastic mulching in agriculture. Trading short-term agronomic benefits for long-term soil degradation? *The Science of the Total Environment*, *550*, 690–705. https://doi.org/10.1016/j.scitotenv.2016.01.153

Stevenson, F. J. (1994). Humus chemistry: Genesis, composition, reactions (2nd ed.). Wiley.

Stock, F., B. Narayana, V. K., Scherer, C., Löder, M. G. J., Brennholt, N., Laforsch, C., & Reifferscheid, G. (2022). Pitfalls and Limitations in Microplastic Analyses. In F. Stock, G. Reifferscheid, N. Brennholt, & E. Kostianaia (Eds.), *Plastics in the Aquatic Environment—Part I* (pp. 13–42). Springer International Publishing. https://doi.org/10.1007/698_2020_654

Strawn, D., Bohn, H. L., & O'Connor, G. A. (2020). *Soil chemistry* (Fifth edition). John Wiley & Sons.

Suresh, B., Maruthamuthu, S., Kannan, M., & Chandramohan, A. (2011). Mechanical and surface properties of low-density polyethylene film modified by photo-oxidation. *Polymer Journal*, *43*(4), 398–406. https://doi.org/10.1038/pj.2010.147

Tanunchai, B., Kalkhof, S., Guliyev, V., Wahdan, S. F. M., Krstic, D., Schädler, M., Geissler, A., Glaser, B., Buscot, F., Blagodatskaya, E., Noll, M., & Purahong, W. (2022). Nitrogen fixing bacteria facilitate microbial biodegradation of a bio-based and biodegradable plastic in soils under ambient and future climatic conditions. *Environmental Science. Processes & Impacts*, *24*(2), 233–241. https://doi.org/10.1039/D1EM00426C

Thompson, R. C., Olsen, Y., Mitchell, R. P., Davis, A., Rowland, S. J., John, A. W. G., McGonigle, D., & Russell, A. E. (2004). Lost at sea: Where is all the plastic? *Science (New York, N.Y.)*, *304*(5672), 838. https://doi.org/10.1126/science.1094559

Totsche, K. U., Amelung, W., Gerzabek, M. H., Guggenberger, G., Klumpp, E., Knief, C., Lehndorff, E., Mikutta, R., Peth, S., Prechtel, A., Ray, N., & Kögel-Knabner, I. (2018). Microaggregates in soils. *Journal of Plant Nutrition and Soil Science*, *181*(1), 104–136. https://doi.org/10.1002/jpln.201600451

Tourinho, P. S., Kočí, V., Loureiro, S., & van Gestel, C. A. M. (2019). Partitioning of chemical contaminants to microplastics: Sorption mechanisms, environmental distribution and effects on toxicity and bioaccumulation. *Environmental Pollution (Barking, Essex : 1987)*, *252*(Pt B), 1246–1256. https://doi.org/10.1016/j.envpol.2019.06.030

Villarrubia-Gómez, P., Carney Almroth, B., Eriksen, M., Ryberg, M., & Cornell., S. E. (2024). Plastics pollution exacerbates the impacts of all planetary boundaries. *One Earth*, *7*(12), 2119–2138. https://doi.org/10.1016/j.oneear.2024.10.017

Wan, Y., Wu, C., Xue, Q., & Hui, X. (2019). Effects of plastic contamination on water evaporation and desiccation cracking in soil. *The Science of the Total Environment*, *654*, 576–582. https://doi.org/10.1016/j.scitotenv.2018.11.123

Wang, F., Wang, Q., Adams, C. A., Sun, Y., & Zhang, S. (2022). Effects of microplastics on soil properties: Current knowledge and future perspectives. *Journal of Hazardous Materials*, *424*(Pt C), 127531. https://doi.org/10.1016/j.jhazmat.2021.127531

Wang, Jie, Jia, M., Zhang, L., Li, X., Zhang, X., & Wang, Z. (2024). Biodegradable microplastics pose greater risks than conventional microplastics to soil properties, microbial community and plant growth, especially under flooded conditions. *The Science of the Total Environment*, *931*, 172949. https://doi.org/10.1016/j.scitotenv.2024.172949

Wang, Jiaxin, Song, M., Lu, M., Wang, C., Zhu, C., & Dou, X. (2024). Insights into effects of conventional and biodegradable microplastics on organic carbon decomposition in different soil aggregates. *Environmental Pollution (Barking, Essex : 1987)*, *359*, 124751. https://doi.org/10.1016/j.envpol.2024.124751

Wang, Q., Feng, X., Liu, Y., Cui, W., Sun, Y., Zhang, S., & Wang, F. (2022). Effects of microplastics and carbon nanotubes on soil geochemical properties and bacterial communities. *Journal of Hazardous Materials*, *433*, 128826. https://doi.org/10.1016/j.jhazmat.2022.128826

Wang, Y., Bai, J., Liu, Z., Zhang, L., Zhang, G., Chen, G., Xia, J., Cui, B., & Rillig, M. C. (2023). Consequences of Microplastics on Global Ecosystem Structure and Function. *Reviews of Environmental Contamination and Toxicology*, *261*(1). https://doi.org/10.1007/s44169-023-00047-9

Watteau, F., Dignac, M.-F., Bouchard, A., Revallier, A., & Houot, S. (2018). Microplastic Detection in Soil Amended With Municipal Solid Waste Composts as Revealed by Transmission Electronic Microscopy and Pyrolysis/GC/MS. *Frontiers in Sustainable Food Systems*, *2*. https://doi.org/10.3389/fsufs.2018.00081

Weig, A. R., Löder, M. G. J., Ramsperger, A. F. R. M., & Laforsch, C. (2021). In situ Prokaryotic and Eukaryotic Communities on Microplastic Particles in a Small Headwater Stream in Germany. *Frontiers in Microbiology*, *12*. https://doi.org/10.3389/fmicb.2021.660024

Weithmann, N., Möller, J. N., Löder, M. G. J., Piehl, S., Laforsch, C., & Freitag, R. (2018). Organic fertilizer as a vehicle for the entry of microplastic into the environment. *Science Advances*, *4*(4), 8060. https://doi.org/10.1126/sciadv.aap8060

Wu, X., Pan, J., Li, M., Li, Y., Bartlam, M., & Wang, Y. (2019). Selective enrichment of bacterial pathogens by microplastic biofilm. *Water Research*, *165*, 114979. https://doi.org/10.1016/j.watres.2019.114979

Xie, Y., Wang, H., Chen, Y., Guo, Y., Wang, C., Cui, H., & Xue, J. (2023). Water retention and hydraulic properties of a natural soil subjected to microplastic contaminations and leachate exposures. *The Science of the Total Environment*, *901*, 166502. https://doi.org/10.1016/j.scitotenv.2023.166502

Xue, Y., Zhao, F., Sun, Z., Bai, W., Zhang, Y., Zhang, Z., Yang, N., Feng, C., & Feng, L. (2023). Long-term mulching of biodegradable plastic film decreased fungal necromass C with potential consequences for soil C storage. *Chemosphere*, *337*, 139280. https://doi.org/10.1016/j.chemosphere.2023.139280

Yang, L., Zhang, Y., Kang, S., Wang, Z., & Wu, C. (2021). Microplastics in soil: A review on methods, occurrence, sources, and potential risk. *The Science of the Total Environment*, *780*, 146546. https://doi.org/10.1016/j.scitotenv.2021.146546

Yoshida, S., Hiraga, K., Takehana, T., Taniguchi, I., Yamaji, H., Maeda, Y., Toyohara, K., Miyamoto, K., Kimura, Y., & Oda, K. (2016). A bacterium that degrades and assimilates poly(ethylene terephthalate). *Science*, *351*(6278), 1196–1199. https://doi.org/10.1126/science.aad6359

Yu, H., Zhang, Z., Zhang, Y., Song, Q., Fan, P., Xi, B., & Tan, W. (2021). Effects of microplastics on soil organic carbon and greenhouse gas emissions in the context of straw incorporation: A comparison with different types of soil. *Environmental Pollution (Barking, Essex : 1987)*, *288*, 117733. https://doi.org/10.1016/j.envpol.2021.117733

Yu, Y., Battu, A. K., Varga, T., Denny, A. C., Zahid, T. M., Chowdhury, I., & Flury, M. (2023). Minimal Impacts of Microplastics on Soil Physical Properties under Environmentally Relevant Concentrations. *Environmental Science & Technology*, *57*(13), 5296–5304. https://doi.org/10.1021/acs.est.2c09822

Yudina, A., & Kuzyakov, Y. (2023). Dual nature of soil structure: The unity of aggregates and pores. *Geoderma*, *434*, 116478. https://doi.org/10.1016/j.geoderma.2023.116478

Zhang, G. S., & Liu, Y. F. (2018). The distribution of microplastics in soil aggregate fractions in southwestern China. *The Science of the Total Environment*, *642*, 12–20. https://doi.org/10.1016/j.scitotenv.2018.06.004

Zhang, S., Lin, T., Zhang, C., Yang, W., Zhou, X., Cable, R., Choi, J., Michaelson, E., Thakre, P., Serrat, C., Tan, Y., Hu, J., Meunier, D., Lai, Y., Duhaime, M., & Chen, Z. (2024). Analysis of

Accelerated Weathering Effect on Polyethylene With Varied Parameters Using a Combination of Analytical Techniques. *ChemistrySelect*, *9*(41), e202404334. https://doi.org/10.1002/slct.202404334

Zhang, Y., Li, X., Xiao, M., Feng, Z., Yu, Y., & Yao, H. (2022). Effects of microplastics on soil carbon dioxide emissions and the microbial functional genes involved in organic carbon decomposition in agricultural soil. *The Science of the Total Environment*, *806*(Pt 3), 150714. https://doi.org/10.1016/j.scitotenv.2021.150714

Zhao, S., Rillig, M. C., Bing, H., Cui, Q., Qiu, T., Cui, Y., Penuelas, J., Liu, B., Bian, S., Monikh, F. A., Chen, J., & Fang, L. (2024). Microplastic pollution promotes soil respiration: A global-scale meta-analysis. *Global Change Biology*, *30*(7), 17415. https://doi.org/10.1111/gcb.17415

Zhao, T., Lozano, Y. M., & Rillig, M. C. (2021). Microplastics Increase Soil pH and Decrease Microbial Activities as a Function of Microplastic Shape, Polymer Type, and Exposure Time. *Frontiers in Environmental Science*, *9*. https://doi.org/10.3389/fenvs.2021.675803

Zhao, W., Ge, Z.-M., Zhu, K.-H., Lyu, Q., Liu, S.-X., Chen, H.-Y., & Li, Z.-F. (2024). Impacts of plastic pollution on soil-plant properties and greenhouse gas emissions in wetlands: A meta-analysis. *Journal of Hazardous Materials*, *480*, 136167. https://doi.org/10.1016/j.jhazmat.2024.136167

Zhou, J., Gui, H., Banfield, C. C., Wen, Y., Zang, H., Dippold, M. A., Charlton, A., & Jones, D. L. (2021). The microplastisphere: Biodegradable microplastics addition alters soil microbial community structure and function. *Soil Biology and Biochemistry*, *156*, 108211. https://doi.org/10.1016/j.soilbio.2021.108211

Zhou, Y., Wang, J., Zou, M., Jia, Z., Zhou, S., & Li, Y. (2020). Microplastics in soils: A review of methods, occurrence, fate, transport, ecological and environmental risks. *The Science of the Total Environment*, *748*, 141368. https://doi.org/10.1016/j.scitotenv.2020.141368

Zumstein, M. T., Schintlmeister, A., Nelson, T. F., Baumgartner, R., Woebken, D., Wagner, M., Kohler, H.-P. E., McNeill, K., & Sander, M. (2018). Biodegradation of synthetic polymers in soils: Tracking carbon into CO2 and microbial biomass. *Science Advances*, *4*(7), 9024. https://doi.org/10.1126/sciadv.aas9024

MANUSCRIPTS

1. Manuscript 1: Physicochemical and Microbial Responses of Agricultural Soils to Biodegradable and Conventional Microplastics

Ryan Bartnick[1], Aileen Jakobs[2], Tillmann Lueders[2], Eva Lehndorff[1]

[1]Soil Ecology, Bayreuth Center of Ecology and Environmental Research (BayCEER), University of Bayreuth, Dr.-Hans-Frisch-Str. 1-3, 95448 Bayreuth, Germany
[2]Ecological Microbiology, Bayreuth Center of Ecology and Environmental Research (BayCEER), University of Bayreuth, Dr.-Hans-Frisch-Str. 1-3, 95448 Bayreuth, Germany

Manuscript completed, planned submission to *Soil Biology and Biochemistry*, 2025.

Physicochemical and Microbial Responses of Agricultural Soils to Biodegradable and Conventional Microplastics

Ryan Bartnick[*1], *Aileen Jakobs*[2], *Tillmann Lueders*[2], *Eva Lehndorff*[1]

[1]Soil Ecology and [2]Ecological Microbiology, Bayreuth Center of Ecology and Environmental Research (BayCEER), University of Bayreuth, Dr.-Hans-Frisch-Str. 1-3, 95448 Bayreuth, Germany

Abstract

Microplastics (MPs) can alter soil physical structure, chemistry, and microbial communities; ultimately affecting plant production. We hypothesized that conventional (CMPs) and biodegradable (BMPs) MPs influence key soil properties depending on their polymer type, size, concentration, degradation, and soil type. MPs may reduce aggregate stability and carbon storage, water holding capacity, pH, and nutrient retention; and BMPs may further alter nutrient availability and microbial communities. Greater aggregate disruption and chemical effects were expected with decreasing size and higher concentrations of MPs, while soil type may exhibit varying responses. To understand this, *Zea mays* was planted in a greenhouse with differing soil types (silty loam and sandy loam) and spiked with CMPs polyethylene (PE) and polyethylene terephthalate (PET), and BMPs polybutylene adipate terephthalate (PBAT), varied by concentration (0%, 0.1%, 1% w/w) and size range (200–400 µm, 75–200 µm, <75 µm); additionally, controls with no MP and pure sand were tested. Aggregate fractionation and stability, water holding capacity, were tested to see changes in physical structure of the soil. An isotopically ^{15}N-labeled ammonium-nitrate fertilizer was added to soil to trace plant nutrient uptake. Biological changes to plant growth and microbial community composition were monitored. Overall, CMPs and size range treatments had minimal impacts on soil parameters. However, the interaction between PBAT and plant growth tended to increase soil microaggregate formation, stability, and WHC in silty loam. In both soil types, PBAT treatments significantly immobilized the added ^{15}N-tracer, which gave different responses to plant uptake dependent on soil structure and nutrient availability. PBAT significantly altered soil prokaryotic communities in both soil types, with stronger shifts in sandy loam, which

enriched unique denitrification and nitrification associated genes and specific microbial taxa, indicating impacts on nitrogen cycling. This study highlights the potential impacts CMPs and BMPs have on distinct soil types and need to elucidate the complex interactions on critical soil functions such as aggregation, chemical cycling, microbial biodiversity, and plant nutrient uptake.

Keywords: carbon storage, soil aggregation, soil fertility, ^{15}N fertilizer, ^{13}C plastic, *Zea mays*

Introduction

The accumulation and fate of plastics in agricultural soils is not yet fully understood, and increased release of microplastics (MPs) to agriculture via mulching, compost and sludge application has a potential to disturb long-term soil health (Corradini et al., 2019; Piehl et al., 2018; Weithmann et al., 2018). While it is difficult to untangle mechanisms of MPs effects on key soil functions and crop production, it is necessary to mitigate the impact plastics have on land use and human health at a global scale (Chang et al., 2024; Chen et al., 2024; Guo et al., 2020). As an alternative to conventional plastics, e.g. mulch films, biodegradable plastics are proposed as a solution to plastic accumulation in agricultural soils (Griffin-LaHue et al., 2022; Huang et al., 2023; Liu et al., 2024). While the accumulation of conventional plastics in agriculture is alarming itself, the degradation of large amounts of biodegradable plastics may come with additional consequences for soil carbon, nutrient cycles, and microbial activities (Hao et al., 2024; Rauscher et al., 2023), which are not yet well understood.

First, the incorporation of small, fragmented plastics is likely to cause changes in soil structure which can affect organic matter accumulation. Plastics <500 µm are likely to begin filling in pore spaces and incorporate within soil aggregates, interacting with complex mineral-associated organic matter and microbial biogeochemical processes (Han et al., 2024; Huang et al., 2005). Soil aggregate formation and stability are essential functions and indicators of soil health as they occlude carbon and nutrients (Amelung et al., 2023; Krause et al., 2018; Lehndorff et al., 2021; Totsche et al., 2018). It has been shown that MPs can affect soil aggregation and the stability of aggregates (Jiaxin Wang et al., 2024). There is concern that the more hydrophobic and less dense MPs are compared to soil mineral particles, they will negatively impact the soil structure leading to instability and carbon leaching (Lehmann et al., 2021; Souza Machado et al., 2018). As MPs decrease in size, their potential to interact with macroaggregates (>250 µm) and microaggregates (<250 µm) increases, and incorporation into specific size fractions would prerequisite a specific plastic size. Additionally, the hydrophobic surfaces of MPs and reduced density compared to soil minerals are likely to cause reduction in

soil water holding capacity (WHC), although researchers have reported mixed effects (Wan et al., 2019; Xie et al., 2023). With reduced WHC, plant production likely decreases, and hydrophobic surfaces may cause additional water potential stress for plant water uptake (Cramer et al., 2023; Shafea et al., 2023).

As MPs differ chemically, this may also help explaining the huge variability of effects that have been reported for MPs soil (Li et al., 2021; Shi et al., 2024; Zhang et al., 2022). Dependent on their chemistry, MPs can alter nutrient cycling, i.e. binding or leaching of ions, which can even impact plant growth (Rillig et al., 2019; Souza Machado et al., 2019; Steinmetz et al., 2016). Conventional MPs (CMPs), e.g. polyethylene (PE) and polyethylene terephthalate (PET), are primarily made of monomers containing carbon, hydrogen, and/or oxygen. Especially biodegradable MPs (BMPs) can degrade to form functional groups, such as carboxyl groups which can alter soil chemistry, pH, and impact sorption behavior of inorganic nutrients, e.g. nitrate and phosphate, and their bioavailability (Meng et al., 2022; Shi et al., 2023). BMPs are typically more quickly degraded through chain scission driven by hydrolysis, UV-reactions, and/or biological enzymes. While the benefit of accelerated degradation is reduced accumulation, this can be of potential harm to stable carbon stocks in soil via the introduction of a labile C source (Liu et al., 2024; Qi et al., 2020; Rauscher et al., 2023). Additionally, the decreasing size of MPs is expected to increase specific polymer effects on soil chemistry (Ma et al., 2023; Rauscher et al., 2023), as smaller sized particles have a larger surface area and can fit into smaller aggregates and pore structures.

MPs in soil are also typically colonized by microbial communities. Some may just colonize a pristine hydrophobic surface, while others may actually benefit by degrading MPs for growth (Miao et al., 2019; Priya et al., 2022; Sander, 2019). MPs have thus been shown to alter soil microbial communities and enzymatic activities, even for hard-to-degrade CMPs such as PE (Huang et al., 2019; Rauscher et al., 2023). Additionally, biofilm formation observed on MPs has been shown to increase the abundance of microbes of potential pathogenic concern (Kirstein et al., 2016; Wu et al., 2019). Moreover, plastics typically contain no nitrogen, thus microbial degradation of MPs is limited by nutrient supply (Sander, 2019; Zumstein et al., 2018). Especially when BMPs are rapidly degraded, a fixation of surplus N in associated microbiota has been observed (Guliyev et al., 2023), likely via N-fixation (Tanunchai et al., 2022; Jie Wang et al., 2024). In summary, a number of important knowledge gaps remain to be addressed, e.g. if conventional mulch films are to be increasingly replaced by biodegradable polymers in routine agricultural practices.

This study aims to address these effects by evaluating how MP type, concentration, and size influence soil aggregation, nutrient dynamics, and microbial communities in two contrasting soil types (a sandy loam and a silty loam). To test this, we performed an 18-week greenhouse experiment, with and without maize growth, in both soils introduced with CMPs (PE and PET) and BMPs (PBAT) at two concentrations (0.1% and 1% w/w) and of various size ranges (<75–400 μm). We assessed physical impacts via aggregate fractionation and WHC measurements, quantified chemical changes by tracing ^{15}N-labeled fertilizer in soil alongside pH, total C, N, plant-available nutrient analyses (NO_3^-, NH_4^+, PO_4^{3-}, K^+), and characterized biological responses using microbial community profiling and measuring maize growth and fertilizer uptake. We hypothesize that higher concentrations and smaller sizes of MPs will disturb soil water retention and aggregate formation. We expect MPs to influence soil C and N, decrease soil pH, and disrupt nutrient sorption dynamics, dependent on polymer type and functionality, as well as concentrations and sizes. Further, BMPs (PBAT) should accelerate the above shifts due to rapid degradation. We also hypothesize that different MPs will select distinct microbial taxa, with more pronounced shifts expected for BMPs as they stimulate microbial activity. Ultimately, combined effects of polymer type, size, and soil structure, could contribute to an overall reduction in plant growth. Only a profound understanding of all the above effects can help to perform a comprehensive ecological risk assessment of MPs in soils and to guide future decision making for more sustainable agricultural practices.

Materials and Methods

Soil properties and quality

The two soil locations were in proximity to have the same climate but very different textures: a silty loam from Bindlach, Germany (49.9725°N, 11.6226°E) and a sandy loam from Bayreuth, Germany (49.9295°N, 11.5545°E) (grain size definition, see *World Reference Base for Soil Resources 2014*, 2014). Maize growth was expected to be more limited in the sandy loam due to its lower water and nutrient retention compared to a fertile silty loam. Soil was collected with topsoil removed to a depth of 30 cm. Soil was then sieved at 2 mm, dried at 40°C over 5 days, and stored at 5°C. Initial texture was analyzed by PARIO (METER Group, Munich, Germany), which uses Stokes' law of sedimentation analysis to determine amounts of sand, silt and clay particles in soil (Table S1, supporting information, SI). For determination of total carbon (C) and nitrogen (N), soil was dried at 50°C, ball-milled, and measured using a varioMAX (Elementar Analysensysteme GmbH, Langenselbold, Germany). A simple organic carbon test was used (Schumacher, 2002) to determine inorganic carbon from loss on ignition (combustion

at 550°C for 12 h) and extrapolate organic carbon from total C analysis. As all soils are likely contaminated with MPs, it is important to know the initial condition of soils used for experimentation. The soils used here had PET contents of 0.27% in silty loam and 0.02% in sandy loam (Table S1, SI; Bartnick et al., 2024). Unfortunately, the determination for PBAT was not possible due to co-pyrolysis effects with PET, as both contain terephthalate ester groups that seemed to interact.

Experimental Design

For a full description of the experimental design, see an extended version in the SI (Experimental Design and Figures S1-2). For experimentation in the greenhouse, soil treatments were set to a specific water holding capacity (WHC) of 60%. A ^{15}N-labeled nitrogen fertilizer was applied to stainless steel mesh bags to trace available nitrogen in soil. The labeled bags (0.5 mm mesh size, 0.32 mm wire thickness; Teichhansel, Bockhorn, Germany) were pre-wetted with deionized (DI) water to prevent soil loss during filling, briefly stored at 5 °C before transplanting. The fertilizer consisted of double-labeled ammonium nitrate, $^{15}NH_4{}^{15}NO_3$ (98 atom %, Sigma-Aldrich, Taufkirchen, Germany), prepared by weighing approximately 1% of the natural abundance equivalent of soil nitrogen (adjusted for molecular weight). This labeled fertilizer was mixed with bulk soil, which was then split and placed into the mesh bags, with two bags used per replicate (see Figure S1, SI).

The maize, *Zea mays*, used for experimentation was a hybrid varietal Benedictio for scientific purposes, (KWS SAAT SE & Co., Einbeck, Germany). Maize plants (n = 5) and two small pots without plant growth were prepared with MP treatments and analyzed at the initial planting stage (T1, 4 weeks) and at harvest (T2, 18 weeks); subsets of plant treatments (3 replicates) with most interest (No MP, PE, and PBAT at 1% conc. MP mix) were selected for subsequent aggregate, and microbial community composition analyses. After 18 weeks of experimentation (14 weeks of maize growth), maize plants were harvested, recording final plant height, leaf count, and leaf area. Leaf area index was measured with a LI-3100C leaf area scanner (LI-COR Environmental, Bad Homburg, Germany). Leaves, stems, fruits, and roots were separated from harvested maize plants, and fresh weight dried at 60°C for 3-5 days and measured for dry biomass. As the entirety of the bulk soil in the pot was infiltrated by maize roots in all treatments, the bulk soil is essentially rhizosphere soil. Isotopically labeled bags were removed by cutting around roots that had penetrated the bag (see Figure S1, SI). For analyses using fresh soil (pH, WHC, available N:P:K, and aggregates), soil was stored at 5°C. Bulk fresh soil was kept for long term storage at -20°C.

Experimental plastics, materials, and fertilizers

Plastic polymers used in experimentation were low density-polyethylene (PE, Lupolen 1800 P-1 – LyondellBasell, Rotterdam, NL), polyethylene terephthalate (PET, CleanPET WF – Veolia Umweltservice, Hamburg, Germany), and polybutylene adipate terephthalate (PBAT, M·VERA® B5026 – BIO-FED, Cologne, Germany). Three MP size ranges (200–400, 75–200, and <75 µm) were prepared by cryomilling (ZM200; Retsch, Haan, Germany) and airjet sieving (E200 LS; Hosokawa Alpine, Augsburg, Germany). The plastic size ranges were obtained by milling plastic beads then sieving to the desired size class resulting in irregularly shaped plastics. Particle size distributions were determined with a particle size and shape analyzer (Microtrac FlowSync, Retsch, Haan, Germany). An additional plastic "size mix" between 75–400 µm was made by combining size fractions in a ratio 6:1 (200–400:75–200 µm); particles <75 µm were not included in the "size mix" due to limited supply. Soil was tested for effects of MPs concentration using the size mix (75–400 µm) at 1% and 0.1% w/w dry soil. MPs size range treatments (200–400, 75–200, and <75 µm) were prepared at 1% w/w, with additional controls of pure cleaned sand (200–400 and 75–200 µm) to compare to MPs size fraction treatments.

Fertilizer was added to all treatments at a concentration of 1% natural abundance to allow isotopic tracing without greatly influencing the natural system. Total N concentrations were measured in each soil type to determine fertilizer amount of N and estimate P and K fertilization, adjusted for atomic weight. Nitrogen fertilizer was ammonium-nitrate (99%, Sigma-Aldrich, Taufkirchen, Germany). Additionally, potassium and phosphorous were added together as potassium dihydrogen phosphate, KH_2PO_4 (≥99.5%, Th. Geyer, Renningen, Germany). All fertilizers were ball-milled with a MM 400 vibrating mill (Retsch, Haan, Germany) for homogeneity and weighed precisely on a M500P microbalance (Sartorius, Güttingen, Germany).

Determination of soil aggregate formation, stability, and water holding capacity

Soil physical conditions were monitored for WHC and soil aggregate stability. Soil pots without plants were taken at starting conditions (4 weeks) and at the same time as the harvest for WHC and aggregate fractionation (18 weeks). WHC was measured as gravimetric water content by slowly submerging fresh soil (5 g) in water with funnel and filter paper for several hours, then subsequent drainage for 24 h overnight (Nelson et al., 2024). Fully saturated funnel columns are then removed from water submersion and covered with aluminum foil and refrigerated (5°C) to prevent evaporation. Water weight in soil is recorded after drainage and compared to dried soil weight, resulting in the maximum WHC as the weight of water per weight of dry soil at full saturation.

Soil aggregation was determined with a wet sieving method (Krause et al., 2018) and aggregate stability was tested with ultrasonic at 60 J ml^{-1} and subsequent sieving of non-occluded, destabilized particles (Amelung et al., 2023, 2024; Mentler et al., 2011). Briefly, fresh soil water content was measured and the amount of soil tested was adjusted to correspond to 20 g dry weight. Fresh soil was slowly immersed in water in a sieve tower with specific fractions (2800, 2000, 500, 250, and 53 µm) and gently shaken for 10 min to gravimetrically separate aggregates by size. Soil aggregates and particles <53 µm remaining at the bottom were collected and additionally sieved at 20 µm. The sieve fraction containing the macroaggregate fractions (2800–250 µm) was collected for ultrasonic treatment, while "free" microaggregate contents (250–53, 53–20, and <20 µm without ultrasonication) was measured. Ultrasonic probing was performed using a Branson 250 sonifier (Emerson, St. Louis, USA). After ultrasonic treatment, a subsequent sieving as before was performed to determine the occluded microaggregates and macroaggregates (2800–2000, 2000–500, and 500–250 µm). Each sieve fraction was then freeze-dried and weighed for aggregate content.

Determination of soil pH and available nutrients (N_{min}, P_{CAL}, K_{CAL})

Soil pH was measured with DI water using a basic field method (1:2.5, soil:solution ratio, Kabała et al., 2016) taken at week 4, 10, and 18 of experimentation to track changes throughout experimentation. Plant-available phosphorus (PO_4^{3-}) and potassium (K^+) were determined using a Calcium-Acetate-Lactate (CAL) extraction method (van Laak et al., 2018; VDLUFA, 2012). Available mineral nitrogen (N_{min}), ammonium (NH_4^+) and nitrate (NO_3^-), were determined using a standard extraction filtration method with 1 M KCl (Mulvaney, 1996). Concentrations of CAL-extractable P_{CAL} and K_{CAL} were measured via ICP-OES (5800, Agilent Technologies, Waldbronn, Germany) and concentrations of N_{min} via Flow Injection Analysis (FIA-LAB, MLE Dresden, Radebeul, Germany).

Isotopic determination of $^{15}N_{change}$

Soil isotopic $\delta^{15}N$ signals were analyzed from isotopically labeled bags with dry milled soil using an isotope ratio mass spectrometer (Delta XP Plus, Thermo Fisher Scientific, Bremen, Germany), calibrated with atmospheric nitrogen (AIR). Maize roots and leaves were also analyzed for uptake of ^{15}N-fertilizer. Atom percent (atom %) values for ^{15}N were calculated from the δ-values and isotope ratio, $^{15}N/^{14}N$ (Fry, 2006). Absolute amounts of heavy isotopes (eq 1) were then calculated with [N] concentration:

$$^{15}N_{amount} = \left(\frac{\text{atom \% } ^{15}N}{100}\right) \times [N] \quad (1)$$

Changes in soil ^{15}N dynamics were determined by comparing labeled MP treatments to a labeled control soil without MPs. The absolute difference in ^{15}N content can then be calculated as:

$$^{15}N_{change} = {}^{15}N_{sample} - {}^{15}N_{control} \quad (2)$$

The $^{15}N_{change}$ (eq 2) will be used to compare isotopic composition between MP treatments and controls.

Determination of microbial communities

For microbial community analysis, the aggregate separation protocol was adapted by using 10 g of fresh soil and sterile purified water (deionized and demineralized). Sieve fractions of 2000–500 µm, 500–250 µm, and 250–53 µm were collected and stored at -20°C until nucleic acid extraction. Nucleic acids were extracted from approximately 0.7 g wet soil aggregate fraction using a phenol-chloroform extraction protocol modified after Lueders et al. (2004) and as described in Rauscher et al. (2023). The quality and integrity of DNA extracts were assessed by agarose gel electrophoresis and spectrophotometric analysis (NanoDrop, Thermo Fisher Scientific, USA). Amplicon PCR targeting V4 regions of prokaryotic 16S rRNA genes was performed using the universal primer pair 515F (5'-GTGYCAGCMGCCGCGGTAA-3′, Parada et al., 2016) and 806r (5'-GGACTACNVGGTWTCTAAT-3′, Apprill et al., 2015) including phasing spacer of different length (0-2 bases) between Illumina adapter and target region on the forward primer. PCR reactions were prepared using the NEBNext® Ultra™ II Q5® Master Mix (M0544; New England Biolabs, USA) following the manufacturer's protocol with the addition of 4 µg BSA (20 µg/µl; Roche, Switzerland) per reaction. Thermocycling was performed under the following conditions: initial denaturation at 98°C for 30 sec, 25 cycles of 98°C for 10 sec, 51°C for 30 sec, and 72°C for 30 sec, followed by a final extension at 72°C for 2 min. Amplification of each sample was carried out in duplicates and pooled before downstream processing. After successful amplification, the PCR product quality and concentration were assessed by capillary electrophoresis on a Fragment Analyzer (Agilent Technologies, USA). Amplicons were purified with the NucleoMag 96 PCR purification kit (744100, Macherey-Nagel, Germany). In a subsequent PCR, amplicons were indexed using the Nextera XT Index Kit v2 Set A (FC-131-2001, Illumina, United States) and purified as described above. Sequencing was performed on an iSeq™ 100-System (Illumina, United States) in a custom 300 bp single-end mode. Raw sequencing reads were demultiplexed, Illumina adapters, and primer sequences were removed before deposition in the European Nucleotide Archive under accession number XX.

Downstream sequence processing and community analyses were conducted in R (version 4.5.0). Raw reads were processed using the DADA2 pipeline version 1.36.0 (Callahan et al., 2016). Forward reads were quality-filtered and truncated to 288 bp. The pipeline used default parameters, except for the maximum expected error (maxEE), which was set to 3 to enhance quality filtering, and the sample interference used the pooling approach. Amplicon sequence variants (ASVs) were taxonomically assigned to the Silva database version 138.1 (Quast et al., 2012) by using a trained dataset (McLaren & Callahan, 2021). Negative controls were extracted, amplified, and sequenced with the samples to identify and remove reads classified as contaminants with the decontam package (version 1.28.0, Davis et al., 2018) using the prevalence-based filtering with a default threshold of 0.1. Further, ASVs classified as chloroplasts, mitochondria, or unassigned ASVs at the kingdom or phylum level were filtered from the dataset, resulting in a dataset of 1,823,669 recovered reads with a minimum of 4,927 reads per sample.

Alpha diversity metrics (richness and Pielou's evenness) were calculated from square root-transformed ASV counts. Due to varying sequencing depths across samples, data were rarefied without replacement to the minimum sample read depth using the rrarefy function from the vegan package (version 2.6.10, Oksanen et al., 2001), with results averaged over 1,000 bootstrap replicates. Bray-Curtis dissimilarities were computed from square root-transformed ASV counts using the avgdist function from the vegan package, with 1,000 subsampling iterations based on the sample with the lowest read depth before averaging. For visualization, non-metric multidimensional scaling (NMDS) was performed on the Bray-Curtis distance matrix using the metaMDS function (vegan). Functional potential of communities was predicted using PICRUSt2 (version 2.6.2, Douglas et al., 2020) with default parameters and the implemented tools EPA-NG (Barbera et al., 2019), gappa (Czech et al., 2020), SEPP (Mirarab et al., 2011), castor (Louca & Doebeli, 2018) and MinPath (Ye & Doak, 2009) on non-transformed ASV counts.

Statistical analyses and figures

The statistical analyses were performed and figures produced in R version to evaluate the effects of MPs concentration and size, with and without maize growth, on multiple soil and plant response variables across different soil types. Quantitative results were expressed as mean ± standard deviation of plant replicates ($n = 5$) in each treatment. ANOVA tests were performed to in each separate soil type to compare significance differences for each measured variable in the treatment groups ($p < 0.05$), then Tukey's HSD post-hoc tests were performed comparing each treatment group to determine significant differences between MP treatments and control

($p < 0.05$). The Shapiro-Wilk test for normal distribution was applied to each measured variable in each treatment group ($p > 0.05$); normal distribution was mostly fulfilled, and QQ plots revealed that because of the low sample size, the Shapiro-Wilk test was sensitive to single values of plant replicates; therefore, variation and normal distribution were consistent with QQ plots. Additionally, homogeneity of variance was analyzed with Levene's test ("car" package), which showed no significant variances across treatment groups ($p > 0.05$). Residuals of ANOVA tests were assessed visually with QQ plots and found the residuals to be approximately normally distributed with minor deviations. Additionally, principal component analysis (PCA) was performed to reduce the dimensionality of multiple measured parameters to relate soil nutrient cycling with MP treatments in each soil type.

Differences in alpha diversity metrics between groups were assessed using the Kruskal-Wallis test (rstatix version 0.7.2, Kassambara, 2023), followed by Dunn's rank sum post hoc test for pairwise comparisons (FSA version 0.10.0, Ogle et al., 2025). Only comparisons between MP treatments and their respective no MP controls were considered to evaluate the impact of MP treatment on richness and evenness. The resulting p-values were adjusted for multiple testing using the Benjamini-Hochberg correction. Statistically significant groupings were visualized using compact letter displays. The influence of each explanatory variable (soil type, aggregate size fraction, MP type) on the community structure was evaluated using permutational multivariate analysis of variance (PERMANOVA) on Bray-Curtis dissimilarities, with 1,000 permutations performed for significance testing. The dataset was subset to the respective groups for pairwise comparisons, and significance was tested using adonis2 with Benjamini-Hochberg p-value correction. Differences in within-group variation (dispersion) were assessed with the function betadisper (vegan) and followed by ANOVA.

Differentially abundant taxa between MP treatments and unamended controls were detected using the ancombc2 function from the package ANCOMBC (version 2.10.0, Lin & Peddada, 2024). Analyses were conducted on the absolute and non-rarefied ASV count table, aggregated to genus level (or lowest resolved taxonomic rank). Linear models were constructed for each soil type and aggregate size fraction, with default settings, Dunnett's type pairwise comparison, and Benjamini-Hochberg p-value correction. Taxa were considered differentially abundant if they had an adjusted p-value < 0.05 and passed sensitivity analyses to control for false positive detections. Statistical differences in predicted gene families derived from PICRUSt2 were assessed using ALDEx2 (Fernandes et al., 2014) on centered log-ratio-transformed predicted counts, with Benjamini-Hochberg p-value correction, as implemented in the ggpicrust2

package (version 2.1.2, C. Yang & Zhang, 2025). Key gene families (KEGG Orthology) involved in nitrogen transformations were compared between each MP treatment and the no MP controls. Results were reported as statistically significant when the adjusted p-value was < 0.05 in both Welch's t-test and Wilcoxon rank test. Community plots were generated using the ggplot (Wickham, 2016) and ComplexHeatmap (Gu, 2016) packages.

Results

Among the MP treatments (PE, PET, and PBAT), low concentrations of 0.1% in soil (w/w) caused no significant effects ($p < 0.05$, Tukey's HSD) compared to the controls except for available nutrients. Therefore, the results reported here focus on 1% MPs amendments to reduce dimensionality of the large sample set. For aggregate and microbial analyses in planted treatments, a reduced set of treatments was used—control, PE, and PBAT (1%, 75–400 µm). PET treatments often showed minimal or no effects and therefore were excluded from the main text but are included in the statistical analyses and reported in the SI.

Microplastics effects on soil physical aggregation and stability

Soil aggregation data was highly variable for samples with plants (T2 maize). Significant differences ($p < 0.05$, Tukey's HSD) were not observed between plastic treatments (PE and PBAT) and the control in either soil type for aggregation formation or stability. Soil treatments without plant growth (T1 and T2) had no replicates, as aggregation fractionation was taken as a bulk sum of each sample; therefore, results were qualitatively compared.

Aggregation occurred at a higher degree in silty loam compared to sandy loam, likely as more building blocks, i.e. silt, clay, and organic matter, for aggregation were present. In silty loam after 4 weeks (T1), all plastic treatments (at 1%) decreased occluded microaggregates and increased free microaggregates, while macroaggregates remained unchanged (Figure 1). With plant growth (T2 maize), reduction of occluded aggregates was observed for controls and PE treatments, while occluded aggregates remained stable for PBAT and plant. This treatment showed a trend of increasing occluded microaggregates (<250 µm), with values of $40.3 \pm 12.3\%$ compared to $27.2 \pm 18.7\%$ in controls. Still, the large variability within sample groups prevented statistically significant findings ($p = 0.5$). Sandy loam remained unstructured over experimentation time, even with maize growth, with a large portion of free microaggregates (Figure 1).

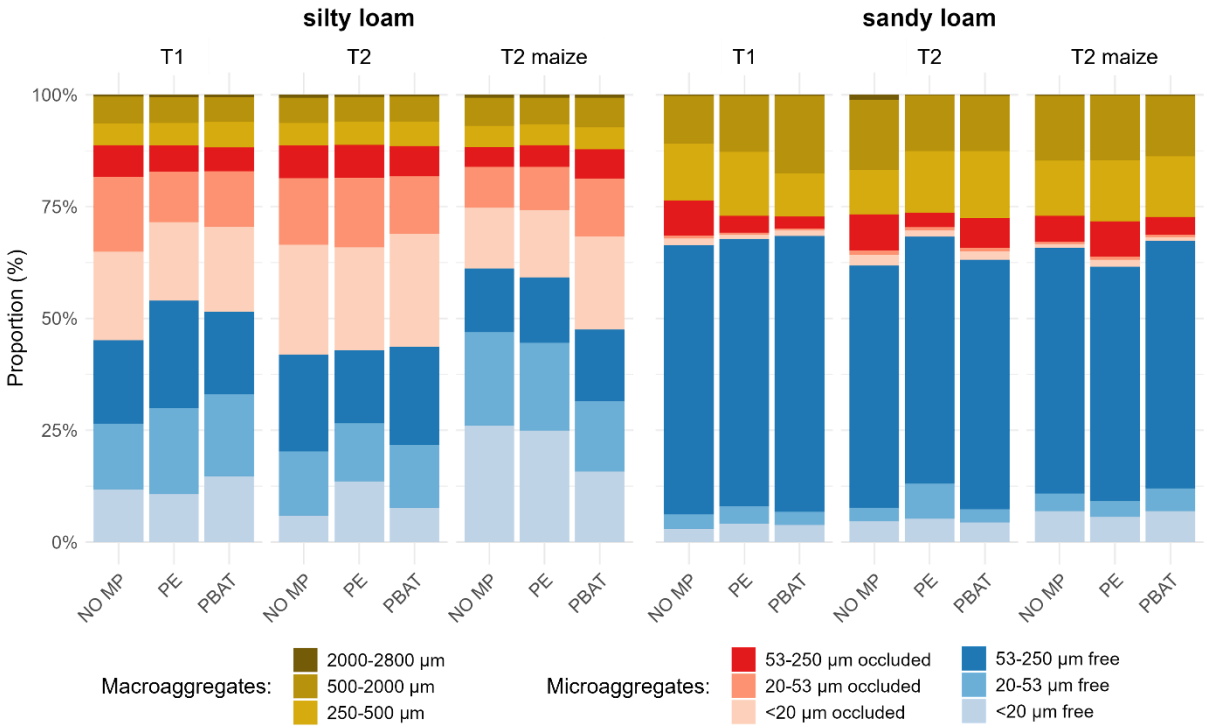

Figure 1. Fractionation of macroaggregates (2800–250 µm), free and occluded (stabilized inside macroaggregates) microaggregates (<250 µm) in silty loam (left) and sandy loam (right) of MP treatments (1% w/w, 75–400 µm) vs. controls (NO MP).

Specific aggregate size fractions (200–400, 75–200, and <75 µm) were compared at T1 and T2 (18 weeks) without maize growth (Figure S3, SI). Silty loam at T1 showed a reduction in occluded microaggregates among every MPs size fraction except for the 75–200 µm treatments which maintained occluded microaggregates comparable to controls. At T2, MP treatments were closer to controls with stable aggregation over time (see silty loam, Figure S6, SI). In sandy loam at T1, specific MP sizes had little impact on aggregation, although PET 75–200 and 75–400 µm increased occluded aggregation (see sandy loam, Figure S3, SI), as well as PE 200–400 µm at T2.

Water holding capacity (WHC) of both soils increased over time with soil structuring from wetting and drying cycles. In silty loam with plant growth, PBAT significantly increased (p = 0.004) WHC (Figure S4, SI). However, pure sand controls (200–400 µm) were also observed to increase WHC. As with aggregation, WHC of the sandy loam was poor compared to silty loam. In sandy loam, MP treatments had no effect on WHC ($p < 0.05$), however plant growth increased WHC unlike silty loam (Figure S4, SI).

Plastic effects on soil and plant chemical nutrient cycling

Due to the complex effects of treatments observed on the multiple measured variables (ANOVA and Tukey's HSD tests), a PCA was conducted on each soil type grouping MP

treatments (1%) by type to reduce dimensionality and explore relationships among treatments and variables (Figure 2). In silty loam, PE treatments were positively correlated with soil C and phosphate (P). MP treatments formed more distinct groupings than in sandy loam. PBAT associated negatively with plant biomass growth, pH, and bulk soil $^{15}N_{change}$ and positively with occluded microaggregates (MA). Changes in pH, WHC, potassium (K), and nitrate (NO_3) were less influential in distinguishing MP treatments in the PCA.

In sandy loam, PCA showed less marked distinctions in effects between plastic types, but still a distinction between MP treatments and controls was indicated (Figure 2). Soil C, biomass growth, pH, and bulk soil $^{15}N_{change}$ appeared positively correlated with PE. Maize root N values were positively correlated with PBAT in both soil types, but plant biomass was negatively correlated with PBAT.

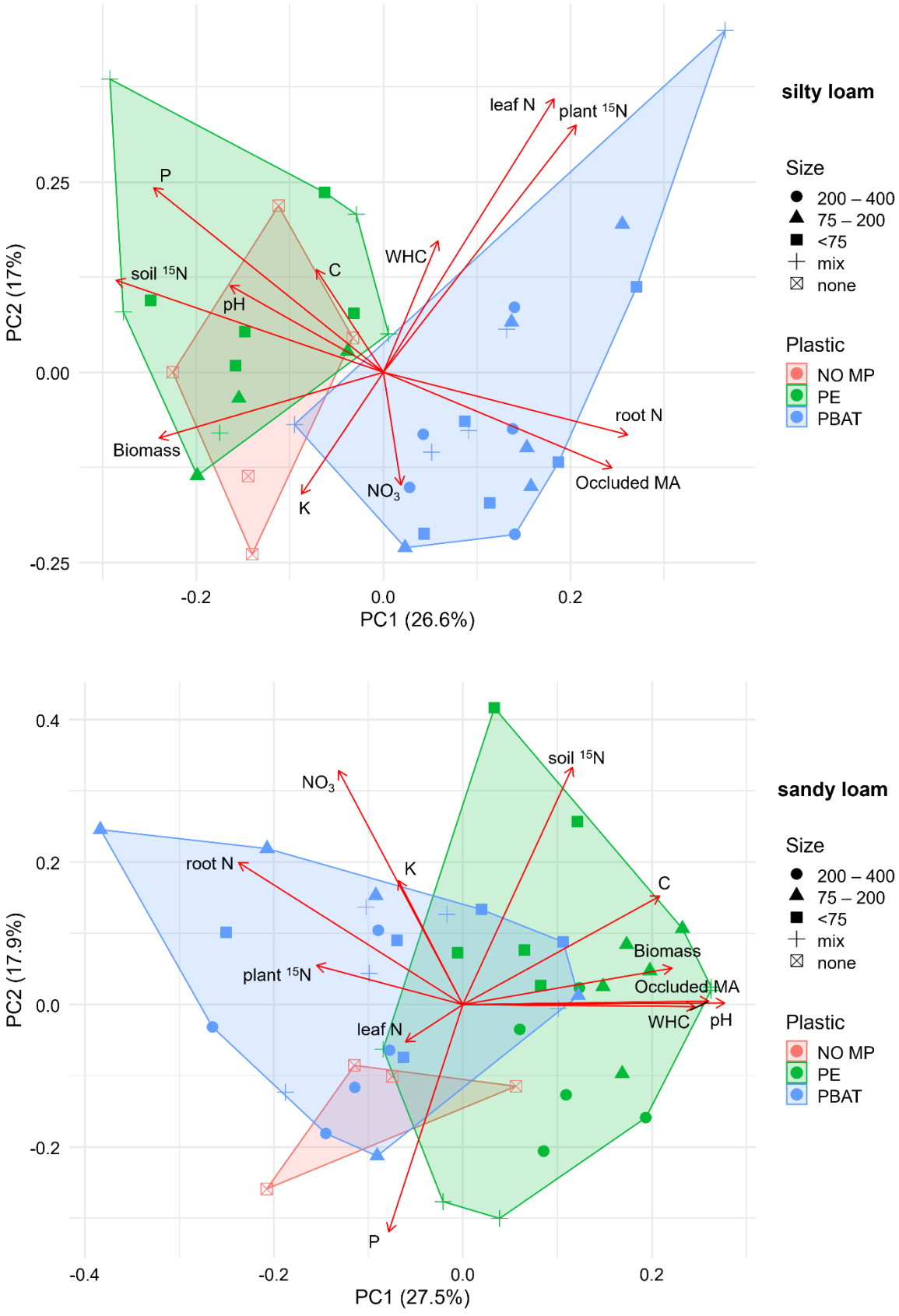

Figure 2. Principal component analysis of silty loam and sandy loam soils, showing relatedness of soil nutrient cycling dependent variables with different groups of plastic types (PE and PBAT, 1% w/w) and controls (NO MP).

pH

Soil pH only slightly changed over time without plants (T1 to T2); pH of controls decreased in silty loam (6.5 ± 0.1 to 6.1 ± 0.1) (mean ± s.d.) but increased in sandy loam (6.7 ± 0.1 to 7.2 ± 0.1) (Figure S5, SI). In silty loam, pH at T1 was slightly reduced (≈6.3) in CMP treatments, which was significant vs. controls ($p < 0.05$). At T2, significant distinctions were no longer observed, and plant growth caused an increase in pH (to ≈6.5) in all respective treatments. Size range treatments did not show any differences for silty loam. MP addition to sandy loam had no effect on soil pH vs. controls except that PBAT <75 µm (T2, without plant) reduced pH from 7.2 ± 0.1 to 6.8 ± 0.1 ($p = 0.001$; Figure S6, SI).

Soil Carbon

As expected, added MPs (1% w/w) increased total C content in both soils. Additionally, there was no further significant increase ($p < 0.05$) over time or with maize growth (Figure S7, SI). The PE amendment increased soil C from 1.61 ± 0.03% to 2.47 ± 0.11% in silty loam; and from 0.55 ± 0.01% to 1.42 ± 0.18% in sandy loam. This equaled an increase of ~0.86% in total C in both soils. However, as C content varied between soils, PE contributed to 61% of the total C in sandy loam and to 35% in silty loam.

Total Soil Nitrogen

Soil total N varied between sandy loam and silty loam, with mixed effects of maize growth and MPs addition (Tables S3-4, SI). In silty loam at T1, 1% PBAT reduced N content compared to controls ($p = 0.0002$; Figure S8, SI). Among the size range treatments, PET had reduced N content compared to control ($p < 0.05$, Figure S9, SI), whereas PBAT was significantly different only for the size mix. At T2 without plants, N content did not vary between treatments and controls. With maize growth, N content increased in controls, but PET and PBAT reduced soil N content at both 0.1% and 1% w/w ($p < 0.01$) and a trend to further reduction with smaller MPs size.

In sandy loam, opposite trends were observed to silty loam at T1; CMPs increased N content ($p < 0.005$) at both 0.1% and 1% w/w compared to controls and PBAT (Figure S8, SI). In sandy loam at T1, the smaller size ranges of PET (75–200 and <75 µm) had no significant effects, whereas the larger size range (200–400 µm) and size mix (75–400 µm) seemed to increase soil N content (Figure S9, SI). Trends switched between MP treatments at T2, where PBAT appeared to increase N content at both 0.1% and 1% concentrations ($p < 0.0001$), while CMPs had no impacts. With maize growth in sandy loam, N content only increased significantly in PE <75 µm ($p < 0.05$).

Plant-available nutrients N_{min}, P_{CAL}, K_{CAL}

Plant-available nutrients substantially decreased from T1 to T2 and were further depleted with plant growth. Available ammonium was not traceable in both soils after T1. Silty loam retained more initial ammonium than sandy loam, and PET and PBAT reduced ammonium in silty loam and oppositely increased ammonium in sandy loam ($p < 0.05$, Figure S10, SI); whereas size treatments led to wider variation.

In silty loam, nitrate content increased from T1 to T2 without plants. MP treatments at T1 all increased nitrate content compared to controls ($p < 0.05$), even at 0.1% concentrations, with PET and PBAT having stronger effects (Figure S11, SI). At T2 without plants, PE at 1% had the greatest increase in nitrate, whilst PBAT treatments had the lowest effect. In sandy loam at T1, CMPs increased nitrate concentrations compared to controls ($p < 0.05$). Nitrate was depleted faster than in silty loam at T2, regardless of the presence of MPs (Figure S11, SI). Size treatments showed some variation that followed no distinct pattern, although trends at T1 in sandy loam were opposite for MPs size range treatments, where we see increased nitrate in PBAT treatments (Figure S12, SI).

Plant-available phosphate (P_{CAL}) and potassium (K_{CAL}) decreased over time in both soils, with minor responses with CMPs at T1 (not shown) which were no longer observed at T2 and were further decreased with maize growth. In silty loam, PBAT treatments showed a reduction in P_{CAL} and decreasing PBAT size further reduced P_{CAL} ($p < 0.05$, Table S3, SI). In sandy loam, P_{CAL} showed no variation between treatments. In both soils with plant growth, K_{CAL} showed no variation between MPs treatments and controls.

^{15}N fertilizer tracing in soils and plants

Isotopically labeled fertilizer bags were added to the soil to trace $\delta^{15}N$ signals to bulk soil, plant roots and leaves. $\delta^{15}N$ signatures in bulk soil of control treatments for sandy loam increased from 10.2 ± 0.6‰ to 27.3 ± 1.9‰ from T1 to T2, while silty loam increased from 9.8 ± 0.3‰ to 14.0 ± 1.3‰. In the bulk soil and labeled bags of silty loam, absolute ^{15}N ($^{15}N_{change}$) in PBAT treatments (1% w/w) showed reduction of the label ($p < 0.01$, Figure 3). Decreasing size of PBAT showed further reduction in ^{15}N in bulk soil ($p < 0.001$, Figure S13A, SI).

In sandy loam, opposite to silty loam, MPs treatments increased bulk soil 15N, although only PE <75 um was significantly different to controls ($p < 0.01$, Figure S13B, SI). In the labeled bags, PBAT treatments retained a higher amount of ^{15}N ($p < 0.05$, Figure 3), with further label retention at the smallest size ($p < 0.01$, Figure S13B, SI).

Plant uptake of ^{15}N-fertilizer showed maize roots had increased ^{15}N with PBAT compared to controls in silty loam ($p < 0.05$, Figure 3), although maize leaves were unaffected. In sandy loam, both maize roots and leaves were increased in ^{15}N, although statistically non-significant

due to the large variation in controls (Figure 3). Size treatments in both soils did not elicit further effects on plant ^{15}N-fertilizer uptake.

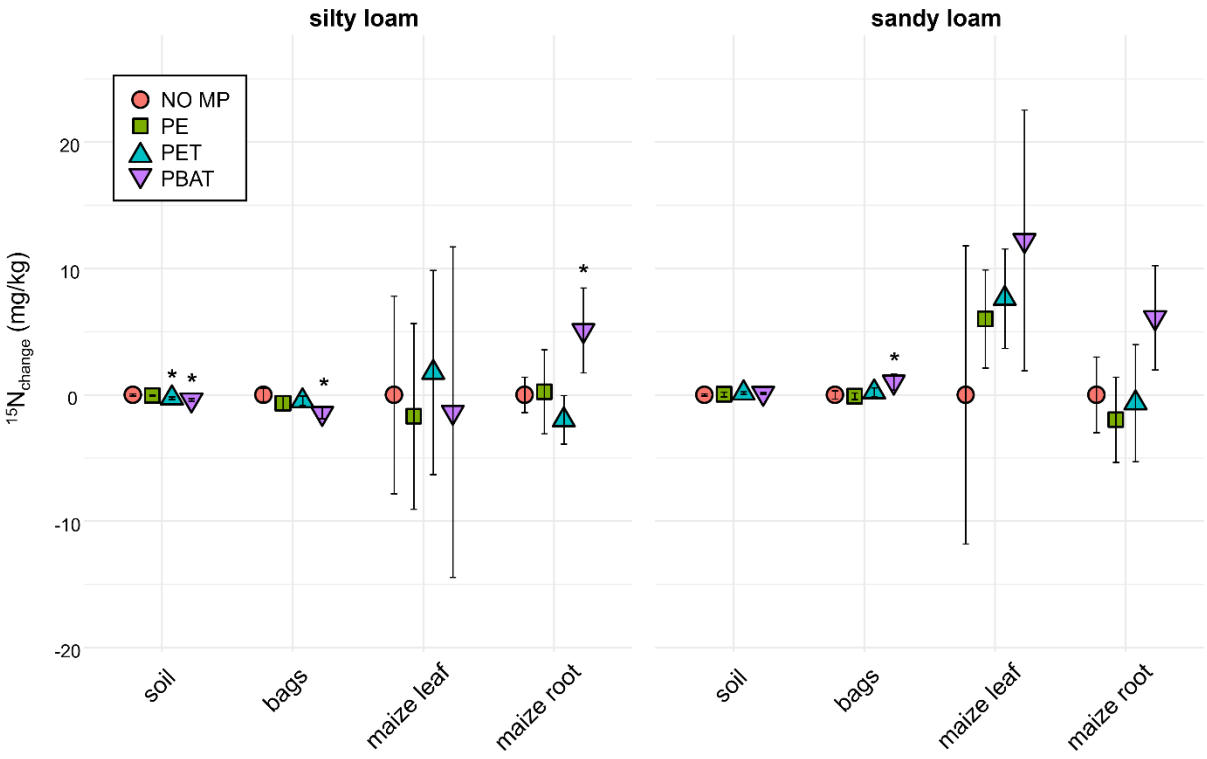

Figure 3. $^{15}N_{change}$ in bulk soil, isotopically labeled bags, maize leaf, and maize root from ^{15}N-fertilizer application, comparing controls without MPs vs. MPs treatments (1% w/w, 75–400 µm). Asterisks indicate significant difference to controls ($p < 0.05$, Tukey's HSD).

Plastic effects on soil prokaryotic communities

Changes in microbial community structure were first assessed in relation to soil type, aggregate size fractions, plant presence, and MP treatments by PERMANOVA of Bray-Curtis dissimilarity. A clear separation of microbiomes was observed between sandy and silty loam (p = 0.001, R^2 = 0.306, Table S5, SI). While differences in group dispersion were detected (homogeneity of group variance, p = 0.025, F = 5.282, Table S5, SI), the magnitude of separation between the groups (Figure S14C, SI) indicated compositional differences rather than shifts due to within-group variability (Figure S14D, SI).

Plant presence in silty loam significantly altered microbiome composition, regardless of aggregate size fraction or MPs treatment (p = 0.001, R^2 = 0.05, Figure S14A, SI). A similar but less pronounced shift was observed in sandy loam (p = 0.001, R^2 = 0.049, Figure S14B, SI), though this may have been driven by an increased within-group variance (homogeneity of group variance: p = 0.008, F = 7.947, Figure S14E, SI). Furthermore, communities in planted silty loam diverged by MP type, with those exposed to LDPE clustering closely to the controls, both

clearly separating from PBAT-treated communities (p = 0.001, R^2 = 0.092, Figure 4A). A comparable and statistically significant clustering by MP type was observed for planted sandy loams (p = 0.001, R^2 = 0.111, Figure 4B). Although group dispersion varied (Figure S14F, SI), the directional shift of PBAT communities from PE and controls suggested a consistent compositional change induced by this polymer. Moreover, aggregate size classes influenced microbiomes in planted sandy loams (p = 0.008, R^2 = 0.087), with a gradual shift observed across size classes and a statistically significant difference between microaggregates and macroaggregates (p = 0.003, R^2 = 0.079, Figure 4B, Table S5, SI). In contrast, aggregate size did not significantly affect planted silty loam communities. Overall, planted silty loam exhibited higher taxonomic richness (Kruskal-Wallis test: $p < 0.001$, H = 32.7) and evenness (Kruskal-Wallis test: $p < 0.001$, H = 17.2) than sandy loam communities, independent of aggregate size class and MP treatment (Figure S15A+B, SI). Additionally, a trend of higher richness in macroaggregates was observed for both soils (Figure S15C, SI). None of the MP treatments differed statistically from controls (Figure S15D+E, SI).

Genera with significant abundance shifts included members of the *Actinobacteriota*, *Bacteroidota*, *Cyanobacteria*, *Patescibacteria*, *Alpha-* and *Betaproteobacteria* (Figure 4B). Most notably, differential abundance shifts were almost exclusively observed in PBAT-treated sandy loams. Of the 15 genera identified, 13 showed an enrichment relative to the control without MP addition, with the highest enrichment observed for *Xylophilus* spp. The genera *Pseudarthrobacter*, *Noviherbaspirillum* and members of the *Micrococcaceae* (unclassified) were consistently enriched across all aggregate size classes. The remaining genera were enriched only in one specific aggregate size fraction: *Mucilaginibacter*, *Burkholderia-Caballeronia-Paraburkholderia*, *Oxalicibacterium Arcticibacter*, and *Caulobacter spp., as well as* unclassified *Sericytochromatia* and the LWQ8 taxon. In addition, *Paenarthrobacter* spp. and unclassified *Comamonadaceae* were enriched in two specific aggregate size fractions. In contrast, the most substantial depletion was observed for *Azospirillum spp.*, while also unclassified *Solirubrobacteraceae* showed a reduction in abundance compared to the respective control. For the silty loam, only the unclassified LWQ8 lineage (*Saccharimonadales*) was detected to increase with PBAT.

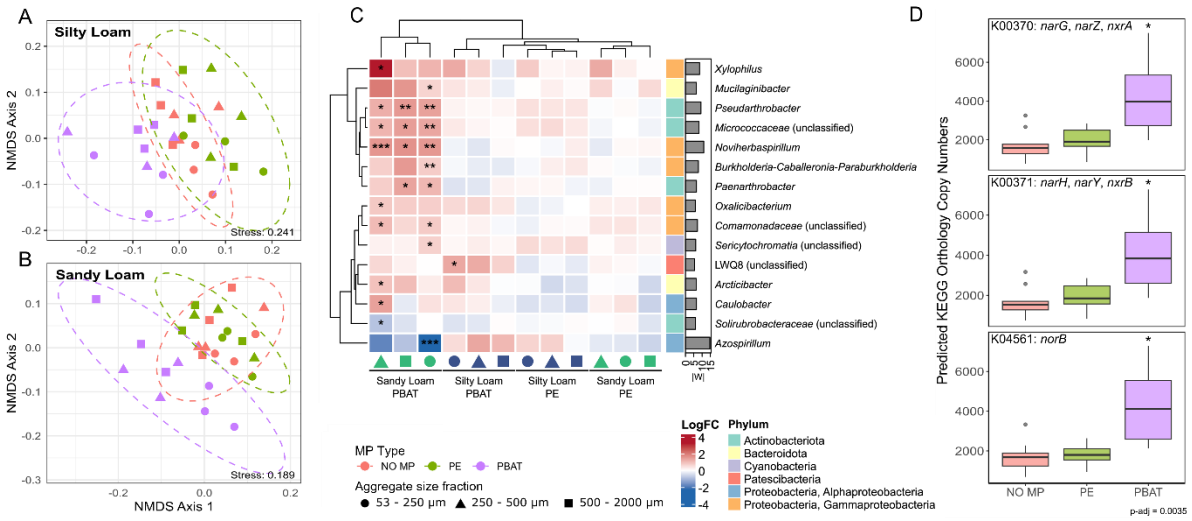

Figure 4. Response of silty and sandy loam prokaryotic communities to MP treatment, based on 16S rRNA gene metabarcoding. Impacts on community structure, differential taxonomic abundance, and predicted functional potential. A+B) NMDS ordination of Bray-Curtis dissimilarities and ellipses with 95% confidence level. C) Statistically significant differential abundant taxa aggregated at genus level in MP treatments (relative to the no MP control) were identified by ANCOM. The test statistics (W) are expressed as absolute value. D) Statistically significant predicted gene abundances of KEGG orthologs associated with nitrogen cycling in sandy loams grouped by MP treatment. Statistical analysis was performed using ALDEx2 on centered log-ratio-transformed predicted counts. Reported p-values (Benjamini-Hochberg corrected) were derived from the Wilcoxon rank test.

Lastly, we performed a metagenomic extrapolation on our 16S rRNA amplicon sequences using PICRUSt2, to gain initial predictive perspective of functional capabilities of the detected soil microbiomes. Given the patterns observed in our physicochemical soil data, we focused the analysis on gene families involved in nitrogen transformations. Therefore, functional profiles of our samples were filtered to genes associated with nitrogen fixation (*nifH*), nitrification (*amoA*, *hao*, *nxrB*), denitrification (*napA*, *narG*, *nirS*/*nirK*, *norB*, *nosZ*), dissimilatory nitrate reduction to ammonium (*nrfA*), and assimilatory nitrite reduction (*nasA*, *nirA*), and anaerobic ammonium oxidation (*hdh*). Indeed, we found that three KEGG orthologs (K04561, K00371, K00370) showed significantly predicted gene abundance in PBAT-treated sandy loam communities. These orthologs are associated with denitrification (K04561, K00371, K00370), dissimilatory nitrate reduction (K00371, K00370), and nitrification (K00371, K00370).

Plant biomass growth unaffected by microplastics

There were no significant effects ($p > 0.05$) of MP treatments on plant growth for any of the measured parameters (plant biomass, height, leaf count, leaf area, or root to shoot ratio). Still, we observed a trend of plastic amendments to slightly increase plant biomass in sandy loam, and decreasing biomass in silty loam (Figure 5). However, maize root N content was shown to increase in silty loam for 1% PBAT treatments ($p = 0.003$, Table S3, SI).

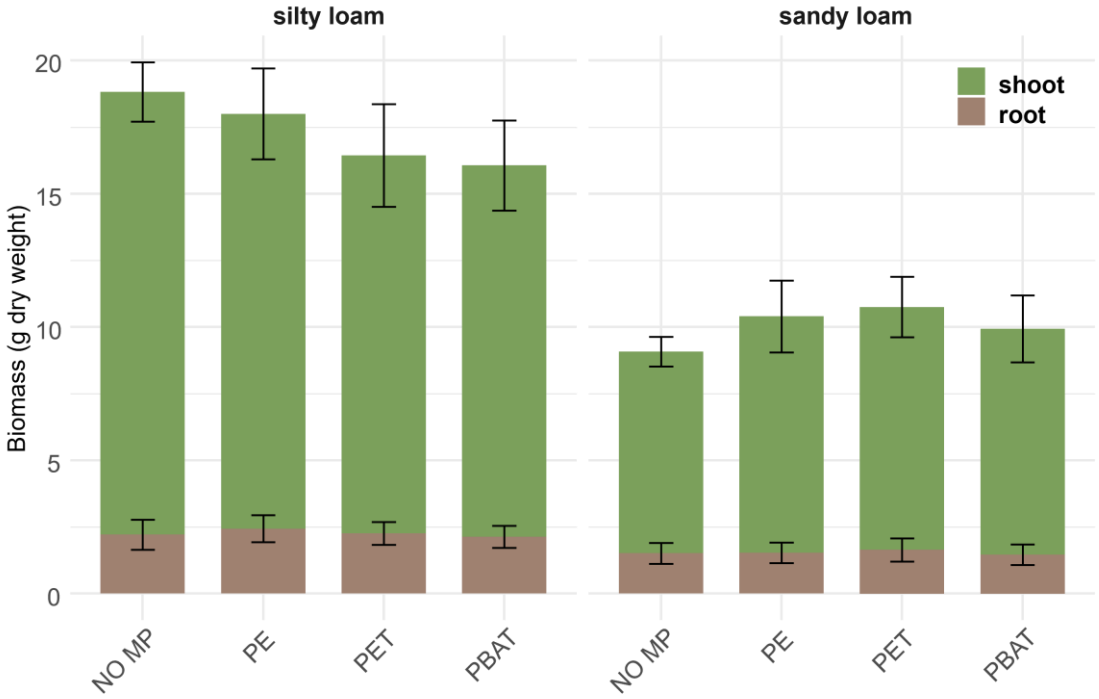

Figure 5. Plant biomass dry weight with no significant differences ($p > 0.5$, Tukey's HSD), although a trend that shoot biomass decreased in silty loam and increased in sandy loam with MPs (1% w/w).

Discussion

PBAT degradation tends to increase aggregation stability and WHC in silty loam

Soil aggregation in loamy soils might be affected by MPs as disruption of microaggregate stability by MPs has been previously shown, as well as decreased water-stability from the presence of CMPs (Lehmann et al., 2021; Souza Machado et al., 2018). BMPs were also shown to increase extracellular microbial enzyme activity (Jiaxin Wang, et al., 2024; Zumstein et al., 2018), likely increasing byproducts through microbial degradation, which could act as potential gluing agents for aggregates. Therefore, MPs may affect soil aggregation due to structural change of soil or due to their degradation effects dependent on multiple factors of polymer type, degradation state, soil type, and soil biota (Han et al., 2024).

In our experiment, soil aggregation and stability were not significantly affected by the presence of MPs, although clear trends were observed, especially with PBAT degradation, that

highlight soil type dependent responses (Figure 1 and Figure S3, SI). Disruption of microaggregates by CMPs occurred at early experimentation (4 weeks), but effects were mediated after experimentation time (18 weeks). The hypothesis that CMPs reduce soil aggregate stability with plant growth was not confirmed, as CMPs at environmentally realistic concentrations (<1%) exhibit some destabilizing trends, but often are statistically non-significant (Y. Yu et al., 2023). Size-fraction experiments further suggested that 75–200 µm MPs integrate with forming macroaggregates more than other size classes, which was contrary to our hypothesis that smaller MPs sizes would further disrupt aggregate formation and stability. At 18 weeks, PBAT contributed to improved soil aggregation in silty loam by stimulating microbial activity and likely associated mechanisms, e.g. gluing and physical pressure. PBAT promoted the formation of occluded microaggregates and maintained microaggregate stability, likely through its degradation and the resulting microbial residues.

Mixed effects were reported for MPs impact on WHC, with both positive and negative trends depending on soil and polymer type (Wan et al., 2019; Wang et al., 2023; Xie et al., 2023). Studies often report declines in water retention, and higher soil water repellency, tied to MPs hydrophobicity (Cramer et al., 2023; Shafea et al., 2023). In our experiment, we observed that CMPs had minimal impact on WHC in sandy loam, whereas the combination of PBAT and plant growth led to a significant increase in WHC (Figure S4, SI); related to aggregation formation and stability, PBAT was shown to increase microaggregate stability, and therefore the degradation of PBAT likely increased microaggregate formation and WHC in tandem. The observed increase in WHC from PBAT degradation may reflect combined effects of promoting aggregation and polymer hydrophilicity under plant-mediated soil structuring. However, the control treatments with pure sand also increased WHC in the same manner, which demonstrates changes in WHC are not strictly related to polymer type but also depend on soil structure and polymer size (Wang et al., 2023). Effects of MPs on soil are often very context-dependent, and plants, especially more resistant species to environmental stressors such as maize, can mediate the negative effects of MPs associated to soil physical properties, e.g. WHC and soil structure (Krehl et al., 2022). However, with further experimentation time, or multiple plant growth cycles, these aggregation dynamics could change.

Microplastics exhibit variable effects on chemical nutrient cycling distinct to soil and polymer type

Plant-available nutrient cycling in soils is influenced by underlying soil properties, e.g. physical structure, pH, soil fertility, and the effects of MPs have been found to vary based on polymer type and size with sometimes opposing influences which appear dependent on soil

type and characteristics (Rauscher et al., 2023; Shi et al., 2024; Zhang et al., 2023). To generalize soil responses to MPs in our study, PCA (Figure 2) suggested that MP effects are strongly shaped by soil type, with observed responses often contrasting between silty loam and sandy loam. In general, CMPs showed minimal deviation from controls, whereas PBAT was distinguished in silty loam, suggesting more pronounced interactions in this soil type. MPs effects in sandy loam were generally less distinct, possibly due to its lower structural complexity and organic matter content.

The variability in pH responses across treatments highlights how soil-specific factors influence soil responses to MPs. While polymer type can affect pH depending on conditions (Gharahi & Zamani-Ahmadmahmoodi, 2022; Qi et al., 2020; Tang et al., 2024), our results indicate that soil type and microbial activity play a major role. The decreased pH in sandy loam with the smallest PBAT size treatment (<75 µm) suggests faster microbial degradation and organic acid release due to greater surface area (Rauscher et al., 2023). In contrast, plant growth appeared to mask pH shifts, consistent with studies showing plants can moderate MP effects in soil systems (Krehl et al., 2022). Opposite trends in silty and sandy soils further show that soil type is a key factor in how soils respond to MPs.

Soil total C content increased by MPs input, proportional to the C content of the plastic type. Since plastics are primarily carbon-based and considered part of the soil C pool when incorporated (Rillig, 2018), effects of MPs on total C are more pronounced in low-C soils such as our sandy loam (Figure S7, SI). PBAT degradation can co-occur with organic matter decomposition, as microbes use PBAT-C for energy; however, this process is dependent on soil N availability (Guliyev et al., 2023; Zumstein et al., 2018). This may trigger priming effects, disrupting C sequestration and C:N dynamics at short time-scales (K. Jia et al., 2024; Meng et al., 2022).

Major plant-available nutrients—ammonium, nitrate, phosphate, and potassium—could be affected due to a lack of physical protection within soil aggregates and altered soil sorption properties. Previous studies have shown that CMPs can disrupt nutrient retention (Ding et al., 2023; Meng et al., 2022) and that BMPs, including PBAT, may further affect nitrogen cycling via priming effects that accelerate microbial activity and nutrient turnover (Liu et al., 2024; Tanunchai et al., 2022). Addition of fertilizer in our experiment was minimal and came from agricultural lands, and soil nutrient conditions were not optimal for large biomass production without further fertilization. Although the sandy loam retained higher levels of available nutrients towards the end of the experiment than silty loam, much of this nitrogen was immobilized and not accessible to plants, as poor soil structure limited uptake.

In both soils, CMPs exhibited effects primarily during early experimentation (4 weeks), often retaining more available nutrients. While contrary to our hypothesis that CMPs would reduce the amount of available nutrients, long-term agricultural practices could show trends of depletion over many cycles (Ding et al., 2023). This indicates that without plants, CMPs can exhibit more complex interactions with soil nutrients indicating a role of plant–microbe interactions in shaping nutrient availability. However, plant growth mitigates much of the nutrient changes that CMPs can exhibit.

BMPs were confirmed to exhibit more rapid turnover of nutrients through a priming effect and immobilization of the nutrient pool, although impacts were different between sandy loam and silty loam. In sandy loam, PBAT appeared to alter sorption behavior, possibly by introducing new charged surfaces, enhancing microbial-driven immobilization of nitrogen and actively promoted priming effects that redistributed fertilizer-derived nitrogen (Jie Wang et al., 2024; Zumstein et al., 2018). In silty loam, PBAT still accelerated nutrient cycling, but its impact was masked by the better aggregation and moisture retention of the silty texture, helping to maintain nitrogen availability. Therefore, PBAT led to higher production of available nitrogen and increased fertilizer spread in sandy loam compared to silty loam, likely due to increased pore space and permeability of sandy loams; and even small amounts of PBAT (0.1%) had impacts on nitrogen cycling. These findings emphasize that MP-induced effects to nutrient cycling and sorption dynamics are strongly soil-dependent, with sandy loam being more vulnerable to PBAT induced nutrient immobilization and disruption.

PBAT immobilizes ammonium-nitrate fertilizer and affects maize plant uptake of nitrogen in differing soil types

MPs were expected to reduce plant biomass production by impacting sorption behavior (Rillig et al., 2019; Steinmetz et al., 2016), and many studies have confirmed now that N-cycling is affected through biodegradation of BMPs by microbes, which require N for biomass production in conjunction with the readily available C source from BMPs (Huang et al., 2023; Inubushi et al., 2022; Xue et al., 2023). In silty loam, an increase in plant root uptake of fertilizer in the presence of PBAT (Figure 3) combined with increased N allocation to maize roots likely is a response to increased immobilized N by the degradation of PBAT and resulted in decreased shoot production. Contrarily, sandy loam exhibited a large increase in ^{15}N-fertilizer uptake into maize leaves in the presence of PBAT, although with no benefits to biomass production.

Therefore, we conclude that early biodegradation of PBAT led to N-immobilization in both systems before plant growth, although plant responses varied with soil type: in silty loam maize plants had reduced availability of N-fertilizer with PBAT present in soils, and sandy loam maize

plants had more N-fertilizer distributed in the system from PBAT presence but could not utilize it for increased biomass production. While this phenomenon in sandy loam could have multiple explanations, PBAT byproducts from microbial degradation could exhibit toxic behavior to plants (Martínez et al., 2024), which also explains in silty loam the fertilizer-N primed by microbes was avoided by plants where other labile N sources were still available. However, in sandy loam the N-limitations required the maize plant mitigate effects, and re-mobilize the immobilized fertilizer pool, indicative of a delayed priming-type immobilization by PBAT.

Microplastic effects on soil microbiological community

Soil type emerged as the main driver of the community structure, with distinct compositional differences in the planted soils by the end of the experimentation time (Table S5, SI). Aggregate size fractions also contributed to the community structure, particularly in the sand loam. This additive effect was driven by dissimilarities between micro- (53-250 µm) and macro- (500-2000 µm) aggregates (Figure 4B) and is likely attributed to the textural characteristics of the soils. The coarser texture of sandy loams might have promoted habitat differentiation across aggregate sizes. In contrast, silty loam with finer and more cohesive texture might have facilitated a more uniform community establishment with less pronounced compositional differences across aggregate size fractions (Xia et al., 2020).

Most notably, PBAT-exposed communities differed statistically significantly from unamended and PE-treated soils, regardless of soil type (Figure 4A+B), highlighting a selective microbial response to PBAT. In contrast, PE had a minimal impact on community structure, consistent with observations from other incubation studies (Hao et al., 2024; Li et al., 2022; Song et al., 2024). This greater shift is assumed to result from the higher release of organic carbon from biodegradable plastics, which could stimulate soil microbes by serving as alternative carbon sources (Qiu et al., 2024; Zumstein et al., 2018).

Although PBAT-induced community shifts occurred in both soil types, differential abundant taxa were almost exclusively detected in sandy loam communities and nearly exclusively enriched compared to the respective unamended controls (Figure 4C). This compositional restructuring of the community could have been a response to the newly introduced carbon source. Soil type has been shown to influence PBAT degradability and the aging process of different plastic types (Han et al., 2021; Ren et al., 2024). Additionally, microbial carbon transformations of organic matter, such as plant residuals, vary across soils with different fertilities (Liu et al., 2021). Since sandy loam is rather nutrient-deficient relative to silty loam, adding biodegradable PBAT may stimulate taxa involved in the degradation of intrinsic organic matter. This could allow microbes to meet their stoichiometric nutrient demands to access the

added carbon source, which would explain the apparent enrichment of particular taxa in the sandy loam but not in the silty loam. In this context, microbes in the sandy loam may prioritize energy conservation for extracellular enzyme production to decompose organic matter and eventually mobilize nutrients, resulting in soil carbon destabilization and CO_2 emission rather than biomass production (Liu et al., 2021; Sinsabaugh et al., 2013; Spohn et al., 2016). Indeed, in our previous lab-scale study, we observed increased soil CO_2 emission following PBAT amendment in sandy loam incubation compared to loam (Rauscher et al., 2023). Further, resource allocation toward exoenzyme production to mine nutrients would also induce soil organic carbon priming (Bernard et al., 2022). Thus, sandy loam with lower nutrient availability than silty loam could eventually destabilize soil organic carbon.

Interestingly, the genera *Pseudarthrobacter* (*Micrococcaceae*), unclassified genera affiliated to *Micrococcaceae*, and *Noviherbaspirillum* (*Oxalobacteraceae*) were consistently enriched across all sandy loam aggregate fractions. In previous studies, these taxa have also been enriched in biodegradable MP soils (Meng et al., 2023; Jie Wang et al., 2024; Zhang et al., 2024). *Micrococcaceae* were found in other polluted soils and seem to be involved in the degradation of polycyclic aromatic hydrocarbon and phthalic acid esters and potentially also in plant-growth promoting traits such as nitrogen fixation and phosphorous solubilization (Bushra et al., 2023; De La Cruz-Barrón et al., 2017; Li et al., 2024; Ortiz-Cornejo et al., 2017). Similarly, species within the genus *Noviherbaspirillum* include denitrifiers and taxa found in oil-polluted sites, supporting their potential involvement in pollutant transformations and nitrogen cycling (Ishii et al., 2017; Lin et al., 2013).

The remaining differential abundant taxa were found in one or two aggregate size fractions, suggesting specific niche preferences, likely shaped by microhabitat conditions and potentially carbon availability (Davinic et al., 2012; Fox et al., 2018). The highest number of differentially abundant taxa was found in the microaggregate and small macroaggregate fraction, possibly due to their similar size range to the applied MP particles, leading to increased exposure to the microbial communities. Moreover, microaggregates often harbor more recalcitrant organic carbon, whereas macroaggregates contain more labile carbon (Totsche et al., 2018). Consequently, microbes may experience greater carbon limitation, potentially enhancing their responsiveness to PBAT.

Members of the family *Comamonadaceae* have been associated with biodegradable plastics (Bandopadhyay et al., 2020; Meng et al., 2023). They are metabolically versatile and may participate in the degradation of complex carbon sources such as lignin and hydrocarbons (Wilhelm et al., 2019; Yi et al., 2022). Within this family, *Xylophilus spp.* was identified,

showing the highest log-fold in the PBAT-exposed communities. Described species of this genus are chemoorganotrophs that have been reported as pathogens of grapevines (Desai, 2025). Moreover, *Comamonadaceae* mediate various nitrogen transformations. While some species were described to fix nitrogen, they seem involved in denitrification and nitrate reduction (Kampfer et al., 2008; Song et al., 2025; Yi et al., 2022).

Similarly, a potential coupling of carbon and nitrogen transformations may also be a feature of *Burkholderia-Caballeronia-Paraburkholderia*. Members have broad metabolic capacities to degrade complex organic compounds, including phenols and hydrocarbons (Pérez-Pantoja et al., 2012; Wilhelm et al., 2020), and they are involved in nitrogen transformation processes such as nitrogen fixation and denitrification (Palleroni, 2015). We performed functional gene predictions, which provided estimates of the abundance of genes involved in key nitrogen transformation processes (Figure 4D). These estimates suggest a possible increase in the abundance of genes encoding enzymes reducing nitrate to nitrite (K00370, K00371), a reaction in several nitrogen transformations, including dissimilatory nitrate reduction to ammonium, nitrification, and denitrification. Furthermore, a concurrent increased predicted abundance of nitric oxide reductase genes facilitates the reduction of NO to N_2O (K04561), which gives evidence of a potential stimulation of denitrifies in PBAT treatments.

In contrast, unclassified genera within the *Solirubrobacteraceae* and the genus *Azospirillum spp.* were depleted in PBAT-amended soils. *Solirubrobacteraceae* has been associated with improved plant growth, suggesting their potential role as plant-beneficial microbes (Chen et al., 2022; Özbolat et al., 2023). *Azospirillum spp.* are known for their plant growth-promoting traits, including nitrogen fixation (Steenhoudt & Vanderleyden, 2000). The observed decline of *Azospirillum spp.* abundance may have been a direct or indirect consequence of PBAT addition and potentially further promoting the mobilization of native nitrogen pools.

Microplastic effects on maize biomass production

The impacts of conventional MPs (CMPs) and biodegradable MPs (BMPs) on soil physical, chemical, and biological properties that relate to plant production are complex and context-dependent, likely varying significantly with soil type and environmental conditions (Bartnick & Lehndorff, 2025). In our experiment, although MPs had an influence on nutrient cycling, and even increased nitrate and available nutrients especially with PBAT, this did not correspond to a significant change in plant production, however a trend that MPs decreased plant production in silty loam and increased production in sandy loam (Figure 4). This could be related to a further complex interaction of soil structure being modified by plastics, and a combined change of physicochemical soil properties elicit difference effects in different soil types based on their

mineral and organic matter content (Chang et al., 2024; Chen et al., 2024; Ding et al., 2023). This makes soil type the largest confounder for MPs behavior in soil, and studies should focus on this when compiling review data, as MPs likely have substantially different responses based on soil type.

Conclusion

This study investigated the effects of CMPs (PE and PET) and BMPs (PBAT) of varying concentration, size ranges, and in contrasting soil types (sandy and silty loam) on soil physical, chemical, and biological properties in a controlled greenhouse experiment with and without maize plants. MPs increased soil total C dependent on polymer stoichiometry, PE contributing more than PET or PBAT, which impacts the perceived organic carbon pool to a higher degree in sandy loam than silty loam. PBAT showed signs of early biodegradation at 4 weeks of experimentation, demonstrated by depleted $\delta^{13}C$ signals, associated priming of ^{15}N-fertilizer, and microbial activity. Physically, PBAT degradation led to increased microaggregate stability and WHC in silty loam, likely through the formation of microbial residues acting as gluing agents, whereas sandy loam remained largely unstructured. Surprisingly, decreasing sizes of MPs had minimal effects on aggregation formation and stability. Chemically, MPs altered soil nutrient cycling depending on polymer type, concentration, and soil type. PBAT was found to immobilize our added ^{15}N-fertilizer and reduce plant uptake in silty loam, while sandy loam plants accessed more ^{15}N in a larger soil ^{15}N pool which was immobilized early by microbes, but this did not translate this into biomass gains, possibly due to stress from PBAT byproducts. These results highlight the complex, soil type dependent interactions between MPs and soil functions, especially as BMPs are proposed as a sustainable alternative to CMPs used in agriculture. Future researchers should prioritize distinguishing polymer-specific effects in identified soil types and nutrient variability and extend studies across multiple plant cycles to better understand long-term consequences of MPs on soil health and plant productivity.

Acknowledgements

This study was performed within the Collaborative Research Center 1357 “Microplastics – Understanding the mechanisms and processes of biological effects, transport and formation: From model to complex systems as a basis for new solutions.” This study was funded by the Deutsche Forschungsgemeinschaft (DFG, German Research Foundation) – SFB 1357 – 391977956. We thank central project Z01, P. Strohriegl, M. Fried, and D. Wagner for polymer preparation and analytics. We also thank A. Frank and G. Gebauer of the BayCEER Laboratory

of Isotope Biogeochemistry (BayCenSI) for isotopic measurements, and M. Obst of the Analytical Chemistry Lab (CAN) of the University of Bayreuth for nutrient analysis. Additionally, a large thanks to K. Söllner, U. Hell, N. Braun, A. L. Dürringer, S. Russ, and M. Detiger for operating the greenhouse and taking soil lab measurements and extensive aggregation separation. We thank Anita Gößner (Ecological Microbiology) for aggregate sieving, microbial community analysis and nucleic acid extractions. Alfons Weig and Michaela Holzinger from the KeyLab Genomics & Bioinformatics (subproject Z02 of the CRC1357) of the University of Bayreuth for 16S rRNA gene amplicon processing, library preparation and Illumina sequencing. Further, we thank Alfons Weig for providing the modified phasing primer sequences and guidance on their implementation. Metabarcoding analysis was supported by the de.NBI Cloud within the German Network for Bioinformatics Infrastructure (de.NBI) and ELIXIR-DE (Forschungszentrum Jülich and W-de.NBI-001, W-de.NBI-004, W-de.NBI-008, W-de.NBI-010, W-de.NBI-013, W-de.NBI-014, W-de.NBI-016, W-de.NBI-022).

Supporting Information

The SI contains an extended experimental design, soil profile information, plastic polymer information, and additional figures of size range treatments, microbial data, and supporting analyses.

*Corresponding author: E-Mail: ryan.bartnick@uni-bayreuth.de

References

Amelung, W., Meyer, N., Rodionov, A., Knief, C., Aehnelt, M., Bauke, S. L., Biesgen, D., Dultz, S., Guggenberger, G., Jaber, M., Klumpp, E., Kögel-Knabner, I., Nischwitz, V., Schweizer, S. A., Wu, B., Totsche, K. U., & Lehndorff, E. (2023). Process sequence of soil aggregate formation disentangled through multi-isotope labelling. *Geoderma*, *429*, 116226. https://doi.org/10.1016/j.geoderma.2022.116226

Amelung, W., Tang, N., Siebers, N., Aehnelt, M., Eusterhues, K., Felde, V. J. M. N. L., Guggenberger, G., Kaiser, K., Kögel-Knabner, I., Klumpp, E., Knief, C., Kruse, J., Lehndorff, E., Mikutta, R., Peth, S., Ray, N., Prechtel, A., Ritschel, T., Schweizer, S. A., … Totsche, K. U. (2024). Architecture of soil microaggregates: Advanced methodologies to explore properties and functions. *Journal of Plant Nutrition and Soil Science*, *187*(1), 17–50. https://doi.org/10.1002/jpln.202300149

Apprill, A., McNally, S., Parsons, R., & Weber, L. (2015). Minor revision to V4 region SSU rRNA 806R gene primer greatly increases detection of SAR11 bacterioplankton. *Aquatic Microbial Ecology*, *75*(2), 129–137. https://doi.org/10.3354/ame01753

Bandopadhyay, S., Liquet Y González, J. E., Henderson, K. B., Anunciado, M. B., Hayes, D. G., & DeBruyn, J. M. (2020). Soil Microbial Communities Associated With Biodegradable Plastic Mulch Films. *Frontiers in Microbiology*, *11*, 587074. https://doi.org/10.3389/fmicb.2020.587074

Barbera, P., Kozlov, A. M., Czech, L., Morel, B., Darriba, D., Flouri, T., & Stamatakis, A. (2019). EPA-ng: Massively Parallel Evolutionary Placement of Genetic Sequences. *Systematic Biology*, *68*(2), 365–369. https://doi.org/10.1093/sysbio/syy054

Bartnick, R., & Lehndorff, E. (2025). From Sea to Land: Setting a Size Definition of Plastics for Soil Ecosystem Studies. *Journal of Plant Nutrition and Soil Science*, *188*(3), 373–375. https://doi.org/10.1002/jpln.12006

Bartnick, R., Rodionov, A., Oster, S. D. J., Löder, M. G. J., & Lehndorff, E. (2024). Plastic Quantification and Polyethylene Overestimation in Agricultural Soil Using Large-Volume Pyrolysis and TD-GC-MS/MS. *Environmental Science & Technology*, *58*(29), 13047–13055. https://doi.org/10.1021/acs.est.3c10101

Bernard, L., Basile-Doelsch, I., Derrien, D., Fanin, N., Fontaine, S., Guenet, B., Karimi, B., Marsden, C., & Maron, P. (2022). Advancing the mechanistic understanding of the priming effect on soil organic matter mineralisation. *Functional Ecology*, *36*(6), 1355–1377. https://doi.org/10.1111/1365-2435.14038

Bushra, R., Uzair, B., Ali, A., Manzoor, S., Abbas, S., & Ahmed, I. (2023). Draft genome sequence of a halotolerant plant growth-promoting bacterium Pseudarthrobacter oxydans NCCP-2145 isolated from rhizospheric soil of mangrove plant Avicennia marina. *Electronic Journal of Biotechnology*, *66*, 52–59. https://doi.org/10.1016/j.ejbt.2023.08.003

Callahan, B. J., McMurdie, P. J., Rosen, M. J., Han, A. W., Johnson, A. J. A., & Holmes, S. P. (2016). DADA2: High-resolution sample inference from Illumina amplicon data. *Nature Methods*, *13*(7), 581–583. https://doi.org/10.1038/nmeth.3869

Chang, N., Chen, L., Wang, N., Cui, Q., Qiu, T., Zhao, S., He, H., Zeng, Y., Dai, W., Duan, C., & Fang, L. (2024). Unveiling the impacts of microplastic pollution on soil health: A comprehensive review. *The Science of the Total Environment*, *951*, 175643. https://doi.org/10.1016/j.scitotenv.2024.175643

Chen, X., Wang, J., You, Y., Wang, R., Chu, S., Chi, Y., Hayat, K., Hui, N., Liu, X., Zhang, D., & Zhou, P. (2022). When nanoparticle and microbes meet: The effect of multi-walled carbon nanotubes on microbial community and nutrient cycling in hyperaccumulator system. *Journal of Hazardous Materials*, *423*, 126947. https://doi.org/10.1016/j.jhazmat.2021.126947

Chen, Z., Carter, L. J., Banwart, S. A., Pramanik, D. D., & Kay, P. (2024). Multifaceted effects of microplastics on soil-plant systems: Exploring the role of particle type and plant species. *The Science of the Total Environment*, *954*, 176641. https://doi.org/10.1016/j.scitotenv.2024.176641

Corradini, F., Meza, P., Eguiluz, R., Casado, F., Huerta-Lwanga, E., & Geissen, V. (2019). Evidence of microplastic accumulation in agricultural soils from sewage sludge disposal. *The Science of the Total Environment*, *671*, 411–420. https://doi.org/10.1016/j.scitotenv.2019.03.368

Cramer, A., Benard, P., Zarebanadkouki, M., Kaestner, A., & Carminati, A. (2023). Microplastic induces soil water repellency and limits capillary flow. *Vadose Zone Journal*, *22*(1). https://doi.org/10.1002/vzj2.20215

Czech, L., Barbera, P., & Stamatakis, A. (2020). Genesis and Gappa: Processing, analyzing and visualizing phylogenetic (placement) data. *Bioinformatics*, *36*(10), 3263–3265. https://doi.org/10.1093/bioinformatics/btaa070

Davinic, M., Fultz, L. M., Acosta-Martinez, V., Calderón, F. J., Cox, S. B., Dowd, S. E., Allen, V. G., Zak, J. C., & Moore-Kucera, J. (2012). Pyrosequencing and mid-infrared spectroscopy reveal distinct aggregate stratification of soil bacterial communities and organic matter composition. *Soil Biology and Biochemistry*, *46*, 63–72. https://doi.org/10.1016/j.soilbio.2011.11.012

Davis, N. M., Proctor, D. M., Holmes, S. P., Relman, D. A., & Callahan, B. J. (2018). Simple statistical identification and removal of contaminant sequences in marker-gene and metagenomics data. *Microbiome*, *6*(1), 226. https://doi.org/10.1186/s40168-018-0605-2

De La Cruz-Barrón, M., Cruz-Mendoza, A., Navarro–Noya, Y. E., Ruiz-Valdiviezo, V. M., Ortíz-Gutiérrez, D., Ramírez-Villanueva, D. A., Luna-Guido, M., Thierfelder, C., Wall, P. C., Verhulst, N., Govaerts, B., & Dendooven, L. (2017). The Bacterial Community Structure and Dynamics of Carbon and Nitrogen when Maize (Zea mays L.) and Its Neutral Detergent Fibre Were Added to Soil from Zimbabwe with Contrasting Management Practices. *Microbial Ecology*, *73*(1), 135–152. https://doi.org/10.1007/s00248-016-0807-8

Desai, I. (2025). Xylophilus. In N. Amaresan & K. Kumar (Eds.), *Compendium of Phytopathogenic Microbes in Agro-Ecology* (pp. 285–293). Springer Nature Switzerland. https://doi.org/10.1007/978-3-031-81999-5_15

Ding, F., Li, S., Lu, J., Penn, C. J., Wang, Q.-W., Lin, G., Sardans, J., Penuelas, J., Wang, J., & Rillig, M. C. (2023). Consequences of 33 Years of Plastic Film Mulching and Nitrogen Fertilization on Maize Growth and Soil Quality. *Environmental Science & Technology*, *57*(25), 9174–9183. https://doi.org/10.1021/acs.est.2c08878

Douglas, G. M., Maffei, V. J., Zaneveld, J. R., Yurgel, S. N., Brown, J. R., Taylor, C. M., Huttenhower, C., & Langille, M. G. I. (2020). PICRUSt2 for prediction of metagenome functions. *Nature Biotechnology*, *38*(6), 685–688. https://doi.org/10.1038/s41587-020-0548-6

Fernandes, A. D., Reid, J. N., Macklaim, J. M., McMurrough, T. A., Edgell, D. R., & Gloor, G. B. (2014). Unifying the analysis of high-throughput sequencing datasets: Characterizing RNA-seq, 16S rRNA gene sequencing and selective growth experiments by compositional data analysis. *Microbiome*, *2*(1), 15. https://doi.org/10.1186/2049-2618-2-15

Fox, A., Ikoyi, I., Torres-Sallan, G., Lanigan, G., Schmalenberger, A., Wakelin, S., & Creamer, R. (2018). The influence of aggregate size fraction and horizon position on microbial community composition. *Applied Soil Ecology*, *127*, 19–29. https://doi.org/10.1016/j.apsoil.2018.02.023

Fry, B. (2006). *Stable Isotope Ecology*. Springer New York. https://doi.org/10.1007/0-387-33745-8

Gharahi, N., & Zamani-Ahmadmahmoodi, R. (2022). Effect of plastic pollution in soil properties and growth of grass species in semi-arid regions: A laboratory experiment. *Environmental Science and Pollution Research International*, *29*(39), 59118–59126. https://doi.org/10.1007/s11356-022-19373-x#citeas

Griffin-LaHue, D., Ghimire, S., Yu, Y., Scheenstra, E. J., Miles, C. A., & Flury, M. (2022). In-field degradation of soil-biodegradable plastic mulch films in a Mediterranean climate. *The Science of the Total Environment*, *806*(Pt 1), 150238. https://doi.org/10.1016/j.scitotenv.2021.150238

Gu, Z. (2016). Complex heatmaps reveal patterns and correlations in multidimensional genomic data. *Bioinformatics*, *32*(18), 2847–2849. https://doi.org/10.1093/bioinformatics/btw313

Guliyev, V., Tanunchai, B., Udovenko, M., Menyailo, O., Glaser, B., Purahong, W., Buscot, F., & Blagodatskaya, E. (2023). Degradation of Bio-Based and Biodegradable Plastic and Its Contribution to Soil Organic Carbon Stock. *Polymers*, *15*(3). https://doi.org/10.3390/polym15030660

Guo, J.-J., Huang, X.-P., Xiang, L., Wang, Y.-Z., Li, Y.-W., Li, H., Cai, Q.-Y., Mo, C.-H., & Wong, M.-H. (2020). Source, migration and toxicology of microplastics in soil. *Environment International*, *137*, 105263. https://doi.org/10.1016/j.envint.2019.105263

Han, L., Chen, L., Feng, Y., Kuzyakov, Y., Chen, Q., Zhang, S., Chao, L., Cai, Y., Ma, C., Sun, K., & Rillig, M. C. (2024). Microplastics alter soil structure and microbial community composition. *Environment International*, *185*, 108508. https://doi.org/10.1016/j.envint.2024.108508

Han, Y., Teng, Y., Wang, X., Ren, W., Wang, X., Luo, Y., Zhang, H., & Christie, P. (2021). Soil Type Driven Change in Microbial Community Affects Poly(butylene adipate- *co* -terephthalate) Degradation Potential. *Environmental Science & Technology*, *55*(8), 4648–4657. https://doi.org/10.1021/acs.est.0c04850

Hao, Y., Min, J., Ju, S., Zeng, X., Xu, J., Li, J., Wang, H., Shaheen, S. M., Bolan, N., Rinklebe, J., & Shi, W. (2024). Possible hazards from biodegradation of soil plastic mulch: Increases in

microplastics and CO2 emissions. *Journal of Hazardous Materials*, *467*, 133680. https://doi.org/10.1016/j.jhazmat.2024.133680

Huang, F., Zhang, Q., Wang, L., Zhang, C., & Zhang, Y. (2023). Are biodegradable mulch films a sustainable solution to microplastic mulch film pollution? A biogeochemical perspective. *Journal of Hazardous Materials*, *459*, 132024. https://doi.org/10.1016/j.jhazmat.2023.132024

Huang, P.-M., Wang, M.-K., & Chiu, C.-Y. (2005). Soil mineral–organic matter–microbe interactions: Impacts on biogeochemical processes and biodiversity in soils. *Pedobiologia*, *49*(6), 609–635. https://doi.org/10.1016/j.pedobi.2005.06.006

Huang, Y., Zhao, Y., Wang, J., Zhang, M., Jia, W., & Qin, X. (2019). LDPE microplastic films alter microbial community composition and enzymatic activities in soil. *Environmental Pollution (Barking, Essex : 1987)*, *254*(Pt A), 112983. https://doi.org/10.1016/j.envpol.2019.112983

Inubushi, K., Kakiuchi, Y., Suzuki, C., Sato, M., Ushiwata, S. Y., & Matsushima, M. Y. (2022). Effects of biodegradable plastics on soil properties and greenhouse gas production. *Soil Science and Plant Nutrition*, *68*(1), 183–188. https://doi.org/10.1080/00380768.2021.2022437

Ishii, S., Ashida, N., Ohno, H., Segawa, T., Yabe, S., Otsuka, S., Yokota, A., & Senoo, K. (2017). Noviherbaspirillum denitrificans sp. Nov., a denitrifying bacterium isolated from rice paddy soil and Noviherbaspirillum autotrophicum sp. Nov., a denitrifying, facultatively autotrophic bacterium isolated from rice paddy soil and proposal to reclassify Herbaspirillum massiliense as Noviherbaspirillum massiliense comb. Nov. *International Journal of Systematic and Evolutionary Microbiology*, *67*(6), 1841–1848. https://doi.org/10.1099/ijsem.0.001875

Jia, K., Nie, S., Tian, M., Sun, W., Gao, Y., Zhang, Y., Xie, X., Xu, Z., Zhao, C., & Li, C. (2024). Biodegradable microplastics can cause more serious loss of soil organic carbon by priming effect than conventional microplastics in farmland shelterbelts. *Functional Ecology*, *38*(11), 2447–2458. https://doi.org/10.1111/1365-2435.14662

Kabała, C., Musztyfaga, E., Gałka, B., Łabuńska, D., & Mańczyńska, P. (2016). Conversion of Soil pH 1:2.5 KCl and 1:2.5 H2O to 1:5 H2O: Conclusions for Soil Management, Environmental Monitoring, and International Soil Databases. *Polish Journal of Environmental Studies*, *25*(2), 647–653. https://doi.org/10.15244/pjoes/61549

Kampfer, P., Thummes, K., Chu, H.-I., Tan, C.-C., Arun, A. B., Chen, W.-M., Lai, W.-A., Shen, F.-T., Rekha, P. D., & Young, C.-C. (2008). Pseudacidovorax intermedius gen. Nov., sp. Nov., a novel nitrogen-fixing betaproteobacterium isolated from soil. *INTERNATIONAL JOURNAL OF SYSTEMATIC AND EVOLUTIONARY MICROBIOLOGY*, *58*(2), 491–495. https://doi.org/10.1099/ijs.0.65175-0

Kassambara, A. (2023). *rstatix: Pipe-Friendly Framework for Basic Statistical Tests* (Version 0.7.2). https://rpkgs.datanovia.com/rstatix/

Kirstein, I. V., Kirmizi, S., Wichels, A., Garin-Fernandez, A., Erler, R., Löder, M., & Gerdts, G. (2016). Dangerous hitchhikers? Evidence for potentially pathogenic Vibrio spp. On microplastic particles. *Marine Environmental Research*, *120*, 1–8. https://doi.org/10.1016/j.marenvres.2016.07.004

Krause, L., Rodionov, A., Schweizer, S. A., Siebers, N., Lehndorff, E., Klumpp, E., & Amelung, W. (2018). Microaggregate stability and storage of organic carbon is affected by clay content in arable Luvisols. *Soil and Tillage Research*, *182*, 123–129. https://doi.org/10.1016/j.still.2018.05.003

Krehl, A., Schöllkopf, U., Májeková, M., Tielbörger, K., & Tomiolo, S. (2022). Effects of plastic fragments on plant performance are mediated by soil properties and drought. *Scientific Reports*, *12*(1), 17771. https://doi.org/10.1038/s41598-022-22270-5

Lehmann, A., Leifheit, E. F., Gerdawischke, M., & Rillig, M. C. (2021). Microplastics have shape- and polymer-dependent effects on soil aggregation and organic matter loss – an experimental and

meta-analytical approach. *Microplastics and Nanoplastics*, *1*(1). https://doi.org/10.1186/s43591-021-00007-x

Lehndorff, E., Rodionov, A., Plümer, L., Rottmann, P., Spiering, B., Dultz, S., & Amelung, W. (2021). Spatial organization of soil microaggregates. *Geoderma*, *386*, 114915. https://doi.org/10.1016/j.geoderma.2020.114915

Li, C., Cui, Q., Li, Y., Zhang, K., Lu, X., & Zhang, Y. (2022). Effect of LDPE and biodegradable PBAT primary microplastics on bacterial community after four months of soil incubation. *Journal of Hazardous Materials*, *429*, 128353. https://doi.org/10.1016/j.jhazmat.2022.128353

Li, H.-Z., Zhu, D., Lindhardt, J. H., Lin, S.-M., Ke, X., & Cui, L. (2021). Long-Term Fertilization History Alters Effects of Microplastics on Soil Properties, Microbial Communities, and Functions in Diverse Farmland Ecosystem. *Environmental Science & Technology*, *55*(8), 4658–4668. https://doi.org/10.1021/acs.est.0c04849

Li, J., Peng, W., Yin, X., Wang, X., Liu, Z., Liu, Q., Deng, Z., Lin, S., & Liang, R. (2024). Identification of an efficient phenanthrene-degrading Pseudarthrobacter sp. L1SW and characterization of its metabolites and catabolic pathway. *Journal of Hazardous Materials*, *465*, 133138. https://doi.org/10.1016/j.jhazmat.2023.133138

Lin, H., & Peddada, S. D. (2024). Multigroup analysis of compositions of microbiomes with covariate adjustments and repeated measures. *Nature Methods*, *21*(1), 83–91. https://doi.org/10.1038/s41592-023-02092-7

Lin, S.-Y., Hameed, A., Arun, A. B., Liu, Y.-C., Hsu, Y.-H., Lai, W.-A., Rekha, P. D., & Young, C.-C. (2013). Description of Noviherbaspirillum malthae gen. Nov., sp. Nov., isolated from an oil-contaminated soil, and proposal to reclassify Herbaspirillum soli , Herbaspirillum aurantiacum , Herbaspirillum canariense and Herbaspirillum psychrotolerans as Noviherbaspirillum soli comb. Nov., Noviherbaspirillum aurantiacum comb. Nov., Noviherbaspirillum canariense comb. Nov. And Noviherbaspirillum psychrotolerans comb. Nov. Based on polyphasic analysis. *International Journal of Systematic and Evolutionary Microbiology*, *63*(Pt_11), 4100–4107. https://doi.org/10.1099/ijs.0.048231-0

Liu, B., Bei, Q., Wang, X., Liu, Q., Hu, S., Lin, Z., Zhang, Y., Lin, X., Jin, H., Hu, T., & Xie, Z. (2021). Microbial metabolic efficiency and community stability in high and low fertility soils following wheat residue addition. *Applied Soil Ecology*, *159*, 103848. https://doi.org/10.1016/j.apsoil.2020.103848

Liu, Z., Wu, Z., Zhang, Y., Wen, J., Su, Z., Wei, H., & Zhang, J. (2024). Impacts of conventional and biodegradable microplastics in maize-soil ecosystems: Above and below ground. *Journal of Hazardous Materials*, *477*, 135129. https://doi.org/10.1016/j.jhazmat.2024.135129

Louca, S., & Doebeli, M. (2018). Efficient comparative phylogenetics on large trees. *Bioinformatics*, *34*(6), 1053–1055. https://doi.org/10.1093/bioinformatics/btx701

Lueders, T., Manefield, M., & Friedrich, M. W. (2004). Enhanced sensitivity of DNA- and rRNA-based stable isotope probing by fractionation and quantitative analysis of isopycnic centrifugation gradients. *Environmental Microbiology*, *6*(1), 73–78. https://doi.org/10.1046/j.1462-2920.2003.00536.x

Ma, J., Xu, M., Wu, J., Yang, G., Zhang, X., Song, C., Long, L., Chen, C., Xu, C., & Wang, Y. (2023). Effects of variable-sized polyethylene microplastics on soil chemical properties and functions and microbial communities in purple soil. *The Science of the Total Environment*, *868*, 161642. https://doi.org/10.1016/j.scitotenv.2023.161642

Martínez, A., Perez-Sanchez, E., Caballero, A., Ramírez, R., Quevedo, E., & Salvador-García, D. (2024). PBAT is biodegradable but what about the toxicity of its biodegradation products? *Journal of Molecular Modeling*, *30*(8), 273. https://doi.org/10.1007/s00894-024-06066-0

McLaren, M. R., & Callahan, B. J. (2021). *Silva 138.1 prokaryotic SSU taxonomic training data formatted for DADA2* [Dataset]. Zenodo. https://doi.org/10.5281/ZENODO.4587955

Meng, F., Harkes, P., Van Steenbrugge, J. J. M., & Geissen, V. (2023). Effects of microplastics on common bean rhizosphere bacterial communities. *Applied Soil Ecology*, *181*, 104649. https://doi.org/10.1016/j.apsoil.2022.104649

Meng, F., Yang, X., Riksen, M., & Geissen, V. (2022). Effect of different polymers of microplastics on soil organic carbon and nitrogen—A mesocosm experiment. *Environmental Research*, *204*(Pt A), 111938. https://doi.org/10.1016/j.envres.2021.111938

Mentler, A., Mayer, H., E. H. Blum, W., Schomakers, J., & Degischer, N. (2011). Measurement of soil aggregate stability using low intensity ultrasonic vibration. *Spanish Journal of Soil Science*, *1*. https://doi.org/10.3232/SJSS.2011.V1.N1.01

Miao, L., Wang, P., Hou, J., Yao, Y., Liu, Z., Liu, S., & Li, T. (2019). Distinct community structure and microbial functions of biofilms colonizing microplastics. *The Science of the Total Environment*, *650*(Pt 2), 2395–2402. https://doi.org/10.1016/j.scitotenv.2018.09.378

Mirarab, S., Nguyen, N., & Warnow, T. (2011). SEPP: SATé-Enabled Phylogenetic Placement. *Biocomputing 2012*, 247–258. https://doi.org/10.1142/9789814366496_0024

Mulvaney, R. L. (1996). Nitrogen-Inorganic Forms. In D. L. Sparks, A. L. Page, P. A. Helmke, R. H. Loeppert, P. N. Soltanpour, M. A. Tabatabai, C. T. Johnston, & M. E. Sumner (Eds.), *Methods of Soil Analysis* (pp. 1123–1184). Soil Science Society of America, American Society of Agronomy. https://doi.org/10.2136/sssabookser5.3.c38

Nelson, J. T., Adjuik, T. A., Moore, E. B., VanLoocke, A. D., Ramirez Reyes, A., & McDaniel, M. D. (2024). A Simple, Affordable, Do-It-Yourself Method for Measuring Soil Maximum Water Holding Capacity. *Communications in Soil Science and Plant Analysis*, *55*(8), 1190–1204. https://doi.org/10.1080/00103624.2023.2296988

Ogle, D. H., Doll, J. C., Wheeler, A. P., & Dinno, A. (2025). *FSA: Simple Fisheries Stock Assessment Methods* (Version 0.10.0). https://fishr-core-team.github.io/FSA/

Oksanen, J., Simpson, G. L., Blanchet, F. G., Kindt, R., Legendre, P., Minchin, P. R., O'Hara, R. B., Solymos, P., Stevens, M. H. H., Szoecs, E., Wagner, H., Barbour, M., Bedward, M., Bolker, B., Borcard, D., Carvalho, G., Chirico, M., De Caceres, M., Durand, S., … Borman, T. (2001). *vegan: Community Ecology Package* (p. 2.6-10) [Dataset]. https://doi.org/10.32614/CRAN.package.vegan

Ortiz-Cornejo, N. L., Romero-Salas, E. A., Navarro-Noya, Y. E., González-Zúñiga, J. C., Ramirez-Villanueva, D. A., Vásquez-Murrieta, M. S., Verhulst, N., Govaerts, B., Dendooven, L., & Luna-Guido, M. (2017). Incorporation of bean plant residue in soil with different agricultural practices and its effect on the soil bacteria. *Applied Soil Ecology*, *119*, 417–427. https://doi.org/10.1016/j.apsoil.2017.07.014

Özbolat, O., Sánchez-Navarro, V., Zornoza, R., Egea-Cortines, M., Cuartero, J., Ros, M., Pascual, J. A., Boix-Fayos, C., Almagro, M., De Vente, J., Díaz-Pereira, E., & Martínez-Mena, M. (2023). Long-term adoption of reduced tillage and green manure improves soil physicochemical properties and increases the abundance of beneficial bacteria in a Mediterranean rainfed almond orchard. *Geoderma*, *429*, 116218. https://doi.org/10.1016/j.geoderma.2022.116218

Palleroni, N. J. (2015). *Burkholderia*. In W. B. Whitman (Ed.), *Bergey's Manual of Systematics of Archaea and Bacteria* (1st ed., pp. 1–50). Wiley. https://doi.org/10.1002/9781118960608.gbm00935

Parada, A. E., Needham, D. M., & Fuhrman, J. A. (2016). Every base matters: Assessing small subunit rRNA primers for marine microbiomes with mock communities, time series and global field samples. *Environmental Microbiology*, *18*(5), 1403–1414. https://doi.org/10.1111/1462-2920.13023

Pérez-Pantoja, D., Donoso, R., Agulló, L., Córdova, M., Seeger, M., Pieper, D. H., & González, B. (2012). Genomic analysis of the potential for aromatic compounds biodegradation in

Burkholderiales. *Environmental Microbiology*, *14*(5), 1091–1117. https://doi.org/10.1111/j.1462-2920.2011.02613.x

Piehl, S., Leibner, A., Löder, M. G. J., Dris, R., Bogner, C., & Laforsch, C. (2018). Identification and quantification of macro- and microplastics on an agricultural farmland. *Scientific Reports*, *8*(1), 17950. https://doi.org/10.1038/s41598-018-36172-y

Priya, A., Dutta, K., & Daverey, A. (2022). A comprehensive biotechnological and molecular insight into plastic degradation by microbial community. *Journal of Chemical Technology & Biotechnology*, *97*(2), 381–390. https://doi.org/10.1002/jctb.6675

Qi, Y., Ossowicki, A., Yang, X., Huerta Lwanga, E., Dini-Andreote, F., Geissen, V., & Garbeva, P. (2020). Effects of plastic mulch film residues on wheat rhizosphere and soil properties. *Journal of Hazardous Materials*, *387*, 121711. https://doi.org/10.1016/j.jhazmat.2019.121711

Qiu, X., Ma, S., Pan, J., Cui, Q., Zheng, W., Ding, L., Liang, X., Xu, B., Guo, X., & Rillig, M. C. (2024). Microbial metabolism influences microplastic perturbation of dissolved organic matter in agricultural soils. *The ISME Journal*, *18*(1), wrad017. https://doi.org/10.1093/ismejo/wrad017

Quast, C., Pruesse, E., Yilmaz, P., Gerken, J., Schweer, T., Yarza, P., Peplies, J., & Glöckner, F. O. (2012). The SILVA ribosomal RNA gene database project: Improved data processing and web-based tools. *Nucleic Acids Research*, *41*(D1), D590–D596. https://doi.org/10.1093/nar/gks1219

Rauscher, A., Meyer, N., Jakobs, A., Bartnick, R., Lueders, T., & Lehndorff, E. (2023). Biodegradable microplastic increases CO2 emission and alters microbial biomass and bacterial community composition in different soil types. *Applied Soil Ecology*, *182*, 104714. https://doi.org/10.1016/j.apsoil.2022.104714

Ren, Z., Xu, X., Liang, J., Yuan, C., Zhao, L., Qiu, H., & Cao, X. (2024). Aging Dynamics of Polyvinyl Chloride Microplastics in Three Soils with Different Properties. *Environmental Science & Technology*, *58*(50), 22332–22342. https://doi.org/10.1021/acs.est.4c06317

Rillig, M. C. (2018). Microplastic Disguising As Soil Carbon Storage. *Environmental Science & Technology*, *52*(11), 6079–6080. https://doi.org/10.1021/acs.est.8b02338

Rillig, M. C., Lehmann, A., Souza Machado, A. A., & Yang, G. (2019). Microplastic effects on plants. *The New Phytologist*, *223*(3), 1066–1070. https://doi.org/10.1111/nph.15794

Sander, M. (2019). Biodegradation of Polymeric Mulch Films in Agricultural Soils: Concepts, Knowledge Gaps, and Future Research Directions. *Environmental Science & Technology*, *53*(5), 2304–2315. https://doi.org/10.1021/acs.est.8b05208

Schumacher, B. (2002). Methods for the determination of total organic carbon (TOC) in soils and sediments: Ecological risk assessment support center. *Method NCEA-C-1282: United States Environmental Protection Agency*, 1–23.

Shafea, L., Felde, V. J. M. N. L., Woche, S. K., Bachmann, J., & Peth, S. (2023). Microplastics effects on wettability, pore sizes and saturated hydraulic conductivity of a loess topsoil. *Geoderma*, *437*, 116566. https://doi.org/10.1016/j.geoderma.2023.116566

Shi, J., Wang, Z., Peng, Y., Fan, Z., Zhang, Z., Wang, X., Zhu, K., Shang, J., & Wang, J. (2023). Effects of Microplastics on Soil Carbon Mineralization: The Crucial Role of Oxygen Dynamics and Electron Transfer. *Environmental Science & Technology*, *57*(36), 13588–13600. https://doi.org/10.1021/acs.est.3c02133

Shi, W., Wu, N., Zhang, Z., Liu, Y., Chen, J., & Li, J. (2024). A global review on the abundance and threats of microplastics in soils to terrestrial ecosystem and human health. *The Science of the Total Environment*, *912*, 169469. https://doi.org/10.1016/j.scitotenv.2023.169469

Sinsabaugh, R. L., Manzoni, S., Moorhead, D. L., & Richter, A. (2013). Carbon use efficiency of microbial communities: Stoichiometry, methodology and modelling. *Ecology Letters*, *16*(7), 930–939. https://doi.org/10.1111/ele.12113

Song, Q., Zhou, B., Song, Y., Du, X., Chen, H., Zuo, R., Zheng, J., Yang, T., Sang, Y., & Li, J. (2025). Microbial community dynamics and bioremediation strategies for petroleum contamination in

an in-service oil Depot, middle-lower Yellow River Basin. *Frontiers in Microbiology*, *16*, 1544233. https://doi.org/10.3389/fmicb.2025.1544233

Song, T., Liu, J., Han, S., Li, Y., Xu, T., Xi, J., Hou, L., & Lin, Y. (2024). Effect of conventional and biodegradable microplastics on the soil-soybean system: A perspective on rhizosphere microbial community and soil element cycling. *Environment International*, *190*, 108781. https://doi.org/10.1016/j.envint.2024.108781

Souza Machado, A. A., Lau, C. W., Kloas, W., Bergmann, J., Bachelier, J. B., Faltin, E., Becker, R., Görlich, A. S., & Rillig, M. C. (2019). Microplastics Can Change Soil Properties and Affect Plant Performance. *Environmental Science & Technology*, *53*(10), 6044–6052. https://doi.org/10.1021/acs.est.9b01339

Souza Machado, A. A., Lau, C. W., Till, J., Kloas, W., Lehmann, A., Becker, R., & Rillig, M. C. (2018). Impacts of Microplastics on the Soil Biophysical Environment. *Environmental Science & Technology*, *52*(17), 9656–9665. https://doi.org/10.1021/acs.est.8b02212

Spohn, M., Pötsch, E. M., Eichorst, S. A., Woebken, D., Wanek, W., & Richter, A. (2016). Soil microbial carbon use efficiency and biomass turnover in a long-term fertilization experiment in a temperate grassland. *Soil Biology and Biochemistry*, *97*, 168–175. https://doi.org/10.1016/j.soilbio.2016.03.008

Steenhoudt, O., & Vanderleyden, J. (2000). *Azospirillum* , a free-living nitrogen-fixing bacterium closely associated with grasses: Genetic, biochemical and ecological aspects. *FEMS Microbiology Reviews*, *24*(4), 487–506. https://doi.org/10.1111/j.1574-6976.2000.tb00552.x

Steinmetz, Z., Wollmann, C., Schaefer, M., Buchmann, C., David, J., Tröger, J., Muñoz, K., Frör, O., & Schaumann, G. E. (2016). Plastic mulching in agriculture. Trading short-term agronomic benefits for long-term soil degradation? *The Science of the Total Environment*, *550*, 690–705. https://doi.org/10.1016/j.scitotenv.2016.01.153

Tang, Y., Xing, Y., Wang, X., Ya, H., Zhang, T., Lv, M., Wang, J., Zhang, H., Dai, W., Zhang, D., Zheng, R., & Jiang, B. (2024). PET microplastics influenced microbial community and heavy metal speciation in heavy-metal contaminated soils. *Applied Soil Ecology*, *201*, 105488. https://doi.org/10.1016/j.apsoil.2024.105488

Tanunchai, B., Kalkhof, S., Guliyev, V., Wahdan, S. F. M., Krstic, D., Schädler, M., Geissler, A., Glaser, B., Buscot, F., Blagodatskaya, E., Noll, M., & Purahong, W. (2022). Nitrogen fixing bacteria facilitate microbial biodegradation of a bio-based and biodegradable plastic in soils under ambient and future climatic conditions. *Environmental Science. Processes & Impacts*, *24*(2), 233–241. https://doi.org/10.1039/D1EM00426C

Totsche, K. U., Amelung, W., Gerzabek, M. H., Guggenberger, G., Klumpp, E., Knief, C., Lehndorff, E., Mikutta, R., Peth, S., Prechtel, A., Ray, N., & Kögel-Knabner, I. (2018). Microaggregates in soils. *Journal of Plant Nutrition and Soil Science*, *181*(1), 104–136. https://doi.org/10.1002/jpln.201600451

van Laak, M., Klingenberg, U., Peiter, E., Reitz, T., Zimmer, D., & Buczko, U. (2018). The equivalence of the Calcium-Acetate-Lactate and Double-Lactate extraction methods to assess soil phosphorus fertility. *Journal of Plant Nutrition and Soil Science*, *181*(5), 795–801. https://doi.org/10.1002/jpln.201700366

VDLUFA. (2012). *Methode A 6.2.1.1: Bestimmung von Phosphor und Kalium im Calcium-Acetat-Lactat-Auszug, in Verband Deutscher Landwirtschaftlicher Untersuchungs- und Forschungsanstalten: Vol. Band I* (6th ed.). VDLUFA-Verlag.

Wan, Y., Wu, C., Xue, Q., & Hui, X. (2019). Effects of plastic contamination on water evaporation and desiccation cracking in soil. *The Science of the Total Environment*, *654*, 576–582. https://doi.org/10.1016/j.scitotenv.2018.11.123

Wang, Jie, Jia, M., Zhang, L., Li, X., Zhang, X., & Wang, Z. (2024). Biodegradable microplastics pose greater risks than conventional microplastics to soil properties, microbial community and plant

growth, especially under flooded conditions. *The Science of the Total Environment*, *931*, 172949. https://doi.org/10.1016/j.scitotenv.2024.172949

Wang, Jiaxin, Song, M., Lu, M., Wang, C., Zhu, C., & Dou, X. (2024). Insights into effects of conventional and biodegradable microplastics on organic carbon decomposition in different soil aggregates. *Environmental Pollution (Barking, Essex : 1987)*, *359*, 124751. https://doi.org/10.1016/j.envpol.2024.124751

Wang, Z., Li, W., Li, W., Yang, W., & Jing, S. (2023). Effects of microplastics on the water characteristic curve of soils with different textures. *Chemosphere*, *317*, 137762. https://doi.org/10.1016/j.chemosphere.2023.137762

Weithmann, N., Möller, J. N., Löder, M. G. J., Piehl, S., Laforsch, C., & Freitag, R. (2018). Organic fertilizer as a vehicle for the entry of microplastic into the environment. *Science Advances*, *4*(4), 8060. https://doi.org/10.1126/sciadv.aap8060

Wickham, H. (2016). *ggplot2: Elegant Graphics for Data Analysis*. Springer-Verlag New York. https://ggplot2.tidyverse.org

Wilhelm, R. C., Murphy, S. J. L., Feriancek, N. M., Karasz, D. C., DeRito, C. M., Newman, J. D., & Buckley, D. H. (2020). Paraburkholderia madseniana sp. Nov., a phenolic acid-degrading bacterium isolated from acidic forest soil. *International Journal of Systematic and Evolutionary Microbiology*, *70*(3), 2137–2146. https://doi.org/10.1099/ijsem.0.004029

Wilhelm, R. C., Singh, R., Eltis, L. D., & Mohn, W. W. (2019). Bacterial contributions to delignification and lignocellulose degradation in forest soils with metagenomic and quantitative stable isotope probing. *The ISME Journal*, *13*(2), 413–429. https://doi.org/10.1038/s41396-018-0279-6

World reference base for soil resources 2014: International soil classification system for naming soils and creating legends for soil maps ([3. ed.]). (2014). FAO.

Wu, X., Pan, J., Li, M., Li, Y., Bartlam, M., & Wang, Y. (2019). Selective enrichment of bacterial pathogens by microplastic biofilm. *Water Research*, *165*, 114979. https://doi.org/10.1016/j.watres.2019.114979

Xia, Q., Rufty, T., & Shi, W. (2020). Soil microbial diversity and composition: Links to soil texture and associated properties. *Soil Biology and Biochemistry*, *149*, 107953. https://doi.org/10.1016/j.soilbio.2020.107953

Xie, Y., Wang, H., Chen, Y., Guo, Y., Wang, C., Cui, H., & Xue, J. (2023). Water retention and hydraulic properties of a natural soil subjected to microplastic contaminations and leachate exposures. *The Science of the Total Environment*, *901*, 166502. https://doi.org/10.1016/j.scitotenv.2023.166502

Xue, Y., Zhao, F., Sun, Z., Bai, W., Zhang, Y., Zhang, Z., Yang, N., Feng, C., & Feng, L. (2023). Long-term mulching of biodegradable plastic film decreased fungal necromass C with potential consequences for soil C storage. *Chemosphere*, *337*, 139280. https://doi.org/10.1016/j.chemosphere.2023.139280

Yang, C., & Zhang, L. (2025). *ggpicrust2: Make "PICRUSt2" Output Analysis and Visualization Easier* (Version 2.1.2). https://github.com/cafferychen777/ggpicrust2

Ye, Y., & Doak, T. G. (2009). A Parsimony Approach to Biological Pathway Reconstruction/Inference for Genomes and Metagenomes. *PLoS Computational Biology*, *5*(8), e1000465. https://doi.org/10.1371/journal.pcbi.1000465

Yi, M., Zhang, L., Qin, C., Lu, P., Bai, H., Han, X., & Yuan, S. (2022). Temporal changes of microbial community structure and nitrogen cycling processes during the aerobic degradation of phenanthrene. *Chemosphere*, *286*, 131709. https://doi.org/10.1016/j.chemosphere.2021.131709

Yu, Y., Battu, A. K., Varga, T., Denny, A. C., Zahid, T. M., Chowdhury, I., & Flury, M. (2023). Minimal Impacts of Microplastics on Soil Physical Properties under Environmentally Relevant Concentrations. *Environmental Science & Technology*, *57*(13), 5296–5304. https://doi.org/10.1021/acs.est.2c09822

Zhang, P., Yuan, Y., Zhang, J., Wen, T., Wang, H., Qu, C., Tan, W., Xi, B., Hui, K., & Tang, J. (2023). Specific response of soil properties to microplastics pollution: A review. *Environmental Research*, *232*, 116427. https://doi.org/10.1016/j.envres.2023.116427

Zhang, Z., Wang, W., Liu, J., & Wu, H. (2024). Discrepant responses of bacterial community and enzyme activities to conventional and biodegradable microplastics in paddy soil. *Science of The Total Environment*, *909*, 168513. https://doi.org/10.1016/j.scitotenv.2023.168513

Zhang, Z., Zhao, S., Chen, L., Duan, C., Zhang, X., & Fang, L. (2022). A review of microplastics in soil: Occurrence, analytical methods, combined contamination and risks. *Environmental Pollution (Barking, Essex : 1987)*, *306*, 119374. https://doi.org/10.1016/j.envpol.2022.119374

Zumstein, M. T., Schintlmeister, A., Nelson, T. F., Baumgartner, R., Woebken, D., Wagner, M., Kohler, H.-P. E., McNeill, K., & Sander, M. (2018). Biodegradation of synthetic polymers in soils: Tracking carbon into CO2 and microbial biomass. *Science Advances*, *4*(7), 9024. https://doi.org/10.1126/sciadv.aas9024

Differing Physicochemical Responses of Agricultural Soil Types to Biodegradable PBAT Compared to Conventional Plastic

Ryan Bartnick[*1], Aileen Jakobs[2], Tillmann Lueders[2], Eva Lehndorff[1]

[1]Soil Ecology, University of Bayreuth, Dr.-Hans-Frisch-Str. 1-3, 95448 Bayreuth, Germany
[2]Ecological Microbiology, University of Bayreuth, Dr.-Hans-Frisch-Str. 1-3, 95448 Bayreuth, Germany

[*]Corresponding author: Email: ryan.bartnick@uni-bayreuth.de

This supporting information includes:

Experimental Design
Tables S1-S4
Figures S1-S15

Supporting Information

The SI contains an extended experimental design, soil profile information, plastic polymer information, and additional figures of size range treatments, microbial data, and supporting analyses.

Experimental Design

Soil treatments were put into pots in Feb. 2022 with to a water holding capacity (WHC) of 60% (initial measurements before treatment) and watered every 3-4 days to maintain this WHC. Each treatment was made in bulk by mixing soil (≈6 kg) and plastic in an overhead shaker gently for three hours. This bulk treatment was then homogeneous and split into replicates of 5 large pots (around 1200 g each) for plant growth and 2 small pots (180 g each) for no plant growth. Each large pot was initially filled approx. 2/3 full of soil, then two isotopically labeled bags of soil were placed at an approx. depth of 5 cm. The remaining soil was filled to reach the final dry weight (Figure S1, SI). The 5 large pots were replicated for each treatment to represent one maize plant life cycle in the greenhouse. The two small pots were used for testing soil conditions and aggregate analysis without plant growth at the initial planting stage (4 weeks) and at harvest (18 weeks); subsets of plant treatments (3 replicates) with most interest (No MP, PE, PBAT at 1% conc. MP mix) were selected for subsequent aggregate, and microbial community composition analyses. This treatment sub-selection was due to the large sample sizes and analytical time limitations.

The plants were placed in a greenhouse with LED lights (wavelength 410–780 nm) on a light cycle of 14 hours/day with constant air flow and maintained temperatures between 18-28°C (see Figure S2, SI). Treatments were randomized and rotated when watered to distribute light evenly. Initial wetting of the dry soil was done slowly and carefully to ensure plastics incorporate into the soil and prevent plastics from floating to the top of the soil (in the case of low-density PE). First, water was slowly sprayed on top of soil and in the bottom saucer to evenly introduce wetting to soil from top and bottom. Continued slow watering occurred until 60% WHC of each corresponding soil type was achieved. Soil was then watered every 3-4 days to the set WHC to mimic naturally wetting and drying of soil over a period of 4 weeks to establish first aggregation of soil. After 4 weeks, the first set of small soil pots were taken for analytical measurements as the starting point for beginning soil conditions in each treatment.

Maize seedlings were sterilized with H_2O_2 and germinated for 5 days before planting., then they were planted at approx. 2 cm, one per replicate. Later after maize saplings were established, to prevent moss growth and other invasive species, small pebbles were weighed and placed in a layer to cover and protect the topsoil. During experimentation, maize height (to top node) and leaf count were monitored weekly. Soil in which the maize seedlings (17/175) had died after the first planting were replanted one week later with a second batch of germinated seedling. A final replant occurred two weeks later for a few soils (4). At harvest, only seven plants (of 175) with questionable growth were removed from analyses.

Table S1. Basic measured parameters of soil investigated.

	sand	silt
location (coordinate)	Bayreuth (49.9295°N, 11.5545°E)	Bindlach (49.9725°N, 11.6226°E)
classification (WRB)	sandy loam (SL)	silt loam (SiL)
sand (%)	78.5	22.5
silt (%)	9.7	63.7
clay (%)	11.8	13.8
pH value	6.7	6.5
total C [g kg^{-1}]	10.92	15.54
$C_{organic}$ [g kg^{-1}]	10.71	15.44
$C_{inorganic}$ [g kg^{-1}]	0.21	0.10
total N [g kg^{-1}]	0.95	1.57
PE [g kg^{-1}]	0.07	0.27
PET [g kg^{-1}]	0.17	2.67

Table S2. Experimental plastic carbon percentage and $\delta^{13}C$ values.

plastic polymer	C [%]	$\delta^{13}C$ [‰]
LDPE	88	-32.9
PET	63	-28.1
PBAT	62	-31.5

Table S3. List of measured parameters in silty loam with maize growth.

silty loam	No MP	PE				PBAT				
		0.1%	1%			0.1%	1%			
parameter	control	75-400 µm	75-400 µm	75-200 µm	<75 µm	75-400 µm	75-400 µm	200-400 µm	75-200 µm	<75 µm
pH value	6.5 ± 0.0	6.4 ± 0.0	6.5 ± 0.2	6.4 ± 0.1	6.4 ± 0.1	6.4 ± 0.1	6.4 ± 0.0	6.3 ± 0.2	6.4 ± 0.1	6.4 ± 0.1
soil total C [g/kg]	16.4 ± 0.4	16.8 ± 0.3	25.2 ± 1.1***	24.4 ± 0.8***	24.5 ± 0.4***	16.0 ± 0.3	21.5 ± 0.3***	22.5 ± 1.4***	20.8 ± 0.6***	21.0 ± 0.3***
soil total N [g/kg]	1.7 ± 0.0	1.6 ± 0.0*	1.6 ± 0.0	1.6 ± 0.0	1.6 ± 0.0	1.6 ± 0.0***	1.5 ± 0.0***	1.6 ± 0.0***	1.5 ± 0.0***	1.5 ± 0.0***
nitrate [mg/kg]	20.3 ± 3.8	20.8 ± 9.3	10.9 ± 6.3	24.5 ± 5.8	21.1 ± 2.7	14.9 ± 3.6	12.6 ± 6.1	21.1 ± 4.7	15.5 ± 3.7	17.7 ± 5.5
K_{CAL} [mg/kg]	4.9 ± 2.8	10.2 ± 10.4	3.8 ± 0.9	3.9 ± 1.6	3.9 ± 2.6	3.0 ± 1.3	5.6 ± 2.6	3.7 ± 0.5	3.5 ± 1.6	4.8 ± 2.6
P_{CAL} [mg/kg]	6.0 ± 0.5	6.7 ± 0.9	6.5 ± 1.5	6.2 ± 0.9	7.1 ± 1.3	4.2 ± 0.3	5.4 ± 0.8	4.8 ± 0.3*	4.6 ± 0.2*	4.3 ± 0.4**
Maize biomass [g]	18.8 ± 1.5	17.1 ± 2.8	18.5 ± 1.4	17.8 ± 3.5	17.7 ± 1.0	17.5 ± 1.2	15.9 ± 3.6	16.1 ± 0.8	16.1 ± 1.6	16.2 ± 1.5
root N [g/kg]	4.3 ± 0.3	4.4 ± 1.0	4.5 ± 0.7	4.7 ± 0.9	3.6 ± 0.6	5.6 ± 0.3	6.0 ± 0.9**	5.5 ± 0.5	5.8 ± 1.0*	5.4 ± 0.6
leaf N [g/kg]	6.4 ± 1.5	9.0 ± 3.1	6.2 ± 1.4	9.7 ± 7.7	6.6 ± 0.9	6.5 ± 0.7	6.9 ± 2.5	6.0 ± 1.2	6.7 ± 2.4	6.7 ± 1.8
WHC [g water/g soil]	0.4 ± 0.0	0.5 ± 0.0	0.5 ± 0.1	0.4 ± 0.0	0.5 ± 0.1	0.5 ± 0.1	0.5 ± 0.0*	0.5 ± 0.1	0.5 ± 0.1	0.4 ± 0.0
macroaggregates [%]	0.1 ± 0.0		0.1 ± 0.0				0.1 ± 0.0			
occluded MA [%]	0.3 ± 0.2		0.3 ± 0.2				0.4 ± 0.1			
free MA [%]	0.6 ± 0.2		0.6 ± 0.2				0.5 ± 0.1			

Significance codes: * $p < 0.05$, ** $p < 0.01$, *** $p < 0.001$
CAL: calcium-acetate-lactate extraction
WHC: water holding capacity
MA: microaggregates

silty loam	No MP	PET				
		0.1%	1%			
parameter	control	75-400 µm	75-400 µm	200-400 µm	75-200 µm	<75 µm
pH value	6.5 ± 0.0	6.4 ± 0.1	6.4 ± 0.0	6.4 ± 0.1	6.3 ± 0.1	6.3 ± 0.1
soil total C [g/kg]	16.4 ± 0.4	16.9 ± 0.7	21.4 ± 0.9***	21.7 ± 1.5***	21.9 ± 0.6***	21.4 ± 0.2***
soil total N [g/kg]	1.7 ± 0.0	1.6 ± 0.0**	1.6 ± 0.0***	1.6 ± 0.1	1.6 ± 0.0**	1.6 ± 0.0***
nitrate [mg/kg]	20.3 ± 3.8	19.7 ± 5.0	21.7 ± 8.9	16.7 ± 5.9	18.1 ± 9.6	17.8 ± 10.4
K_{CAL} [mg/kg]	4.9 ± 2.8	7.7 ± 3.9	3.4 ± 0.6	5.5 ± 2.2	3.7 ± 0.6	3.4 ± 1.7
P_{CAL} [mg/kg]	6.0 ± 0.5	5.3 ± 0.9	5.5 ± 0.7	5.1 ± 0.3	5.0 ± 0.1	5.0 ± 0.3
Maize biomass [g]	18.8 ± 1.5	15.8 ± 2.8	16.4 ± 2.5	15.3 ± 2.3	16.9 ± 1.1	17.2 ± 2.3
root N [g/kg]	4.3 ± 0.3	4.8 ± 0.7	4.2 ± 0.5	4.2 ± 0.6	3.8 ± 0.4	5.9 ± 0.6**
leaf N [g/kg]	6.4 ± 1.5	6.3 ± 1.7	7.4 ± 1.3	4.9 ± 1.4	6.5 ± 2.7	7.1 ± 0.7
WHC [g water/g soil]	0.4 ± 0.0	0.5 ± 0.0	0.5 ± 0.1	0.6 ± 0.0**	0.4 ± 0.1	0.5 ± 0.1
macroaggregates [%]	0.1 ± 0.0					
occluded MA [%]	0.3 ± 0.2					
free MA [%]	0.6 ± 0.2					

Table S4. List of measured parameters in sandy loam with maize growth.

sandy loam	No MP	PE					PBAT				
		0.10%	1%				0.10%	1%			
parameter	control	75-400 µm	75-400 µm	200-400 µm	75-200 µm	<75 µm	75-400 µm	75-400 µm	200-400 µm	75-200 µm	<75 µm
pH value	6.9 ± 0.1	7.1 ± 0.1	7.0 ± 0.1	7.0 ± 0.1	7.0 ± 0.1	7.0 ± 0.1	6.8 ± 0.2	6.8 ± 0.2	6.9 ± 0.1	6.9 ± 0.1	6.9 ± 0.1
soil total C [g/kg]	6.4 ± 0.2	6.9 ± 0.4	14.9 ± 1.6***	13.7 ± 2.1***	15.3 ± 0.6***	15.6 ± 0.7***	7.3 ± 0.5	12.3 ± 1.9***	11.2 ± 1.1***	12.0 ± 0.5***	12.0 ± 0.4***
soil total N [g/kg]	0.5 ± 0.0	0.5 ± 0.0	0.5 ± 0.0	0.5 ± 0.0	0.6 ± 0.0	0.6 ± 0.0**	0.6 ± 0.0	0.6 ± 0.0	0.5 ± 0.0	0.5 ± 0.0	0.6 ± 0.0
nitrate [mg/kg]	13.3 ± 6.1	14.3 ± 6.4	7.1 ± 6.7	8.3 ± 7.2	17.5 ± 7.1	19.6 ± 3.6	17.5 ± 7.3	15.2 ± 9.1	12.2 ± 6.3	22.4 ± 15.3	17.4 ± 6.5
K_{CAL} [mg/kg]	10.3 ± 1.8	11.0 ± 1.5	11.4 ± 2.4	10.3 ± 2.2	11.2 ± 1.5	14.6 ± 9.5	12.4 ± 3.2	12.6 ± 0.9	13.0 ± 1.3	12.4 ± 3.0	12.8 ± 1.4
P_{CAL} [mg/kg]	62.8 ± 13.7	69.1 ± 27.0	75.7 ± 24.4	62.1 ± 16.9	55.7 ± 7.3	55.7 ± 5.0	70.5 ± 37.8	56.1 ± 20.5	74.5 ± 23.1	51.0 ± 19.2	52.1 ± 23.6
Maize biomass [g]	9.1 ± 0.6	10.2 ± 0.7	9.4 ± 1.8	11.3 ± 0.7	11.2 ± 0.9	9.6 ± 1.4	11.0 ± 1.1	10.7 ± 0.9	9.6 ± 2.0	9.6 ± 2.0	9.9 ± 1.2
root N [g/kg]	6.3 ± 0.7	5.7 ± 0.4	6.0 ± 0.7	5.4 ± 0.4	5.2 ± 0.4	7.0 ± 0.7	6.7 ± 0.6	6.4 ± 0.3	7.0 ± 0.9	7.2 ± 1.7	6.6 ± 0.5
leaf N [g/kg]	5.0 ± 2.3	6.2 ± 0.9	6.2 ± 0.7	5.9 ± 0.4	4.2 ± 1.2	4.4 ± 1.2	5.0 ± 1.2	5.9 ± 1.3	5.3 ± 1.9	5.8 ± 1.0	4.4 ± 1.8
WHC [g water/g soil]	0.3 ± 0.0	0.3 ± 0.0	0.3 ± 0.0	0.3 ± 0.0	0.3 ± 0.0	0.3 ± 0.0	0.3 ± 0.0	0.3 ± 0.0	0.3 ± 0.0	0.3 ± 0.0	0.3 ± 0.0
macroaggregates [%]	0.3 ± 0.0		0.3 ± 0.0					0.3 ± 0.0			
occluded MA [%]	0.1 ± 0.0		0.1 ± 0.0					0.1 ± 0.0			
free MA [%]	0.7 ± 0.0		0.6 ± 0.1					0.7 ± 0.0			

Significance codes: * $p < 0.05$, ** $p < 0.01$, *** $p < 0.001$
CAL: calcium-acetate-lactate extraction
WHC: water holding capacity
MA: microaggregates

sandy loam	No MP	PET				
		0.10%	1%			
parameter	control	75-400 µm	75-400 µm	200-400 µm	75-200 µm	<75 µm
pH value	6.9 ± 0.1	7.1 ± 0.1	7.1 ± 0.1	6.9 ± 0.2	6.8 ± 0.3	6.9 ± 0.1
soil total C [g/kg]	6.4 ± 0.2	7.5 ± 1.0	13.8 ± 1.9***	11.4 ± 1.9***	12.5 ± 1.0***	11.9 ± 0.8***
soil total N [g/kg]	0.5 ± 0.0	0.6 ± 0.0	0.6 ± 0.0	0.6 ± 0.0	0.6 ± 0.0	0.5 ± 0.0
nitrate [mg/kg]	13.3 ± 6.1	13.0 ± 8.2	8.2 ± 7.2	15.6 ± 9.7	13.0 ± 11.1	18.1 ± 10.8
K_{CAL} [mg/kg]	10.3 ± 1.8	14.2 ± 3.2	11.4 ± 2.8	13.7 ± 6.5	12.0 ± 1.8	11.3 ± 0.7
P_{CAL} [mg/kg]	62.8 ± 13.7	73.8 ± 24.0	78.5 ± 25.7	67.3 ± 43.2	62.3 ± 18.3	44.4 ± 3.6
Maize biomass [g]	9.1 ± 0.6	10.3 ± 0.9	10.9 ± 1.1	10.8 ± 1.2	11.5 ± 1.3	9.8 ± 1.6
root N [g/kg]	6.3 ± 0.7	5.5 ± 0.8	5.8 ± 0.4	5.7 ± 0.2	6.4 ± 0.6	6.4 ± 0.3
leaf N [g/kg]	5.0 ± 2.3	6.5 ± 0.7	5.9 ± 1.0	5.3 ± 1.8	5.4 ± 0.7	4.1 ± 1.1
WHC [g water/g soil]	0.3 ± 0.0	0.3 ± 0.0	0.3 ± 0.0	0.3 ± 0.0	0.3 ± 0.0	0.3 ± 0.0
macroaggregates [%]	0.3 ± 0.0					
occluded MA [%]	0.1 ± 0.0					
free MA [%]	0.7 ± 0.0					

Table S5. Summary of statistical analysis of Bray-Curtis dissimilarities between treatments, assessed using PERMANOVA. Homogeneity of group dispersions was evaluated using PERMDISP2 followed by ANOVA.

soil type	comparison	PERMANOVA			homogeneity of group dispersions	
		p	F	R^2	p	F
both	soil type	0.001	30.804	0.306	0.025	5.282
sandy loam	plant presence	0.001	1.738	0.049	0.008	7.947
silty loam	plant presence	0.001	1.793	0.05	0.19	1.786
sandy loam	plastic polymer	0.001	1.51	0.111	0.022	4.486
sandy loam	aggregate	0.008	1.175	0.087	0.869	0.141
sandy loam	plastic polymer:aggregate	0.956	0.934	0.138	NA	NA
silty loam	plastic polymer	0.001	1.208	0.092	0.817	0.204
silty loam	aggregate	0.108	1.035	0.079	0.855	0.158
silty loam	plastic polymer:aggregate	0.996	0.957	0.145	NA	NA
sandy loam	aggregate: small vs medium	0.091	1.097	0.064	0.894	0.018
sandy loam	aggregate: small vs large	0.003	1.378	0.079	0.657	0.205
sandy loam	aggregate: medium vs large	0.74	0.94	0.056	0.652	0.211
sandy loam	plastic polymer: none vs LDPE	0.179	1.066	0.062	0.367	0.863
sandy loam	plastic polymer: none vs PBAT	0.001	1.707	0.096	0.014	7.7
sandy loam	plastic polymer: LDPE vs PBAT	0.001	1.705	0.096	0.026	5.986
silty loam	plastic polymer: none vs LDPE	0.09	1.045	0.061	0.527	0.419
silty loam	plastic polymer: none vs PBAT	0.001	1.212	0.07	0.784	0.078
silty loam	plastic polymer: LDPE vs PBAT	0.001	1.382	0.08	0.727	0.126

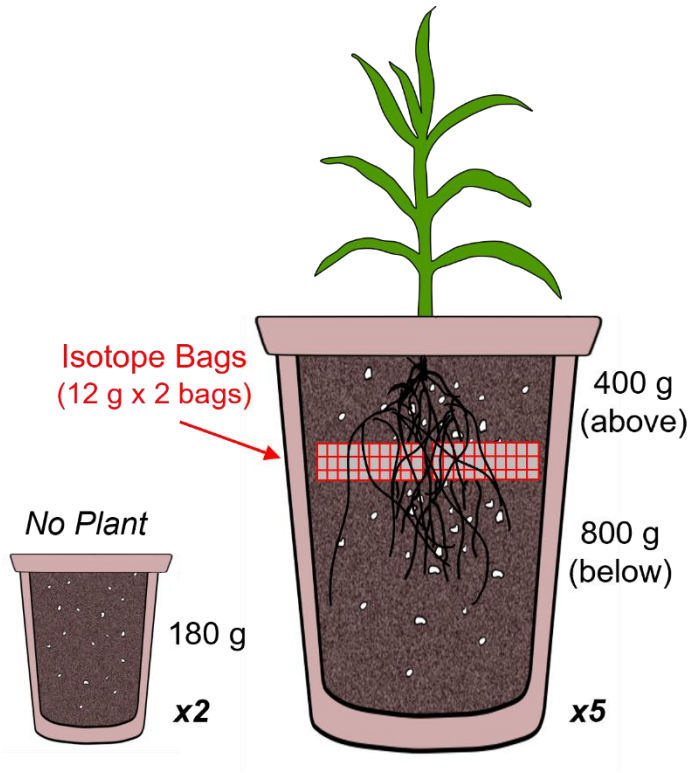

Figure S1. Greenhouse experimental pots with isotopically labeled bags.

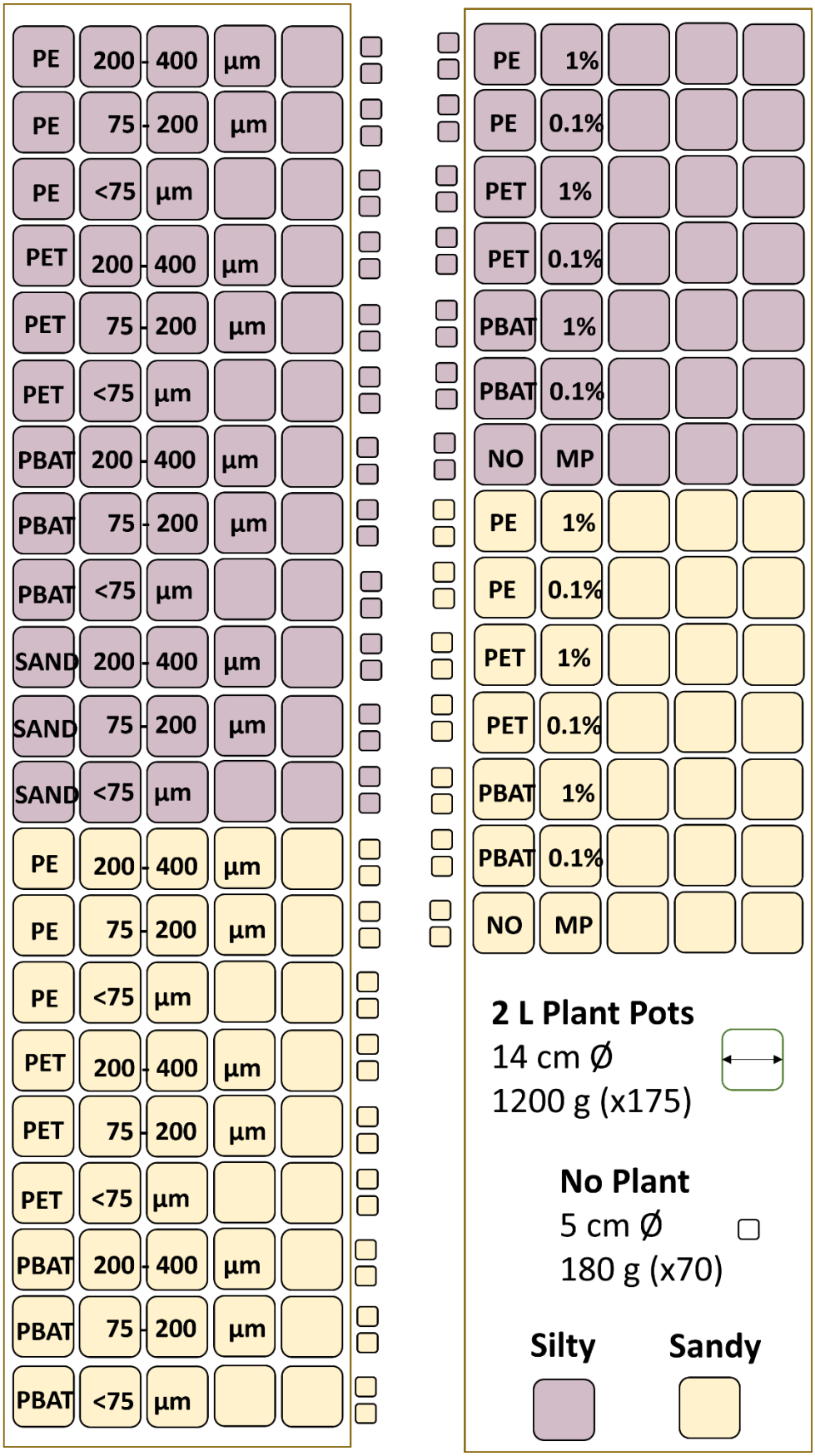

Figure S2. Greenhouse layout and design; treatments later randomized and rotated when watered to distribute light evenly.

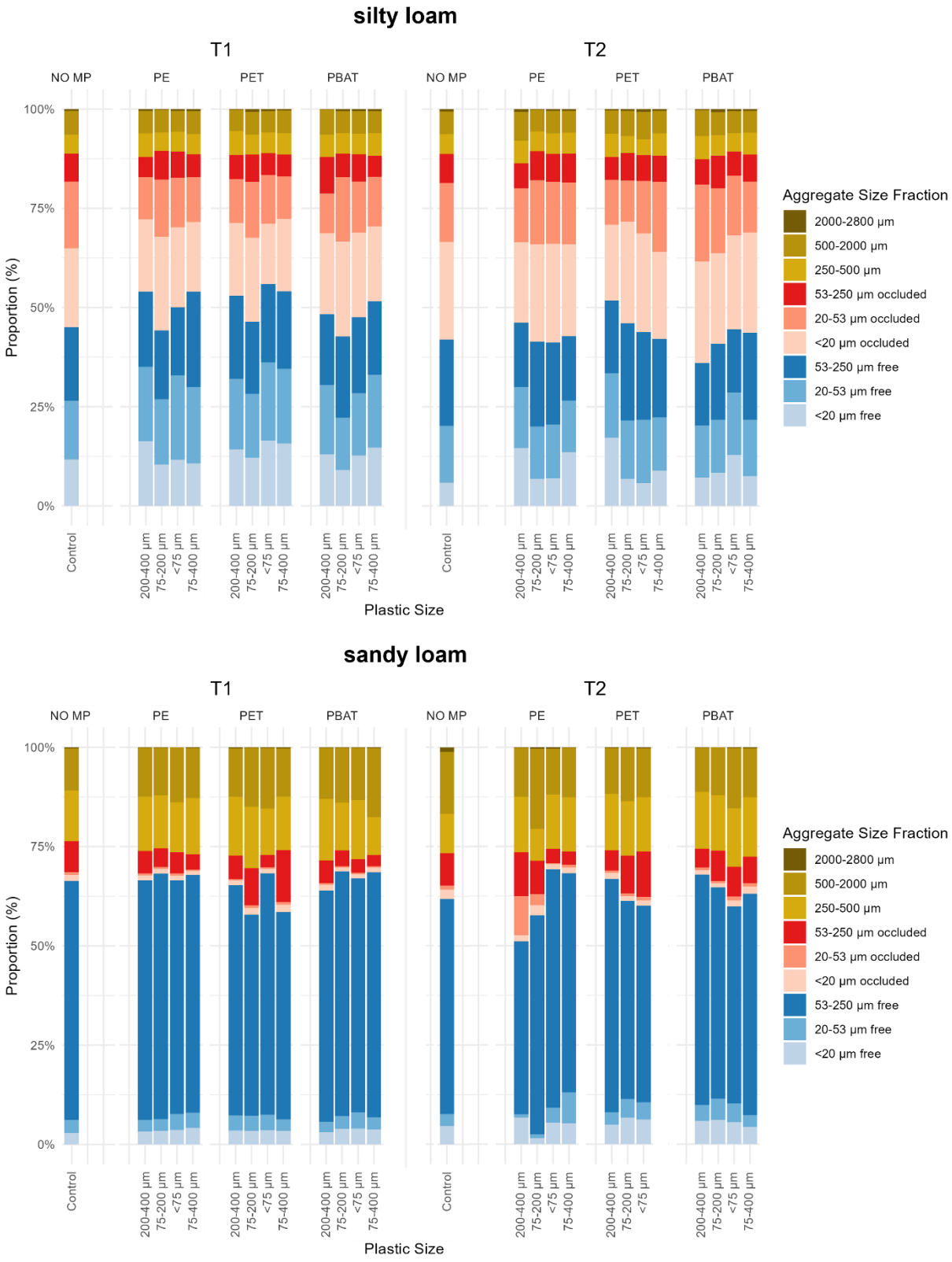

Figure S3. Aggregation fractionation in silty loam (top) and sandy loam (bottom) comparing MPs size range treatments (200–400, 75–200, <75, and 75–400 µm) to control. Aggregation fractionation in silty loam without plant growth with various MPs sizes between T1 (4 weeks) and T2 (18 weeks).

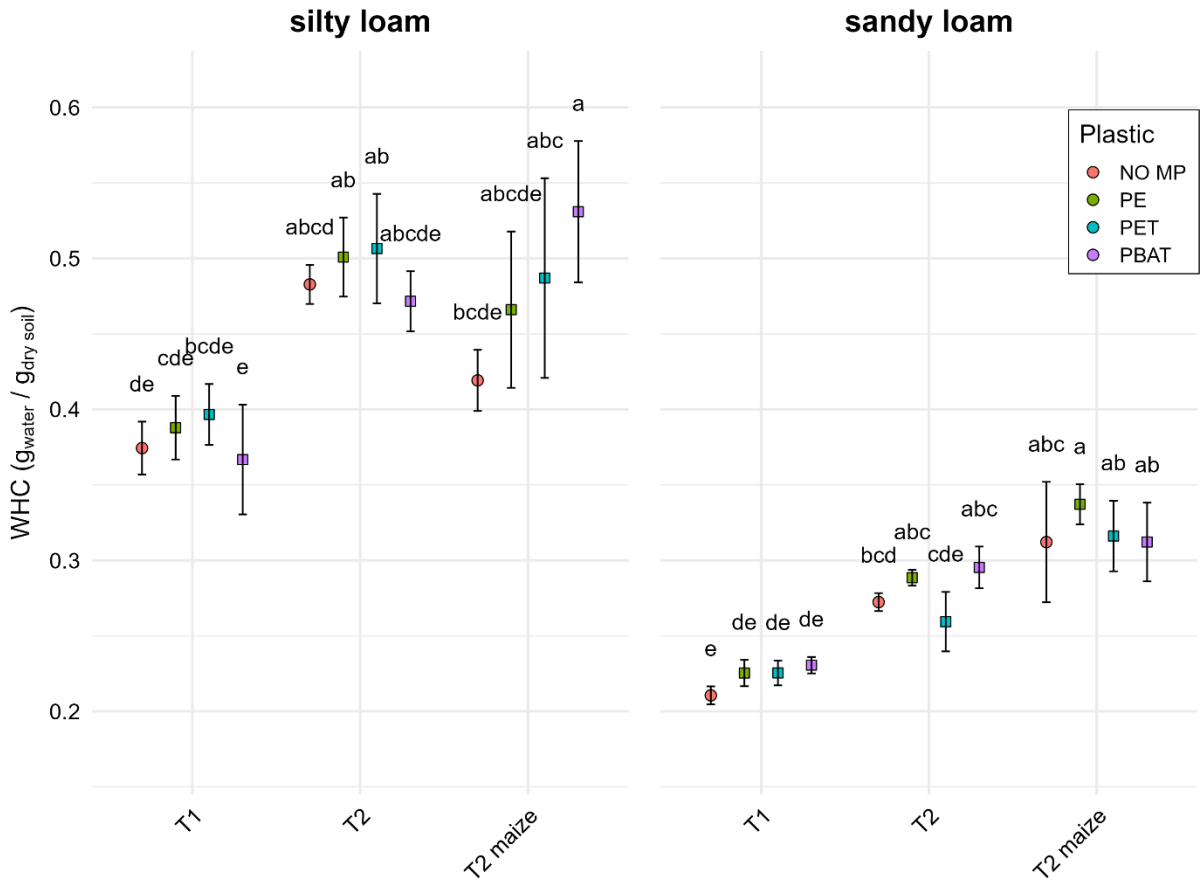

Figure S4. Water holding capacity (WHC) of silty loam (left) and sandy loam (right) with MPs (1% w/w) over experimentation time and maize growth.

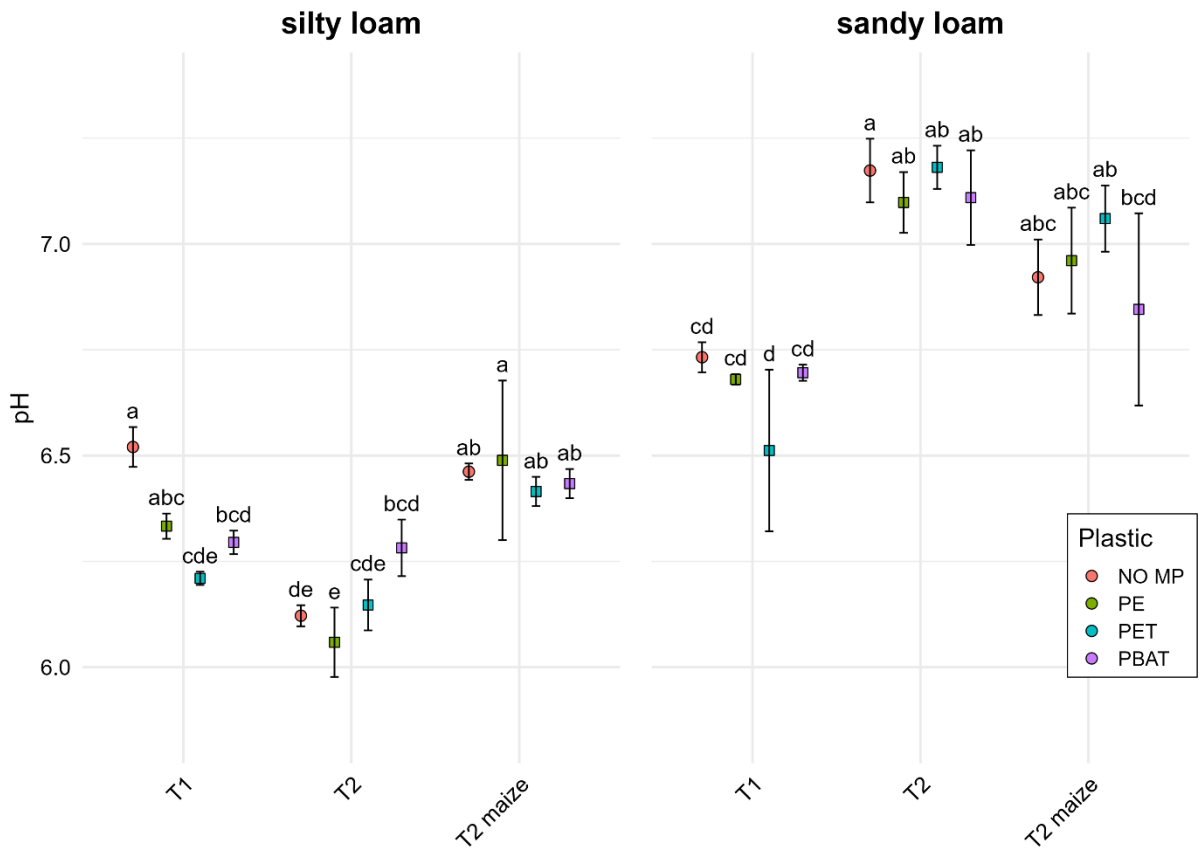

Figure S5. pH values of silty loam (left) and sandy loam (right) with MPs (1% w/w) over experimentation time and maize growth.

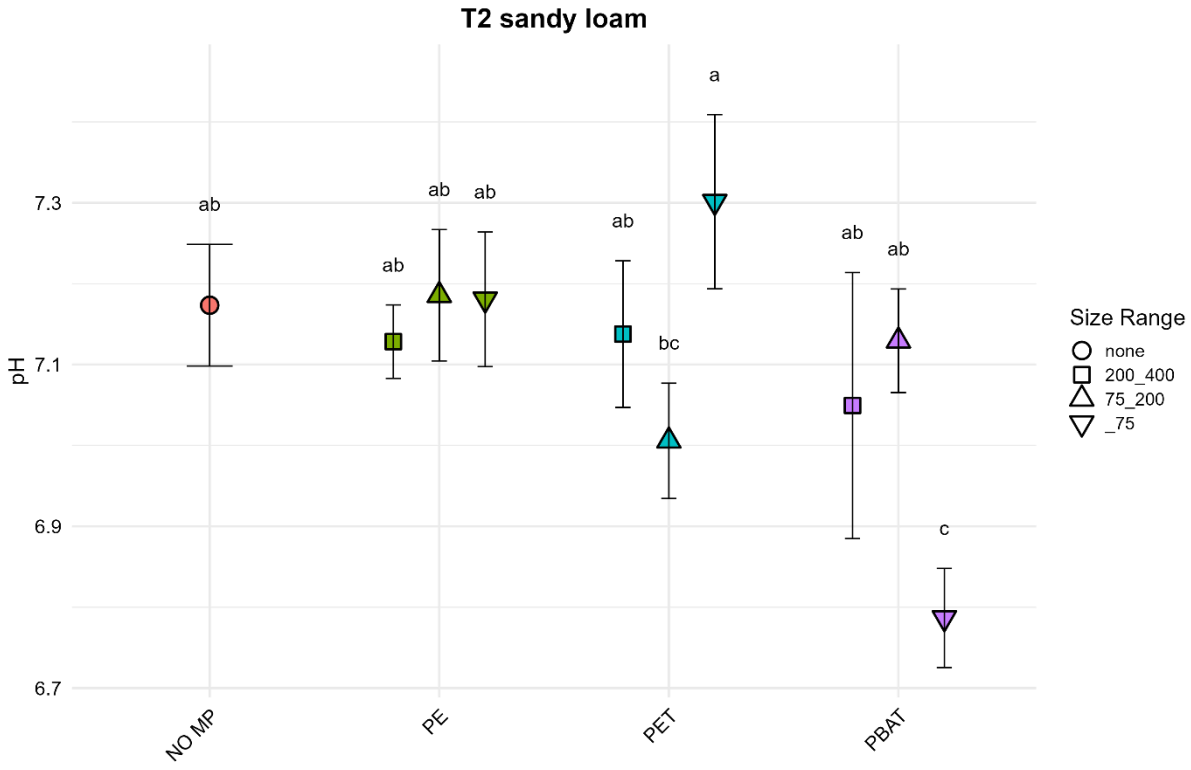

Figure S6. Sandy loam pH values with differing sizes of MPs (200–400, 75–200, and <75 µm).

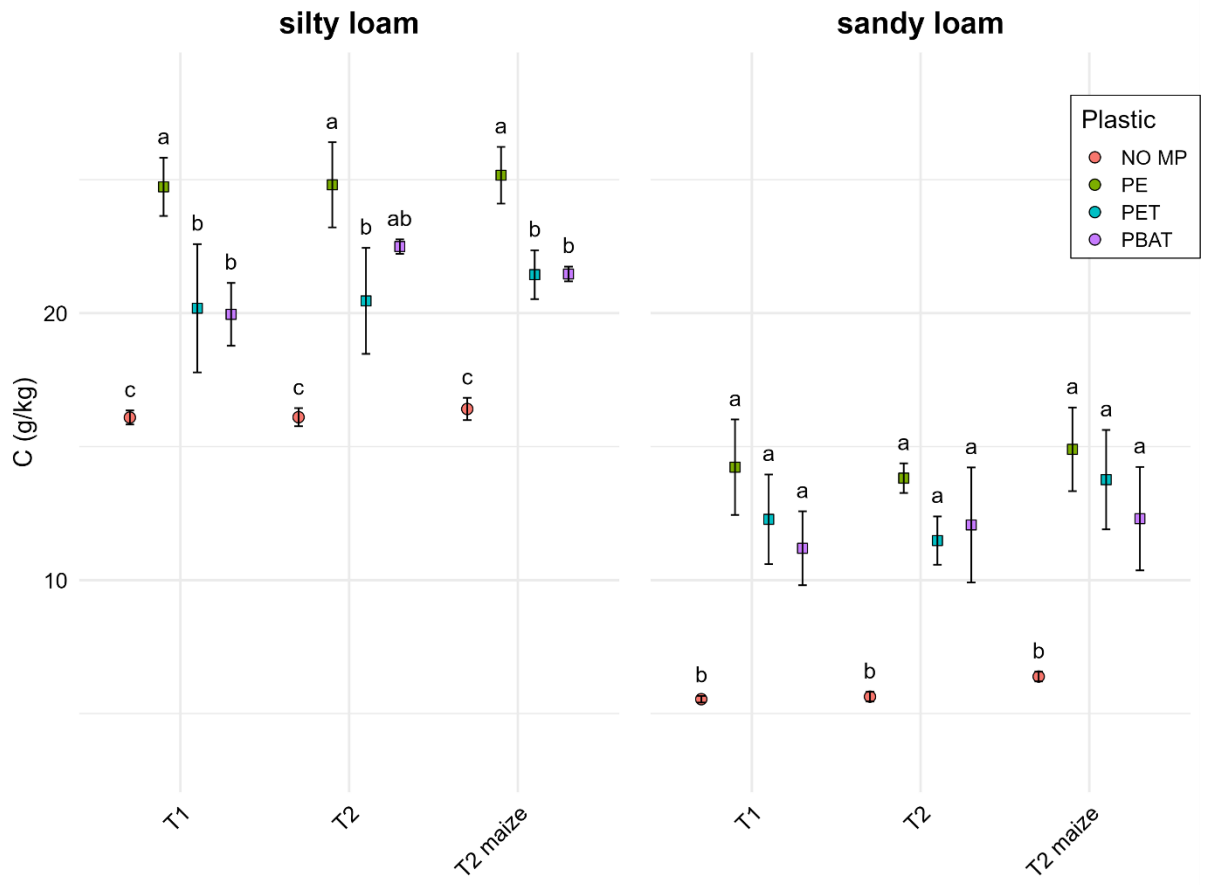

Figure S7. Total carbon content of silty loam (left) and sandy loam (right) increased in proportion to addition of 1% MPs respective C content.

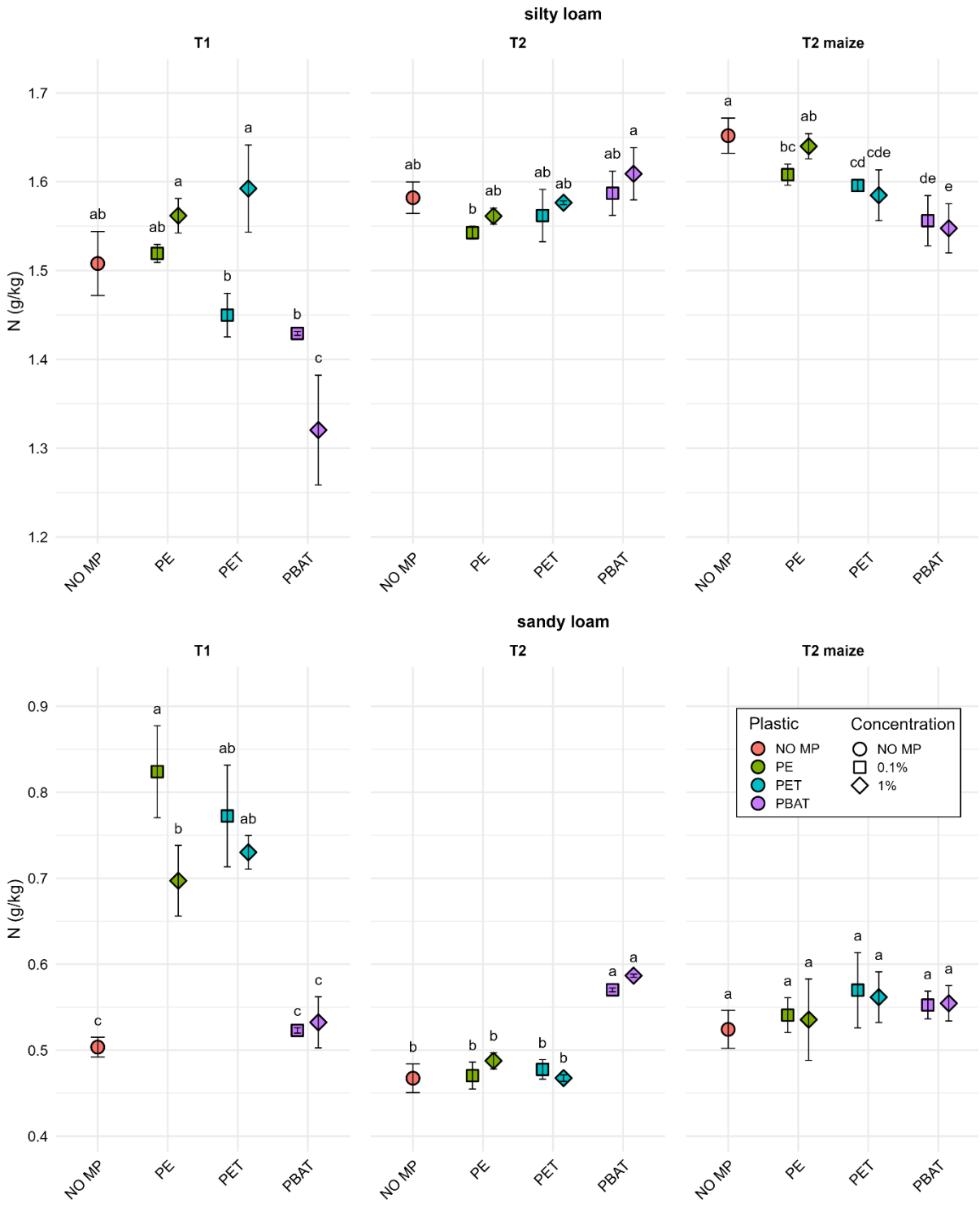

Figure S8. Soil total nitrogen of silty loam (top) and sandy loam (bottom) affected by concentration of MPs (0.1% and 1% w/w).

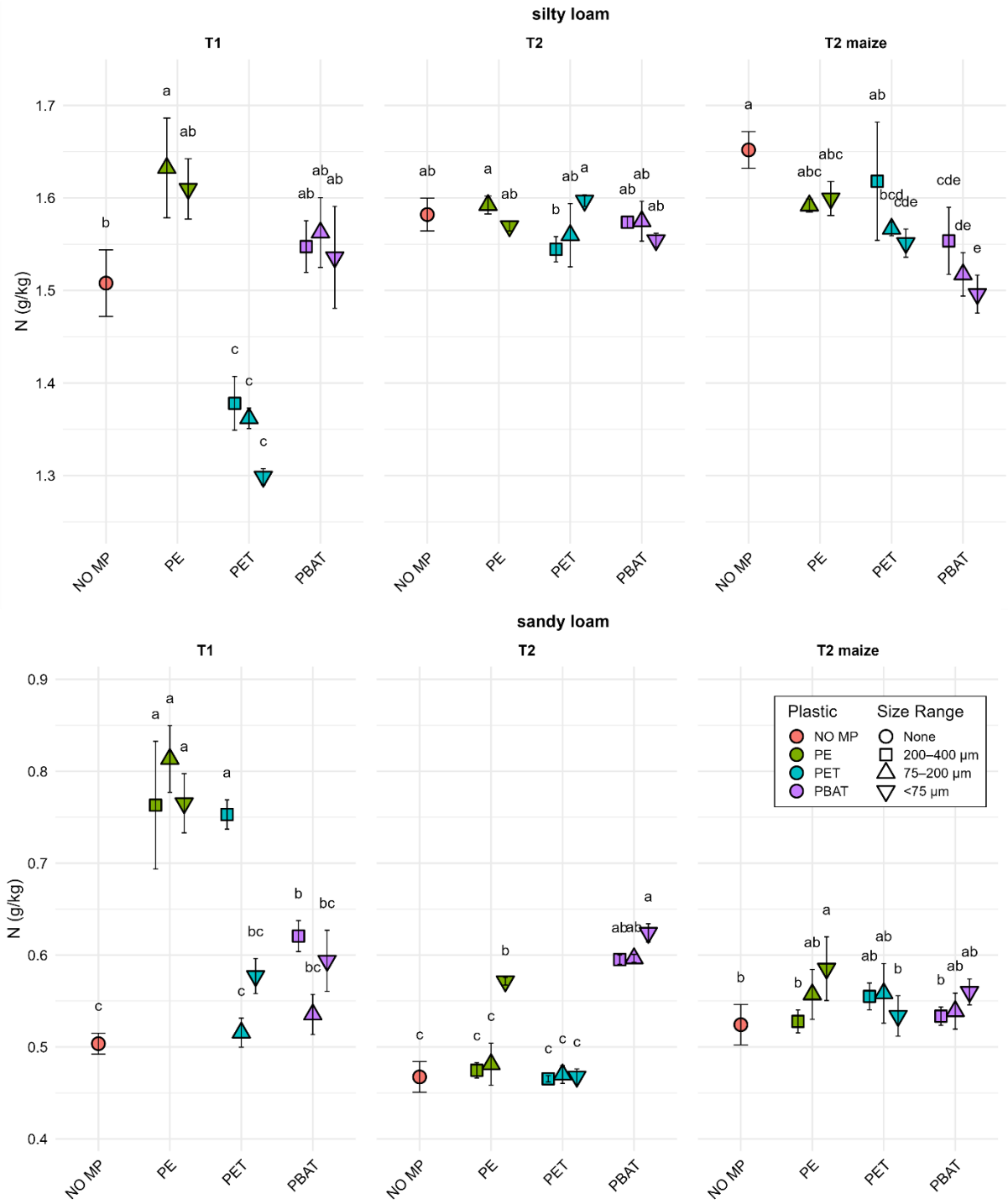

Figure S9. Soil total nitrogen of silty loam (top) and sandy loam (bottom) affected by size treatments of MPs (200–400, 75–200, and <75 µm).

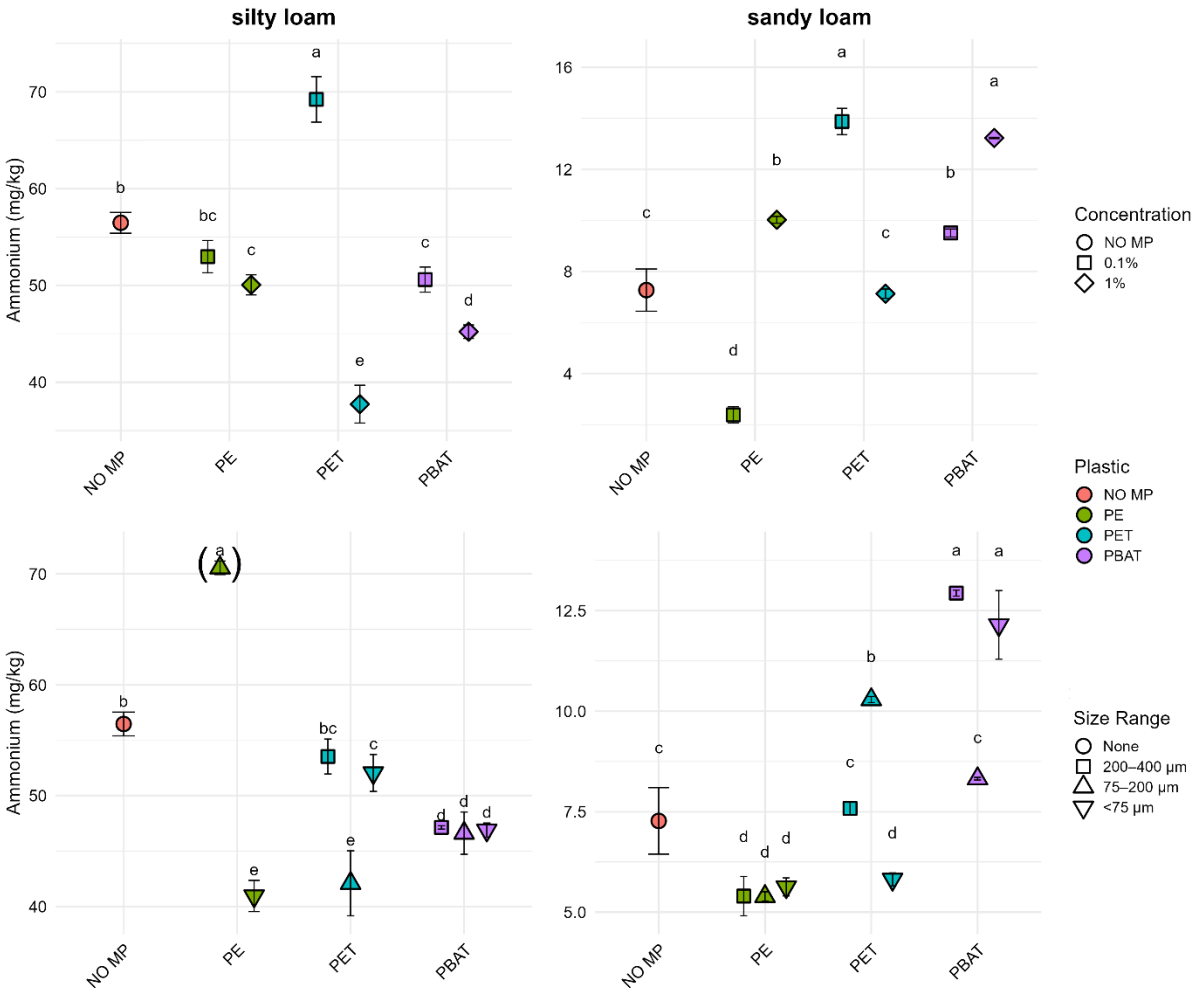

Figure S10. Plant-available ammonium at T1 (4 weeks) in silty loam (left) and sandy loam (right) with different concentrations (top) and different size ranges (bottom) of MPs treatments. PE 75–200 µm indicated as outlier (brackets).

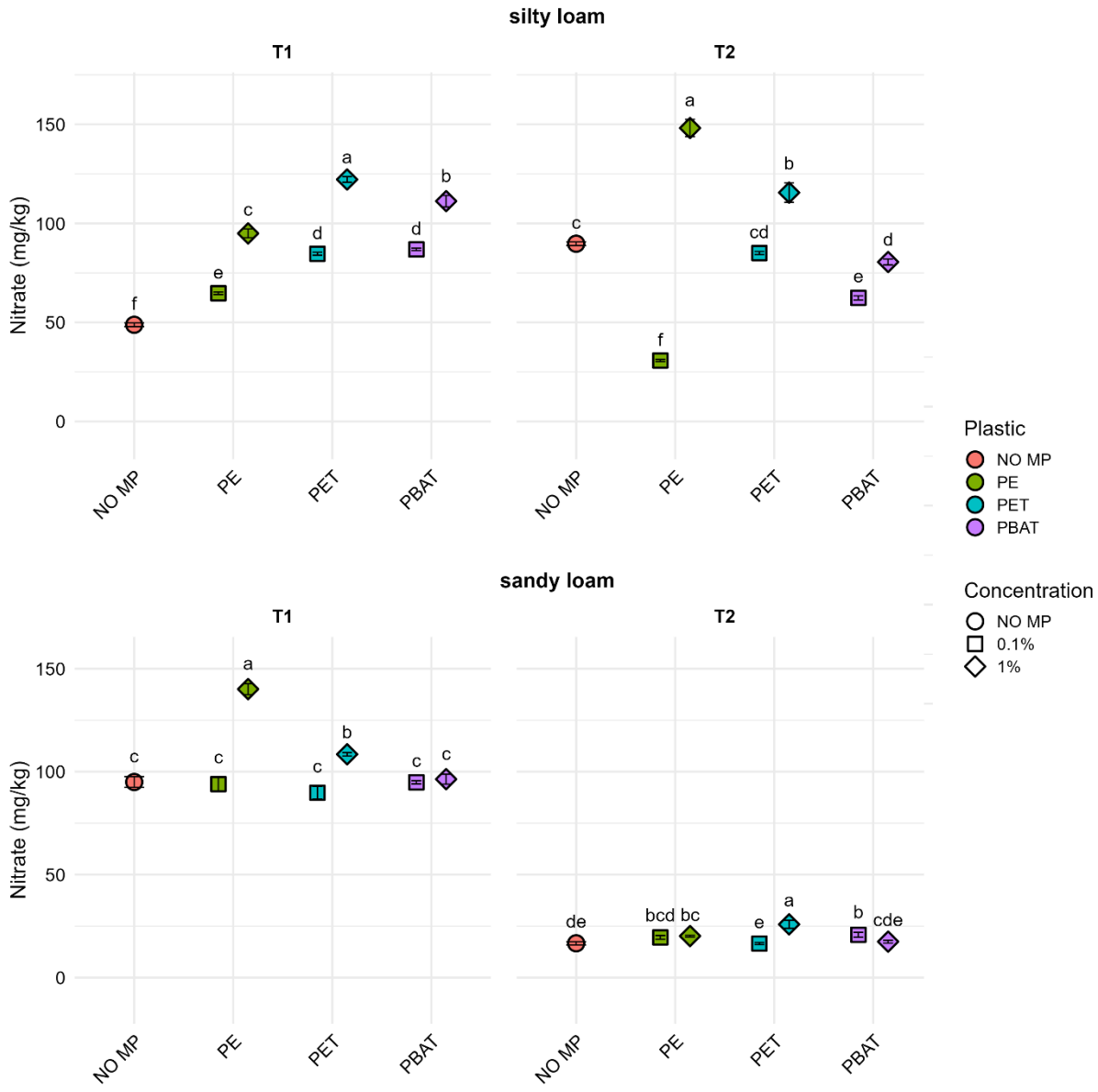

Figure S11. Plant-available nitrate in silty loam (top) and sandy loam (bottom) with MPs concentrations (0.1% and 1% w/w).

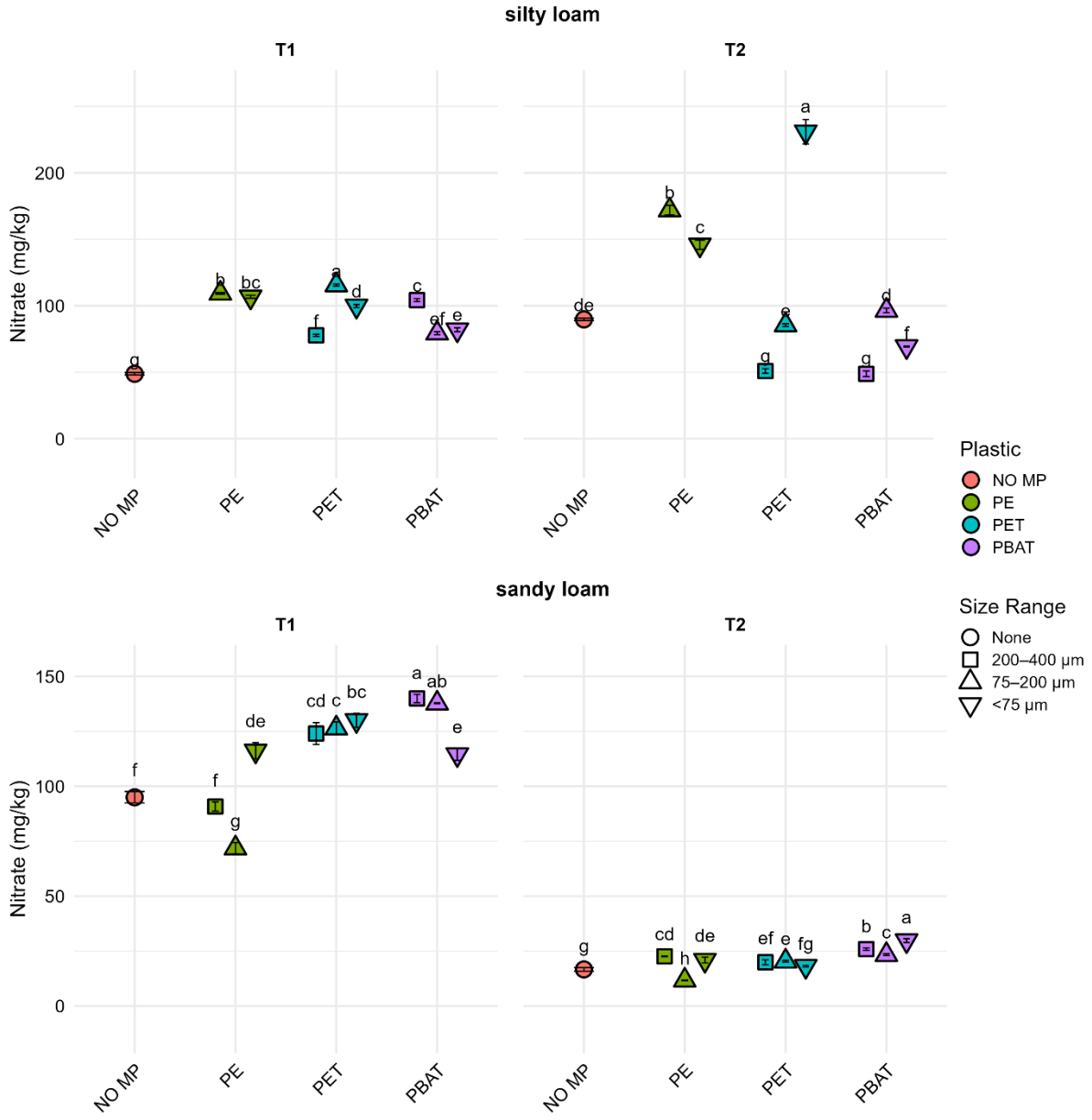

Figure S12. Plant-available nitrate in silty loam (top) and sandy loam (bottom) with MPs size ranges (200–400, 75–200, and <75 µm).

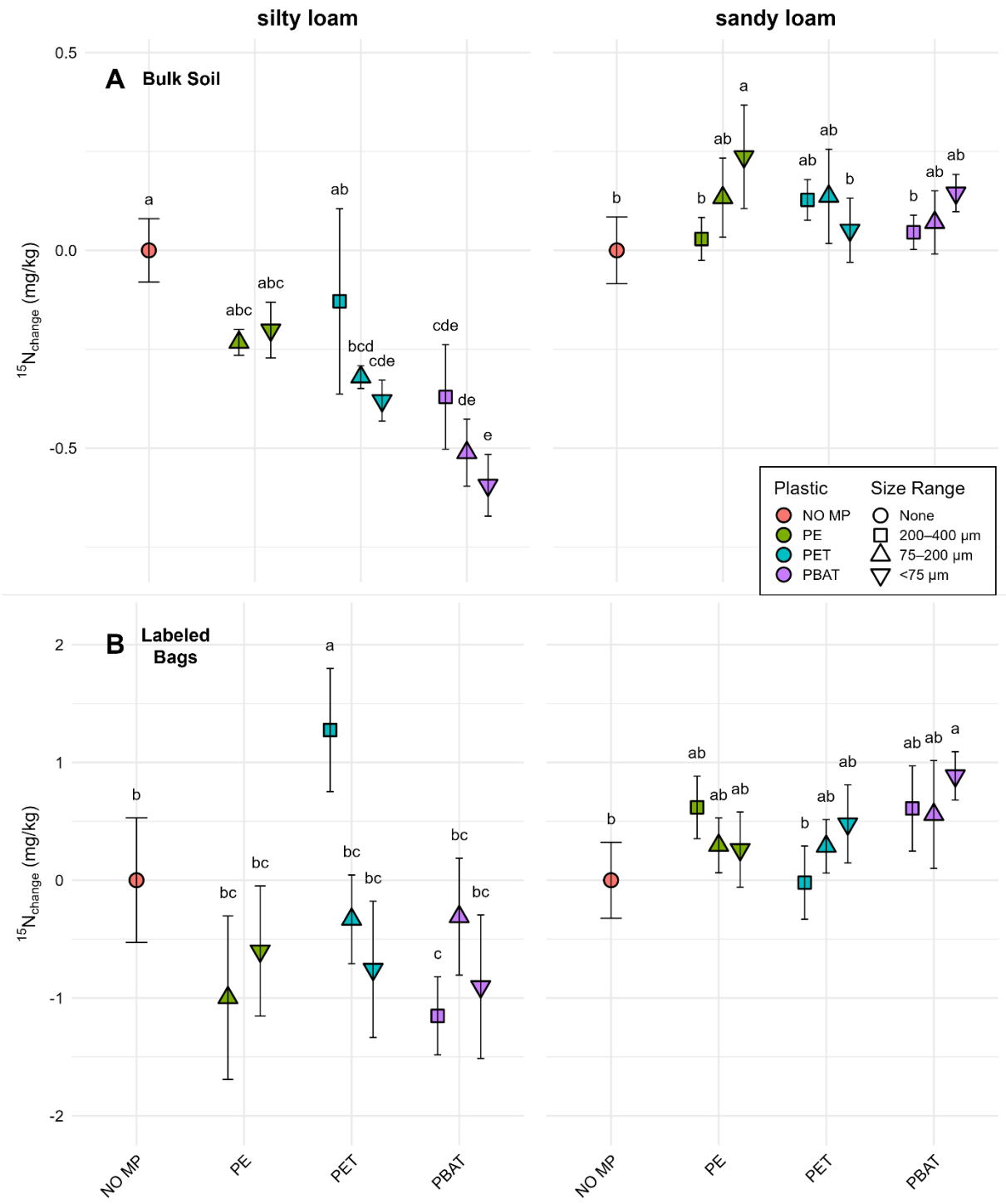

Figure S13. $^{15}N_{change}$ in bulk soil (A) and ^{15}N-fertilizer labeled bags (B) with MP size treatments (200–400, 75–200, and <75 µm) in silty loam (left) and sandy loam (right). Letters indicate significant effects ($p < 0.05$, Tukey's HSD) in each soil type.

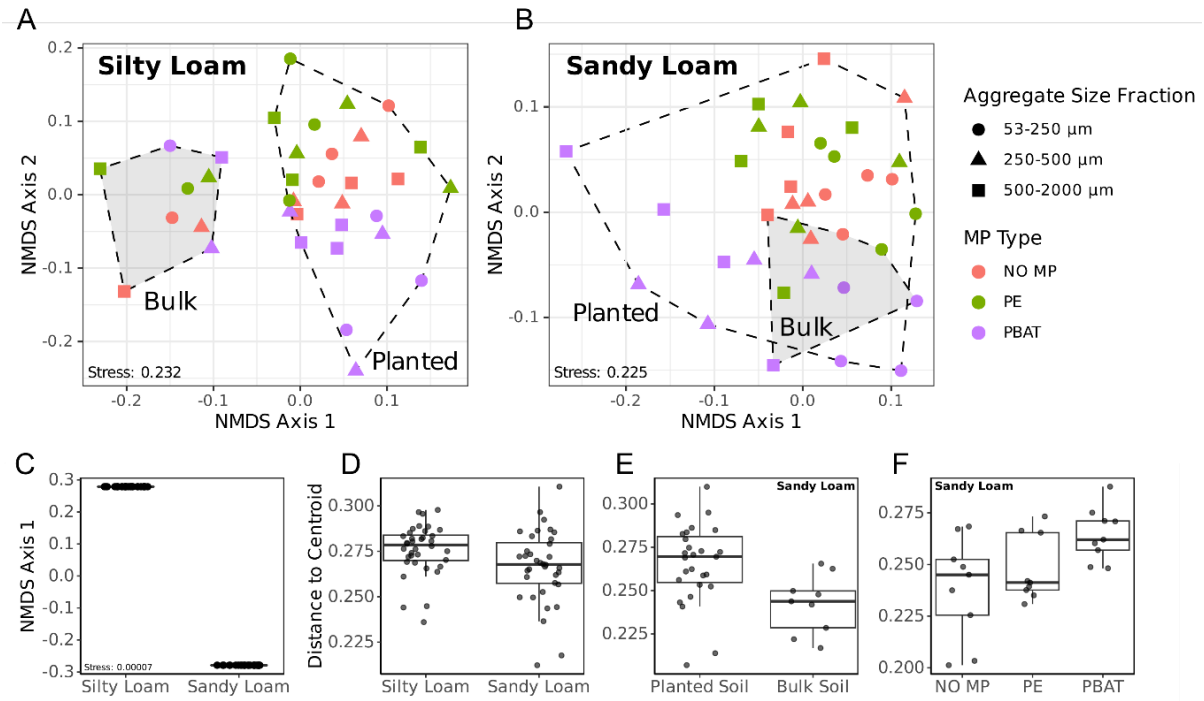

Figure S14. Beta diversity of bulk and planted soils. NMDS ordination based on Bray-Curtis dissimilarities between treatments in A) silty loam and B) sandy loam. C) NMDS axis 1 scores by soil type. Community dispersion to group centroids shown for D) soil type, E) planted and bulk sandy loam communities, and F) sandy loam MP treatments.

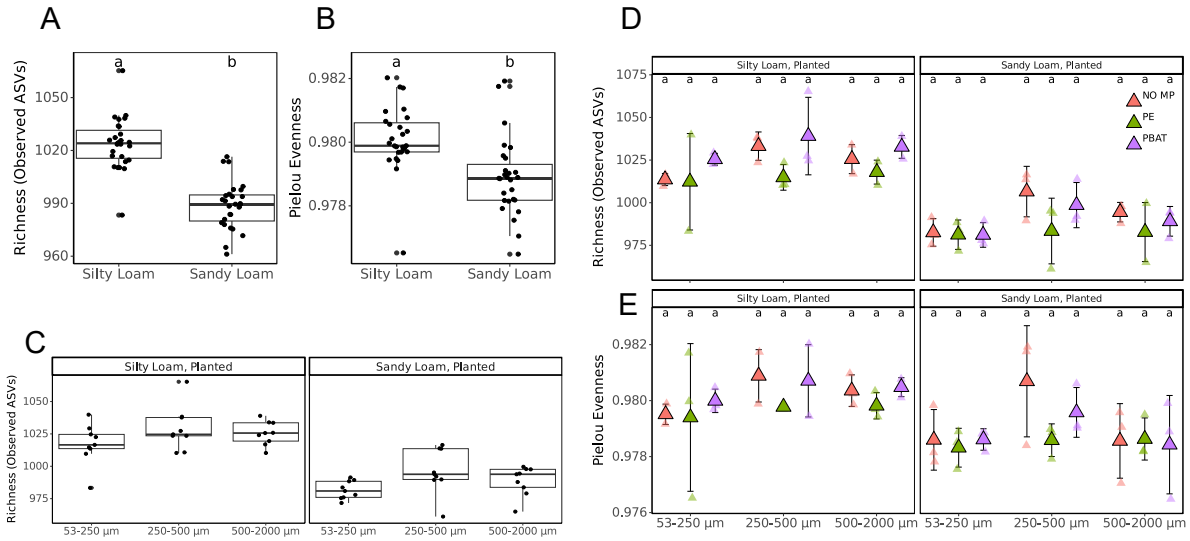

Figure S15. Alpha diversity metrics across soil type and MP treatments. ASV richness by A) soil type, B) Pielou's evenness by soil type, C) richness by aggregate size fraction, and D) MP treatment within each aggregate size fraction and soil type. E) Pielou's evenness for each MP amendment grouped by aggregate size fraction and soil type. Statistical analysis was performed using the Kruskal-Wallis and Dunn's rank sum post hoc tests with Benjamini-Hochberg correction. MP treatments were only compared to their respective no MP controls, and statistically significant differences were expressed using compact letter displays.

2. Manuscript 2: Biodegradable Microplastic Increases CO_2 Emission and Alters Microbial Biomass and Bacterial Community Composition in Different Soil Types

Adina Rauscher[1], Nele Meyer[1], Aileen Jakobs[2], **Ryan Bartnick**[1], Tillmann Lueders[2], Eva Lehndorff[1]

[1]Soil Ecology, Bayreuth Center of Ecology and Environmental Research (BayCEER), University of Bayreuth, Dr.-Hans-Frisch-Str. 1-3, 95448 Bayreuth, Germany
[2]Ecological Microbiology, Bayreuth Center of Ecology and Environmental Research (BayCEER), University of Bayreuth, Dr.-Hans-Frisch-Str. 1-3, 95448 Bayreuth, Germany

Applied Soil Ecology, *182*, 104714, 2023. https://doi.org/10.1016/j.apsoil.2022.104714

Applied Soil Ecology 182 (2023) 104714

Contents lists available at ScienceDirect

Applied Soil Ecology

journal homepage: www.elsevier.com/locate/apsoil

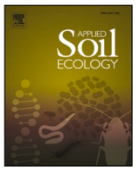

Biodegradable microplastic increases CO_2 emission and alters microbial biomass and bacterial community composition in different soil types

Adina Rauscher [a], Nele Meyer [a,*], Aileen Jakobs [b], Ryan Bartnick [a], Tillmann Lueders [b], Eva Lehndorff [a]

[a] Soil Ecology, Bayreuth Center of Ecology and Environmental Research (BayCEER), University of Bayreuth, Dr.-Hans-Frisch-Str. 1-3, 95448 Bayreuth, Germany
[b] Ecological Microbiology, Bayreuth Center of Ecology and Environmental Research (BayCEER), University of Bayreuth, Dr.-Hans-Frisch-Str. 1-3, 95448 Bayreuth, Germany

ARTICLE INFO

Keywords:
Microplastic
Low-density polyethylene
Polybutylene adipate-*co*-terephthalate
Soil respiration
Microbial activity
Microbial community

ABSTRACT

Plastic input to the terrestrial environment is of global concern and the still increasing production and release worldwide reinforces this problem. It has been shown that microplastics (MPs) can affect soil structure and soil organisms, possibly leading to an increase in soil carbon turnover, microbial activity and resulting CO_2 emissions. Yet, the response of soil CO_2 emissions to various types, quantities, and sizes of microplastic is not well understood. The aim of this work was to investigate the effect of conventional and biodegradable microplastics on soil microbial biomass, bacterial community composition and CO_2 development. Two types of plastics, LDPE (low-density polyethylene) and PBAT (polybutylene adipate-*co*-terephthalate), at low (0.1 %) and high (1 %) concentrations and in three different size ranges (50–200 μm, 200–500 μm, and 0.63–1.2 mm) were amended to a sandy loam and a loamy soil and CO_2 emissions were measured over four weeks. Afterwards, microbial biomass and growth were estimated, and prokaryotic community shifts were inferred by amplicon sequencing. No effect of LDPE on soil CO_2 emissions could be detected, but higher CO_2 emissions (13–57 %), microbial biomass (1–7 %), and a shift in community composition was induced by addition of the biodegradable PBAT when added at high concentration. Soil CO_2 emissions were 10–13 % greater when small PBAT particles were added compared to large ones. PBAT addition at low concentration had no significant effect independent of its size. Overall, the effect of PBAT addition on soil CO_2 emissions was larger in sandy loam than in loam. Several bacterial lineages known to degrade polyesters and other biodegradable MPs, such as members of the *Caulobacteraceae* and *Comamonadaceae* were found enriched after PBAT amendment, but effects were soil specific. We conclude that direct impacts of plastic on soil properties are not the main reason for increased soil CO_2 emissions, but rather relate to the different recalcitrance of polymer types. Soils contaminated with biodegradable plastic may emit larger amounts of CO_2, which needs to be considered in predictions of global impacts of plastic pollution and its mitigation.

1. Introduction

Today's world is hard to imagine without plastic. The global production of resins and fibers, from which the known plastic is produced with the addition of additives, increased from 2 Mt. in 1950 to 380 Mt. in 2015 (Geyer et al., 2017). Forecasts show a further increase in production, so that 34,000 Mt. of primary plastic could be produced by 2050 (Geyer et al., 2017). If plastic enters the soil, larger particles often break to smaller ones forming microplastics (MPs), typically defined in a size range < 5 mm (De Souza Machado et al., 2018b). Studies have shown that soil MPs can have impacts on various soil physical and chemical properties as well as on organisms such as earthworms and microbes (De Souza Machado et al., 2018a, 2018b; Huerta Lwanga et al., 2016; Lozano and Rillig, 2020; Wang et al., 2022a; Wang et al., 2022b). Although the fate of MPs in soil receives increasing attention, many questions remain unanswered. In particular, its influence on microbial biomass and soil CO_2 emissions is not well understood (Rillig et al., 2021), despite the great importance of soil for the global carbon budget and thus also climate change (Raich and Tufekcioglu, 2000).

After plastic is released into the environment, many of the commonly

* Corresponding author.
E-mail address: nele.meyer@uni-bayreuth.de (N. Meyer).

https://doi.org/10.1016/j.apsoil.2022.104714
Received 17 June 2022; Received in revised form 20 October 2022; Accepted 22 October 2022
Available online 29 October 2022

used types of plastic cannot be degraded in a short time but accumulate in ecosystems. Resistance to hydrolytic and enzymatic degradation is provided by the polymers' carbon skeletons (Ng et al., 2018). Widely used plastic types with high stability are, for example, polyethylene (PE) and polypropylene (PP), for which a very long lifetime is predicted (Kyrikou and Briassoulis, 2007; Ng et al., 2018). In contrast to conventional polymer types, which are produced due to their high resistance to degradation, there are also so-called biodegradable polymers. These have heteroatoms (O, N, S) along their carbon structure, at which hydrolytic or enzymatic reactions can take place, which leads to a significant reduction in the persistence of plastics (Ng et al., 2018). This, in turn, allows microorganisms to absorb the plastic particles, mineralize it to CO_2, CH_4 and H_2O, and to incorporate degradation products into their biomass (Ng et al., 2018). Examples of biodegradable plastics are polylactides (PLA), polycaprolactone (PCL), and polybutylenadipat-*co*-terephthalate (PBAT) (Ng et al., 2018; Jian et al., 2020). Indeed, for PBAT, Kijchavengkul and Auras (2008) could demonstrate biodegradation caused by microbial degradation and hydrolysis.

Several studies showed that both conventional and biodegradable MPs have an effect on physical and chemical soil properties (De Souza Machado et al., 2018a, 2018b; Wang et al., 2022a; Wang et al., 2022c). For instance, Rillig et al. (2021) reported a significant increase in the number of water-stable soil aggregates and in their mean weight diameter (MWD). As a result, air permeability and oxygen supply increased slightly. De Souza Machado et al. (2018a, 2018b), however, reported contrasting results and found a significant decrease in water-stable aggregates by MPs. Besides physical effects, also changes in soil pH and nutrient concentrations were reported (reviewed by Wang et al., 2022a), though results varied with plastic type, concentration, and size. As microorganisms are strongly influenced by chemical and physical soil properties, MPs have also been reported to alter microbial activity (De Souza Machado et al., 2018a, 2018b) and community composition (Yu et al., 2021; Wang et al., 2022c). As microorganisms are driving the degradation of plastic and the decomposition of soil organic matter, a changed microbial community, biomass, and activity may ultimately also affect CO_2 emissions from soil. Indeed, Rillig et al. (2021) reported a significant increase in CO_2 emissions by 5 to 26 % caused by MP addition. Also, Zhang et al. (2022) observed that LDPE at a concentration of 1 % increased CO_2 emissions significantly by 15–17 %. Yet, lower concentrations showed no significant effect.

Assuming that MPs affect soil CO_2 emissions especially through their impact on soil physical properties (cf. Rillig et al., 2021), such as aggregate stability and porosity, soil specific effects may be expected. For instance, the ability of soils to form aggregates considerably depends on their texture: the higher the sand content, the less aggregation (Totsche et al., 2018; Simon et al., 2020). Also, sandy soils are usually already well aerated, leading to the assumption that improved porosity caused by MP addition will not alter soil CO_2 emissions as much as in poorly aerated soils. Yet, the soil specific effect of MPs has rarely been considered so far.

Previous studies showed that the effect of MP on soil microorganisms depends on plastic type (Feng et al., 2022; Wang et al., 2022c). Especially biodegradable plastics may result in increasing soil CO_2 emissions. This can be explained by its impact on physical and chemical soil properties but also by its degradation, which leads to additional CO_2 emissions. For instance, the application of 10 % poly(3-hydroxybutyrate co-3-hydroxyvalerate) (PHBV), which is considered biodegradable, showed an increased CO_2 emission from soil, which could mainly be attributed to its degradation (Zhou et al., 2021).

The aim of this study was to investigate the effect of conventional and biodegradable microplastics on soil microbial biomass, bacterial community composition and CO_2 emissions. We added two different types of microplastic (LDPE and PBAT) to two soils (sandy loam and loam), in two quantities (0.1 % and 1 % of the dry soil weight), and three size ranges (50–200 µm, 200–500 µm, and 0.63–1.2 mm). We measured soil CO_2 emissions, substrate-induced respiration as an indicator of microbial biomass and growth (MBC; Anderson and Domsch, 1978), as well as prokaryotic community composition. We hypothesized that biodegradable PBAT, which is more susceptible to degradation, will increase soil CO_2 emissions and biomass and cause more pronounced shifts in microbiome composition in comparison with LDPE. Further, due to their larger specific surface, smaller PBAT particles are more easily accessible to microorganisms and may be more rapidly degraded than coarse PBAT particles. We further hypothesized that MP addition will cause more CO_2 release from loamy soil compared to sandy loam soil due to physical impact on soil structure.

Table 1
Basic parameters of the two soils investigated.

	Sandy loam	Loam
C content [g kg^{-1}]	13.25	13.45
N content [g kg^{-1}]	1.25	1.34
pH-value	6.9	5.8
WHC [g water g^{-1} soil]	0.59	0.79
Sand (%)	76.4	50
Silt (%)	7.3	29
Clay (%)	16.3	21

WHC = water holding capacity.

2. Methods

2.1. Sampling and preparation of soil

The soil used for the study was taken from the premises of the Agricultural Training Institute of the District of Upper Franconia in Bayreuth. From a grassland site (49.9267°N, 11.5476°E) a loam was sampled and from a cropland site (fallow at the time of sampling; 49.9295°N, 11.5545°E) a sandy loam (Table 1). Soil was taken at one location per field side from the top 30 cm with a spade after removal of vegetation. The soil was sieved to 2 mm (smaller soil aggregates stayed intact) and stored at 5 °C until use. For C/N analysis, soil was dried at 50 °C and grinded using a vibrating mill (Retsch MM 400) in a zirconium oxide coated container and measurements were conducted using a varioMAX (Elementar Analysesysteme, Hanau, Germany). As soils were free of carbonate by testing with 10 % HCl, we assume that total C represents the concentration of organic C. Gravimetric water content and water holding capacity were measured by submerging fresh soil in water for 30 min with subsequent drainage for 24 h and drying at 105 °C. The pH value was measured in H_2O with a soil:solution ratio of 1:2.5 (DIN 19682–13:2009–01). Texture was measured using PARIO, where the amounts of silt and clay particles are determined using Stokes' law in a sedimentation analysis, and the amount of sand particles is separated by sieving (METER Group, 2018). The soils were classified as loam and sandy loam according to the World Reference Base.

2.2. Preparation of the plastic

Low-density polyethylene (LDPE) and polybutyleneadipate-*co*-terephthalate (PBAT) were used for this study. The LDPE was produced by the company LyondellBasell (product name Lupolen 1800 P), was not additivated, and had a density of 0.918 g cm^{-3}. PBAT was produced by the company AKROPLASTIC GmbH (product name M-VERA B5026 (B0104)) and had a density of 1.25 g cm^{-3}. The C content of PBAT was 62.16 % while N was below the detection limit. Three size classes were applied: “small” (50–200 µm),”medium” (200–500 µm), and “large” (630–1200 µm). The small and medium size classes were obtained by milling of larger particles with subsequent sieving to the desired size class. The large size class was obtained by manual fragmentation of larger particles using a scalpel and subsequent sieving to the desired size class. Due to differences in production, the distribution of particle sizes within each class varied slightly between LDPE and PBAT. The small-sized LDPE mainly ranged from 75 to 200 µm while PBAT covered the

entire range from 50 to 200 µm. The medium-sized LDPE mainly ranged between 200 and 400 µm, while PBAT covered the entire range from 200 to 500 µm. Gloves have been used when cutting the plastic manually and all equipment had been cleaned thoroughly to avoid contamination of the plastic during handling.

2.3. Incubation experiment

The incubation experiment was conducted using a Respicond V system, which allows incubating 95 samples in parallel (Nordgren, 1988). The Respicond system provides a measurement of CO_2 evolution every 60 min by trapping CO_2 in potassium hydroxide (KOH) (Nordgren, 1988).

For the experiment, 39 vessels (250 ml) were filled with 50 g (based on dry weight) of sandy loam or loamy soil, respectively, brought to a water holding capacity of 40 %, and compressed to a density of 1 g per cm^3 using a stamp. As soil structure is affected by sieving, we decided not to readjust the bulk density to original values as this would not have resulted in a similar structure as in the undisturbed soil. Instead, 1 g per cm^3 was chosen to create standardized and comparable conditions of soil samples. All samples were pre-incubated for 12 days at 22 °C. Subsequently, plastic was added to the soil. For both types of plastic, a concentration of 0.1 % and 1 % of soil weight was added from each of the three size classes and carefully mixed with a spatula. In addition, controls without plastic were also mixed with a spatula. Each treatment was with three replicates. Afterwards, the measurement ran for another four weeks at 22 °C in the dark. Vessels were kept closed throughout the measurement. Soil CO_2 emissions were expressed as the cumulative CO_2 release during the incubation.

Subsequently, substrate-induced respiration was measured for determination of microbial biomass (Anderson and Domsch, 1978) and growth characteristics (Blagodatsky et al., 2000; Meyer et al., 2017). This method bases on the principle that the addition of a highly labile C source (i.e. glucose) activates all living microorganisms in the soil sample. The resulting higher level of soil CO_2 emissions is therefore proportional to the amount of microbial biomass in the soil (Anderson and Domsch, 1978). After a lag time of a few hours, microorganisms start to grow on the added glucose resulting in an exponential growth phase which persists until a peak respiration rate is reached, where glucose or nutrient availability limits further growth. The growth rate and the maximum peak respiration rate can therefore inform about microbial activity (Blagodatsky et al., 2000) and nutrient availability (Meyer et al., 2017; Nordgren, 1992) in soil. For this experiment, 300 mg glucose (6 mg glucose per g soil; recommended for mineral soils by Lin and Brookes, 1999) per vessel was added and mixed with a spatula. In total, substrate-induced respiration was measured for 13 days. Vessels were opened several times during the experiment to replace the KOH solution and to allow ventilation. Microbial biomass carbon (MBC) in each vessel was determined leaning on the formula described by Anderson and Domsch (1978) (Eq. (1)), in which the amount of CO_2 from the lag phase (e.g. within the first 6 h after glucose addition) before the exponential increase in substrate-induced respiration was used.

$$\mathrm{MBC}\ \left[\mathrm{mg\ kg\ soil^{-1}}\right] = \left(\mathrm{CO_2}\ \left[\mathrm{ml\ g\ soil^{-1}\ h^{-1}}\right]\ \mathrm{x}\ 40,04 + 0{,}37\right)\ \mathrm{x}\ 1000 \quad (1)$$

2.4. Prokaryotic community analysis

DNA extraction was performed from ~500 ± 54 mg (wet weight) soil samples after incubation of the 1 % small MPs amended soils, controls and from initial soil. The treatments with 1 % small MPs were chosen as they revealed the larges effect on soil CO_2 efflux and microbial biomass and was therefore most suitable to investigate potential effects of MPs on the soil prokaryotic community. DNA extraction was performed following the protocol of Lueders et al. (2004) with minor modifications. For this, samples were mixed with 0.2 ml of a 1:1 mixture of Ø 0.1 mm and Ø 0.7 mm zirconia/silica beads (BioSpec Products, USA), 800 µl PTN buffer (120 mM Na_2HPO_4/NaH_2PO_4, 125 mM Tris-HCl/Tris-Base, 0.25 mM NaCl, pH 8. 0), 100 µl of a 20 % SDS solution, 200 µl phenol/chloroform/isoamyl alcohol (in the ratio 25:24:1, pH 8.0; Carl Roth GmbH + Co. KG, Germany) and comminuted using a TissueLyzer II (QIAGEN, Germany) for 1 min at 30 Hz. Samples were then centrifuged for 4 min at 14000 rpm and 4 °C (1-15 K microcentrifuge, Sartorius, Germany). 850 µl supernatant was transferred to 2 ml Phase-Lock-Gel-Heavy tubes (VWR, Germany) and extracted with 1 volume of phenol/chloroform/isoamyl alcohol. After another centrifugation step and supernatant transfer into a new Phase-Lock-Gel-Heavy tube, 1 volume of chloroform/isoamyl alcohol (ratio 24:1; Carl Roth) was added, shaken vigorously and centrifuged again. Subsequently, the supernatant was mixed with 2 volumes of PEG (30 % PEG, 1.6 M NaCl; Carl Roth, Germany) and DNA was then precipitated for 2.5 h at 4 °C. After a 45 min centrifugation, supernatant was discarded and pellet was washed with 300 µl ice-cold 70 % (*v*/v) ethanol. Followed by a 4 min centrifugation and ethanol discard, the pellet was dried for 5 min at room temperature and DNA was dissolved in 30 µl elution buffer (QIAGEN, Germany).

Preparation of 16S rRNA amplicons for Illumina sequencing was performed using primer pair 515F (5'-GTGYCAGCMGCCGCGGTAA-3′; Parada et al., 2016) and 806R (5'-GGACTACNVGGTWTCTAAT-3′; Apprill et al., 2015) targeting the V4 hypervariable region of bacterial and archaeal 16S SSU rRNA, extended with Illumina-specific universal adapters. PCRs were prepared in 50 µl reactions using NEBNext® High-Fidelity 2× PCR Master Mix (New England Biolabs, USA) following manufacturer's instructions with addition of 0.4 µl BSA (20 µg/µl; Roche, Switzerland) and 12 ± 3.4 ng DNA/per reaction. The thermal profile consisted of an initial denaturation for 30 s at 98 °C, followed by 25 cycles of 10 s denaturation at 98 °C, 30 s annealing at 55 °C, and 30 s elongation at 72 °C. Followed by a 2 min final elongation at 72 °C. After a second round of PCR to generate the final barcoded amplicon constructs, sequencing was performed in a custom 300-bp paired-end read mode on an Illumina iSeq 100 sequencer. Size-based purification of PCR products (after first and second round of PCR) was performed using a Pippin Prep instrument (Biozym Scientific, Germany), and subsequent size and concentration determination of amplicons was carried out via automated capillary electrophoresis on an Agilent Fragment Analyzer System (Agilent, USA).

Raw 16S rRNA amplicon reads were demultiplexed and 291 bp forward reads were bioinformatically analyzed in single-end mode with the bioinformatics platform QIIME2 (Bolyen et al., 2019). In this process, adapter sequences, forward and reverse primers sequences, and regions with a Phred quality score below 25 (Q25) were clipped from the reads. Denoising, dereplication and chimera removal were performed using the DADA2 pipeline (Callahan et al., 2016). The assignment of the reads to amplicon sequence variants (ASVs) was performed with the naïve Bayes classifiers (Bokulich et al., 2018) trained on the SILVA reference database (version 138; Quast et al., 2013). Beta diversity was calculated based on unweighted UniFrac distances (Lozupone et al., 2007) and principal coordinates analysis (PCoA) plot generated via the Emperor plugin (Vázquez-Baeza et al., 2013) implemented in Qiime2. All raw sequencing data have been deposited with the NCBI Sequence Read Archive (SRA) under the project number PRJNA844606.

2.5. Statistical analysis

All statistics were calculated by R (version 3.6.1, R Core Team, 2013). Results were expressed as mean and standard deviation of the three replicates per soil and treatment. In addition, we calculated the averaged percent deviation from the control value.

The results of the measurements were tested for normal distribution using the Shapiro-Wilk test and for homogeneity of variances using Levene's test ("car" package; Fox and Weisberg, 2019). For soil CO_2 emissions with plastic, substrate-induced respiration, and microbial biomass, we tested for significant differences with a multifactorial anova with soil type, plastic type, plastic size, and plastic content as factors. If

Table 2
Results of the multifactorial ANOVA for basal respiration and microbial biomass.

Factor	*P* value	
	Basal respiration	Microbial biomass
Soil type	<0.0001	<0.0001
Plastic type	<0.0001	<0.0001
Plastic size	0.012	<0.001
Plastic content	<0.0001	<0.0001
Soil type x Plastic type	0.023	0.995
Soil type x Plastic size	0.864	0.426
Plastic type x Plastic size	0.912	0.111
Soil type x plastic size	<0.0001	0.684
Plastic type x Plastic content	<0.0001	0.001
Plastic size x Plastic content	0.364	0.104
Soil type x Plastic type x Plastic size	0.675	0.195
Soil type x Plastic type x Plastic size	0.676	0.780
Soil type x Plastic size x Plastic content	0.105	0.086
Plastic type x Plastic size x Plastic content	0.059	0.459
Soil type x Plastic type x Plastic size x Plastic content	0.038	0.106

the multi-factorial anova showed significant differences, a single-factor anova was used to compare the individual treatments of the same plastic type and soil type. If there was a significant difference between the treatments, the Tukey HSD test ("agricolae" package; De Mendiburu and Yaseen, 2020) was used to differentiate exactly which of the treatments differed significantly from each other. If the normal distribution for the single factorial anova was not given, the Kruskal-Wallis test was used. Significance between different treatments was assumed from a *p*-value <0.05.

Differences in beta diversity between incubations were tested for statistical significance ($p < 0.05$) using a permutational multivariate analysis of variance (PERMANOVA) test implemented in QIIME2 with 999 permutations based on the weighted UniFrac distance metrics calculated for ASV composition. Moreover, analyses of composition of microbiomes (ANCOM) as implemented in QIIME2 was done to identify the taxa with the most marked differential abundance patterns during soil incubation or upon MPs treatment. Family-level taxa with the most marked distinctions for ANCOM discriminant indicators (sandy loam: $W > 27$, $clr > 28$; loam: $W > 48$, $clr > 33$) were selected for relative abundance comparison between samples.

3. Results

3.1. Soil CO_2 emissions

Soil CO_2 emissions differed significantly between the two soil types and were on average higher in loamy soil than in sandy loam soil (significant soil type effect; Table 2). Plastic addition had a significant effect on soil CO_2 emissions but this effect was dependent on soil type, plastic type, plastic size, and plastic content (significant interaction; Table 2). Treatments with PBAT had on average higher soil CO_2 emissions compared with the control when added at high concentration of 1 % (Fig. 1). In the sandy loam soil, 1 % PBAT always showed significantly higher CO_2 emissions than the control, which increased with decreasing size of the particles (up to 57 % increase; Fig. 1b). Lower concentrations, in contrast, had no significant effect on soil CO_2 emissions. The same trend applied to loamy soil. Here, however, only small and medium sized particles in high concentrations (1 %) increased soil CO_2 emissions significantly in comparison with the unamended control. The addition of LDPE had no significant effect on soil CO_2 emissions in comparison with the control, neither in sandy loam soil (Fig. 1a) nor in loamy soil (Fig. 1c).

The course of substrate-induced growth was not affected by plastic addition as can be inferred form visual inspection of Fig. 3, which revealed no distinct separation between the treatments. However, when comparing the growth curves between measurements with sandy loam and loam, it was noticeable that microbial growth during the exponential growth phase occurred faster in the sandy loam. This was evidenced by a higher and earlier occurring peak respiration rate in sandy loam than in loam. The loamy soil reached a lower maximum respiration rate and the corresponding peaked appeared several hours later (Fig. 3).

3.2. Microbial biomass

In general, MBC was larger in treatments with sandy loam soil compared to the treatments with loamy soil (significant soil type effect; Table 2; Fig. 2). The addition of plastic had, on average, a positive effect on MBC (Table 2; Fig. 2). Yet, this effect was dependent on plastic type and size (Table 2). LDPE did not affect MBC, neither in sandy loam soil

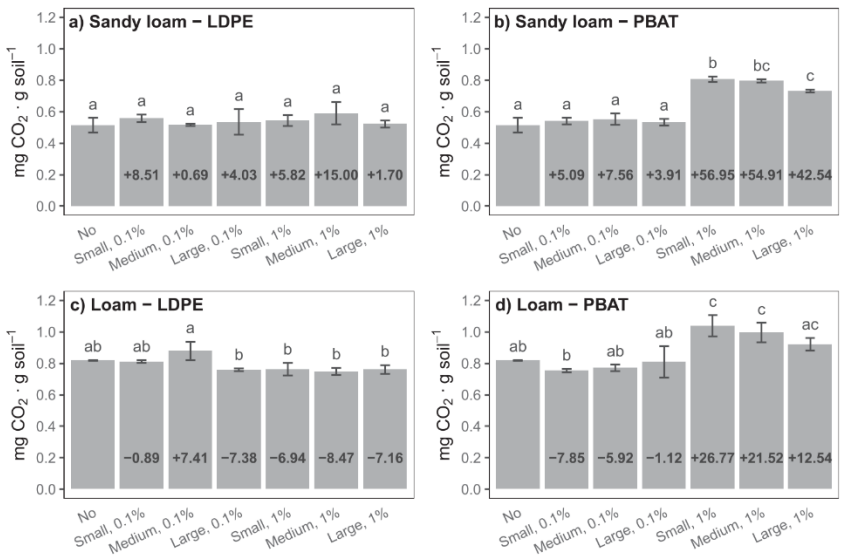

Fig. 1. Accumulated CO_2 emissions during four weeks of incubation, a) in sandy loam soil after LDPE addition, b) in sandy loam soil after PBAT addition, c) in loamy soil after LDPE addition, d) in loamy soil after PBAT addition. Bars represent mean value and standard deviation of the three replicates. sp., mp, and lp represent small, medium, and large plastic particles, and -p is the control without plastic addition. In each subfigure, different letters indicate significant differences between treatments. The percent deviation of the treatments from the control without plastic is shown in the bars.

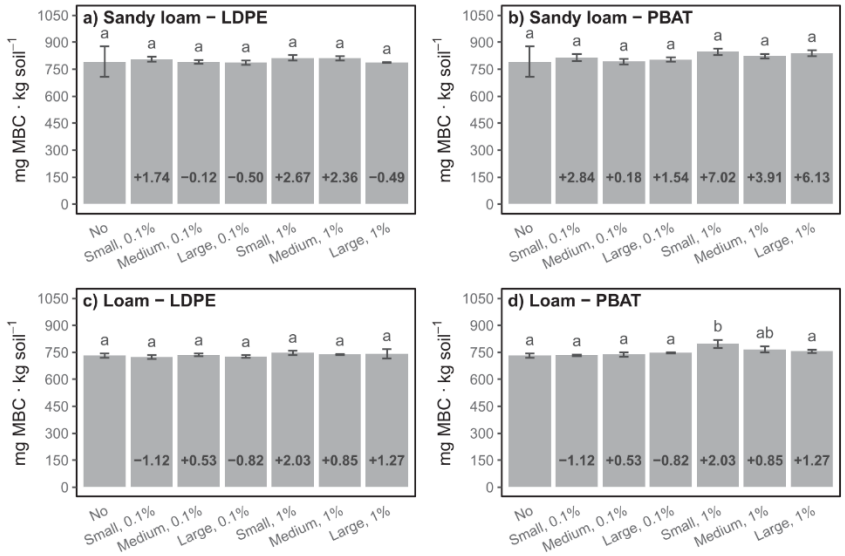

Fig. 2. Microbial biomass, a) in sandy loam soil after LDPE addition, b) in sandy loam soil after PBAT addition, c) in loamy soil after LDPE addition, d) in loamy soil after PBAT addition. The bars represent mean value and standard deviation of the three replicates. sp., mp and lp represent small, medium, and large plastic particles, and -p is the control without plastic addition. In each subfigure, different letters indicate significant differences between treatments. The percent deviation of the treatments from the control without plastic is shown in the bars.

(Fig. 2a) nor in loamy soil (Fig. 2c). Addition of PBAT, in contrast, consistently increased MBC both in sandy loam (Fig. 2b) and loamy soil (Fig. 2d) when added in large concentration (1 %).

3.3. Prokaryotic community structure

Assignment of representative 16S rRNA gene sequences to taxonomic groups of bacteria and archaea revealed that the majority of sequences in incubations with loamy (79.3–81.8 %) and sandy loam soil (67.6–72.8 %) were assigned to the phyla *Proteobacteria*, *Verrucomicrobiota*, *Actinobacteriota* and *Acidobacteriota* (Fig. 4). Phylum-level taxa with a maximum abundance below 1 % were grouped in the category "diverse" and accounted for max. 2.5 % in each sample. The top 5 most abundant taxa at family level in treatments with loamy soil were *Chthoniobacteraceae* (21.8 ± 0.4 % - 22.5 ± 1.2 %), *Xanthobacteraceae* (5.1 ± 0.2 % - 6.2 ± 0.4 %), uncultured *Vicinamibacterales* (3.4 ± 0.1 % - 5.1 ± 0.2 %), KD4–96 within the *Chloroflexi* (2.0 ± 0.3 % - 3.7 ± 0.3 %) and *Gemmataceae* (2.3 ± 0.2 % - 3.5 ± 0.5 %) (Fig. 4). In treatments with sandy loam soil the most abundant groups were *Nitrososphaeraceae* (4.0 ± 0.7 % - 6.9 ± 0.3 %), *Chthoniobacteraceae* (5.2 ± 0.3 % - 6.0 ± 0.4 %), uncultured *Vicinamibacterales* (4.4 ± 0.3–5.5 ± 0.0 %), *Vicinamibacteraceae* (4.1 ± 0.1 % - 4.5 ± 0.5 %) and *Xanthobacteraceae* (3.4 ± 0.4 % - 4.4 ± 0.2 %) (Fig. 4).

Weighted UniFrac distance metrics were used to compare the prokaryotic community similarity across samples (beta-diversity, Fig. 5). Incubations showed a clustering by soil type with a separation of incubations with loamy soil and sandy loam soil. In addition, the samples after incubation (loam/sandy loam, loam/sandy loam PBAT, loam/sandy loam LDPE) clustered distinctly from the initial soil inocula (loam t0, sandy loam t0). Moreover, communities of sandy loam soils showed a higher dissimilarity after incubation than those in loamy soils. Variation of prokaryotic community composition appeared slightly larger for PBAT amended soils than for PE- or unamended soils (Fig. S1), albeit statistically not significant (data not shown).

To more clearly elaborate potential effects of plastic treatment and polymer type on soil microbiota, ANCOM analysis was done to identify bacterial taxa with the most marked differential abundance patterns in our soil incubations (Fig. 6). Especially, amplicon reads within the family *Caulobacteraceae* were identified to increase in relative abundance in both PBAT amended soils compared to controls and PE-amendments (~2.1 to ~3.8-fold increase in loam and sandy loam, respectively), while reads within the *Comamonadaceae* increase only in PBAT amended sandy loam (~2.3-fold increase). In addition, an appearance of reads within the Ca. *Nomurabacteria*, albeit at minor abundance (~0.05 %), was only observed for PBAT-incubated sandy loam. A number of further taxa was observed to either increase or decrease in relative abundance during incubation, but here no further marked plastic-specific effects were observed.

4. Discussion

4.1. Does biodegradable PBAT alter soil CO_2 emissions, biomass, and microbiome composition more than LDPE?

LDPE amendment did not show any effect on CO_2 emissions, suggesting that plastic amendment alone did not affect microbial activity. This is surprising as MPs have been reported to alter porosity, bulk density, and aggregation (De Souza Machado et al., 2018a, 2018b; Rillig et al., 2021), known to affect microbial activity. Yet, both previous studies applied plastic fibers, which may well differ in effect on physical soil properties from the irregular fragmented particles used here. Indeed, De Souza Machado et al. (2018a, 2018b) also demonstrated that compact particles induced much smaller effects than fibers. The structure of the LDPE used, a carbon skeleton without functional groups, gives it a high chemical stability in soil, and microbes are mostly unable to access and degrade it (Meng et al., 2022; Ng et al., 2018). This was evident by the lack of influence of LDPE on soil CO_2 emissions, microbial biomass, and also prokaryotic community composition. Thus, we can conclude that the LDPE amendment was in an (almost) unaltered state after the completion of our experiment compared, which was unsurprising given the relative short incubation time of 14 days.

In contrast, PBAT addition clearly increased soil CO_2 emissions, microbial biomass carbon, and altered soil prokaryotic community composition. This can be attributed to the much lower chemical stability of PBAT compared to LDPE (Jian et al., 2020; Ng et al., 2018). The chemical structure of PBAT, interspersed with heteroatoms, allows the attack of hydrolytic and enzymatic reactions (Ng et al., 2018). This allowed microbes to access and mineralize PBAT to CO_2, incorporating polymer-derived carbon into their own biomass, as suggested by the increase in soil CO_2 emissions and microbial biomass. The assumption

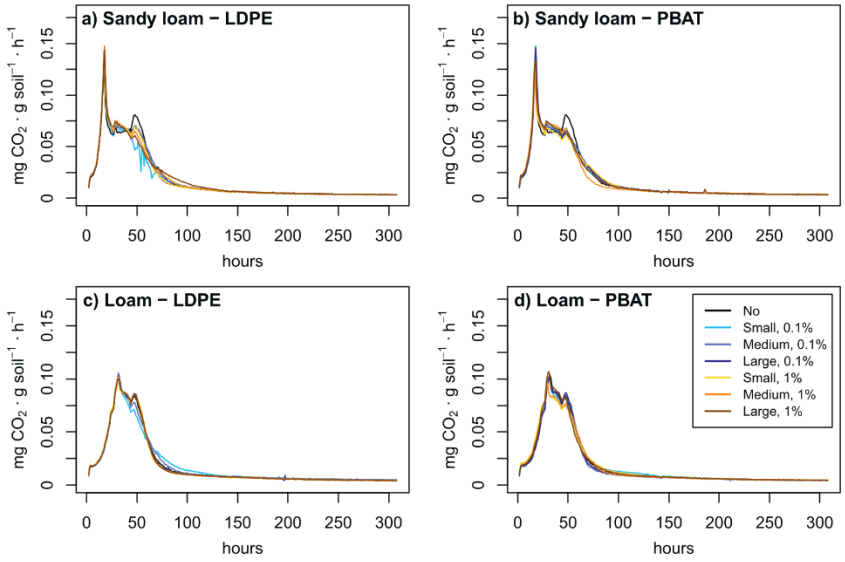

Fig. 3. Course of substrate-induced respiration a) for the combination of sandy loam and LDPE, b) for the combination of sandy loam and PBAT, c) for the combination of loam and LDPE, and d) for the combination of loam and PBAT. Concentration and size of MPs is depicted by different colours as indicated in the legend.

that larger CO_2 emissions actually result from degradation of PBAT and not from indirect effects, e.g. from alteration of physical soil properties which in turn affect CO_2 emissions, is evidenced by the finding that LDPE addition in similar size and concentration had no measurable effect. This is consistent with the study of Meng et al. (2022), which showed no mass loss of LDPE in a mesocosm experiment over 105 days, while the mass of PBAT decreased significantly during that time. This confirms the hypothesis that plastic degradability has an influence on soil CO_2 emissions and biomass even within a few weeks of soil incubation.

However, the fact that this effect was not observed at a PBAT concentration of 0.1 % can be explained by the much smaller amount of added substrate available for microorganisms. It was apparently not sufficient to trigger a significant change in soil CO_2 emissions. These results are in line with the findings of Zhou et al. (2021), who found an increase in CO_2 emission from soil by adding high concentrations (10 %) of the biodegradable poly (3-hydroxybutyrate-*co*-3-hydroxyvalerate), or PHBV, in a short-term measurement.

Most pronouncedly, a selective impact of PBAT amendment was observed on bacteria within the *Caulobacteraceae* (both soils), *Comamonadaceae* (sandy loam) and Ca. Nomurabacteria (sandy loam only). Members of the *Caulobacteraceae* have been previously identified to increase in relative abundance in the plastisphere of biodegradable polymers such as PBAT or PLA in alpine soils (Rüthi et al., 2020), while *Comamonadaceae* were reported to be enriched on starch-based biodegradable mulch films in a sandy soil (Qi et al., 2020). Furthermore, the *Comamonadaceae* include arguably one of the most prominent degraders of polyesters known to date, *Ideonella sakaiensis* (Yoshida et al., 2016), and both lineages have been frequently reported for plastisphere microbiomes in aquatic environments (Nguyen et al., 2021; Weig et al., 2021). Thus, not only an enrichment, but direct involvement of members of these taxa in PBAT degradation in our soil microcosms seems likely. The most significant PBAT-related enrichment, albeit at very low abundance, was observed for reads within the Ca. Nomurabacteria, associated with the Candidate Phyla Radiation (CPR) of the *Patescibacteria*. Here, functional context can clearly not be inferred, but the still enigmatic Ca. Nomurabacteria seem to be recently reported from the rhizosphere of agricultural plants such as tobacco or ginseng (Chen et al., 2022; Wang et al., 2020).

4.2. Does the effect of plastic particles increases with decreasing size?

Size effects of degradable plastics on CO_2 emission from our soils were also observed. Size dependent degradation processes are well known in the environment, e.g. the decay of fine particulate organic matter is more rapid compared to coarse particulate organic matter (Sinsabaugh and Linkins, 1990). This is explained by a different specific surface area of the particles. Since the surface area to volume ratio increases with decreasing particle size (increasing specific surface area; Petersen et al., 1996), smaller particles provided a larger surface area for microbial degradation. In a similar way we observed here that fine-grained PBAT went along with higher elevated CO_2 emissions than large particles. Thus, the hypothesis that small sized microplastic particles have a greater effect on soil CO_2 emissions could be supported, though only for PBAT and not for LDPE.

4.3. Does the effect of microplastic depend on soil texture?

We hypothesized that MP addition will cause more CO_2 release from loamy soil compared to sandy loam soil due to physical impact on soil structure, i.e. MP may affect soil CO_2 emissions through its impact on soil physical properties, such as aggregate stability and porosity, ultimately increasing its aeration (Rillig et al., 2021). According to our results, we have to reject this hypothesis. In line with this argumentation, we expected lower effects in the sandier soil, in which aeration is already high. Yet, the opposite was observed and soil CO_2 emissions increased significantly more by MP addition in the sandy loam compared to the loam. Further, significant differences between soils only applied to PBAT and at high concentrations. The finding that soil specific effects of MP addition were only observed for PBAT but not for LDPE indicate that MP effects on physical soil properties are not the main mechanisms for the observed differences.

It therefore seems more likely that soils differ in their response to MP addition due to their different accessibility of MPs to microorganisms and hence degradation rate. Our results may indicate a better availability of PBAT to microorganisms in the sandy loam. This difference

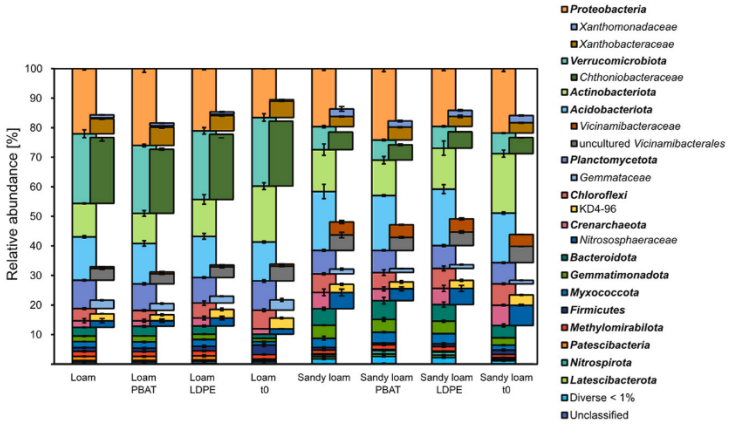

Fig. 4. Relative abundances of prokaryotic 16S rRNA gene amplicons in soil incubations without (loam, sandy loam) and with plastic amendment (loam PBAT, loam LDPE, sandy loam PBAT, sandy loam LDPE), and untreated soil before incubation (loam t0, sandy loam t0). Family level taxonomic units are highlighted only for the 5 most abundant taxa per soil. Bars represent mean values of biologically triplicated amplicon libraries, standard deviations are shown.

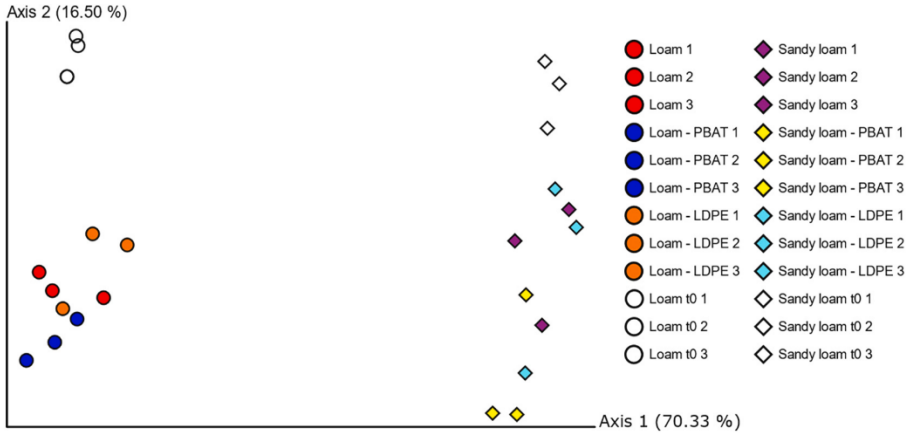

Fig. 5. Two-dimensional principal component analysis (PCoA) based on weighted UniFrac distance metrics of prokaryotic 16S rRNA amplicons from soil incubations without (loam, sandy loam) and with plastic amendment (loam PBAT, loam LDPE, sandy loam PBAT, sandy loam LDPE), and plain soil before incubation (loam t0, sandy loam t0).

could be attributed to texture, as other soil properties (C and N content, pH, and gravimetric water content) did not show relevant differences between the two soils (Table 1). Soils with a high clay and silt content tend to have more pronounced aggregation than sandier soils (De Gryze et al., 2006) and aggregate occluded matter is protected from microbial degradation (Totsche et al., 2018). The assumption that texture affected the accessibility of carbon-rich substrates in our experiment is also supported by the course of the substrate-induced respiration (Fig. 3). The faster microbial growth on added glucose in sandy loam soil may indicate a better accessibility of added sugar compared to the loamy soil. When the glucose was mixed into the soil, it probably distributed more evenly in the sandy loam and was less occluded in aggregates or adsorbed on mineral surfaces, resulting in better accessibility to the microorganisms. In turn, microorganisms in the loamy soil required a longer time to access a similar amount of glucose, which could explain the flattened substrate-induced respiration pattern. The same mechanisms may have played a role in the degradation of the added microplastic. A greater accessibility of PBAT in sandy loam could explain the greater increase in soil CO_2 emissions compared to loam.

5. Conclusion

Plastic is continuously accumulating in soils, including agricultural systems. Therefore, it is relevant to understand and predict how long MPs will remain in the soil and how it affects soil microbial properties. We were able to show that LDPE, classified as a conventional plastic type, does not affect CO_2 emissions from two different soils, and that a degradation of LDPE during a time course of four weeks was unlikely. In contrast, PBAT, a biodegradable plastic, was shown to stimulate soil microorganisms and CO_2 emissions, probably involving direct degradation. This was also supported by a marked increase in relative abundance of bacterial lineages previously reported to degrade polyesters and other biodegradable MPs. The effect of MPs increased with decreasing size of the plastic particles and with increasing concentration. This can cause increased CO_2 emissions from soils contaminated with biodegradable microplastics depending on soil texture. In the future, it must be clarified whether the addition of biodegradable plastic increases CO_2 emissions from soils through direct degradation, or whether the increased microbial activity also stimulates the degradation

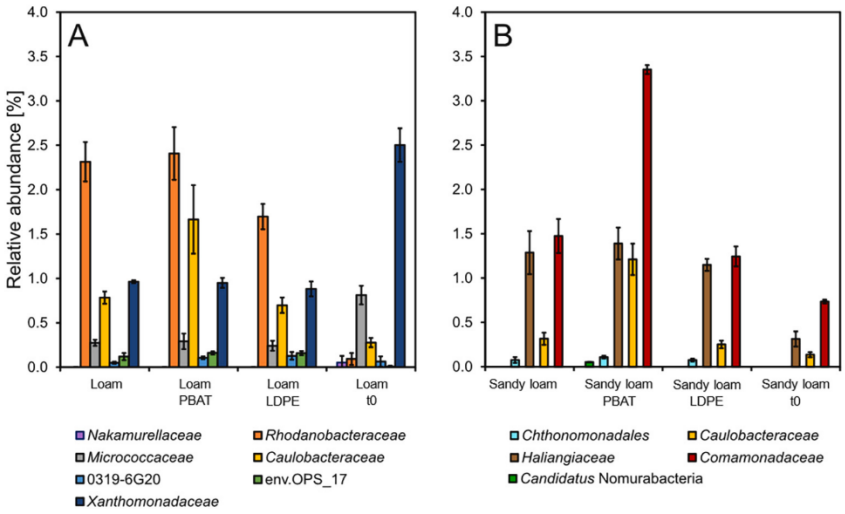

Fig. 6. Relative abundance comparison of bacterial taxa identified via ANCOM analyses to respond most markedly to plastic amendment (PBAT, LDPE) and microcosm incubation (t0 and after incubation) per soil type (loam, sandy loam).

of SOM (i.e. an unwanted "priming" effect).

Supplementary data to this article can be found online at https://doi.org/10.1016/j.apsoil.2022.104714.

Declaration of competing interest

The authors declare that they have no known competing financial interests or personal relationships that could have appeared to influence the work reported in this paper.

Data availability

Data will be made available on request.

Acknowledgements

This study was funded as part of the Collaborative Research Center 1357 "Microplastics - Understanding the mechanisms and processes of biological effects, transport and formation: From model to complex systems as a basis for new solutions" by the Deutsche Forschungsgemeinschaft (DFG, German Research Foundation) – SFB 1357 – Grant no. 391977956 – Subproject A06 to E.L. and T.L. We thank Seema Agarwal for providing PBAT (subproject C02 of the CRC1375) and we thank the KeyLab Genomics & Bioinformatics (subproject Z02 of the CRC1357) of the University of Bayreuth under the direction of Alfons Weig for library preparation and Illumina sequencing. Furthermore, bioinformatics was done within the BMBF-funded de.NBI Cloud within the German Network for Bioinformatics Infrastructure (de.NBI) (031A537B, 031A533A, 031A538A, 031A533B, 031A535A, 031A537C, 031A534A, 031A532B).

References

Anderson, J.P.E., Domsch, K.H., 1978. A physiological method for the quantitative measurement of microbial biomass in soils. Soil Biol. Biochem. 10, 215–221. https://doi.org/10.1016/0038-0717(78)90099-8.

Apprill, A., Mcnally, S., Parsons, R., Weber, L., 2015. Minor revision to V4 region SSU rRNA 806R gene primer greatly increases detection of SAR11 bacterioplankton. Aquat. Microb. Ecol. 75, 129–137. https://doi.org/10.3354/ame01753.

Blagodatsky, S.A., Heinemeyer, O., Richter, J., 2000. Estimating the active and total soil microbial biomass by kinetic respiration analysis. Biol. Fertil. Soils 32, 73–81. https://doi.org/10.1007/s003740000219.

Bokulich, N.A., Kaehler, B.D., Rideout, J.R., Dillon, M., Bolyen, E., Knight, R., Huttley, G. A., Caporaso, J.G., 2018. Optimizing taxonomic classification of marker-gene amplicon sequences with QIIME 2's q2-feature-classifier plugin. Microbiome 6, 90. https://doi.org/10.1186/s40168-018-0470-z.

Bolyen, E., Rideout, J.R., Dillon, et al., 2019. Reproducible, interactive, scalable and extensible microbiome data science using QIIME 2. Nat. Biotechnol. 37, 852–857. https://doi.org/10.1038/s41587-019-0209-9.

Callahan, B.J., McMurdie, P.J., Rosen, M.J., Han, A.W., Johnson, A.J.A., Holmes, S.P., 2016. DADA2: high-resolution sample inference from Illumina amplicon data. Nat. Methods 13, 581–583. https://doi.org/10.1038/nmeth.3869.

Chen, D., Zhou, Y., Wang, M., Mujtaba Munir, M.A., Lian, J., Yu, S., Dai, K., Yang, X., 2022. Succession pattern in soil micro-ecology under tobacco (Nicotiana tabacum L.) continuous cropping circumstances in Yunnan Province of Southwest China. Front. Microbiol. 12 https://doi.org/10.3389/fmicb.2021.785110.

De Gryze, S., Jassogne, L., Bossuyt, H., Six, J., Merckx, R., 2006. Water repellence and soil aggregate dynamics in a loamy grassland soil as affected by texture. Eur. J. Soil Sci. 57, 235–246. https://doi.org/10.1111/j.1365-2389.2005.00733.x.

De Mendiburu, F., Yaseen, M., 2020. agricolae: Statistical Procedures for Agricultural Research. R package version 1.4.0. https://myaseen208.github.io/agricolae/https://cran.r-project.org/package=agricolae.

De Souza Machado, A.A., Kloas, W., Zarfl, C., Hempel, S., Rillig, M.C., 2018. Microplastics as an emerging threat to terrestrial ecosystems. Glob. Chang. Biol. 24, 1405–1416. https://doi.org/10.1111/gcb.14020.

De Souza MacHado, A.A., Lau, C.W., Till, J., Kloas, W., Lehmann, A., Becker, R., Rillig, M.C., 2018. Impacts of microplastics on the soil biophysical environment. Environ. Sci. Technol. 52, 9656–9665. https://doi.org/10.1021/acs.est.8b02212.

Feng, X., Wang, Q., Sun, Y., Zhang, S., Wang, F., 2022. Microplastics change soil properties, heavy metal availability and bacterial community in a Pb-Zn-contaminated soil. J. Hazard. Mater. 424, 127364 https://doi.org/10.1016/j.jhazmat.2021.127364.

Fox, J., Weisberg, S., 2019. An R Companion to Applied Regression, Third edition. Thousand Oaks, CA, Sage. https://socialsciences.mcmaster.ca/jfox/Books/Companion/.

Geyer, R., Jambeck, J.R., Law, K.L., 2017. Production, use, and fate of all plastics ever made. Sci. Adv. 3, 3–8. https://doi.org/10.1126/sciadv.1700782.

Huerta Lwanga, E., Gertsen, H., Gooren, H., Peters, P., Salánki, T., Van Der Ploeg, M., Besseling, E., Koelmans, A.A., Geissen, V., 2016. Microplastics in the terrestrial ecosystem: implications for Lumbricus terrestris (Oligochaeta, Lumbricidae). Environ. Sci. Technol. 50, 2685–2691. https://doi.org/10.1021/acs.est.5b05478.

Jian, J., Xiangbin, Z., Xianbo, H., 2020. An overview on synthesis, properties and applications of poly(butylene-adipate-co-terephthalate)–PBAT. Adv. Ind. Eng. Polym. Res. 3, 19–26. https://doi.org/10.1016/j.aiepr.2020.01.001.

Kijchavengkul, T., Auras, R., 2008. Perspective compostability of polymers. Polym. Int. 57, 793–804.

Kyrikou, I., Briassoulis, D., 2007. Biodegradation of agricultural plastic films: a critical review. J. Polym. Environ. 15, 125–150. https://doi.org/10.1007/s10924-007-0053-8.

Lin, Q., Brookes, P.C., 1999. An evaluation of the substrate-induced respiration method. Soil Biol. Biochem. 31, 1969–1983. https://doi.org/10.1016/S0038-0717(99)00120-0.

Lozano, Y.M., Rillig, M.C., 2020. Effects of microplastic fibers and drought on plant communities. Environ. Sci. Technol. 54, 6166–6173. https://doi.org/10.1021/acs.est.0c01051.

Lozupone, C.A., Hamady, M., Kelley, S.T., Knight, R., 2007. Quantitative and qualitative β diversity measures lead to different insights into factors that structure microbial communities. Appl. Environ. Microbiol. 73 (5), 1576–1585. https://doi.org/10.1128/AEM.01996-06.

Lueders, T., Manefield, M., Friedrich, M.W., 2004. Enhanced sensitivity of DNA- and rRNA-based stable isotope probing by fractionation and quantitative analysis of isopycnic centrifugation gradients. Environ. Microbiol. 6, 73–78. https://doi.org/10.1046/j.1462-2920.2003.00536.x.

Meng, F., Yang, X., Riksen, M., Geissen, V., 2022. Effect of different polymers of microplastics on soil organic carbon and nitrogen – a mesocosm experiment. Environ. Res. 204 https://doi.org/10.1016/j.envres.2021.111938.

METER Group, 2018. Bedienungsanleitung PARIO. http://library.metergroup.com/%0AManuals/20780_PARIO_Manual_Web.pdf.

Meyer, N., Welp, G., Bornemann, L., Amelung, W., 2017. Microbial nitrogen mining affects spatio-temporal patterns of substrate-induced respiration during seven years of bare fallow. Soil Biol. Biochem. 104, 175–184. https://doi.org/10.1016/j.soilbio.2016.10.019.

Ng, E.L., Huerta Lwanga, E., Eldridge, S.M., Johnston, P., Hu, H.W., Geissen, V., Chen, D., 2018. An overview of microplastic and nanoplastic pollution in agroecosystems. Sci. Total Environ. 627, 1377–1388. https://doi.org/10.1016/j.scitotenv.2018.01.341.

Nguyen, N.H.A., El-Temsah, Y.S., Cambier, S., Calusinska, M., Hrabak, P., Pouzar, M., Boruvka, M., Kejzlar, P., Bakalova, T., Gutleb, A.C., Sevcu, A., 2021. Attached and planktonic bacterial communities on bio-based plastic granules and micro-debris in seawater and freshwater. Sci. Total Environ. 785, 147413 https://doi.org/10.1016/j.scitotenv.2021.147413.

Nordgren, A., 1988. Apparatus for the continuous, long-term monitoring of soil respiration rate in large numbers of samples. Soil Biol. Biochem. 20, 955–957.

Nordgren, A., 1992. A method for determining microbially available N and P in an organic soil. Biol. Fertil. Soils 13, 195–199. https://doi.org/10.1007/BF00340575.

Parada, A.E., Needham, D.M., Fuhrman, J.A., 2016. Every base matters: assessing small subunit rRNA primers for marine microbiomes with mock communities, time series and global field samples. Environ. Microbiol. 18, 1403–1414. https://doi.org/10.1111/1462-2920.13023.

Petersen, L.W., Moldrup, P., Jacobsen, O.H., Rolston, D.E., 1996. Relations between specific surface area and soil physical and chemical properties. Soil Sci. 161, 9–20. https://doi.org/10.1097/00010694-199601000-00003.

Qi, Y., Ossowicki, A., Yang, X., Huerta Lwanga, E., Dini-Andreote, F., Geissen, V., Garbeva, P., 2020. Effects of plastic mulch film residues on wheat rhizosphere and soil properties. J. Hazard. Mater. 387, 121711 https://doi.org/10.1016/j.jhazmat.2019.121711.

Quast, C., Pruesse, E., Yilmaz, P., Gerken, J., Schweer, T., Yarza, P., Peplies, J., Glöckner, F.O., 2013. The SILVA ribosomal RNA gene database project: improved data processing and web-based tools. Nucleic Acids Res. 41, 590–596. https://doi.org/10.1093/nar/gks1219.

R Core Team, 2013. R: a language and environment for statistical computing. R Foundation for Statistical Computing. http://www.R-project.org/.

Raich, J.W., Tufekcioglu, A., 2000. Vegetation and soil respiration: correlations and controls. Biogeochemistry 48, 71–90. https://doi.org/10.1023/A:1006112000616.

Rillig, M.C., Hoffmann, M., Lehmann, A., Liang, Y., Lück, M., Augustin, J., 2021. In: Microplastic Fibers Affect Dynamics and Intensity of CO2 and N2O Fluxes From Soil Differently, 1, pp. 1–11. https://doi.org/10.1186/s43591-021-00004-0.

Rüthi, J., Bölsterli, D., Pardi-Comensoli, L., Brunner, I., Frey, B., 2020. The "plastisphere" of biodegradable plastics is characterized by specific microbial taxa of alpine and arctic soils. Front. Environ. Sci. 8 https://doi.org/10.3389/fenvs.2020.562263.

Simon, M., Lehndorff, E., Wrede, A., Amelung, W., 2020. In-field heterogeneity of apple replant disease: relations to abiotic soil properties. Sci. Hortic. 259, 108809 https://doi.org/10.1016/j.scienta.2019.108809.

Sinsabaugh, R.L., Linkins, A.E., 1990. Enzymic and chemical analysis of particulate organic matter from a boreal river. Freshw. Biol. 301–309 https://doi.org/10.1111/j.1365-2427.1990.tb00273.x.

Totsche, K.U., Amelung, W., Gerzabek, M.H., Guggenberger, G., Klumpp, E., Knief, C., Lehndorff, E., Mikutta, R., Peth, S., Prechtel, A., Ray, N., Kögel-Knabner, I., 2018. Microaggregates in soils. J. Plant Nutr. Soil Sci. 181, 104–136. https://doi.org/10.1002/jpln.201600451.

Vázquez-Baeza, Y., Pirrung, M., Gonzalez, A., Knight, R., 2013. EMPeror: a tool for visualizing high-throughput microbial community data. Gigascience 2, 15. https://doi.org/10.1186/2047-217X-2-16.

Wang, F., Wang, Q., Adams, C.A., Sun, Y., Zhang, S., 2022a. Effects of microplastics on soil properties: current knowledge and future perspectives. J. Hazard. Mater. 424, 127531 https://doi.org/10.1016/j.jhazmat.2021.127531.

Wang, Q., Sun, H., Li, M., Xu, C., Zhang, Y., 2020. Different age-induced changes in rhizosphere microbial composition and function of panax ginseng in transplantation mode. Front. Plant Sci. 11 https://doi.org/10.3389/fpls.2020.563240.

Wang, Q., Adams, C.A., Wang, F., Sun, Y., Zhang, S., 2022b. Interactions between microplastics and soil fauna: a critical review. Crit. Rev. Environ. Sci. Technol. 52, 3211–3243. https://doi.org/10.1080/10643389.2021.1915035.

Wang, Q., Feng, X., Liu, Y., Cui, W., Sun, Y., Zhang, S., Wang, F., 2022c. Effects of microplastics and carbon nanotubes on soil geochemical properties and bacterial communities. J. Hazard. Mater. 433, 128826 https://doi.org/10.1016/j.jhazmat.2022.128826.

Weig, A.R., Löder, M.G.J., Ramsperger, A.F.R.M., Laforsch, C., 2021. In situ prokaryotic and eukaryotic communities on microplastic particles in a small headwater stream in Germany. Front. Microbiol. 12, 3634. https://doi.org/10.3389/fmicb.2021.660024.

Yoshida, S., Hiraga, K., Takehana, T., Taniguchi, I., Yamaji, H., Maeda, Y., Toyohara, K., Miyamoto, K., Kimura, Y., Oda, K., 2016. A bacterium that degrades and assimilates poly(ethylene terephthalate). Science 351, 1196–1199. https://doi.org/10.1126/science.aad6359.

Yu, H., Zhang, Z., Zhang, Y., Song, Q., Fan, P., Xi, B., Tan, W., 2021. Effects of microplastics on soil organic carbon and greenhouse gas emissions in the context of straw incorporation: a comparison with different types of soil. Environ. Pollut. 288, 117733 https://doi.org/10.1016/j.envpol.2021.117733.

Zhang, Y., Li, X., Xiao, M., Feng, Z., Yu, Y., Yao, H., 2022. Effects of microplastics on soil carbon dioxide emissions and the microbial functional genes involved in organic carbon decomposition in agricultural soil. Sci. Total Environ. 806, 150714 https://doi.org/10.1016/j.scitotenv.2021.150714.

Zhou, J., Gui, H., Banfield, C.C., Wen, Y., Zang, H., Dippold, M.A., Charlton, A., Jones, D. L., 2021. The microplastisphere: biodegradable microplastics addition alters soil microbial community structure and function. Soil Biol. Biochem. 156, 108211 https://doi.org/10.1016/j.soilbio.2021.108211.

Supplementary Information

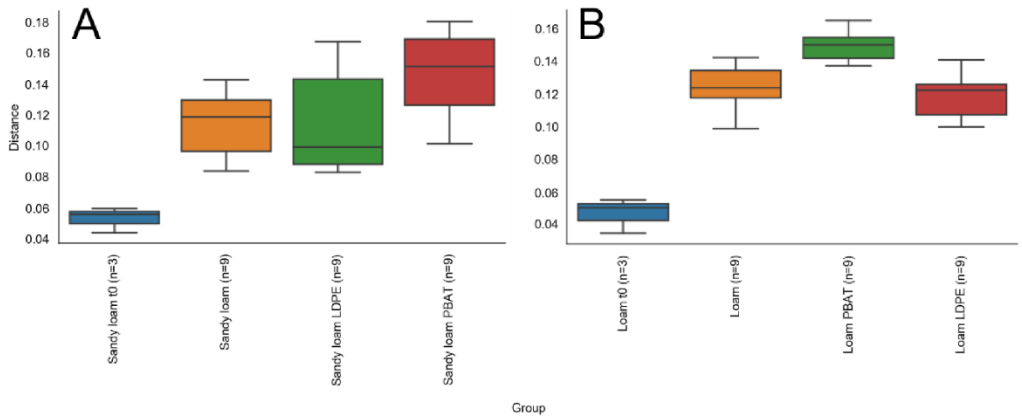

Figure S1: Distance comparison of the beta diversity via a PERMANOVA test with 999 permutations based on weighted UniFrac distance metrics from incubations with (PBAT, LDPE) and without plastic amendment (loam, sand) and initial soil (t0). Distance comparisons were carried out from incubations within one soil type (A, sandy soil; B, loamy soil) to the respective initial soil.

3. Manuscript 3: UV-Degraded Polyethylene Exhibits Variable Charge and Enhanced Cation Adsorption

Ryan Bartnick[1], Shahin Shahriari[1], Günter Auernhammer[2], Ulrich Mansfeld[3], Werner Reichstein[4], Lisa Hülsmann[5], Eva Lehndorff[1]

[1]Soil Ecology, Bayreuth Center of Ecology and Environmental Research (BayCEER), University of Bayreuth, Dr.-Hans-Frisch-Str. 1-3, 95448 Bayreuth, Germany

[2]Polymer Interfaces, Leibniz-Institut für Polymerforschung Dresden e.V., Hohe Straße 6, 01069 Dresden, Germany

[3]Keylab Electron and Optical Microscopy, Bavarian Polymer Institute, University of Bayreuth, Universitätsstr. 30, 95447 Bayreuth, Germany

[4]Ceramic Materials Engineering, University of Bayreuth, Prof.-Rüdiger-Bormann-Str. 1, 95447 Bayreuth, Germany

[5]Ecosystem Analysis and Simulation, Bayreuth Center of Ecology and Environmental Research (BayCEER), University of Bayreuth, Dr.-Hans-Frisch-Str. 1-3, 95448 Bayreuth, Germany

Manuscript completed, submitted to *Geoderma*, June 2025.

UV-Degraded Polyethylene Exhibits Variable Charge and Enhanced Cation Adsorption

Ryan Bartnick[*1], *Shahin Shahriari*[1], *Günter K. Auernhammer*[2], *Ulrich Mansfeld*[3], *Werner Reichstein*[4], *Lisa Hülsmann*[5], *Eva Lehndorff*[1]

[1]Soil Ecology, [5]Ecosystem Analysis and Simulation, Bayreuth Center of Ecology and Environmental Research (BayCEER), University of Bayreuth, Dr.-Hans-Frisch-Str. 1-3, 95448 Bayreuth, Germany

[2]Polymer Interfaces, Leibniz-Institut für Polymerforschung Dresden e.V., Hohe Straße 6, 01069 Dresden, Germany

[3]Keylab Electron and Optical Microscopy, Bavarian Polymer Institute, University of Bayreuth, Universitätsstr. 30, 95447 Bayreuth, Germany

[4]Ceramic Materials Engineering, University of Bayreuth, Prof.-Rüdiger-Bormann-Str. 1, 95447 Bayreuth, Germany

Abstract

The widespread use of plastics has led to an omnipresence in soils. We aim to understand whether transformation of polyethylene (PE) and polyethylene terephthalate (PET) in the atmosphere alters their surface properties which, after input of MP to soil, leads to an increase of reactive surfaces in soils. PE and PET particles (sieved 200 – 400 µm) were exposed to accelerated UV degradation. Changes in particle size and surface morphology were measured (using electron microscopy) and compared to pH dependent variation in surface charge parameters (zeta potential and cation exchange capacity). Fourier transform infrared spectroscopy and X-ray photoemission spectroscopy detected the formation of functional groups and surface atomic composition. After 2000 hours of degradation, PE particles reduced in size from 375±117 µm to 8±7 µm, while PET particles showed only a slight decrease in size, from 653±219 µm to 484±274 µm. Reduction of particle sizes correlated with increased absolute zeta potential and a decrease of the isoelectric point. Hydrated surface charge of degraded PE after 2000 hours was unstable under alkaline conditions,

related to the formation of carbonyl groups on its surface and increase in hydrophilicity. PET showed fewer surface chemical changes. Especially for weathered PE incorporated in soil, the alteration of its surface can exhibit comparatively one-tenth the cation sorption power of clay in alkaline environments. This study demonstrates that PE undergoes substantial physicochemical changes during UV degradation, increasing its reactivity, while PET remains relatively stable. These findings highlight the need for further studies to differentiate and understand the effects of diverse plastic types on soil ecosystems.

Keywords: cation exchange capacity, ultra-violet, accelerated degradation, microplastics, polyethylene terephthalate

Highlights

- Polyethylene (PE) undergoes size reduction and increase in surface area
- PE develops oxidative functional groups and shifts to hydrophilic behavior
- PE develops cation exchange capacity under alkaline conditions
- Polyethylene terephthalate remains stable in size and chemical surface properties

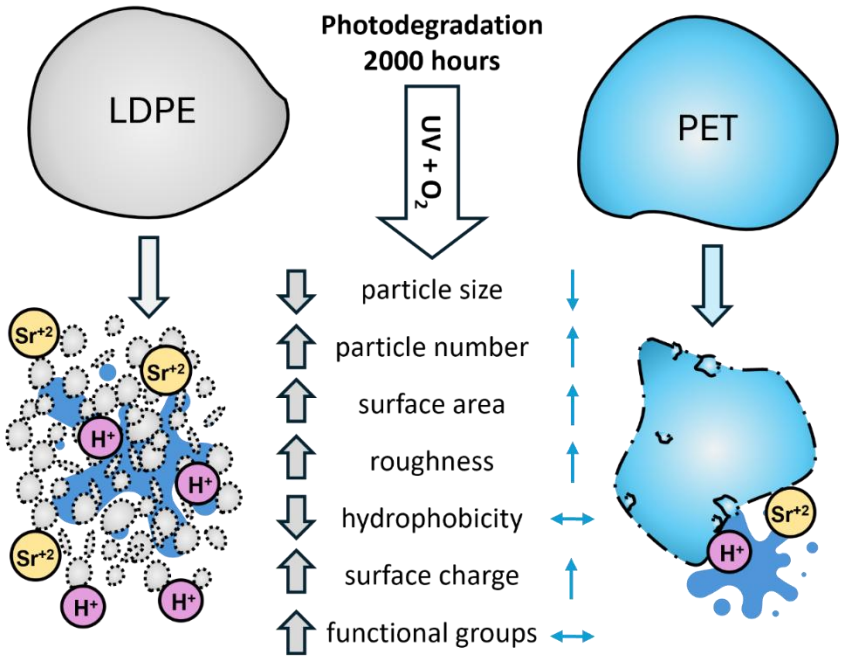

Graphical Abstract. Polyethylene (PE) and polyethylene terephthalate (PET) after 2000 hours of accelerated UV-degradation; PE substantially reduced in size, hydrophobicity, and increased in surface oxidation forming functional groups, whereas PET showed minor surface defects but remained chemically stable.

Introduction

Poor waste management and high plastic production have led to a significant accumulation of plastic waste in soils where nutrient and carbon storage can be affected (Andrady, 2017; Priya et al., 2022). Plastics effect on soil functions as a foreign reactive surface is not fully understood, as the change of plastic surface properties during environmental exposure must be considered. The environmental fate of microplastics (MPs) depends on their chemical composition, weathering rate, and interaction with other environmental particles (Imhof et al., 2012; Mattsson et al., 2015). Among all sinks for MPs, agricultural soil may be a main hotspot for MPs pollution because of intensive agricultural activities (Braun et al., 2023; Huang et al., 2020; Kumar et al., 2020; Zhang et al., 2022).

Polyethylene (PE) is the most widely used plastic in the world, accounting for around 30% of all plastics (Geyer et al., 2017). PE degrades relatively easily when exposed to ultraviolet (UV) light (Kissin, 2020). Polyethylene terephthalate (PET) is also a widespread plastic and of environmental concern due to its strong resistance to degradation (Hopewell et al., 2009). When exposed to UV light, PET can break down into smaller particles, but this process is slow, and the particles can persist in the environment. For these reasons, PE and PET were chosen in this study to understand the physicochemical transformations during UV degradation.

One key problem with plastic pollution is the breakdown of larger plastics into MPs and nanoplastics (NPs). As plastics weather, they break down into smaller pieces due to sunlight, temperature changes, physical abrasion, and biological processes (Bhagat et al., 2022; He & Luo, 2020), causing their properties to change and affecting their behavior in the environment (Andrady, 2011; Meides et al., 2022). Size reduction increases the number of particles and their surface area, enhancing their environmental mobility and interaction potential, however, this still needs to be related to surface properties of MPs.

To understand how degraded MPs interact with complex environments like soil, it is essential to determine how weathering processes alter the physical and chemical properties of pristine (unweathered) MPs. Photodegradation, driven by exposure to UV radiation, leads to the breakdown of polymer chains and the formation of new functional groups such as carbonyls and hydroxyls on the particle surfaces, which increase their reactive surface (Andrady, 2011; Meides et al., 2022). Fourier-transform infrared spectroscopy (FTIR), a powerful analytical technique widely used to identify functional groups and chemical bonds in organic compounds, shows these chemical changes, indicating oxidative degradation (Khan et al., 2018). By analyzing the specific wavelengths of light absorbed by a sample, FTIR can provide detailed information about molecular vibrations, providing analysis to

changes to plastic molecular composition throughout UV-degradation. Additionally, X-Ray photoelectron spectroscopy (XPS) can be used to provide surface chemical composition of polymeric structures at 2 – 10 nm sampling depth at high precision (Giglio et al., 2014). By observing the bonding energies of emitted electrons from X-ray irradiation of the polymer surface, molecular information can be obtained to characterize changes in degraded polymers. Changes in plastic surface chemical speciation can be detected throughout the plastic degradation process.

To evaluate the change in surface charge of weathered MPs, the zeta potential of degraded PE and PET MPs can be analyzed to understand surface charge variations. Zeta potential, or electrokinetic potential (symbolized as ζ), is the electrical potential difference across the mobile portion of the electrical double layer surrounding a colloidal particle. The isoelectric point (IEP), or point of zero charge, is a crucial marker for understanding how particles behave in solutions of a specific, because it gives the pH at which the surface appears neutral to the surrounding. Instead of using zeta potential, the IEP allows seeing if particles have potential to react with other soil constituents (Healy & Fuerstenau, 2007; Jang et al., 2022; Pergande & Cologna, 2017; Yeganeh et al., 1999).

While pristine plastics may be considered inert and exhibit no ion exchange, degraded plastics have more potential to significantly influence soil properties, e.g. cation exchange capacity (CEC), which is vital for nutrient retention and availability in soils. The CEC of soil measures the quantity (moles) of negatively charged sites on soil particles that attract positively charged ions, such as soil nutrients. Degraded MPs could incorporate and aggregate with soil components, potentially changing soil structure and chemical properties (Boots et al., 2019; Ingraffia et al., 2022; Souza Machado et al., 2018; Zhang et al., 2019). Alterations in CEC can be attributed to complex and various factors, including the physicochemical traits of MPs, their interaction with soil particles and microorganisms, and changes in soil pH and organic matter content caused by MPs (Sharma et al., 2021; Yuan Wang et al., 2022; Yu Wang et al., 2022; Wen et al., 2022). Soil pH has a significant impact on the effective CEC, changing the quantity and direction of charge of soil constituents (mainly OM and oxidic phases). Whether degraded MPs of decreasing size may alter soil CEC by varying the amount of charged surfaces due to their increased surface area needs to be studied.

The main goal of this study was to understand how the UV-degradation of PE and PET influences their surface chemistry and adsorption capacity for ions that potentially affect the

quality of soil. We investigated if a UV-weathering process significantly altered the size, surface morphology, surface charge, and chemical composition of PE and PET using a combination of light microscopy, scanning electron microscopy (SEM), as well as their potential to affect cation exchange as expected in soils. In this study, we quantified the change in size of PE and PET during degradation and visualized changes in hydrophobicity and roughness with ESEM; we used FTIR and XPS to identify functional group formation on the surface of degraded PE and PET; and we quantified the alteration of CEC and zeta potential of degraded PE and PET. The polymers used in this study had an initial sieved size of 200 – 400 µm and have been weathered for up to 2000 hours by UV radiation under controlled, moist conditions.

Materials and Methods

Experimental plastics, materials, and artificial degradation

The plastic materials used in this study were low density-polyethylene (LD-PE, Lupolen 1800 P-1 – LyondellBasell, Rotterdam, NL) and polyethylene terephthalate (PET, CleanPET WF – Veolia Umweltservice, Hamburg, Germany). Plastics were initially prepared by cryomilling (ZM200; Retsch, Haan, Germany) and airjet sieving (E200 LS; Hosokawa Alpine, Augsburg, Germany) to a size range of 200 – 400 µm of irregular shape. All materials were kept in glass containers and handled with metal utensils.

In a Q-SUN XE-3 accelerated weathering chamber (Q-LAB, Westlake, OH) equipped with three xenon lamps and a Daylight-Q filter, MPs samples were subjected to various conditions to simulate natural degradation processes (Meides et al., 2021, 2022). MPs were exposed to UV radiation to mimic solar radiation (UVA), irradiated with 60 W/m^2 (at 300–400 nm), corresponding to a total irradiance of 594 W/m^2, comparable to the spectrum of natural sunlight, with an estimated accelerated degradation 5x faster than in the environment (Menzel et al., 2022). MPs were maintained at a constant temperature of 38°C, immersed in deionized water, and under mechanical stress from stirring. The continuous stirring ensured that the particles were uniformly irradiated from all sides. To study how weathering affects surface changes and ion adsorption, three sets of both PE and PET samples were produced: non-degraded (0 hours), and exposed samples in an accelerated weathering chamber for 400 and 2000 hours.

Size and visual characterization of MPs

Scanning electron microscopy was performed at 3 kV on a LEO 1530 (Zeiss, Oberkochen, Germany). Prior imaging, the particles were coated with a thin layer of platinum using a

Cressington 208 HR sputter coater. ESEM was performed on a FEI Quanta FEG 250 (Thermo Fisher Scientific, Waltham, USA) equipped with a cooling stage and a gaseous secondary electron detector (GSED). The pristine samples were placed on a polished graphite support and cooled down to 2 °C at 400-600 Pa for 30 min. For the wetting experiments, the pressure was increased to a range of 725-800 Pa (rate 600 Pa/min) depending on the wettability, and wetting was imaged at 10 kV at constant pressure.

The size and distribution of particles were measured using images taken by SEM and a transmitted light ECHO Revolve microscope with 10x magnification, which allowed detection of particles with a lower limit around 1 µm in size. In each image (n_i = 4 - 37), the diameter of each particle was measured (n_p = 107 - 861) using Fiji 2.9.0 image processing software (Schindelin et al., 2012), and then frequency distribution graphs were produced using OriginPro 2024b software (OriginLab). Due to the random, oblong shapes of particles following size fractionation, diameter of each detected particle was measured at the longest and shortest sides that could pass through the airjet sieve, which results in a larger detected distribution then what is expected from airjet sieving which can pass particles that are narrower than 400 µm on one side but longer on another.

Surface chemical characterization of MPs

FTIR detected functional group change in the plastic surfaces at a penetration depth of few micrometers, while XPS measured at higher resolution at the top surface of a few nanometers. The FTIR surface analysis of PE and PET MPs was conducted using an Alpha II spectrometer (Bruker, Billerica, USA). The MPs samples were prepared by placing dry particles directly onto the analyzer without any specific sample preparation. The FTIR measurements covered a range of wavenumbers from approx. 4000 to 500 cm^{-1}, capturing the absorption bands of different functional groups present on the particle surface. This allows quick identification of changes in the IR spectra of MPs after degradation.

XPS measurements were taken with a PHI 5000 VersaProbe III (ULVAC-PHI, Chigasaki, Japan), peaks identified by binding energy (Briggs, 1981), and spectra produced with MultiPak 9.8.0.19 software. Plastic samples were fixed on a sample holder with double-sided tape. Measurements were taken in triplicate as a collection, which were neutralized (electron and argon) and binding energy corrected. Excitation energy was monochromatic aluminum K-alpha. Surveys for elemental composition were taken as a scan (pass energy = 224 eV, step size = 0.8 eV), and curve fitting of C1s peak was performed with a high resolution, detailed spectrum (pass energy = 26 eV, step size = 0.1 eV).

Streaming zeta potential

The surface potential (ψ) of particles can be calculated by using the experimentally measured zeta potential (ζ), although the actual zeta potential typically remains lower than the surface potential calculated from the diffuse double-layer theory. Zeta potential shows the difference in potential between the shear plane and the bulk solution (Kontogeorgis & Kiil, 2016; Stumm & Morgan, 1996). In the streaming zeta potential process, a solution is pushed through a capillary channel with a specific applied pressure. The SurPASS 3 (Anton Paar, Graz, Austria) was used to measure both streaming potential and streaming current (Bukšek et al., 2010).

For these measurements the respective amount of powder was fixed with 20 µm membranes, pore size chosen by the size distribution values, in the powder sample holder. This part was inserted in the cylindrical cell of the instrument equipped with Ag/AgCl-electrodes. The permeability index was adjusted around 100. The measuring fluid was streamed through this powder plug in the pressure range from 600 to 200 mbar. The zeta potential ζ was calculated according to Smoluchowski equation:

$$\zeta = \frac{dU}{dp} \times \frac{\eta\kappa}{\varepsilon_r \varepsilon_0}$$

[Eq. 1]

Where U is the streaming potential, p is the pressure loss, ε_r and ε_0 are the dielectric constant and the vacuum permittivity, η is the viscosity and κ the conductivity of the measuring fluid. The pH-dependence of zeta potential or the powder was determined in the presence of KCl solution, concentration of 10^{-3} mol/L, as function of the pH value. We started at pH ~6 and adjusted the pH value by stepwise adding HCl or KOH. By looking at the shape of the zeta potential versus pH curves and where the zeta potential is zero (at the IEP), we can understand the types of the functional groups on the surface of the fibers (see Figure S1, SI); for non-polar or non-dissociating surfaces, the IEP was determined around pH 4. To compare the absolute values accurately, we needed to ensure the same testing conditions. We made efforts to maintain consistent flow conditions, but because of differences in particle structure after degradation, the weight and surface area varied between PE and PET. PE, with its more fibrous structure, could be compressed strongly with a smaller sample amount, while the PET's particle-shaped structure required a larger sample amount to achieve similar flow properties. We note that the IEP is only little influenced by these changes in permeability.

Cation exchange capacity determination

To determine CEC, we followed modified methods by Liu et al. (2001) and Schäfer & Steiger (2002). In addition to testing weathered and non-weathered MPs, we also included adsorption to montmorillonite clay as a reference material for highly charged soil particles and a control of pure, inert quartz sand. Potential CEC is measured as strontium (Sr^{+2}) through a reverse desorption reaction via replacement of the sites via magnesium (Mg^{+2}). Initially, cation and material equilibration occurred by percolating the sample with 0.1 M strontium chloride-triethanolamine buffered at pH 4, 7, and 9 (pH adjusted with HCl or KOH, column filled with 0.1 to 0.4 mm quartz sand, pre-cleaned by rinsing with acetone:cyclohexane (1:1) and heating to 900 °C). Triethanolamine helped disperse MPs and minerals.

The magnesium chloride ($MgCl_2$, 0.1 M) solution from the reverse exchange was filtered through a 0.45 μm cellulose acetate filter and analyzed for total Sr using inductively coupled plasma-optical emission spectroscopy (ICP-OES 5800, Agilent Technologies, Waldbronn, Germany). The number of charges from Sr^{2+} ions in the volumetric flask was estimated as the CEC of the sample. This value would be equivalent to the CEC $cmol_c$ / kg of our sample as follows:

$$\frac{mg\ Sr^{2+}}{kg\ sample} \times \frac{1\ g}{1000\ mg} \times \frac{1\ mol\ Sr^{2+}}{87.62\ g} \times \frac{100\ cmol}{1\ mol} \times \frac{2\ cmol_c\ valence\ Sr^{2+}}{1\ cmol} = CEC\ cmol_c/kg$$

[Eq. 2]

Sample concentration of Sr^{2+} was converted to CEC from sample weight, and the atomic weight and valence of Sr^{2+}. Each sample treatment was performed in triplicate, with blanks measured below the detection limit (0.05 mg/L).

Statistical analyses and figures

Statistical analyses were performed in R 4.4.3 to evaluate differences in particle size distribution and CEC across polymer types and degradation times. We compared PE and PET treatments separately for significant differences in particle size distribution with degradation time using one-way ANOVA and Tukey HSD post-hoc tests ($p < 0.05$). The Shapiro-Wilk test for normal distribution was determined for particle size in the sample treatments which showed improved normality in particle size distribution when log-transformed. The Shapiro–Wilk test indicated a significant deviation from normality ($p < 0.05$), however the W statistic was relatively high ($W > 0.97$), due to the large sample size of particle counts. The PE 2000 hour degraded sample was found to contain NPs (<1 μm) present outside of our detection limit of the microscope; therefore, we fitted a truncated normal distribution to log-

transformed particle size data using lower truncation point at log(1) (the detection limit) to the observed particle size distribution and predicted the entire normal distribution with the estimated mean and standard deviation.

One-way ANOVA, followed by Tukey's HSD post-hoc tests, was used to compare PE and PET at each pH level and degradation time for significant differences in CEC ($p < 0.05$). The Shapiro-Wilk test confirmed a normal distribution for CEC samples of PE and PET at each pH level and degradation time ($W > 0.78$, $p > 0.05$). Homogeneity of variances was assessed using Levene's test ("car" package), which showed no significant differences in variances across treatment groups ($F = 1.67$, $p > 0.05$).

Results

Particle size distribution of degradation MPs

To understand how UV-degradation affects MPs particle size, we measured the size of particles for PE and PET: 1) exposed for 400 hours in the weathering chamber, 2) exposed for another 2000 hours, and 3) a set of non-degraded, pristine MPs (0 hours) (UV exposure in de-ionized water, stirred). The resolution of the transmitted light microscope was 0.56 µm per pixel, therefore a lower limit of particle detection was set at 1 µm.

For PE particles, a large decrease in particle size with degradation time was observed (Figure 1). ANOVA of PE treatments showed a significant reduction in particle size over degradation time ($F = 2531$, $p < 0.001$; log-transformed to normalize distribution). Quantitative measurements revealed no significant changes from Tukey HSD post-hoc tests indicated no significant difference in particle size between pristine PE (0 hours) and degraded PE at 400 hours, but a large significant reduction at 2000 hours ($p = 1.9 \times 10^{-13}$; see Figure S2, SI). The mean particle size for PE was 375 µm, 370 µm, and 8 µm at degradation times of 0, 400, and 2000 hours, respectively (see Table S1, SI). Combining histograms and Gaussian graphs showed that with increased degradation, the frequency of larger particles decreased while the frequency of smaller particles increased. The decrease in particle size was accompanied by a narrowing of the particle size distribution width (Figure 1). The starting observed particle range for PE was 161-689 µm. After 2000 hours of degradation, then ranged from below detection (< 1 µm) to the largest detected particle at 66 µm. Therefore, to assess the amount of NPs produced which we could not detect under the microscope, we fitted a truncated normal distribution, which estimated 2.5% of particles (<1 µm) are missing from our observed size measurements (see Figure S3, SI). The sharp reduction in particle size of PE suggests accelerated fragmentation with degradation time, and

the truncated normal distribution estimation statistically indicates a likely transition into the nanoplastic size range with further degradation.

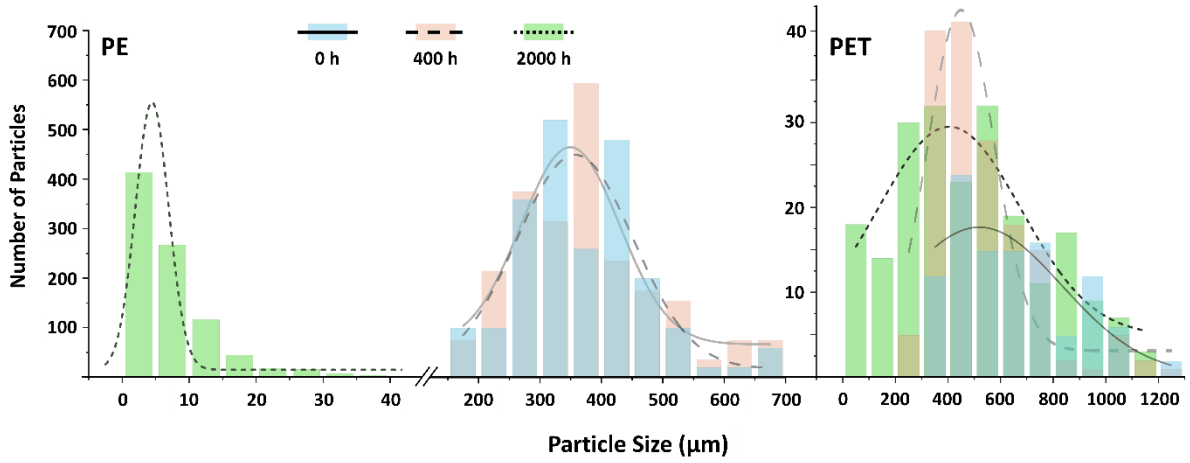

Figure 1. Particle size distribution of PE (left) and PET (right) microplastics at 0, 400, and 2000 hours of degradation (solid and blue, dashed and red, and dotted line and green, respectively); the left y-axis corresponds to PE 2000 h and the right y-axis corresponds to all other treatments.

For PET particles, weathering led to a significant decrease in particle size at each degradation step from 0 to 400 hours (ANOVA: $F = 25$, $p < 0.001$). Tukey's HSD showed a significant reduction from 0 to 400 hours ($p = 0.01$) and 2000 hours ($p = 1.4 \times 10^{-10}$), likely due to the large dataset of particle counts; and quantitative measures revealed a subtle decrease in particle size over degradation times, with means of 653 µm, 531 µm, and 484 µm, respectively. However, PET reduced in size to 74% on average at 2000 hours of degradation compared to the large reduction to 2% of the initial size of PE (see Table S1, Figure S2, SI). For PET 0 h, particles were in a range of 333-1239 µm, and after 2000 hours degradation, the range was 24-1165 µm.

Surface characteristics of degraded MPs

Scanning Electron Microscopy (SEM) provided detailed images of the surface structure of MPs, showing features like cracks, holes, and grooves that formed during degradation. For PE particles, SEM images showed a consistent decrease in particle size (Figure 2). During the first 400 hours of degradation, the particles became more rounded and resembled crumpled paper. Fragmentation occurred mainly from 400 to 2000 hours of degradation, with particle size decreasing severely and surfaces turning rougher. After 2000 hours, a significant fragmentation into NPs formed.

For PET particles, the decrease in the size of particles during degradation was not recognizable by visualization alone (Figure 2). Only by measuring the average diameter of particles under a light microscope, the tiny flaky fragments that were detached from the outer layer of larger particles could be recognized. The surface of particles did not change during the first 400 hours of degradation. However, on the surface of PET particles after 2000 hours of degradation, traces of abrasion appeared. The roughness of the surface increased, and consequently, we observed more tiny flaky fragments on the surface, which had the potential of detaching from their larger initial particle. In summary, the size of PET during degradation did not change much; only tiny flaky fragments likely detached from the outer layer of the larger particles (see SEM images, Figure S4, SI).

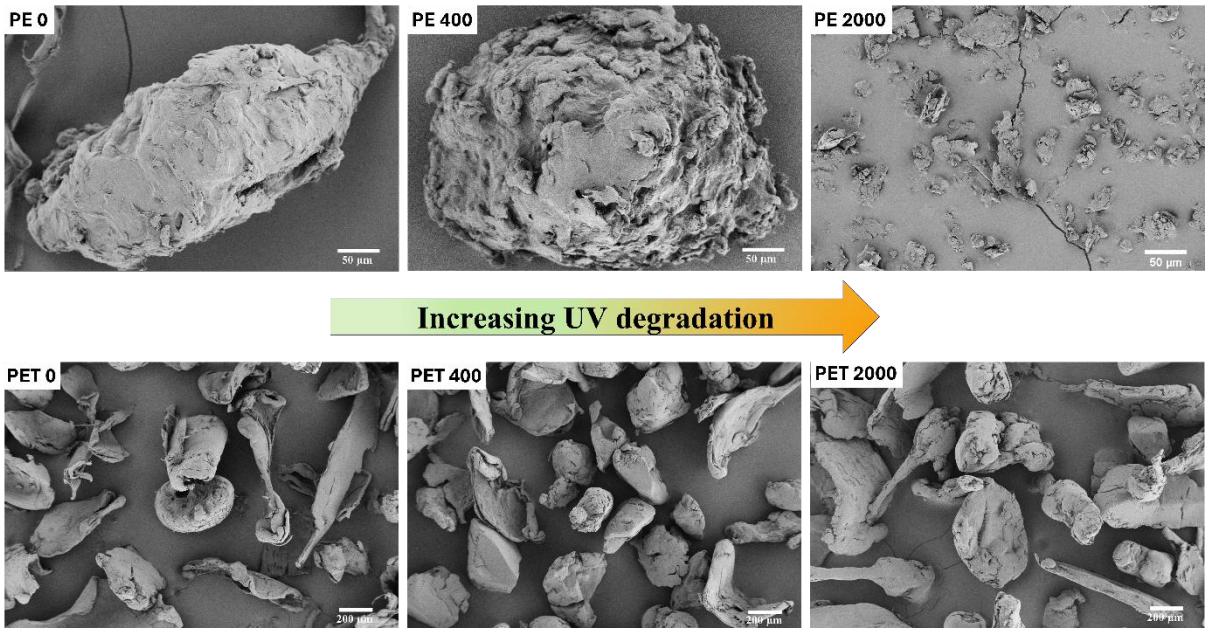

Figure 2. SEM images of PE (top row) and PET (bottom row) at 0 h and degraded at 400 h and 2000 h. Degradation decreases the size of PE particles, while PET particles show no significant size changes.

ESEM shows wetting as a function of water pressure in the SEM chamber. This allows for qualitative evaluation of hydrophilicity of surfaces in the degraded polymers at 2 °C. The smaller the contact angle the more hydrophilic the surface is. An additional kinetic indication for increased hydrophilicity is that less pressure is needed for the observable condensation to start.

For PE, pristine particles without degradation (PE 0) were primarily hydrophobic (Figure 3), with large contact angles (CA) as expected of hydrophobic surfaces, and wetting started at 750-800 Pa. At 400 hours of degradation, PE remained mainly hydrophobic, with some areas

showing small CA, e.g. particle gaps filling; wetting starting earlier at 730 Pa indicating less hydrophobicity than pristine PE. At 2000 hours, PE became hydrophilic, with low contact angles, gaps filling, and particles surrounding wetting regions; wetting started immediately at 720 Pa and before the graphite support became wetted.

For PET, all kinds of contact angles were present: hydrophilic and hydrophobic areas. There was no significant difference between pristine and degraded particles (Figure S5, SI).

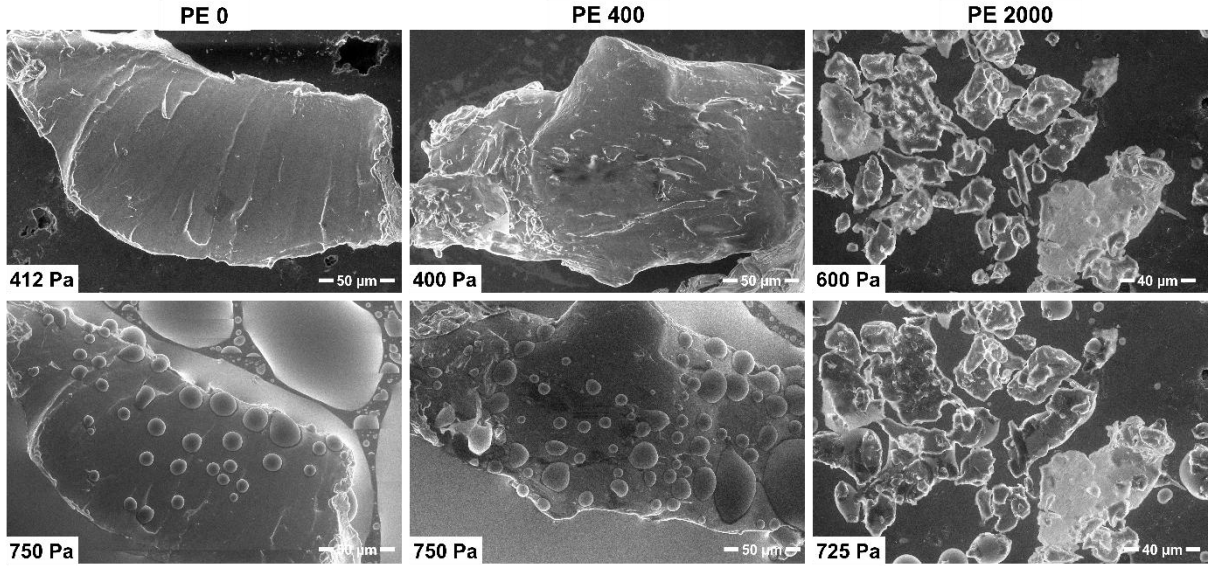

Figure 3. Representative ESEM images at 2°C of PE at 0, 400, and 2000 h of degradation. Especially hydrophobic particles (water droplets with high contact angles) started to drift because of earlier wetting of the carbon support. Degradation changed the surface wetting behavior of PE from hydrophobic to hydrophilic.

Changes in surface chemistry of degraded MPs

The FTIR spectra of pristine PE at 0 hours and degraded PE at 400 hours were similar (Figure 4), with only a small peak appearing for PE at 400 hours at wavenumber 1714 cm^{-1}, indicative of carbonyl (C=O) group formation. The increased broadening in the carbonyl peak of PE at 2000 hours up to 1750 cm^{-1} indicates further ester and ketone formation. In PE at 2000 hours, not only did the peak at wavenumber 1714 cm^{-1} increase, but we also observed an increase in transmittance and the appearance of new peaks from 850 cm^{-1} to 1300 cm^{-1}, which could indicate a variety of carbon-oxygen single bonds (C-O) as carboxylic acids, ethers, alcohols, and peroxides. The FTIR spectra for pristine and degraded PET showed no differences (Figure 4), although the peak heights for PET at 400 hours were lower than the others.

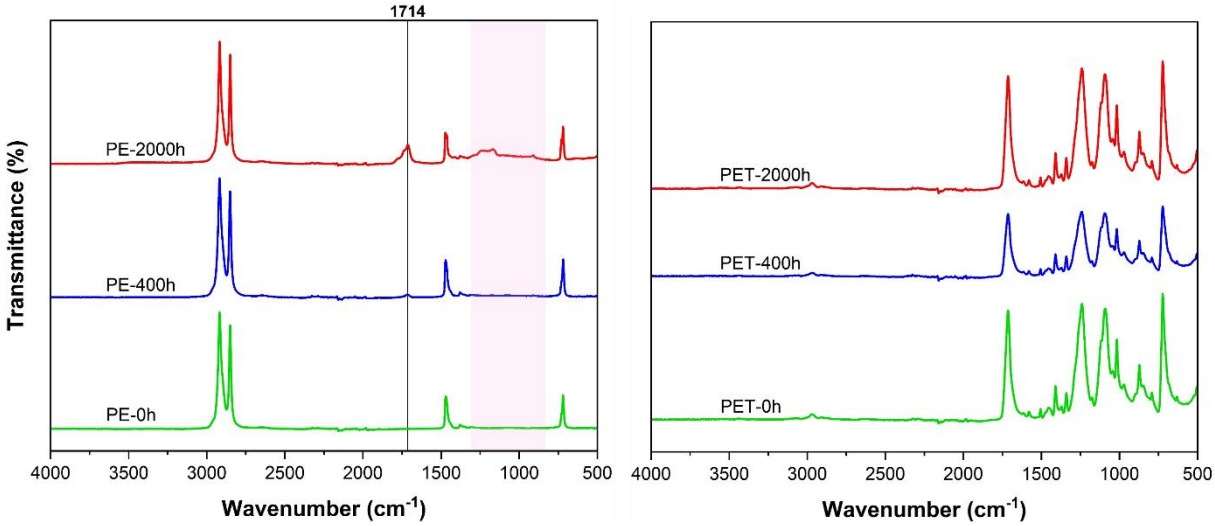

Figure 4. FTIR spectra of PE (left) and PET (right) at each degradation time; new peak marked at wavenumber 1714 cm^{-1} in PE after 2000 hours of degradation (top).

XPS analysis of the surface polymer chemistry (≈5 nm) of pristine and degraded PE and PET was performed. XPS quantitated and compared atomic ratios of elements to carbon which appeared on the plastic surface (Table 1). After degradation, the surface of PE increased in atomic concentration of oxygen (O), silicon (Si), and fluorine (F), with a subsequent reduction in carbon (C). Pristine PE revealed some initial O concentration bound to the polymer surface, which more than doubled after 400 hours, and further increased with 2000 hours of degradation (Table 1). Si was detected on pristine and degraded PE as C-Si organic bonds (Figure 5), its presence likely due to Si-containing lubricants used in the polymerization process, which subsequently increased with degradation. PE in its structure consists only of C and H, but impurities are often present even in specialized production. Traces of F were also detected after degradation, which was not present in pristine PE, likely introduced as surface contamination during degradation.

Table 1. XPS element ratios of the surface composition of PE from 0 to 2000 hours degradation.

plastic	element ratios		
	O/C	Si/C	F/C
PE 0 h	0.023	0.012	ND
PE 400 h	0.069	0.029	ND
PE 2000 h	0.110	0.040	0.026
PET 0 h	0.348	0.011	ND
PET 400 h	0.291	0.012	ND
PET 2000 h	0.340	ND	0.105

ND = Not Detected

In XPS, the different binding states of the carbon can be analyzed by the deconvolution of the corresponding high-resolution element spectra (curve fitting) of the C1s spectra (Figure 5). On the surface of PE, the C1s spectra consists mainly of C-C bonds (eV = 284.5) with a tailing to C-Si bonds (eV = 283) (Briggs & Beamson, 1992). At 400 hours of degradation, PE exhibits a strong shift away from C-C bonds on the surface and towards C-O (eV 286) and C=O carbonyl (eV 287-288) and carboxyl (eV = 289) bonds. At 2000 hours, the PE surface recovers its C-C bonds closer to when it was pristine, however with wider tails exhibiting C-O formation. This suggests functional group formation on plastic polymer surfaces is dynamic with degradation time, as size fractionation of particles reveals fresher surfaces.

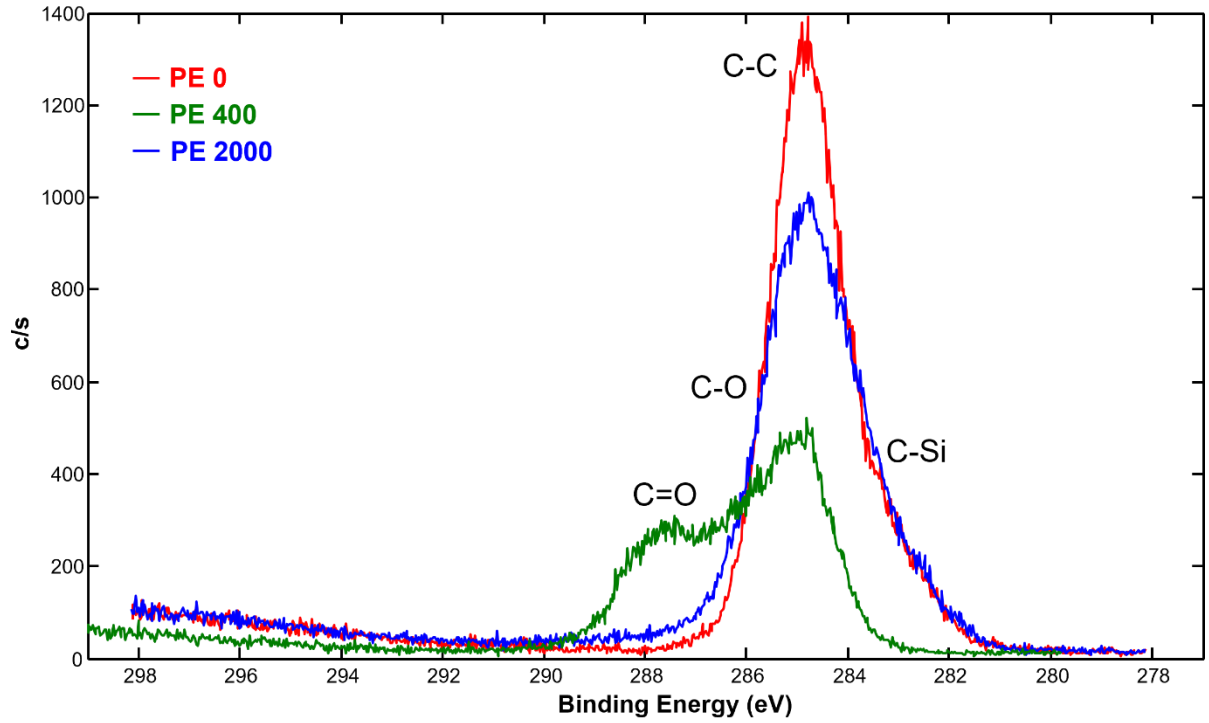

Figure 5. XPS spectra overlay of carbon C1s spectra, showing change in functional group formation of PE during degradation.

PET contains C and O, single and double bonds in its polymer structure. After degradation, no increase in O concentration was found in PET (Table 1), instead the formation of organic C-F bonds (F1s, eV = 689, not shown) were introduced during the degradation process similar to PE. However, contrary to PE, initial Si content decreased over degradation time on the surface of PET and was not detected after 2000 hours. The C1s spectra of the pristine PET surface shows C-O and C=O and other carboxyl and ester groups (Figure S6, SI). After degradation at 400 hours, a more pronounced shift to C=O bonds and reduction in C-O bonds occurs, but after 2000 hours of degradation these peaks recover. While slight dynamic changes to surface chemical functionality occur with PET over degradation time, these changes are minimal compared to PE.

Zeta potential and isoelectric point

Surprisingly, all IEP values were lower than what we would normally expect for non-polar surfaces (pH 4, Figure S1, SI), with the IEP of pristine PE and PET around pH 3, possibly as the increase in surface area and roughness from the milling process to produce MPs.

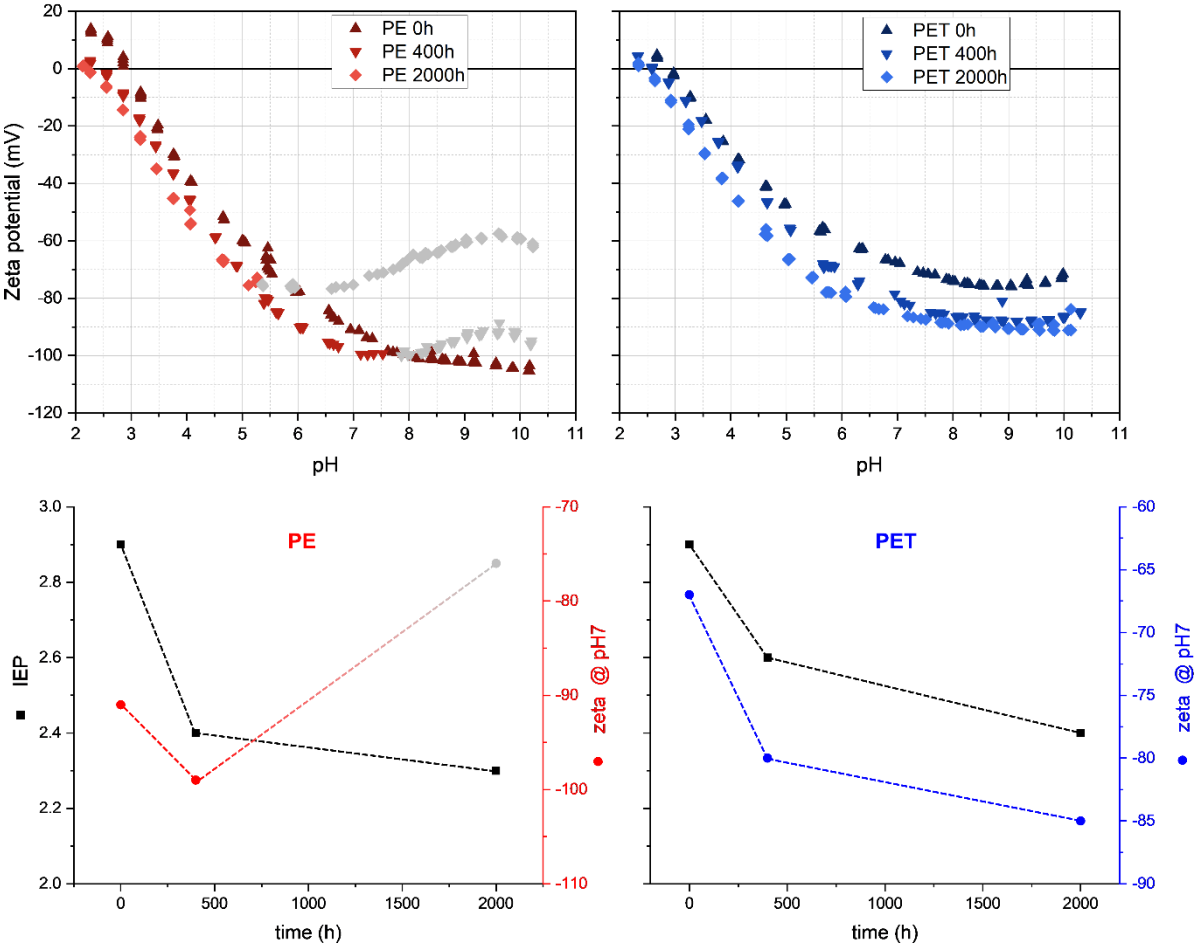

Figure 6. Effect of weathering rate on zeta potential values (top) and isoelectric point (IEP, bottom) of PE (left) and PET (right) at different degradation times. Gray symbols in PE degraded plastics show instability in alkaline region.

The IEP of non-degraded PE (0 h) was around pH 3, with the plateau having high absolute zeta potential values, and after artificial weathering, the IEP decreased (Figure 6). This change seemed to reach its lowest point after long weathering times. In the pH range below pH 4.5, close to the IEP, the zeta potential values were less than ±30 mV. In non-degraded PE, as pH increased, the absolute zeta potential values steadily increased. However, around neutral pH, the rate of increase slowed down, and zeta potential values rose smoothly. In PE 400 h, as pH increased, the decreasing trend changed to an increasing trend (strange instability) around pH 7.5. In PE 2000 h, the turning point was around pH 5.5, and as pH increased beyond 6, the trend changed to an increasing one with lower zeta potential values. In both PE 400 h and PE 2000 h, at pH above 9.5, the trends started decreasing again. We attribute this behavior to an instability of the particles or the particle surfaces in alkaline conditions.

The IEP of non-degraded PET was similar to PE, also with high absolute plateau values and a decreased IEP after artificial weathering. In the pH range below pH 5, close to the IEP, the zeta potential values were less than ±30 mV. In non-degraded PET, as pH increased, the absolute zeta potential values steadily increased. However, above neutral pH, the rate of increase slowed down. Both PET 400 h and PET 2000 h showed similar trends to non-degraded PET but with higher absolute zeta potential values.

Cation exchange capacity of weathered MPs particles

Degradation of PE led to a significant increase in CEC values dependent on pH (ANOVA: $F = 325$, $p < 0.001$). The CEC values for both non-degraded PE (PE 0) and PE degraded for 400 hours (PE 400) were very low and close to the control sand, meaning they were near zero charge from pH 4 to 7 (Figure 7). At pH 9, the CEC values for both PE 0 and PE 400 increased slightly to about 0.8 ± 0.2 $cmol_c$ / kg (mean ± s.d.), significantly above the control at pH 9 (Tukey's HSD: $p < 0.005$). However, for PE exposed for 2000 hours (PE 2000), significant differences in CEC occurred compared to control at pH 7 ($p = 5.7 \times 10^{-5}$) and pH 9 ($p = 1.1 \times 10^{-12}$). The charges on PE 2000 varied and increased with an increase in pH; at low pH, PE 2000 had a net negative CEC because it had more positive charges than negative ones. As the pH increased to 7, the CEC values rose to about 0.9 ± 0.1 $cmol_c$ / kg in the positive range of PE 2000. When the pH was increased to 9, the CEC dramatically rose to mean value of 7.5 ± 0.5 $cmol_c$ / kg. To better understand the absolute CEC values of degraded MPs, we compared to the CEC of montmorillonite, one of the most reactive soil constituents. Using montmorillonite as a reference, at pH 9, the CEC of PE degraded for 2000 hours was about one-tenth of montmorillonite's adsorption capacity. Even at pH 7, the CEC of 2000 h PE was about one-seventieth of montmorillonite's adsorption capacity.

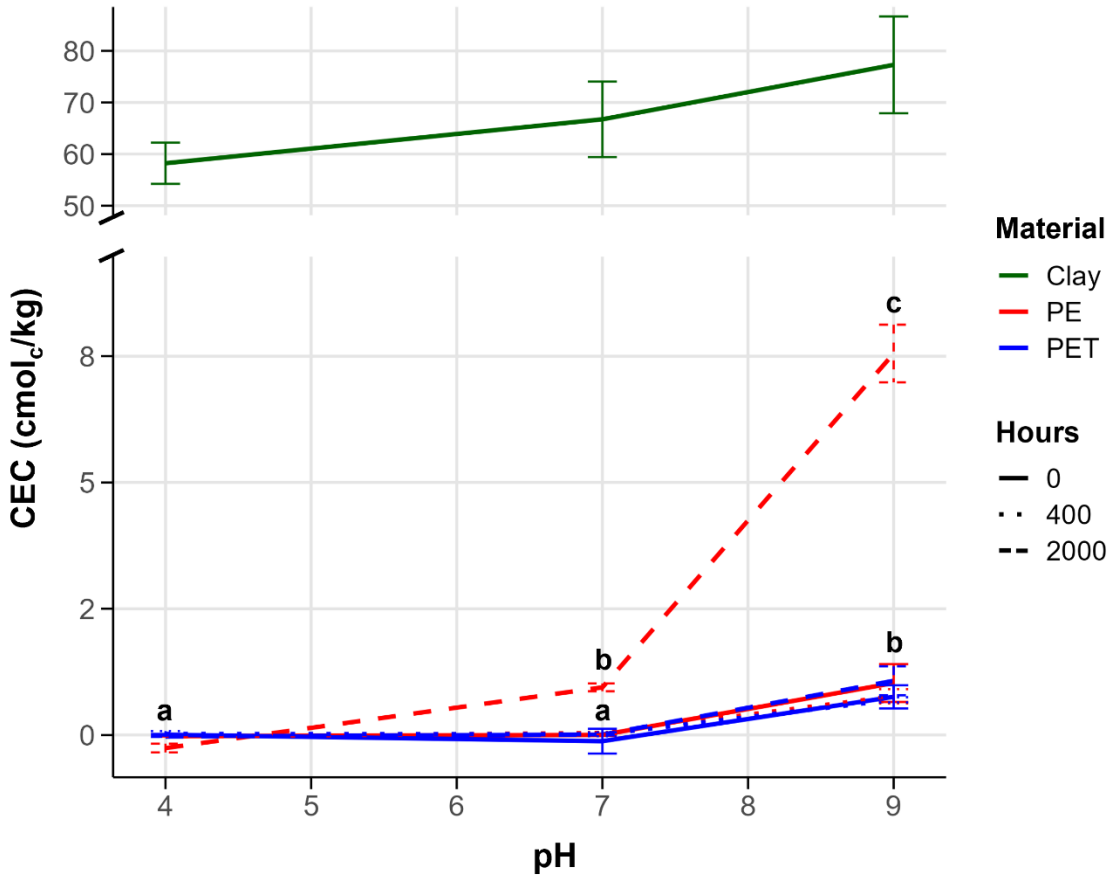

Figure 7. CEC values for pristine and degraded PE and PET, and montmorillonite clay at three pH levels with standard deviation and significance letters from Tukey HSD post-hoc tests.

Although to a lesser degree than PE, degradation of PET also led to a significant increase in CEC values dependent on pH (ANOVA: F = 26, $p < 0.001$). From pH 4 to 7, the CEC values for non-degraded PET (PET 0), PET 400, and PET 2000 were very low and close to the control sand, meaning near zero ($p = 1$). When the pH was increased to 9, the CEC values for both non-degraded and PET 400 significantly differed from control ($p < 0.05$) and reached a mean of 0.7 ± 0.1 $cmol_c$ / kg. However, for PET 2000 h, the CEC slightly increased to 1.1 ± 0.2 $cmol_c$ / kg compared to control ($p = 5.4 \times 10^{-6}$). Comparing the absolute CEC values of PET with montmorillonite showed that PET had very low CEC values, around one-seventieth of montmorillonite's adsorption capacity, even after 2000 hours of degradation (Figure 7). This demonstrates that longer degradation times increase surface reactivity, especially in alkaline environments, but the extent of reactivity is dependent on plastic polymer type.

Discussion

Reduction of PE and PET particle size and increase in surface area due to UV weathering

UV-weathering significantly impacts the particle size distribution of PE, whereas for PET this is less clear. It was shown before that the degree of crystallinity plays a crucial role in forming microcracks on the surface of MPs (Meides et al., 2021; Menzel et al., 2022), with lower crystallinity leading to more microcracks appearing earlier during degradation. Changes in MPs particles during degradation varied greatly depending on the composition and degree of crystallinity of the polymers. Menzel et al. (2022) concluded that the break-up of PE is driven by surface fragmentation. Indeed, we could show that PE particles significantly decreased in size after 2000 h of UV degradation, an average 46x smaller in magnitude on average compared to starting particles. For PE, fragments of various sizes were seen on the particle surfaces after 2000 degradation hours. The particles were very small but had sharp edges, and secondary NPs were attached to larger ones (Figure 2). A significant number of PE NPs particles formed after 2000 hours of weathering, an estimated 2.5% (see Figure S3, SI), which would predict a larger pool of NPs formed from sunlight exposure also in the environment with respective consequences for their accumulation and reactivity in soil.

Weathering and fragmentation should also affect the roughness of MPs. Accordingly, Menzel et al. (2022) observed that the first 400 hours of PE degradation resulted in smoother surfaces of PE due to abrasion, but did not reduce particle size. However, in our study, we did not observe significant smoothing of PE during the first 400 hours; instead, the particles became more rounded and resembled crumpled paper (Figure 3). Fragmentation was the main process from 400 to 2000 hours, with particle size decreasing exponentially and surfaces turning rougher, indicating rapid break-up, which was consistent to Menzel et al.'s observations. In our study, we did not consider degradation of PE after 2000 hours because, according to Menzel et al. (2022), after 2000 hours particle sizes remained stable. Particle disintegration continued mainly at the nanoscale, but a plateau occurred as disintegration was balanced by agglomeration (NPs particles sticking to larger ones). The substantial reduction in size of degraded PE and increased surface area may exhibit increased reactivity in soils, and the formation of NPs have largely unknown consequences but may be more environmentally relevant due to their highly changed properties.

For PET, fragmentation is less likely to occur, as photodegradation and the associated decrease in mechanical properties have been shown to be limited to a thin affected layer, about 15 μm, and chemical changes were detectable only within the top 50 μm surface of PET (Day & Wiles, 1972; Grossetête et al., 2000; Wang et al., 1998). The limited surface

penetration of UV radiation and oxygen into the bulk of the material explains why deeper layers remained relatively unaffected. The degradation products formed at the surface act as a barrier, preventing further weathering effects in the bulk (Lewandowski et al., 2013). In our study, PET particles showed some reduction in size at each degradation step, however with only tiny flaky fragments detaching from the surface. For PET particles, the decrease in the size of particles during degradation was not recognizable in SEM images (Figure 2); only by measuring the average diameter of particles under a microscope, the tiny flaky fragments that were detached from the outer layer of larger particles could be recognized (Figure S2, SI).

UV exposure of PET leads to significant changes in surface morphology, such as increased roughness and the formation of microcracks, which were evident in the SEM images. These changes were accompanied by variations in color and gloss, which are more noticeable in the early stages of degradation (Cañadas et al., 2019). However, we did not observe significant changes in color or the formation of microcracks until 2000 hours of accelerated degradation, where traces of abrasion first appeared. The roughness of the PET surface also increased (Figure S4, SI) and consequently, we observed more tiny flaky fragments on the surface, which had the potential of detaching from their larger particle. These are aligned with previous research on PET degradation, indicating that photodegradation primarily affects the surface of the polymer (Grossetête et al., 2000; Wang et al., 1998). The lack of significant particle size reduction in the initial 400 hours suggested that surface abrasion did not substantially reduce size early on. However, after 2000 hours, the increased roughness and tiny flaky fragments indicated more advanced degradation that could continue with increased weathering time. In the soil environment, the fragmentation of PET is very slow compared to PE, leading to prolonged accumulation and persistence in soils (Chamas et al., 2020). Over time, the increased surface roughness of degraded PET may interact with soil mineral and microbial components, affecting long-term soil dynamics.

Surface chemical changes in weathered PE and PET

Degradation of MPs in the environment, particularly under sunlight exposure, initiates change in their surface chemistry. Ultraviolet (UV) irradiation, a key component of sunlight, induces alterations in the polymer structure. For PE, this process introduces carboxyl, hydroxyl, hydroperoxides and oxygen containing functional groups, ultimately leading to chain scission (Andrady, 2011; Benítez et al., 2013; Bhagat et al., 2022; Pandey & Singh, 2001). Consequently, as a result of this chemical degradation process, the physicochemical properties of PE are transformed, resulting in an increase in the presence of functional groups on PE polymers due to accelerated weathering rates (Mauel et al., 2022; Meides et al., 2022).

Indeed, as seen here in the FTIR and XPS spectrum of degraded PE, especially for PE exposed for 2000 hours, new functional groups such as carboxylic acids were observed. Specifically, C-O stretching vibrations, characteristic of oxidation products such as alcohols, carbonyl compounds, esters, ethers, or ketals/acetals. The presence of these peaks suggested the formation of new functional groups due to the degradation process, indicating chemical changes on the surface of PE which will likely change its reactivity in the environment (Menzel et al., 2022). It is likely not possible to incorporate much more than 10% oxygen into the surface, as the oxidation is not controlled during degradation: in a first step, hydroxyl groups (alcohols) are formed, a portion of them are oxidized to ketones, then forming carboxylic acid groups, and eventually volatilizing as CO_2 (Mohanan et al., 2020; Yao et al., 2022). This is perhaps why our PE degraded for 400 hours showed a high increase in surface oxidized functional groups in the XPS (Figure 5), before major fractionation at 2000 hours into smaller sizes revealed new surfaces, therefore functional group formation over degradation time is dynamic with particle size reduction and surface exposure (Menzel et al., 2022). Degradation of PE at 2000 hours caused more fragmentation into smaller pieces, creating new submicron surfaces with higher surface areas, which increased its reactivity in combination with functional group formation. The increased surface area, decreased hydrophobicity, and introduction of hydroxyl, hydroperoxides, and other polar functional groups can affect pH-dependent charges, such as surface chemistry in soil minerals and organic matter.

All measured samples for both PE and PET showed strongly negative zeta potential values because of large hydrophobic surface area without water adsorption (Figure 6). As the size of PE particles decreased, the absolute zeta potential values increased. This happened because smaller particles have a larger surface area, leading to higher zeta potential values (Bhagat et al., 2022; Sarkar et al., 2021; Y. K. Song et al., 2017). Generally, when we increased the pH, the absolute zeta potential values of MPs also increased. The specific reaction of weathered PE particles to alkalinity could be interpreted as a swelling of the surface (gray symbols, Figure 6), however, this would need further investigation. ESEM imaging showed a shift from hydrophobic behavior in pristine PE to hydrophilic after degradation (Figure 3). This indicated a shift in polarity and the ability of PE to interact with the polar phase of water, which is confirmed in recent studies also showing hydrophilic changes to PE artificially or naturally degraded (Shang et al., 2022; Zhang et al., 2024). Over time, the increased interaction of PE with water would change its chemical behavior in soils, suggesting changes in plastic chemical sorption over degradation time based on the change from hydrophobic to

hydrophilic interactions. PE that has undergone significant degradation could then interact with pollutants, nutrients, and influence soil pH by interaction with H+ and OH- species in water.

For PET, other studies have shown that UV-degradation was more subtle and limited to the surface (Lewandowski et al., 2013; Suresh et al., 2011; Wang et al., 1998). PET contains ester and aromatic groups that could become more oxidized to introduce carbonyl or hydrolyze ester bonds to form carboxyl and hydroxyl groups. This happens because acidic groups might form or settle on the particle surface (Benítez et al., 2013; Bhagat et al., 2022; Pandey & Singh, 2001). The height of the initial peaks in the spectra of pristine PET at 1711 cm^{-1} (carbonyl stretching) and 1233 cm^{-1} (C-O stretching) increased with increasing degrees of weathering (Sang et al., 2020). In our study, PET did not exhibit a large change in chemical functional groups after degradation. While FTIR did not detect functional group change in the top surface (few micrometers), XPS revealed an initial shift away at the surface (few nanometers) after 400 degradation hours, from oxidized carbon to more single carbon bonds (see Figure S6, SI). At 2000 hours the shift remained the same, suggesting early transformation after 400 hours of the very top surface of PET which becomes stabilized. XPS analysis revealed only slight changes in atomic ratios between C and O, but the introduction of fluorine compounds during degradation created the largest shift (see Table 1). Therefore, we could conclude that the stable chemical properties of PET were resistant to photooxidation even after accelerated degradation, indicating slow transformation and degradation in natural environments. Hydrophobic properties of PET did not change due to weathering but rather showed variable hydrophilic and hydrophobic on the surface of PET. As the chemical degradation of PET had only little effect on its surface chemistry, then the main factor increasing the CEC values was the increasing surface area (Figure 7). Altogether, size and surface charge analyses indicated that as PE and PET become break down and become smaller in the environment, their reactivity increases, and this reactivity should be most pronounced in alkaline environments.

Potential roles of degraded MPs particles in soils

Research has shown that PE can affect soil physicochemical properties, with PE significantly increasing CEC (Kim et al., 2020; Liu et al., 2020). However, our findings highlighted that the degradation state of PE played a more crucial role in influencing CEC than merely the presence of PE. Generally, the CEC of most soils increases with pH. At very low pH values, the CEC is usually low. In these conditions, only the permanent charges of clay minerals and a small portion of the pH-dependent charges on colloids hold exchangeable

ions. If the input of PE with pH-dependent, variable charge to a soil system is high, especially in limed soil or alkaline soils, this could result in significant changes to nutrient and pollutant cycling. Some research even suggests that increasing MPs in soil could positively affect their fertility by increasing CEC values (Li et al., 2023). However, to give a theoretical calculation example: the measured 77 $cmol_c$ / kg clay for a highly reactive clay such as montmorillonite that might occur to 10% or more in soil would give a total charge of 7.7 $cmol_c$ / kg soil. A soil contaminated with plastic, even under critical management conditions such as ploughing and direct incorporation of PE, might reach 1% plastic content (Büks & Kaupenjohann, 2020; Z. Jia et al., 2024). With a measured charge of around 7.5 $cmol_c$ / kg for degraded PE in alkaline conditions, this would contribute 0.075 $cmol_c$ / kg of soil, a small but potentially relevant contribution. If continued input and accumulation of plastic pollution to soil continues, clay content is reduced or absent in soil (Li et al., 2021), or hotspots occur in specific soil regions where MPs might accumulate >1%, the surface reactivity of degraded PE could start affecting cationic nutrient and pollutant dynamics to a degree comparable or in competition to clay minerals.

Research should focus now on micro-sites in soil where plastic surface charge can matter either due to a massive enrichment compared to bulk soil (Corradini et al., 2019), or due to the attraction of soil microbes that are part of carbon and nutrient cycling. The weathered and charged MPs may then play a role for micro-scale processes such as soil aggregation and, indirectly, for nutrient dynamics. Additionally, it is important to focus research on assessing the ratio between fresh and weathered portions of PE and PET and further plastic types in soil, as this might affect the interpretation of hydrophobic and reactive chemical effects which would be especially relevant for soils under climatic stress or drought conditions.

Conclusion

This study provided information on the physicochemical changes of PE and PET MPs during UV degradation. Studying the degradation of MPs is crucial because weathering alters their physicochemical properties, such as surface area, charge, and chemical composition of these MPs. PE particles showed a significant decrease in size over 46x after 2000 hours of degradation, causing an increase in particle distribution, surface area, and chemical reactivity. PE formed a substantial amount (estimated 2.5%) of NPs <1 µm after 2000 hours of degradation, which has largely unknown environmental consequences. The formation of new functional groups in degraded PE, such as carbonyl groups, carboxylic acids, and its shift to hydrophilic behavior indicate that degraded PE is more environmentally relevant than pristine

PE, as these many changes in surface properties have potential to complex with other soil components, mineral and organic, which require further study to elucidate. In contrast, PET particles showed minimal size reduction and change in surface chemistry, highlighting differences in degradation behavior based on polymer structure and crystallinity. The negative surface charges on both PE and PET increase with degradation, though the increased reactivity of degraded PE, especially at alkaline conditions, exhibits a major shift in chemical behavior due to its changed surface forming new functional groups with increased hydrophilic interactions. PE showed a significant increase in CEC with degradation, particularly at higher pH levels, indicating greater adsorption capacity which is relevant to alkaline soils or soils with low reactive mineral contents. The degradation rate of PE plays a more crucial role in influencing CEC than merely the presence of PE. PET showed minimal changes in CEC, functional group formation, or change in hydrophobicity with degradation, suggesting that its adsorption properties are less affected by degradation compared to PE and will require more degradation time to reach a level of reactivity that is relevant to soil functions. While reactivity of degraded PE and PET are still quite low after degradation compared to natural soil components such as clay, the large accumulation of MPs in agricultural soils and their limited mineralization is still relevant to study the impact of degraded and transformed MPs surface in context to sustainable agroecosystems. This study highlights the need for further research of degraded and transformed MPs interactions in soils to assess the long-term impact of MPs to soil chemical functions.

Acknowledgements

This study was performed within the Collaborative Research Center 1357 “Microplastics - Understanding the mechanisms and processes of biological effects, transport and formation: From model to complex systems as a basis for new solutions.” This study was funded by the Deutsche Forschungsgemeinschaft (DFG, German Research Foundation) – SFB 1357 – 391977956. We thank these members of the University of Bayreuth: N. Meides (Macromolecular Chemistry) for providing degraded microplastics, M. Obst of the Analytical Chemistry Lab (CAN) for chemical analysis, A. Jakobs for assistance with microscopic analysis (Ecological Microbiology), M. Löder for conducting FTIR analysis (Animal Ecology I), and M. Becevic (Soil Ecology) for graphic design support. Additional thanks to F. Simon of Polymer Interfaces, Leibniz-Institut für Polymerforschung Dresden e.V., for XPS support; and M. Heider for her support with SEM analysis at the Keylab Electron and Optical

Microscopy (BPI), Bayreuth Institute of Macromolecular Research (BIMF). A special thanks to T. Glaser for preliminary CEC research and K. Söllner for her technical expertise.

Supporting Information

The Supporting Information contains additional particle size distribution table and figures, additional SEM and ESEM images, and XPS PET analysis.

*Corresponding author: E-Mail: ryan.bartnick@uni-bayreuth.de

References

Andrady, A. L. (2011). Microplastics in the marine environment. *Marine Pollution Bulletin*, *62*(8), 1596–1605. https://doi.org/10.1016/j.marpolbul.2011.05.030

Andrady, A. L. (2017). The plastic in microplastics: A review. *Marine Pollution Bulletin*, *119*(1), 12–22. https://doi.org/10.1016/j.marpolbul.2017.01.082

Benítez, A., Sánchez, J. J., Arnal, M. L., Müller, A. J., Rodríguez, O., & Morales, G. (2013). Abiotic degradation of LDPE and LLDPE formulated with a pro-oxidant additive. *Polymer Degradation and Stability*, *98*(2), 490–501. https://doi.org/10.1016/j.polymdegradstab.2012.12.011

Bhagat, K., Barrios, A. C., Rajwade, K., Kumar, A., Oswald, J., Apul, O., & Perreault, F. (2022). Aging of microplastics increases their adsorption affinity towards organic contaminants. *Chemosphere*, *298*, 134238. https://doi.org/10.1016/j.chemosphere.2022.134238

Boots, B., Russell, C. W., & Green, D. S. (2019). Effects of Microplastics in Soil Ecosystems: Above and Below Ground. *Environmental Science & Technology*, *53*(19), 11496–11506. https://doi.org/10.1021/acs.est.9b03304

Braun, M., Mail, M., Krupp, A. E., & Amelung, W. (2023). Microplastic contamination of soil: Are input pathways by compost overridden by littering? *The Science of the Total Environment*, *855*, 158889. https://doi.org/10.1016/j.scitotenv.2022.158889

Briggs, D. (1981). Handbook of X-ray Photoelectron Spectroscopy C. D. Wanger, W. M. Riggs, L. E. Davis, J. F. Moulder and G. E.Muilenberg Perkin-Elmer Corp., Physical Electronics Division, Eden Prairie, Minnesota, USA, 1979. 190 pp. *Surface and Interface Analysis*, *3*(4). https://doi.org/10.1002/sia.740030412

Briggs, David., & Beamson, Graham. (1992). Primary and secondary oxygen-induced C1s binding energy shifts in x-ray photoelectron spectroscopy of polymers. *Analytical Chemistry*, *64*(15), 1729–1736. https://doi.org/10.1021/ac00039a018

Büks, F., & Kaupenjohann, M. (2020). Global concentrations of microplastics in soils – a review. *SOIL*, *6*(2), 649–662. https://doi.org/10.5194/soil-6-649-2020

Bukšek, H., Luxbacher, T., & Petrinić, I. (2010). Zeta potential determination of polymeric materials using two differently designed measuring cells of an electrokinetic analyzer. *Acta Chimica Slovenica*, *57*(3), 700–706.

Cañadas, J. C., Diego, J. A., Mudarra, M., Parsa, S. E., & Sellarès, J. (2019). Effects of UV radiation on the charge trapping capability of PET. *Journal of Physics D: Applied Physics*, *52*(15), 155301. https://doi.org/10.1088/1361-6463/aafea1

Chamas, A., Moon, H., Zheng, J., Qiu, Y., Tabassum, T., Jang, J. H., Abu-Omar, M., Scott, S. L., & Suh, S. (2020). Degradation Rates of Plastics in the Environment. *ACS Sustainable Chemistry & Engineering*, *8*(9), 3494–3511. https://doi.org/10.1021/acssuschemeng.9b06635

Corradini, F., Meza, P., Eguiluz, R., Casado, F., Huerta-Lwanga, E., & Geissen, V. (2019). Evidence of microplastic accumulation in agricultural soils from sewage sludge disposal. *The Science of the Total Environment*, *671*, 411–420. https://doi.org/10.1016/j.scitotenv.2019.03.368

Day, M., & Wiles, D. M. (1972). Photochemical degradation of poly(ethylene terephthalate). III. Determination of decomposition products and reaction mechanism. *Journal of Applied Polymer Science*, *16*(1), 203–215. https://doi.org/10.1002/app.1972.070160118

Geyer, R., Jambeck, J. R., & Law, K. L. (2017). Production, use, and fate of all plastics ever made. *Science Advances*, *3*(7), 1700782. https://doi.org/10.1126/sciadv.1700782

Giglio, E., Ditaranto, N., & Sabbatini, L. (2014). 3. Polymer surface chemistry: Characterization by XPS. In L. Sabbatini (Ed.), *Polymer Surface Characterization* (pp. 73–112). DE GRUYTER. https://doi.org/10.1515/9783110288117.73

Grossetête, T., Rivaton, A., Gardette, J. L., Hoyle, C. E., Ziemer, M., Fagerburg, D. R., & Clauberg, H. (2000). Photochemical degradation of poly(ethylene terephthalate)-modified copolymer. *Polymer*, *41*(10), 3541–3554. https://doi.org/10.1016/S0032-3861(99)00580-7

He, D., & Luo, Y. (Eds.). (2020). *Microplastics in Terrestrial Environments: Emerging Contaminants and Major Challenges* (Vol. 95). Springer International Publishing. https://doi.org/10.1007/978-3-030-56271-7

Healy, T. W., & Fuerstenau, D. W. (2007). The isoelectric point/point-of zero-charge of interfaces formed by aqueous solutions and nonpolar solids, liquids, and gases. *Journal of Colloid and Interface Science*, *309*(1), 183–188. https://doi.org/10.1016/j.jcis.2007.01.048

Hopewell, J., Dvorak, R., & Kosior, E. (2009). Plastics recycling: Challenges and opportunities. *Philosophical Transactions of the Royal Society of London. Series B, Biological Sciences*, *364*(1526), 2115–2126. https://doi.org/10.1098/rstb.2008.0311

Huang, Y., Liu, Q., Jia, W., Yan, C., & Wang, J. (2020). Agricultural plastic mulching as a source of microplastics in the terrestrial environment. *Environmental Pollution (Barking, Essex : 1987)*, *260*, 114096. https://doi.org/10.1016/j.envpol.2020.114096

Imhof, H. K., Schmid, J., Niessner, R., Ivleva, N. P., & Laforsch, C. (2012). A novel, highly efficient method for the separation and quantification of plastic particles in sediments of aquatic environments. *Limnology and Oceanography: Methods*, *10*(7), 524–537. https://doi.org/10.4319/lom.2012.10.524

Ingraffia, R., Amato, G., Bagarello, V., Carollo, F. G., Giambalvo, D., Iovino, M., Lehmann, A., Rillig, M. C., & Frenda, A. S. (2022). Polyester microplastic fibers affect soil physical properties and erosion as a function of soil type. *SOIL*, *8*(1), 421–435. https://doi.org/10.5194/soil-8-421-2022

Jang, M.-H., Kim, M.-S., Han, M., & Kwak, D.-H. (2022). Experimental application of a zero-point charge based on pH as a simple indicator of microplastic particle aggregation. *Chemosphere*, *299*, 134388. https://doi.org/10.1016/j.chemosphere.2022.134388

Jia, Z., Wei, W., Wang, Y., Chang, Y., Lei, R., & Che, Y. (2024). Occurrence characteristics and risk assessment of microplastics in agricultural soils in the loess hilly gully area of Yan' an, China. *The Science of the Total Environment*, *912*, 169627. https://doi.org/10.1016/j.scitotenv.2023.169627.

Khan, S. A., Khan, S. B., Khan, L. U., Farooq, A., Akhtar, K., & Asiri, A. M. (2018). Fourier Transform Infrared Spectroscopy: Fundamentals and Application in Functional Groups and Nanomaterials Characterization. In S. K. Sharma (Ed.), *Handbook of Materials Characterization* (pp. 317–344). Springer International Publishing. https://doi.org/10.1007/978-3-319-92955-2_9

Kim, S. W., Kim, D., Jeong, S.-W., & An, Y.-J. (2020). Size-dependent effects of polystyrene plastic particles on the nematode Caenorhabditis elegans as related to soil physicochemical properties. *Environmental Pollution (Barking, Essex : 1987)*, *258*, 113740. https://doi.org/10.1016/j.envpol.2019.113740

Kissin, Y. V. (2020). *Polyethylene: End-use properties and their physical meaning* (Second edition). Hanser Publishers.

Kontogeorgis, G. M., & Kiil, S. (2016). *Introduction to Applied Colloid and Surface Chemistry*. Wiley. https://doi.org/10.1002/9781118881194

Kumar, M., Xiong, X., He, M., Tsang, D. C. W., Gupta, J., Khan, E., Harrad, S., Hou, D., Ok, Y. S., & Bolan, N. S. (2020). Microplastics as pollutants in agricultural soils. *Environmental Pollution (Barking, Essex : 1987)*, *265*(Pt A), 114980. https://doi.org/10.1016/j.envpol.2020.114980

Lewandowski, S., Rejsek-Riba, V., Bernès, A., Perraud, S., & Lacabanne, C. (2013). Multilayer films ageing under ultraviolet radiations: Complementary study by dielectric spectroscopy. *Journal of Applied Polymer Science*, *129*(6), 3772–3781. https://doi.org/10.1002/app.38747

Li, J., Yu, Y., Zhang, Z., & Cui, M. (2023). The positive effects of polypropylene and polyvinyl chloride microplastics on agricultural soil quality. *Journal of Soils and Sediments*, *23*(3), 1304–1314. https://doi.org/10.1007/s11368-022-03387-6

Li, M., Zhang, X., Yi, K., He, L., Han, P., & Tong, M. (2021). Transport and deposition of microplastic particles in saturated porous media: Co-effects of clay particles and natural organic matter. *Environmental Pollution*, *287*, 117585. https://doi.org/10.1016/j.envpol.2021.117585

Liu, C. L., Wang, M. K., & Yang, C. C. (2001). Determination of cation exchange capacity by one-step soil leaching column method. *Communications in Soil Science and Plant Analysis*, *32*(15–16), 2359–2372. https://doi.org/10.1081/CSS-120000378

Liu, J., Wang, Z., Hu, F., Xu, C., Ma, R., & Zhao, S. (2020). Soil organic matter and silt contents determine soil particle surface electrochemical properties across a long-term natural restoration grassland. *CATENA*, *190*, 104526. https://doi.org/10.1016/j.catena.2020.104526

Mattsson, K., Hansson, L.-A., & Cedervall, T. (2015). Nano-plastics in the aquatic environment. *Environmental Science. Processes & Impacts*, *17*(10), 1712–1721. https://doi.org/10.1039/C5EM00227C

Mauel, A., Pötzschner, B., Meides, N., Siegel, R., Strohriegl, P., & Senker, J. (2022). Quantification of photooxidative defects in weathered microplastics using 13C multiCP NMR spectroscopy. *RSC Advances*, *12*(18), 10875–10885. https://doi.org/10.1039/d2ra00470d

Meides, N., Mauel, A., Menzel, T., Altstädt, V., Ruckdäschel, H., Senker, J., & Strohriegl, P. (2022). Quantifying the fragmentation of polypropylene upon exposure to accelerated weathering. *Microplastics and Nanoplastics*, *2*(1). https://doi.org/10.1186/s43591-022-00042-2

Meides, N., Menzel, T., Poetzschner, B., Löder, M. G. J., Mansfeld, U., Strohriegl, P., Altstaedt, V., & Senker, J. (2021). Reconstructing the Environmental Degradation of Polystyrene by Accelerated Weathering. *Environmental Science & Technology*, *55*(12), 7930–7938. https://doi.org/10.1021/acs.est.0c07718

Menzel, T., Meides, N., Mauel, A., Mansfeld, U., Kretschmer, W., Kuhn, M., Herzig, E. M., Altstädt, V., Strohriegl, P., Senker, J., & Ruckdäschel, H. (2022). Degradation of low-density polyethylene to nanoplastic particles by accelerated weathering. *The Science of the Total Environment*, *826*, 154035. https://doi.org/10.1016/j.scitotenv.2022.154035

Mohanan, N., Montazer, Z., Sharma, P. K., & Levin, D. B. (2020). Microbial and Enzymatic Degradation of Synthetic Plastics. *Frontiers in Microbiology*, *11*, 580709. https://doi.org/10.3389/fmicb.2020.580709

Pandey, J. K., & Singh, R. P. (2001). UV-irradiated biodegradability of ethylene—Propylene copolymers, LDPE, and I-PP in composting and culture environments. *Biomacromolecules*, *2*(3), 880–885. https://doi.org/10.1021/bm010047s

Pergande, M. R., & Cologna, S. M. (2017). Isoelectric Point Separations of Peptides and Proteins. *Proteomes*, *5*(1). https://doi.org/10.3390/proteomes5010004

Priya, A., Dutta, K., & Daverey, A. (2022). A comprehensive biotechnological and molecular insight into plastic degradation by microbial community. *Journal of Chemical Technology & Biotechnology*, *97*(2), 381–390. https://doi.org/10.1002/jctb.6675

Sang, T., Wallis, C. J., Hill, G., & Britovsek, G. J. P. (2020). Polyethylene terephthalate degradation under natural and accelerated weathering conditions. *European Polymer Journal*, *136*, 109873. https://doi.org/10.1016/j.eurpolymj.2020.109873

Sarkar, A. K., Rubin, A. E., & Zucker, I. (2021). Engineered Polystyrene-Based Microplastics of High Environmental Relevance. *Environmental Science & Technology*, *55*(15), 10491–10501. https://doi.org/10.1021/acs.est.1c02196

Schäfer, M., & Steiger, M. (2002). A rapid method for the determination of cation exchange capacities of sandstones: Preliminary data. *Geological Society, London, Special Publications*, *205*(1), 431–439. https://doi.org/10.1144/GSL.SP.2002.205.01.31

Schindelin, J., Arganda-Carreras, I., Frise, E., Kaynig, V., Longair, M., Pietzsch, T., Preibisch, S., Rueden, C., Saalfeld, S., Schmid, B., Tinevez, J.-Y., White, D. J., Hartenstein, V., Eliceiri, K., Tomancak, P., & Cardona, A. (2012). Fiji: An open-source platform for biological-image analysis. *Nature Methods*, *9*(7), 676–682. https://doi.org/10.1038/nmeth.2019

Shang, C., Wang, B., Guo, W., Huang, J., Zhang, Q., Xie, H., Gao, H., & Feng, Y. (2022). The weathering process of polyethylene microplastics in the paddy soil system: Does the coexistence of pyrochar or hydrochar matter? *Environmental Pollution*, *315*, 120421. https://doi.org/10.1016/j.envpol.2022.120421

Sharma, V. K., Ma, X., Guo, B., & Zhang, K. (2021). Environmental factors-mediated behavior of microplastics and nanoplastics in water: A review. *Chemosphere*, *271*, 129597. https://doi.org/10.1016/j.chemosphere.2021.129597

Song, Y. K., Hong, S. H., Jang, M., Han, G. M., Jung, S. W., & Shim, W. J. (2017). Combined Effects of UV Exposure Duration and Mechanical Abrasion on Microplastic Fragmentation by Polymer Type. *Environmental Science & Technology*, *51*(8), 4368–4376. https://doi.org/10.1021/acs.est.6b06155

Souza Machado, A. A., Lau, C. W., Till, J., Kloas, W., Lehmann, A., Becker, R., & Rillig, M. C. (2018). Impacts of Microplastics on the Soil Biophysical Environment. *Environmental Science & Technology*, *52*(17), 9656–9665. https://doi.org/10.1021/acs.est.8b02212

Stumm, W., & Morgan, J. J. (1996). *Aquatic chemistry: Chemical equilibria and rates in natural waters* (Third edition). John Wiley & Sons, Inc.

Suresh, B., Maruthamuthu, S., Kannan, M., & Chandramohan, A. (2011). Mechanical and surface properties of low-density polyethylene film modified by photo-oxidation. *Polymer Journal*, *43*(4), 398–406. https://doi.org/10.1038/pj.2010.147

Wang, W., Taniguchi, A., Fukuhara, M., & Okada, T. (1998). Surface nature of UV deterioration in properties of solid poly(ethylene terephthalate). *Journal of Applied Polymer Science*, *67*(4), 705–714. https://doi.org/10.1002/(SICI)1097-4628(19980124)67:4%3C705::AID-APP13%3E3.0.CO;2-Q

Wang, Yu, Wang, F., Xiang, L., Bian, Y., Wang, Z., Srivastava, P., Jiang, X., & Xing, B. (2022). Attachment of positively and negatively charged submicron polystyrene plastics on nine typical soils. *Journal of Hazardous Materials*, *431*, 128566. https://doi.org/10.1016/j.jhazmat.2022.128566

Wang, Yuan, Wang, X., Li, Y., Liu, Y., Sun, Y., Hansen, H. C. B., Xia, S., & Zhao, J. (2022). Effects of struvite-loaded zeolite amendment on the fate of copper, tetracycline and antibiotic resistance genes in microplastic-contaminated soil. *Chemical Engineering Journal*, *430*, 130478. https://doi.org/10.1016/j.cej.2021.130478

Wen, X., Yin, L., Zhou, Z., Kang, Z., Sun, Q., Zhang, Y., Long, Y., Nie, X., Wu, Z., & Jiang, C. (2022). Microplastics can affect soil properties and chemical speciation of metals in yellow-brown soil. *Ecotoxicology and Environmental Safety*, *243*, 113958. https://doi.org/10.1016/j.ecoenv.2022.113958

Yao, C., Xia, W., Dou, M., Du, Y., & Wu, J. (2022). Oxidative degradation of UV-irradiated polyethylene by laccase-mediator system. *Journal of Hazardous Materials*, *440*, 129709. https://doi.org/10.1016/j.jhazmat.2022.129709

Yeganeh, M. S., Dougal, S. M., & Pink, H. S. (1999). Vibrational Spectroscopy of Water at Liquid/Solid Interfaces: Crossing the Isoelectric Point of a Solid Surface. *Physical Review Letters*, *83*(6), 1179–1182. https://doi.org/10.1103/PhysRevLett.83.1179

Zhang, G. S., Zhang, F. X., & Li, X. T. (2019). Effects of polyester microfibers on soil physical properties: Perception from a field and a pot experiment. *The Science of the Total Environment*, *670*, 1–7. https://doi.org/10.1016/j.scitotenv.2019.03.149

Zhang, S., Li, Y., Chen, X., Jiang, X., Li, J., Yang, L., Yin, X., & Zhang, X. (2022). Occurrence and distribution of microplastics in organic fertilizers in China. *The Science of the Total Environment*, *844*, 157061. https://doi.org/10.1016/j.scitotenv.2022.157061

Zhang, S., Lin, T., Zhang, C., Yang, W., Zhou, X., Cable, R., Choi, J., Michaelson, E., Thakre, P., Serrat, C., Tan, Y., Hu, J., Meunier, D., Lai, Y., Duhaime, M., & Chen, Z. (2024). Analysis of Accelerated Weathering Effect on Polyethylene With Varied Parameters Using a Combination of Analytical Techniques. *ChemistrySelect*, *9*(41), e202404334. https://doi.org/10.1002/slct.202404334

UV-Degraded Polyethylene Exhibits Variable Charge and Enhanced Cation Adsorption

Ryan Bartnick[*1], Shahin Shahriari[1], Günter K. Auernhammer[2], Ulrich Mansfeld[3], Werner Reichstein[4], Lisa Hülsmann[5], Eva Lehndorff[1]

[1]Soil Ecology, University of Bayreuth, Dr.-Hans-Frisch-Str. 1-3, 95448 Bayreuth, Germany
[2]Leibniz-Institut für Polymerforschung Dresden e.V., Hohe Straße 6, 01069 Dresden, Germany
[3]Keylab Electron and Optical Microscopy, Bavarian Polymer Institute, University of Bayreuth, Universitätsstr. 30, 95447 Bayreuth, Germany

[4]Ceramic Materials Engineering, University of Bayreuth, Prof.-Rüdiger-Bormann-Str. 1, 95447 Bayreuth, Germany

[5]Ecosystem Analysis and Simulation, University of Bayreuth, Dr.-Hans-Frisch-Str. 1-3, 95448 Bayreuth, Germany

[*]Corresponding author: Email: ryan.bartnick@uni-bayreuth.de

This supporting information includes:

Table S1
Figure S1-S6

Supporting Information

The SI contains additional particle size distribution table and figures, additional SEM and ESEM images, and XPS PET analysis.

Table S1. Particle size distribution table of PE and PET after 0, 400, and 2000 hours of degradation.

plastic	mean ± s.d. [µm]	max peak ± s.d. [µm]	width ± s.d. [µm]	range [µm]	
				low	high
PE 0 h	375 ± 117	349 ± 15	189 ± 48	161	689
PE 400 h	370 ± 105	357 ± 17	223 ± 61	160	693
PE 2000 h	7.8 ± 7.5	4.5 ± 0.5	5.9 ± 2.3	< 1	66
PET 0 h	653 ± 219	519 ± 106	740 ± 454	333	1239
PET 400 h	531 ± 196	449 ± 20	298 ± 55	256	1286
PET 2000 h	484 ± 274	405 ± 41	640 ± 177	24	1165

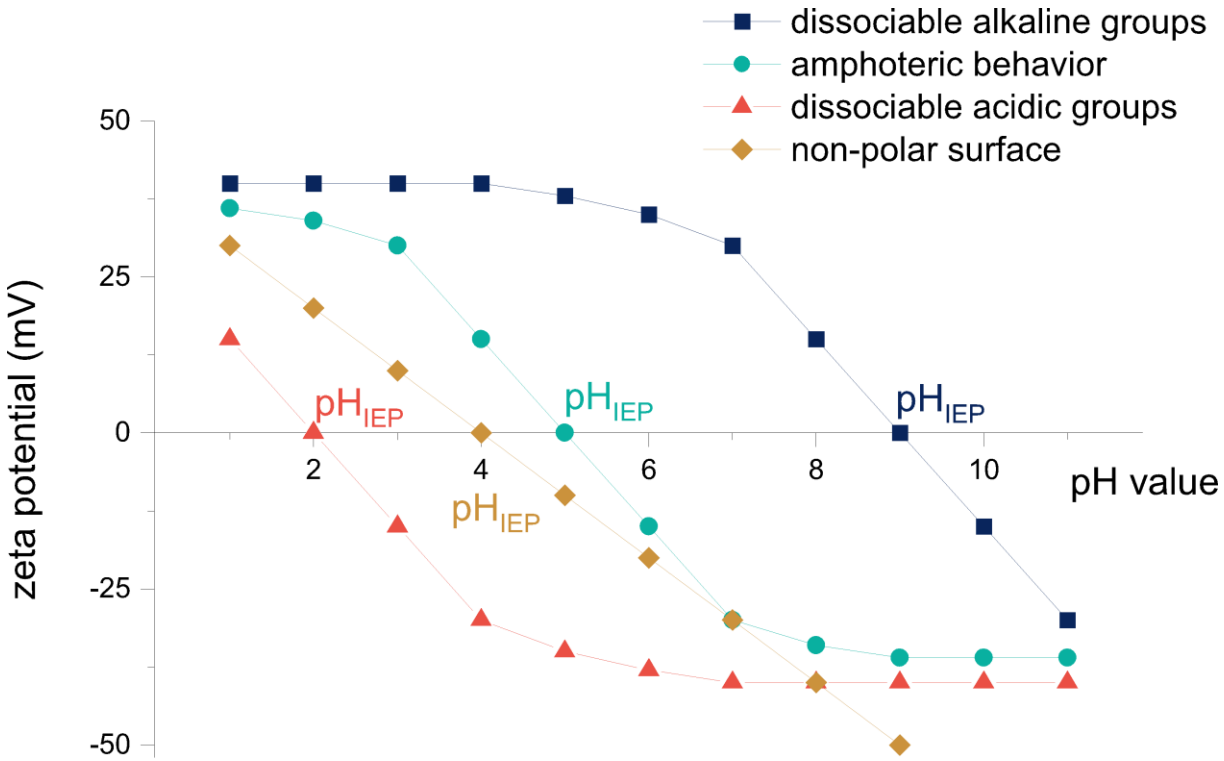

Figure S1. Zeta potential (ζ) of particles with different functional groups in the presence of KCl under different pH conditions. For non-polar / non-dissociating surfaces, the isoelectric point (IEP) is determined around pH 4.

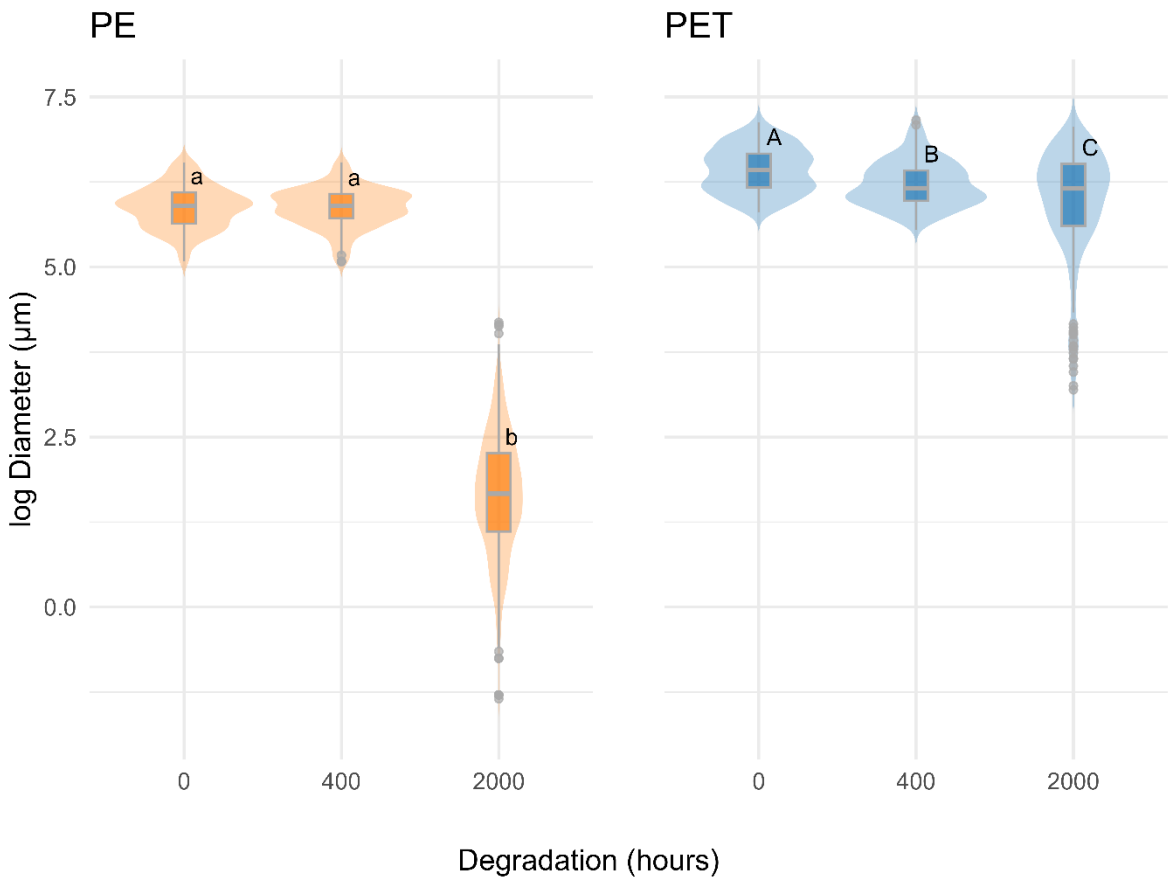

Figure S2. Particle size distribution of PE and PET plastics after degradation (log-transformed). Significant differences from Tukey HSD tests are displayed as different characters.

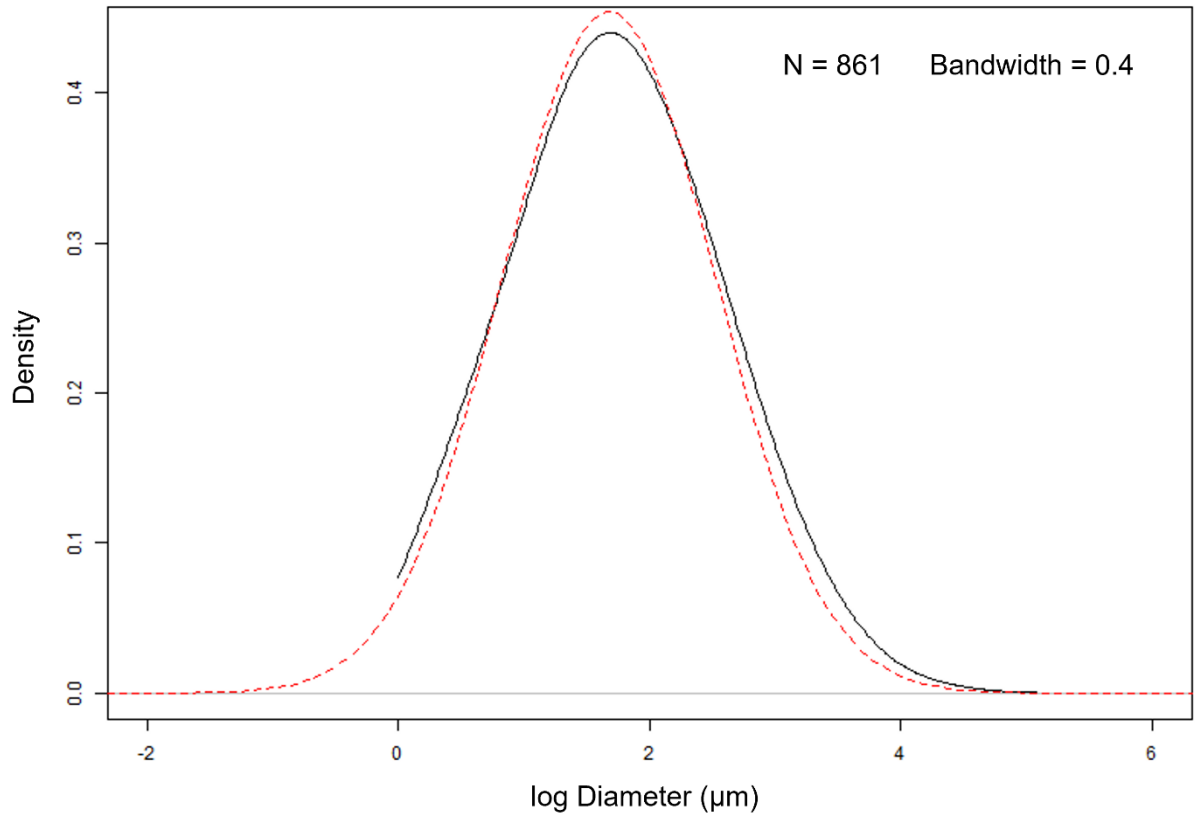

Figure S3. PE 2000 hours degraded observed particle size distribution (log-transformed; black line), with estimated fit of truncated normal distribution (red dashed line) which estimated 2.5% of the distribution as undetected particles <1 µm.

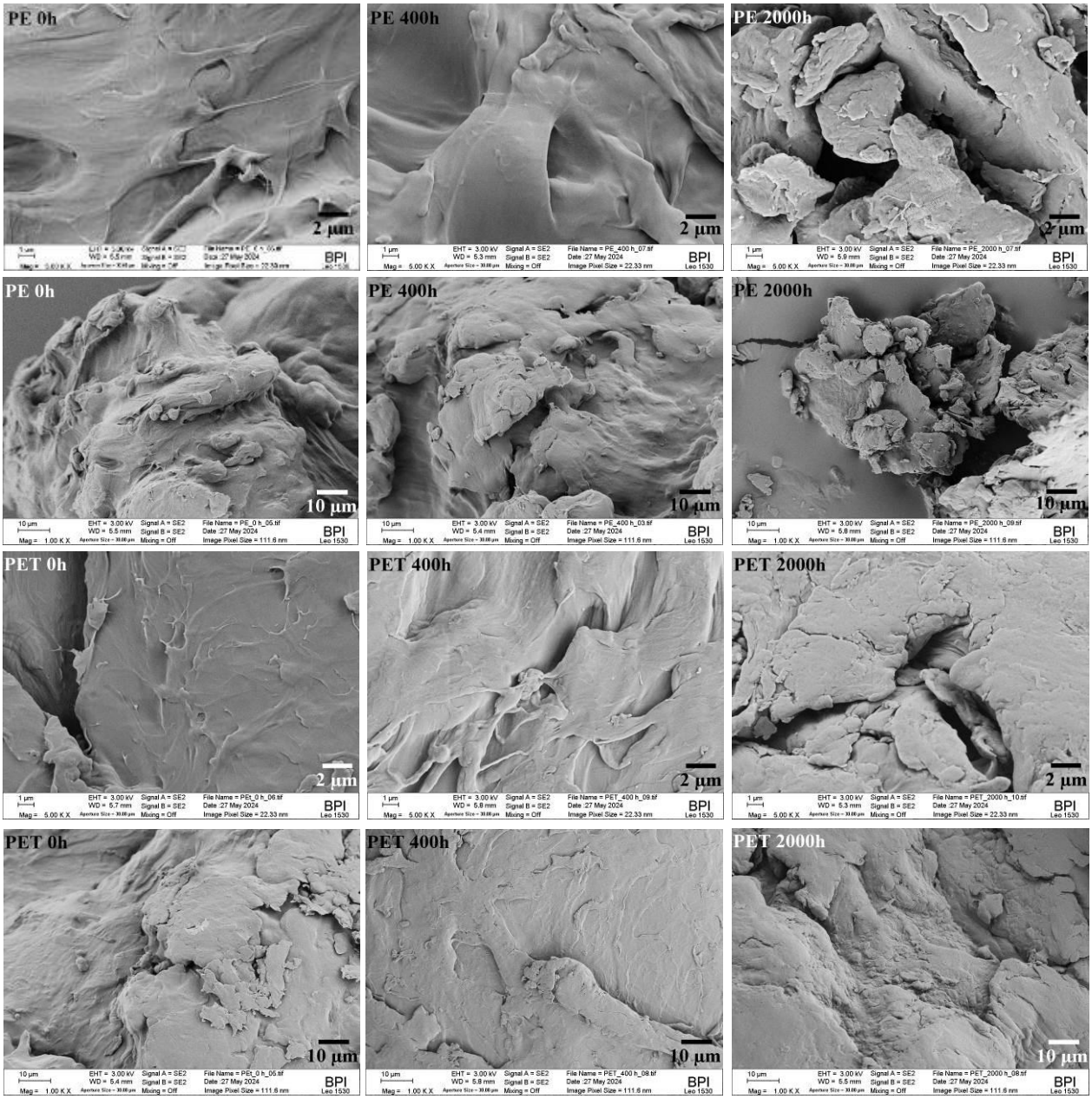

Figure S4. SEM images of PE (top two rows) and PET (bottom two rows), pristine (0 h) and degraded at 400 h and 2000 h (left to right), at 5000x and 1000x magnification. Degradation decreases the size of PE particles, while PET particles show no significant size changes.

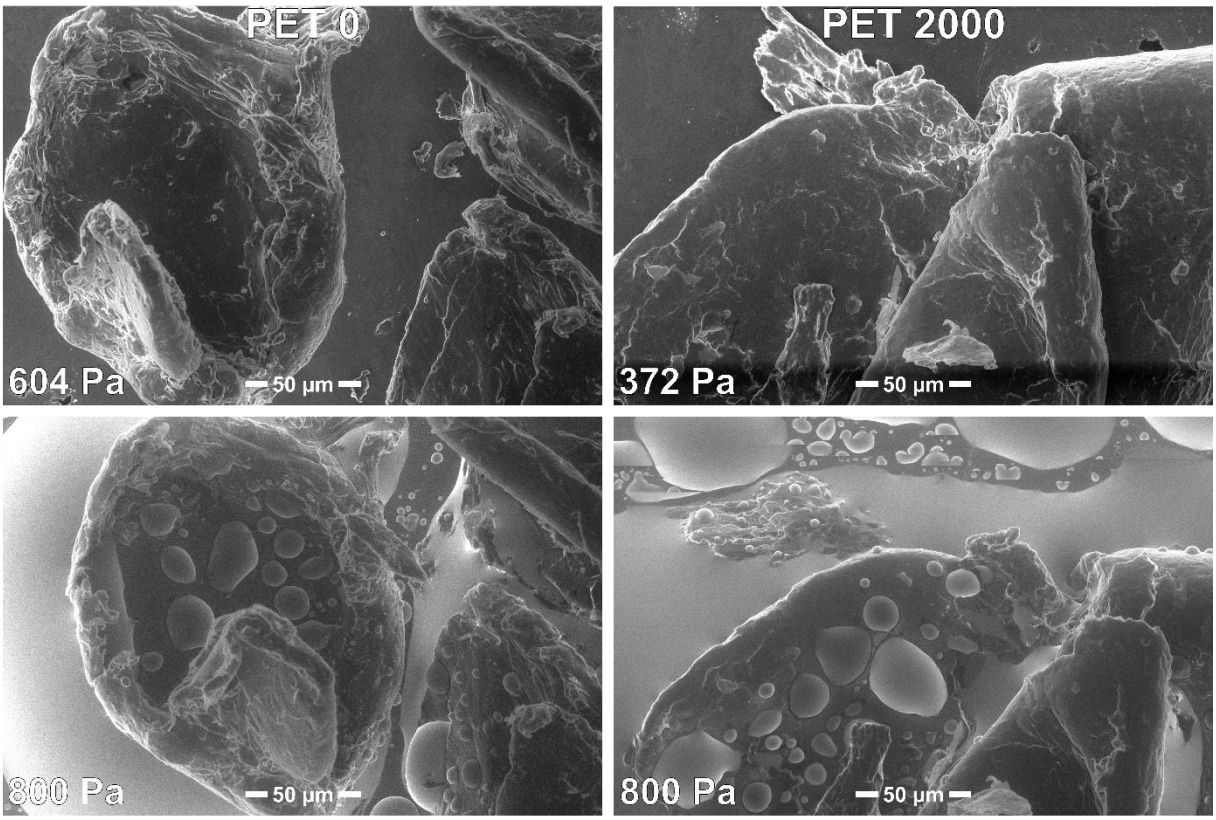

Figure S5. ESEM images of PET pristine (left) and degraded at 2000 hours (right), at 300x magnification. PET particles show no significant changes in wettability over degradation time.

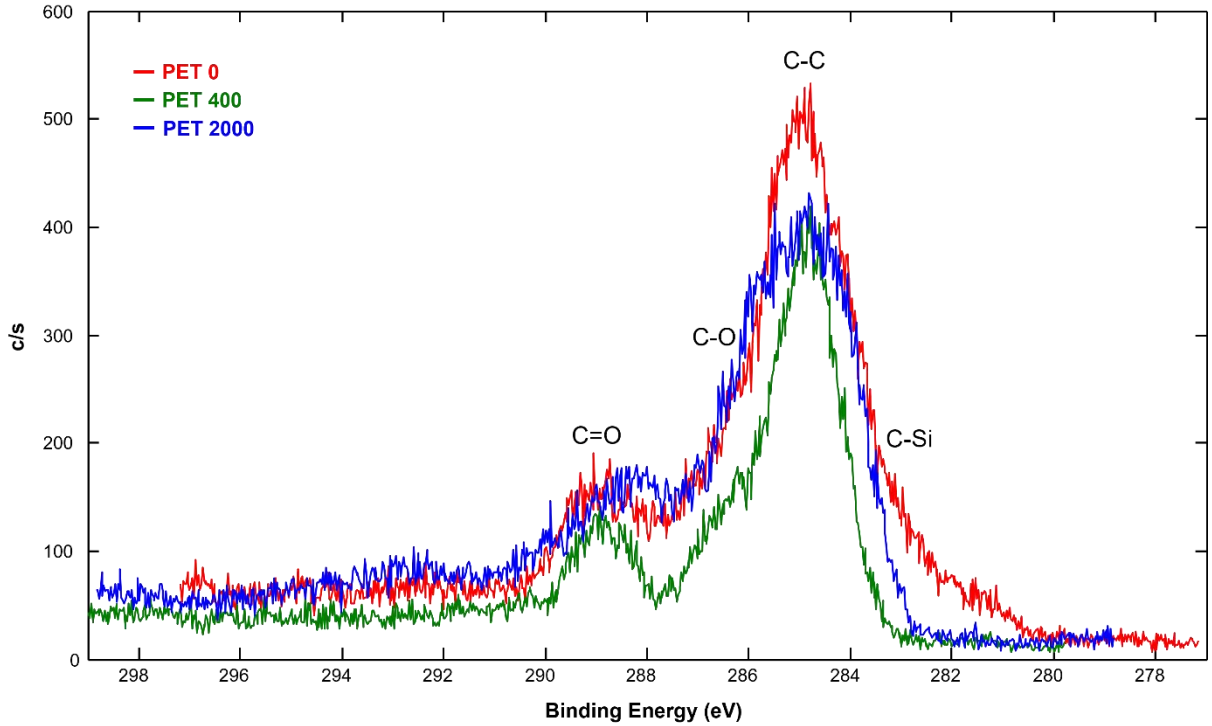

Figure S6. XPS overlay of C1s spectra of PET degraded at 0 (red), 400 (green), and 2000 (blue) hours of degradation.

4. Manuscript 4: Plastic Quantification and Polyethylene Overestimation in Agricultural Soil Using Large-Volume Pyrolysis and TD-GC-MS/MS

Ryan Bartnick[1], Andrei Rodionov[1], Simon D. J. Oster[2], Martin G. J. Löder[2], Eva Lehndorff[1]

[1]Soil Ecology, University of Bayreuth, Dr.-Hans-Frisch-Str. 1-3, 95448 Bayreuth, Germany
[2]Animal Ecology, University of Bayreuth, Universitätsstr. 30, 95447 Bayreuth, Germany

Environmental Science & Technology, *58*(29), 13047–13055, 2024. https://doi.org/10.1021/acs.est.3c10101

Environmental Science & Technology

pubs.acs.org/est

Article

Plastic Quantification and Polyethylene Overestimation in Agricultural Soil Using Large-Volume Pyrolysis and TD-GC-MS/MS

Ryan Bartnick,* Andrei Rodionov, Simon David Jakob Oster, Martin G. J. Löder, and Eva Lehndorff

Cite This: *Environ. Sci. Technol.* 2024, 58, 13047−13055

Read Online

ACCESS | Metrics & More | Article Recommendations | Supporting Information

ABSTRACT: Quantification of microplastics in soil is needed to understand their impact and fate in agricultural areas. Often, low sample volume and removal of organic matter (OM) limit representative quantification. We present a method which allows simultaneous quantification of microplastics in homogenized, large environmental samples (>1 g) and tested polyethylene (PE), polyethylene terephthalate (PET), and polystyrene (PS) (200−400 μm) overestimation by fresh and diagenetically altered OM in agricultural soils using a new combination of large-volume pyrolysis adsorption with thermal desorption−gas chromatography−tandem mass spectrometry (TD-GC-MS/MS). Characteristic MS/MS profiles for PE, PET, and PS were derived from plastic pyrolysis and allowed for a new mass separation of PET. Volume-defined standard particles (125 × 125 × 20 μm^3) were developed with the respective weight (PE: 0.48 ± 0.12, PET: 0.50 ± 0.10, PS: 0.31 ± 0.08 μg), which can be spiked into solid samples. Diagenetically altered OM contained compounds that could be incorrectly identified as PE and suggest a mathematical correction to account for OM contribution. With a standard addition method, we quantified PS, PET, and $PE_{corrected}$ in two agricultural soils. This provides a base to simultaneously quantify a variety of microplastics in many environmental matrices and agricultural soil.

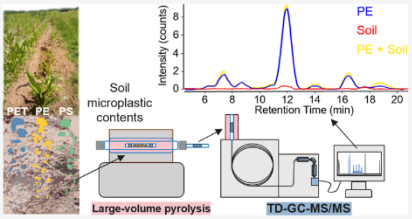

KEYWORDS: *gas chromatography−tandem mass spectrometry, microplastics, polyethylene terephthalate, polystyrene, soil, thermal desorption*

INTRODUCTION

Plastics are ubiquitous to the environment, but their representative quantification is still a challenge. In agricultural soil, microplastics are heterogeneously introduced via atmospheric inputs, fertilizers, sewage sludge, and plastic mulches[1−4] and cover a large size range from millimeters to nanometers.[5,6] Also, all relevant soil processes, like carbon and nutrient cycling and water retention, occur mainly in this range.[7,8] As microscopic methods would fail to cover this,[9] a focus on pyrolysis-based, thermal analytical quantification methods is required.[10] However, until now, quantification is limited by soil plastic concentrations and by the need to separate from other organic matter (OM).[11]

In soils, plastic is most likely rather heterogeneously distributed, e.g., incorporation processes might lead to highly variable distribution of plastic of different sizes and types and shapes in soil pores and aggregates.[12] A method considering the full heterogeneity of soil requires homogenization of a large sample volume, e.g., by milling and subsequent quantification of environmentally relevant plastic mixtures. Still, the concentration of plastics in agricultural soil is expected to be low in many cases,[13,14] but current plastic quantification methods are limited to low sample amounts or require preconcentration steps.[15,16] Often, a plastic extraction from a large sample volume is needed to cover all possible concentrations in soil, and we test whether preconcentration can be avoided when using large-scale pyrolysis of soil samples.

Pyrolysis of soil is already an established method for plastic detection. However, pyrolysis−gas chromatography−mass spectrometry (Py-GC-MS)[17] and pyrolysis adsorption−thermal desorption−GC-MS (e.g., using a TED-GC-MS system)[18,19] methods are still challenged by the presence of other OM. In Py-GC-MS, pyrolyzed plastics and OM would directly enter the GC-MS system. In methods based on pyrolysis adsorption−thermal desorption−GC-MS, only a portion of OM would be transferred for analysis, potentially allowing to reduce a time-consuming sample cleanup; however, a single quadrupole MS would not have the selectivity required for precise detection of every plastic type,[20] e.g., polyethylene (PE) and polypropylene (PP). Hence, a selective cleanup for OM other than plastics has to be implemented to avoid interferences on the GC column and in the detection system. In soil matrices, a huge variety of OM are present, and methods to remove via density separation and enzymatic

Received: December 1, 2023
Revised: April 11, 2024
Accepted: May 29, 2024
Published: July 8, 2024

https://doi.org/10.1021/acs.est.3c10101
Environ. Sci. Technol. 2024, 58, 13047−13055

digestion are extensive.[21] It is, for example, known that both PE and OM when pyrolyzed produce mono-unsaturated hydrocarbons, resulting in OM being the highest contributor to noise and interference.[22] However, a further approach, tandem mass spectrometry (MS/MS), was also shown to improve plastic quantification by reducing interferences compared to using a single quadrupole MS in scan or selected ion monitoring (SIM) mode, as shown by Albignac et al. for PE and PP in water samples.[20] Hence, we here explicitly tested whether an offline large-volume pyrolysis adsorption−thermal desorption−GC-MS/MS method would allow us to avoid the cleanup for quantification of soil samples from an agricultural context.

Microplastic quantification with adequate standard materials is another challenge in thermal analytical techniques. Some methods take advantage of dissolving plastics via pressurized liquid extraction;[23,24] however, this is restricted to materials which can be dissolved and might involve strong solvents and high temperatures. Others considered isotopically labeled standard materials, which were limited to easily dissolvable polymers and might be affected by isotope exchange with the matrix during pyrolysis.[25] The development of solid standard materials would be independent of different solubilities and, hence, be most representative of the intrinsic plastic content of an environmental sample.

In this study, we aim at developing a method that allows analyzing a representative, homogenized sample to then simultaneously quantify soil plastic contents. We hypothesized that using an offline large-volume pyrolysis adsorption−desorption method would improve representativeness, that newly developed solid standard materials facilitate quantification for various types of plastic, and that the benefit of combining large-volume pyrolysis with adsorption−thermal desorption and MS/MS will finally allow one to sufficiently quantify a variety of plastics in agricultural soil without excluding OM. To test this, we developed a new analytical setup for offline large-volume pyrolysis adsorption−thermal desorption−gas chromatography−tandem mass spectrometry (TD-GC-MS/MS) and analyzed materials with increasing complexity and potential for interference; these include lab blanks, polyethylene (PE), polyethylene terephthalate (PET), and polystyrene (PS) as well as fresh and diagenetically altered OM and agricultural soils. This method development is meant to serve as a base for further application in soil science and many other environmental research areas dealing with plastic detection in complex matrices.

MATERIALS AND METHODS

Plastic Materials and Reference Compounds for Identification of Plastic Pyrolysis Products. For the first step, the identification of plastic pyrolysis products, we used pure plastic materials and the respective compounds resulting from pyrolysis (reference compounds).

Throughout the experimental process, contact of samples to other plastics was avoided. All materials were kept in glass containers and handled with only metal tools. The plastic polymers low-density polyethylene (LD-PE, Lupolen 1800 P-1—LyondellBasell, Rotterdam, NL), polyethylene terephthalate (PET, CleanPET WF—Veolia Umweltservice, Hamburg, Germany), and polystyrene (PS 158N/L—INEOS Styrolution, Frankfurt, Germany) were in a size range of 200−400 μm of irregular shape (see the Supporting Information, SI). Plastics were prepared by cryomilling (ZM200; Retsch, Haan, Germany) and air jet sieving (E200 LS; Hosokawa Alpine, Augsburg, Germany). Five supplemental plastics: polypropylene (PP, Moplen HP 5261—LyondellBasell, Rotterdam, NL), polyamide (PA66, Ultramid A27 E—BASF SE, Ludwigshafen, Germany), polybutylene adipate terephthalate (PBAT, M·VERA B5026—BIO-FED, Cologne, Germany), polylactic acid (PLA, Ingeo Biopolymer 7001D—NatureWorks, MN), and polymethyl methacrylate (PMMA—LLV-Shop.de, Niederkassel, Germany) were provided and analyzed.

To identify retention time (t_R) and ions of interest (mass to charge, m/z) of plastic pyrolysis products, reference compounds were purchased or made to compare to plastic pyrolysis products. Reference compounds were the following—PET: vinyl benzoate, ethyl benzoate, benzoic acid, and biphenyl; PS: styrene; and PE: 1,9-decadiene and 1,13-tetradecadiene (all compounds were purchased from Sigma-Aldrich Chemie, Taufkirchen, Germany, with the exception of benzoic acid from Fluka, Buchs, Switzerland). Due to a lack of available PS dimer and trimer compounds for purchase, a solution was made by dissolving 100 mg of PS per mL of tetrahydrofuran. For quality assurance and identification, reference compounds vinyl benzoate, ethyl benzoate, and styrene were diluted in methanol to a concentration of 0.2 μg μL^{-1}; benzoic acid, biphenyl, 1,9-decadiene, and 1,13-tetradecadiene were diluted to a concentration of 2 μg μL^{-1}. 1 μL of reference compound was then injected through the septum of a closed thermal desorption vial directly onto a nonpolar sorbent (Sorb-Star; ENVEA, Karlsfeld, Germany) and analyzed.

Development of Solid Standards for Quantification of Plastics. To overcome the limitations of standards for microplastic analysis, a novel production of rectangular, volume-defined standard particles (125 × 125 × 20 μm^3) was used with an average respective weight (PE 0.48 ± 0.12, PET 0.50 ± 0.10, PS 0.31 ± 0.08 μg per particle), which can be directly introduced into solid samples for pyrolysis. For production of standard plastic particles, a protocol from Oster et al. was used.[26] Injection-molded polymer blocks made of LD-PE, PET, and PS were cut into rectangular pieces (10 × 10 × 4 mm^3). These were then processed using a CNC mill (CMX 600 V; DMG MORI Inc., Bielefeld, Germany) to create columns on a baseplate with the intended diameter of the particles. The columns were then embedded in gelatin, frozen at −19 °C for 10 min, and cut using a cryomicrotome (CM1950; Leica Camera Inc., Wetzlar, Germany) also operated at −19 °C. The resulting slices (20 μm thickness) were subsequently filtered with the help of a 10 μm-pore size stainless-steel filter and 60 °C filtered milli-Q water (0.2 μm-pore size cellulose acetate filters) to remove the gelatin. The standard plastics were then picked up from the filter using a tool made of a single hair attached to the tip of a pipet and transferred into vials for usage in TD-GC-MS/MS analysis.

The use of solid particles, as opposed to adding a solution of internal standard, has several advantages, e.g., steps of dissolution and reprecipitation can be avoided. Plastic particle standards are placed on glass fiber filters, analyzed under a microscope, and inserted into the sample internally for pyrolysis.

Soil and Organic Materials. Past studies have demonstrated that alkadienes are more selective for PE detection, but possible interferences from OM still persist, especially among humic acids and diagenetically altered OM.[22,23] To check for potential signal contribution of natural organic compounds to

https://doi.org/10.1021/acs.est.3c10101
Environ. Sci. Technol. 2024, 58, 13047−13055

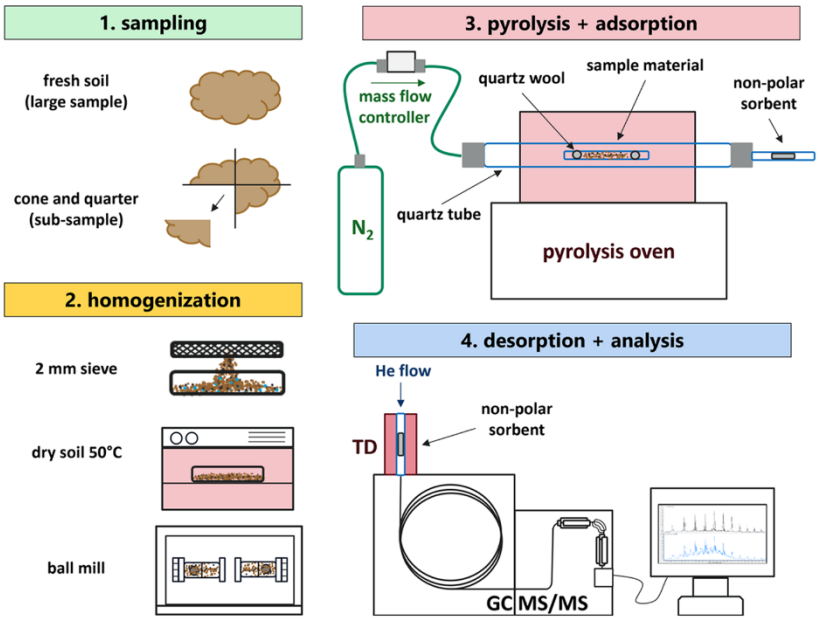

Figure 1. Procedural steps of sampling and homogenization, pyrolysis and adsorption, and analysis with thermal desorption−gas chromatography−tandem mass spectrometry (TD-GC-MS/MS); manual transfer of the trapped sample in the vial between adsorption and desorption steps.

any of the pyrolyzed plastics, we tested fresh biomass such as inner wood from a beech tree (*Fagus sylvatica*) and yeast as well as organic materials of higher maturity and kinetic stability such as leonardite (Humintech, Grevenbroich, Germany) and humic acids (Humintech, Grevenbroich, Germany; Sigma-Aldrich Chemie, Taufkirchen, Germany). As yeast, a *Komagataella pastoris* strain Pi-0702 (DSM 70382; German Collection of Microorganisms and Cell Cultures, Braunschweig, Germany) was cultured at 25 °C in minimal medium;[27] cells were then harvested after centrifugation and freeze drying. Humic acid was obtained from raw lignite via alkaline digestion (Northern Hesse, Germany/Sigma-Aldrich Chemie, received with a standard high-density PE bottle). To avoid contamination from storage in PE bottles, leonardite, a mineraloid of oxidized lignite with a high humic acid content, was collected (North Rhine-Westphalia, Germany/Humintech, provided in glass containers with no contact to plastics). Soil samples of two agricultural fields (several kg of topsoil, 0−30 cm, of a sandy and silty soil; see Table S1, SI) were collected from Bayreuth, Germany. Subsamples were produced by mixing soil using a cone and quartering method,[28] sieved at 2 mm, dried at 50 °C, and ground using a ball mill (MM 400; Retsch, Haan, Germany, for soil preparation, see the analytical scheme, Figure 1). Aliquots of 1 g of soil were initially analyzed for their "natural" plastic contents using a standard addition calibration method (5 replicates) and then reduced to 0.5 g aliquots if plastic contents exceeded the quantification range. To compensate for matrix effects, the standard addition method adds known concentrations of analyte to samples in increasing amounts, "spikes", to then extrapolate the analyte signal in the sample matrix.[29]

Large-Volume Pyrolysis. Pyrolysis was performed in a stand-alone tube furnace with a programmable temperature (Carbolite Gero TF1-1100; Verder Scientific, Haan, Germany). All equipment was precleaned, quartz glass and sand (900 °C, 3 h), glass wool and fiber filters (550 °C, 3 h), sorption vials, and septa (300 °C, 2 h). Samples for pyrolysis were inserted into a quartz sample tube (4 mm inner diameter (i.d.) × 6 mm outer diameter (o.d.) × 100 mm) and fitted with two balls of glass wool on each end to retain the sample. The sample tube was then inserted inside a larger quartz pyrolysis tube (7 mm i.d. × 9 mm o.d. × 400 mm; heating volume: 3.85 cm^3), which was held inside the pyrolysis oven. Another glass tube of a specific length was used to push the sample tube directly into the middle of the pyrolysis oven to ensure equal heating throughout the sample. The large quartz tube was then connected with metal Swagelok connectors (Swagelok Company, OH), with one end to a N_2 carrier gas (99.999%) flow line and the other end to a sorption tube fitted with a Sorb-Star (a polydimethylsiloxane bar with a large surface to trap nonpolar, semivolatile pyrolysis products; see the analytical scheme, Figure 1). Early tests optimizing the pyrolysis flow and heating rates showed reproducibility of the plastic peaks PS, PET, and PE (Figure S1, SI), before accounting for lab blank signal contributions. The tube furnace heating program was from 25 to 600 °C at a rate of 15 °C min^{-1}, then held at 600 °C for 30 min, and flushed with a constant N_2 flow of 8 mL min^{-1} from the sample toward the sorbent during pyrolysis (all parameters tested and optimized as adapted from previous TED-GC-MS applications).[18,19,30] As Dümichen et al. (2014) state, there is no optimum flow rate to cover all polymer applications and a compromise has to be chosen; early testing of our method showed that a flow rate of 8 mL min^{-1} was optimal in our system for peak sensitivity and loading time on the sorbent. The heating ramp was increased from 10 to 15 °C min^{-1} to save time efficiency without affecting peak intensity. The sorption tube consisted of an open glass tube aligned with a Sorb-Star lying flat inside the

https://doi.org/10.1021/acs.est.3c10101
Environ. Sci. Technol. 2024, 58, 13047−13055

Table 1. Pyrolysis Product Compounds of Polyethylene Terephthalate, Polyethylene, and Polystyrene Plastic Polymers[a]

polymer label	compound (pyrolysis product)[b]	t_R (min)	molecular formula	molar mass	SIM (m/z) Q1	SRM (m/z) Q1	SRM (m/z) Q3
PS1	styrene	5.4	C_8H_8	104	104	104	78
PET1	vinyl benzoate	12.2	$C_9H_8O_2$	148	105	148	105
PET2	ethyl benzoate[c]	12.8	$C_9H_{10}O_2$	150	105	150	122
PET3	benzoic acid	13.0	$C_7H_6O_2$	122	105		
PE1	1,12-tridecadiene	15.4	$C_{13}H_{24}$	180	81	81	79
PET4	biphenyl	17.3	$C_{12}H_{10}$	154	154	154	152
PE2	1,13-tetradecadiene[c]	17.4	$C_{14}H_{26}$	194	81	81	79
PE3	1,14-pentadecadiene[c]	19.2	$C_{15}H_{28}$	208	81	81	79
PE4	1,15-hexadecadiene	20.9	$C_{16}H_{30}$	222	81	81	79
PS2	2,4-diphenyl-1-butene[c]	23.2	$C_{16}H_{16}$	208	91	208	104
PS3	2,4,6-triphenyl-1-hexene	32.9	$C_{24}H_{24}$	312	91	312	207

[a]Ordered by the Corresponding Retention Time, t_R. [b]Characterized by selected reaction monitoring (SRM) ions of interest (m/z) at quadrupole 1 (Q1) and quadrupole 3 (Q3) of the tandem mass spectrometer. [c]Used for quantification.

middle of the tube in the direction of the gas flow; nonadsorbed materials were vented. The sorption tube was disconnected after pyrolysis and closed with polytetrafluoroethylene (PTFE) septa and an aluminum cap on the top and bottom. The pyrolysis and sorption systems were cleaned by replacing all glass tubes.

Thermal Desorption−Gas Chromatography−Tandem Mass Spectrometry. Pyrolysis products of plastics were detected and quantified by thermal desorption−gas chromatography−tandem mass spectrometry (TD-GC-MS/MS) using a PAL autosampler with a Chromtech thermal desorption unit (PAL3 RSI TDAS 2020; Chromtech, Bad Camberg, Germany) coupled to a gas chromatograph with a tandem quadrupole mass spectrometer (Agilent 7890B plus 5977B modified to a Chromtech Evolution 3; Chromtech, Bad Camberg, Germany). The GC (fused) silica capillary column was a Macherey-Nagel OPTIMA 5 MS (30 m × 0.25 mm i.d. × 0.25 μm film thickness, split injection: 1:100, inlet temperature: 300 °C, He gas flow: 1 mL min^{-1}).

Before injection into the GC, the sorption tube was flushed with N_2 to remove any gases from the headspace and then transported inside a preheated TD unit for desorption at 300 °C for 5 min. During this, compounds adsorbed to the sorbent are desorbed into the gas phase and, at the end, injected to the GC column via a helium gas flow (followed by 5 min of flushing of the injection system in heated mode). The GC oven temperature program was set to standby at 40 °C for 1 min, ramp to 285 °C at 7 °C min^{-1}, and postrun at 320 °C for 5 min (GC parameters tested and optimized for time efficiency and peak separation, as adapted from previous GC-MS applications).[18,19,23]

The detection system was used either in single quad full scan mode (45−450 m/z) or selected ion monitoring mode (SIM, target ions see Table 1) or in triple quad (tandem MS) selected reaction monitoring (SRM) mode (electron ionization at 70 eV, ion source temperature: 230 °C, quadrupole 1 at 150 °C, mass resolution: ±1.0 m/z in quadrupole 1 and 3, collision energy: −10 V, targeted mass fragments, see Table 1).

Quality Control and Quantification. To account for the lab background signals, a blank was estimated from glass wool, filters, and the N_2 carrier flow during pyrolysis (n = 18 replicates). We defined the blank offset as the average target response of the blank samples. The blank offset was determined as the y-axis origin for calibration (see Table S2, SI). Calibrations were made using plastic mixes weighed on a cut piece of glass fiber filter, inserted into a quartz sample tube, and pyrolyzed to test for the linearity of the signal and limit of quantification (MassHunter Quantitative Analysis software; Agilent, CA). Microplastic contamination is present in nearly all laboratory analyses, and thus, the limit of quantification (LOQ) is defined by the lab background signals and not the analytical instrument. A calibration was made with our novel defined plastic particles and weights of approximately 0.5−250 μg (n = 20, each plastic mixed) to determine the lowest amount standard that could be reliably detected above the lab background signal (see Table S2, Figure S2, SI). For testing detectable concentrations ranging over multiple levels of magnitude as can be expected for agricultural soil, a calibration of approximately 150−850 μg (n = 10, each plastic mixed) was plotted with the lower concentration range as a double log plot to correlate a linear function over several orders of magnitude (see the Results and Discussion section and Figure S3, SI).

Organic substances (triplicates, 20 mg, representative of a typical amount of 2% OM in topsoil) were tested for potential contribution to characteristic signals of plastic pyrolysis products of PS, PE, and PET. For quantification of organic contributions, we used the calibration of pure plastic standard particles (0.5−250 μg). Only for characteristic PE pyrolysis products, i.e., tetradecadiene and pentadecadiene, interferences from OM were found using the method described below. Calculation of potential OM contribution to such alkadienes was estimated from the mass detector response of humic acid, leonardite, wood, and yeast and compared it to the response of the pure PE pyrolysis product (alkadiene_{PE}) ($PE_{\text{overestimation factor}}$, eq 1).

$$\text{PE}_{\text{overestimation factor}} = \frac{(\text{alkadiene}_{OM}[AU] \times OM[SI])}{(\text{alkadiene}_{PE}[AU] \times PE[SI])} \quad (1)$$

For this study, we averaged the PE overestimation factor using tetradecadiene from humic acid and leonardite (see Table S3, SI). Yeast and wood were not considered as they were tested to be under the previously determined LOQ. The use of pentadecadiene is discussed below. We calculated a PE correction for soil samples ($PE_{corrected}$, eq 2) using the PE overestimation factor, sample amount, and soil OM contents, soil organic carbon (OC), from elemental analysis multiplied by a factor 2 to account for other elements in OM.

https://doi.org/10.1021/acs.est.3c10101
Environ. Sci. Technol. 2024, 58, 13047−13055

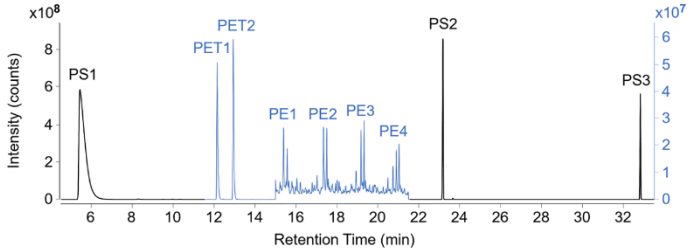

Figure 2. Chromatogram of polystyrene (PS1−3, black scale), polyethylene terephthalate (PET1−2, blue scale), and polyethylene (PE1−4, blue scale) pyrolysis products using selected reaction monitoring (SRM) mode of MS/MS (100 μg each plastic PE, PET, PS; peak names refer to pyrolysis products of each plastic, see Table 1).

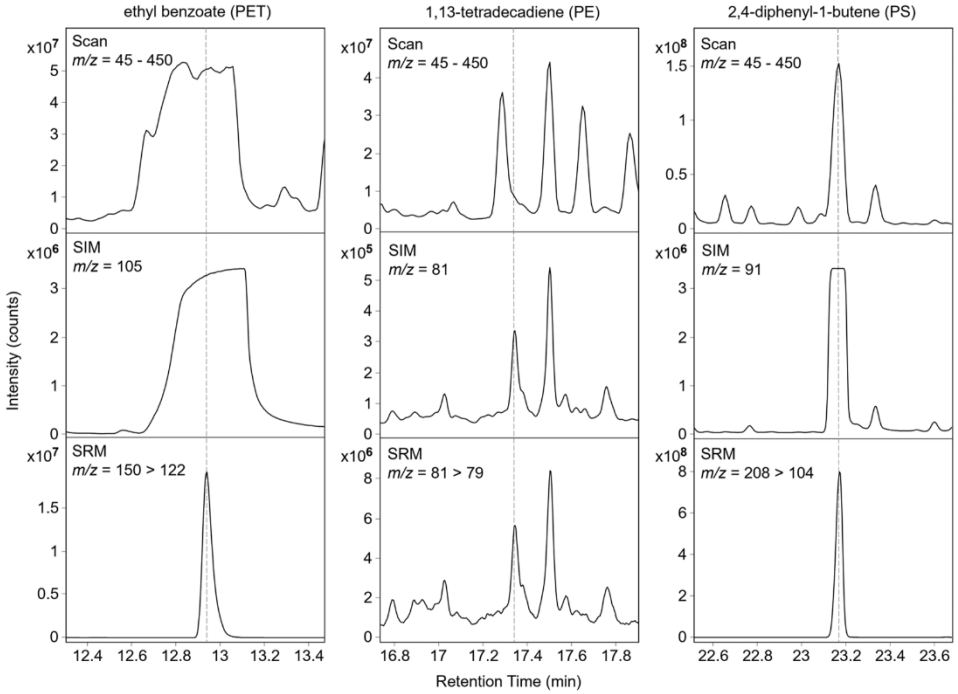

Figure 3. Chromatograms of pyrolyzed products of plastics PE, PET, and PS, 50 μg each. Increasing precision and intensity of signal counts is observed transitioning from MS modes of scan to selected ion monitoring (SIM) and then selected reaction monitoring (SRM) mode of MS/MS.

$$PE_{corrected}[mg\,g^{-1}] = PE_{soil}[mg\,g^{-1}] - (sample[g] \times 2(OC_{sample}[mg\,g^{-1}]) \times PE_{overestimation\ factor}) \quad (2)$$

For PE overestimation from OM, we later discuss whether this can be specified for only the recalcitrant OM portion in soil. In soils, solid standards of PE, PS, and PET were used for standard addition to quantify the respective plastic types and account for matrix effects (soil initially spiked with the expected plastic content of 0.01% and then adjusted to spike at 1× and 2× the estimated plastic content of each polymer; see Figure S4, SI).

RESULTS AND DISCUSSION

Method Development—MS/MS Parameters. Characteristic pyrolysis products from PE, PET, and PS were identified by the respective reference polymer compounds to verify retention times and ions of interest. We selected pyrolysis products which had the lowest risk to coeluate with pyrolysis products from other plastics. First, we could confirm characteristic ions suggested for full scan mode analysis of the mass spectra.[19] Second, a selected ion monitoring (SIM) method was established to set quadrupole 1 (see SIM m/z Q1, Table 1) to the ion with the best selectivity to the specific pyrolysis product, also informed by the literature.[18,19,23,31−33] Third, a product ion scan (PIS) method was used to have another reaction step in a second quadrupole (Q2) with N_2 collision gas and then a scan of the product ions generated at a third quadrupole (Q3). Finally, the selected reaction monitoring (SRM) method was completed for each pyrolysis product (see SRM m/z Q1 and Q3, Table 1, Figure 2; compounds identified by the mass spectrum from the NIST online library[34]).

The pyrolysis products found here (Table 1) agreed well with the previous literature.[18,19] However, for PET, we were

https://doi.org/10.1021/acs.est.3c10101
Environ. Sci. Technol. 2024, 58, 13047−13055

able to improve the peak separation of ethyl benzoate from benzoic acid, which elutes at the same time (Figure 3). During SIM mode, ion 105 is commonly used to detect many PET (PET1−3) compounds, as this ion has the highest response. However, we were now able to separate ethyl and vinyl benzoate by mass from the lower weight benzoic acid, which fronts on the column over ethyl benzoate, by setting Q1 to the entire molar mass of these compounds (see SRM m/z Q1, Table 1). Then, Q3 was set to the highest product ion produced from the Q1 mass separation, creating excellent separation of ethyl benzoate from benzoic acid, which was chosen as the calibration compound for PET over vinyl benzoate due to higher response. It should be noted that PET pyrolysis additionally produces biphenyl (PET4), a compound which could potentially be used to quantify PET; however, its retention time overlapped the signal of PE2, so it was excluded from analysis.

For PE, pyrolysis yields several alkenes and alkadienes, which elute across much of the chromatogram runtime, resulting in many peaks with relatively low intensity. Dümichen et al. used ion 55 to detect alkenes and alkadienes from PE pyrolysis products, but they also found significant contributions to alkenes from OM.[18] Albignac et al. used ion 95; however, we focused on ion 81, which had more intensity for alkadienes (see Q1, Table 1).[20] Of the four alkadienes (PE1−4) with the highest signal intensities from PE pyrolysis, we selected 1,13-tetradecadiene (PE2) as the calibration compound because it had the highest peak response and had an available reference compound. While separation of PE1−4 from other compounds is comparable between SIM and SRM modes (see Figure 3), the benefit of utilizing a second mass detector is a significantly higher signal intensity for environmental samples (see the degree of intensity counts, Figure 2). The benefit of MS/MS application is a higher detector sensitivity due to reduction of untargeted ions.

For PS, we first observed carryover effects that could be minimized by increasing conditioning temperature in the TD unit (from 200 to 300 °C) and running blanks between samples for cleaning needles. PS pyrolysis products of styrene monomer, dimer, and trimer can all produce carryover effects in the TD-GC part of the system if there is inadequate postrun heating. Especially, the heavy styrene trimer can potentially stick in the system between the TD unit and the GC inlet wherever there are unheated areas of the needles. For PS quantification, the monomer styrene (PS1) could not be recommended because it is a pyrolysis byproduct of lignin found in soil.[16] Therefore, the dimer, 2,4-diphenyl-1-butene (PS2), was selected as the calibration compound with the highest peak response for PS, which is well separated from OM and agrees to the literature.[18,19,35] These authors used ion 91 for quantification; however, the signal is too intense in tandem MS when targeting other plastic simultaneously. Therefore, we first fragmented the dimer, excluded m/z 91, and sent the remaining parent molecules (m/z 208) to further fragmentation (m/z 104) (Figure 3). We thus reduced the signal of styrene and improved its simultaneous detection with other types of plastics.

Method Development—Quantification of MP. Plastic concentrations in the environment may cover a large range, from extremely low to spots with high accumulation. Since plastics occur ubiquitously, we recommend to start with accounting for the lab background signal.[23] For our calibration curves, the lab background signal defined the y-axis origin of slope and was removed from contributing to the calibration ("blank offset", Table S2, SI). To further check a range of concentrations, a series of PE, PET, and PS mixtures between 0.5 and 850 μg each was tested, referring to about 0.001−0.1% of the plastics in 1 g of soil. For PET, we found that at concentrations of 0.01−0.1%, vinyl benzoate is recommendable for quantification, while ethyl benzoate is better for testing a lower limit of quantification (0.001−0.01%), as higher sensitivity over vinyl benzoate was achieved.

Responses were linear for PE and PET at the highest tested concentration (850 μg), with coefficients of determination (R^2) of 0.94 and 0.92, respectively. However, for PS, the signal response was not linear at concentrations over 120 μg (Figure S5, SI). Therefore, a double log calibration[36] was made for PS to correlate a linear relationship of concentration ranges over multiple orders of magnitude (see PS2, Table S2, Figure S3, SI), resulting in a good fit (R^2 = 0.97). From personal observation, while calibrating PS in matrices such as sand and soil, responses become much linear at higher concentrations as signals overall are suppressed within a matrix, as was the case with Dierkes et al. who demonstrated a linear range of PS between 0.005 and 1 mg g^{-1} in sand.[23]

The quantification of plastics at low concentrations was until now challenged by the poor solubility of some plastic polymers (PE, PET), limitations in weighing small amounts (<10 μg), and the pyrolysis process. According to Lauschke et al., tests with labeling of environmental samples by adding deuterated styrene showed high variability of recovery due to partial loss of the isotope label during pyrolysis.[25] We solved the problem of weighing by using precisely cut, volume-defined particles out of our plastic standard materials and used these for lower limit calibration.[26] The lower limit of calibration was linear for PE (R^2 = 0.98), PET (R^2 = 0.93), and PS (R^2 = 0.92) and stayed in accordance with Dierkes et al. who reported an R^2 of 0.98 for PE and 0.99 for PS using a calibration range from 0.005 to 10 mg in a Py-GC-MS system.[23]

Method Development—Comparison of Plastic Specific Signals to Organic Materials. In a soil matrix, separation of plastic pyrolysis products from interferences with other OM was the most critical. We could exclude interferences from OM for PS and PET in our method; however, for PE pyrolysis products, tetradecadiene and pentadecadiene, OM interference had to be considered.

The PE pyrolysis compounds 1,13-tetradecadiene and 1,14-pentadecadiene were previously suggested to be suitable for quantifying PE in soils.[18,23] However, previous potential interference of petroleum with PE detection was already discussed.[23] In our study, we checked fresh biomass (wood, yeast) and recalcitrant organic materials (humic acid and leonardite) and for the latter found significant contributions of alkadienes (1,13-tetradecadiene was on average 0.8% and 1,14-pentadecadiene was 2% of our humic reference materials, Table S3, SI). This can be explained by diagenetic alteration of organic compounds, i.e., humic acid formation in soil and coal contributions from geological materials may accumulate kinetically stable organic carbon forms resisting oxidation[37] and yielding alkenes and alkadienes similar to PE from pyrolysis. Hence, as in soil, pedogenic, geogenic, and anthropogenic sources of recalcitrant OM are present, and a quantification method for PE must consider this.

When studies aim at an overall quantification of a variety of plastic types, we suggest correcting the quantification of PE based on pyrolysis and alkadiene detection by the average

https://doi.org/10.1021/acs.est.3c10101
Environ. Sci. Technol. 2024, 58, 13047−13055

Table 2. Quantification of Microplastics via Solid Standard Addition to Two Soil Types[a]

			$PE_{corrected}$[a] quantified via		
soil[b]	OC [g kg^{-1}]	PET [mg kg^{-1}]	1,13-tetradecadiene [mg kg^{-1}]	1,14-pentadecadiene [mg kg^{-1}]	PS [mg kg^{-1}]
clayey sand	10.71	166.4 ± 17.0	67.7 ± 35.7 (245.3 ± 35.1)	<potential OM contribution (389.3 ± 142.3)	<LOQ (0.31)
sandy silt	15.44	2670.1 ± 415.9[c]	OC too high	273.3 ± 159.4[c] (605.3 ± 159.0)[c]	20.8 ± 3.9

[a]For PE, we provide a corrected estimation and the uncorrected, "total PE" amount in brackets. [b]1 g sample aliquot, unless otherwise noted. [c]Quantified with a 0.5 g sample aliquot.

amount of tetradecadiene detected in humic acids and leonardite, as pentadecadiene had double the contribution from humic materials. We here estimated that all soil OM consist of humic substances; however, analyses of recalcitrant carbon forms in the respective samples should allow a more realistic estimate. We thus provide here a conservative correction for PE content analyses in soil.

Plastic Detection in Soil Using TD-GC-MS/MS. We tested plastic detection and quantification for two agricultural soils, a sandy silt and a clayey sand, with comparable pH and organic carbon contents of 1.1 and 1.5%, respectively (see the analytical scheme in Figure 1 and Tables 1, S1, SI). PET was detected in both soils, much higher in sandy silt, while PS was under the LOQ in clayey sand and in low amounts in sandy silt (Table 2). For PE, we estimated a total amount of 0.4 and 0.6 mg g^{-1} in sandy and silty soil, respectively (Table 2), when using pentadecadiene for quantification as suggested by, e.g., Dierkes et al.[23] The advantage of tetradecadiene is that the humic material contribution was lower compared to that of pentadecadiene. However, when organic carbon contents in a soil matrix were above 15 mg g^{-1}, there was too much interference to separate tetradecadiene from other compounds and cleanup steps should be considered. As for pentadecadiene, the overestimation factor was much higher; the total PE contents detected in the clayey sand were lower than the potential overestimation by OM; and a $PE_{corrected}$ could not be estimated (Table 2). In the silty soil, the variation of the pentadecadiene was high due to weak peak separation, and a relation to tetradecadiene was not obvious, and although correction worked, both indicated that organics contributed substantially (Table 2 and example calculation in the SI). Finally, we showed that OM could contribute a maximum of 72% to the PE quantification compound (Table 2). Hence, we expect that previous studies using pyrolysis or TD-GC-MS for river sediments[33] and suspended particulate matter[18,22,35] overestimated PE contents. While PET and PS were well-quantifiable with our method, for PE, we still recommend either a correction for contribution by OM contents or a partial removal by solvent extraction[17,23] or density fractionation.[21,38]

This TD-GC-MS/MS method can be adapted further by including other plastics and marker compounds, such as tire and road wear, that has only recently been approached for lake sediments and road dust.[29,39] We did tests for PP, PA66, PMMA, PLA, and PBAT and see high potential to extend this method to a rather complete variety of plastics (see Table S4, SI).

To summarize, a novel offline large-volume pyrolysis adsorption−thermal desorption−GC-MS/MS method was developed to simultaneously evaluate PS, PE, and PET in larger (>1 g) dried soil samples down to a concentration of 1 mg kg^{-1}, allowing representative analyses of plastic concentrations in homogeneous environmental samples and for larger areas such as agricultural topsoil. Rectangular, volume-defined standard particles (125 × 125 × 20 μm^3) were developed for calibration and lowered the LOQ for PS, PE, and PET than was possible with previous particles (200−400 μm) due to their lower individual weight. For two soil types, sand and silt, a standard addition method was able to quantify PS, PET, and $PE_{corrected}$ in a complete soil matrix, highlighting that plastic quantification in agricultural soil is feasible without any sample cleanup except for interferences of PE with OM.

Of the organics tested, the recalcitrant materials showed relevant contributions to PE quantification, which was highest for 1,14-pentadecadiene compared to 1,13-tetradecadiene. Hence, we proposed a correction for PE and can show that an overestimation of PE contents of up to 70% might appear in environmental studies. For PE detection in samples containing >1.5% organic carbon, correction was not applicable and cleanup is required. As the average agricultural topsoil in temperate regions has 0.9% organic carbon (e.g., Steinmann et al.),[40] we suggest to limit sample cleanup for PE to soils rich in OM and depending on the relevance of PE for the specific research question. If PE quantification would be in the focus of research and cleanup is required, i.e., the removal of OM by density separation, digestion, and organic solvent extraction, we recommend follow-up studies to check for underestimation of PE and other plastics due to potential loss.

We here established a method that builds the base for quantification of various plastic types in complex environmental samples such as biological tissues, sediments, water, and soils. For bringing the method into widespread application in soil science, soils with different properties should be tested, e.g., differing amounts and quality of OM and reactive minerals, to further ensure the method robustness against matrix effects and finally study plastic concentration, composition, and spatial heterogeneity in soils from many geographical and agricultural contexts.

■ ASSOCIATED CONTENT

Supporting Information

The Supporting Information is available free of charge at https://pubs.acs.org/doi/10.1021/acs.est.3c10101.

Soil information, calibration slopes and equations, organic contributions, additional TD-GC-MS/MS analysis of plastic polymers (PLA, PA, PMMA, PP, PBAT), and example calculations (PDF)

■ AUTHOR INFORMATION

Corresponding Author

Ryan Bartnick − *Soil Ecology, University of Bayreuth, 95448 Bayreuth, Germany*; orcid.org/0000-0002-3053-8472; Email: ryan.bartnick@uni-bayreuth.de

https://doi.org/10.1021/acs.est.3c10101
Environ. Sci. Technol. 2024, 58, 13047−13055

Authors

Andrei Rodionov − *Soil Ecology, University of Bayreuth, 95448 Bayreuth, Germany;* orcid.org/0000-0001-5971-1948

Simon David Jakob Oster − *Animal Ecology I, University of Bayreuth, 95447 Bayreuth, Germany;* orcid.org/0000-0002-7021-3488

Martin G. J. Löder − *Animal Ecology I, University of Bayreuth, 95447 Bayreuth, Germany;* orcid.org/0000-0001-9056-8254

Eva Lehndorff − *Soil Ecology, University of Bayreuth, 95448 Bayreuth, Germany;* orcid.org/0000-0001-6247-2976

Complete contact information is available at: https://pubs.acs.org/10.1021/acs.est.3c10101

Notes

The authors declare no competing financial interest.

■ ACKNOWLEDGMENTS

Plastic polymers were provided by central project Z01 in the frame of the Collaborative Research Center 1357 "Microplastics—Understanding the Mechanisms and Processes of Biological Effects, Transport, and Formation: From Model to Complex Systems as a Basis for New Solutions." This study was funded by the Deutsche Forschungsgemeinschaft (DFG, German Research Foundation)—SFB 1357—391977956. We greatly thank Aileen Jakobs (Ecological Microbiology, University of Bayreuth) for cultivating and providing yeast. We thank central project Z01, P. Strohriegl, M. Fried, and D. Wagner for polymer preparation and analytics. We also thank T. van den Berg and Y. Hardi, Chromtech, Germany, for analytical support. Additionally, we are grateful to Alexander Rube of Humintech GmbH, Germany, for providing us with the raw leonardite mineral and humic materials to test.

■ REFERENCES

(1) Steinmetz, Z.; Wollmann, C.; Schaefer, M.; Buchmann, C.; David, J.; Tröger, J.; Muñoz, K.; Frör, O.; Schaumann, G. E. Plastic mulching in agriculture. Trading short-term agronomic benefits for long-term soil degradation? *Sci. Total Environ.* **2016**, *550*, 690−705.

(2) Steinmetz, Z.; Löffler, P.; Eichhöfer, S.; David, J.; Muñoz, K.; Schaumann, G. E. Are agricultural plastic covers a source of plastic debris in soil? A first screening study. *Soil* **2022**, *8* (1), 31−47.

(3) Wang, J.; Liu, X.; Li, Y.; Powell, T.; Wang, X.; Wang, G.; Zhang, P. Microplastics as contaminants in the soil environment: A mini-review. *Sci. Total Environ.* **2019**, *691*, 848−857.

(4) Weithmann, N.; Möller, J. N.; Löder, M. G. J.; Piehl, S.; Laforsch, C.; Freitag, R. Organic fertilizer as a vehicle for the entry of microplastic into the environment. *Sci. Adv.* **2018**, *4* (4), No. eaap8060.

(5) Gigault, J.; Halle, A. t.; Baudrimont, M.; Pascal, P.-Y.; Gauffre, F.; Phi, T.-L.; El Hadri, H.; Grassl, B.; Reynaud, S. Current opinion: What is a nanoplastic? *Environ. Pollut.* **2018**, *235*, 1030−1034.

(6) Hartmann, N. B.; Hüffer, T.; Thompson, R. C.; Hassellöv, M.; Verschoor, A.; Daugaard, A. E.; Rist, S.; Karlsson, T.; Brennholt, N.; Cole, M.; Herrling, M. P.; Hess, M. C.; Ivleva, N. P.; Lusher, A. L.; Wagner, M. Are We Speaking the Same Language? Recommendations for a Definition and Categorization Framework for Plastic Debris. *Environ. Sci. Technol.* **2019**, *53* (3), 1039−1047.

(7) Brady, N. C.; Weil, R. R. *The Nature and Properties of Soils*, Global ed.; Pearson, 2017.

(8) Rillig, M. C.; Leifheit, E.; Lehmann, J. Microplastic effects on carbon cycling processes in soils. *PLoS Biol.* **2021**, *19* (3), No. e3001130.

(9) Primpke, S.; Fischer, M.; Lorenz, C.; Gerdts, G.; Scholz-Böttcher, B. M. Comparison of pyrolysis gas chromatography/mass spectrometry and hyperspectral FTIR imaging spectroscopy for the analysis of microplastics. *Anal. Bioanal. Chem.* **2020**, *412* (30), 8283−8298.

(10) Seeley, M. E.; Lynch, J. M. Previous successes and untapped potential of pyrolysis-GC/MS for the analysis of plastic pollution. *Anal. Bioanal. Chem.* **2023**, *415*, 2873−2890.

(11) Dierkes, G.; Lauschke, T.; Földi, C. Analytical Methods for Plastic (Microplastic) Determination in Environmental Samples. In *Plastics in the Aquatic Environment - Part I*; Stock, F.; Reifferscheid, G.; Brennholt, N.; Kostianaia, E., Eds.; Springer International Publishing, 2022; pp 43−67.

(12) Zhang, G. S.; Liu, Y. F. The distribution of microplastics in soil aggregate fractions in southwestern China. *Sci. Total Environ.* **2018**, *642*, 12−20, DOI: 10.1016/j.scitotenv.2018.06.004.

(13) Bläsing, M.; Amelung, W. Plastics in soil: Analytical methods and possible sources. *Sci. Total Environ.* **2018**, *612*, 422−435.

(14) Corradini, F.; Casado, F.; Leiva, V.; Huerta-Lwanga, E.; Geissen, V. Microplastics occurrence and frequency in soils under different land uses on a regional scale. *Sci. Total Environ.* **2021**, *752*, No. 141917.

(15) Möller, J. N.; Löder, M. G. J.; Laforsch, C. Finding Microplastics in Soils: A Review of Analytical Methods. *Environ. Sci. Technol.* **2020**, *54* (4), 2078−2090.

(16) Stock, F.; B Narayana, V. K.; Scherer, C.; Löder, M. G. J.; Brennholt, N.; Laforsch, C.; Reifferscheid, G. Pitfalls and Limitations in Microplastic Analyses. In *Plastics in the Aquatic Environment - Part I*; Stock, F.; Reifferscheid, G.; Brennholt, N.; Kostianaia, E., Eds.; Springer International Publishing, 2022; pp 13−42.

(17) Steinmetz, Z.; Kintzi, A.; Muñoz, K.; Schaumann, G. E. A simple method for the selective quantification of polyethylene, polypropylene, and polystyrene plastic debris in soil by pyrolysis-gas chromatography/mass spectrometry. *J. Anal. Appl. Pyrolysis* **2020**, *147*, No. 104803.

(18) Dümichen, E.; Eisentraut, P.; Bannick, C. G.; Barthel, A.-K.; Senz, R.; Braun, U. Fast identification of microplastics in complex environmental samples by a thermal degradation method. *Chemosphere* **2017**, *174*, 572−584.

(19) Duemichen, E.; Eisentraut, P.; Celina, M.; Braun, U. Automated thermal extraction-desorption gas chromatography mass spectrometry: A multifunctional tool for comprehensive characterization of polymers and their degradation products. *J. Chromatogr. A* **2019**, *1592*, 133−142.

(20) Albignac, M.; Oliveira, T. d.; Landebrit, L.; Miquel, S.; Auguin, B.; Leroy, E.; Maria, E.; Mingotaud, A. F.; Halle, A. Tandem mass spectrometry enhances the performances of pyrolysis-gas chromatography-mass spectrometry for microplastic quantification. *J. Anal. Appl. Pyrolysis* **2023**, *172*, No. 105993.

(21) Möller, J. N.; Heisel, I.; Satzger, A.; Vizsolyi, E. C.; Oster, S. D. J.; Agarwal, S.; Laforsch, C.; Löder, M. G. J. Tackling the Challenge of Extracting Microplastics from Soils: A Protocol to Purify Soil Samples for Spectroscopic Analysis. *Environ. Toxicol. Chem.* **2022**, *41*, 844−857.

(22) Dümichen, E.; Barthel, A.-K.; Braun, U.; Bannick, C. G.; Brand, K.; Jekel, M.; Senz, R. Analysis of polyethylene microplastics in environmental samples, using a thermal decomposition method. *Water Res.* **2015**, *85*, 451−457.

(23) Dierkes, G.; Lauschke, T.; Becher, S.; Schumacher, H.; Földi, C.; Ternes, T. Quantification of microplastics in environmental samples via pressurized liquid extraction and pyrolysis-gas chromatography. *Anal. Bioanal. Chem.* **2019**, *411* (26), 6959−6968.

(24) Okoffo, E. D.; Ribeiro, F.; O'Brien, J. W.; O'Brien, S.; Tscharke, B. J.; Gallen, M.; Samanipour, S.; Mueller, J. F.; Thomas, K. V. Identification and quantification of selected plastics in biosolids by pressurized liquid extraction combined with double-shot pyrolysis gas chromatography-mass spectrometry. *Sci. Total Environ.* **2020**, *715*, No. 136924.

(25) Lauschke, T.; Dierkes, G.; Schweyen, P.; Ternes, T. A. Evaluation of poly(styrene-d5) and poly(4-fluorostyrene) as internal standards for microplastics quantification by thermoanalytical methods. *J. Anal. Appl. Pyrolysis* **2021**, *159*, No. 105310.
(26) Oster, S. D.; Bräumer, P. E.; Wagner, D.; Rösch, M.; Fried, M.; Narayana, V. K.; Hausinger, E.; Metko, H.; Vizsolyi, E. C.; Schott, M.; Laforsch, C.; Löder, M. G. J. Development of new microplastic reference particles for usage in pre-defined numbers. Preprint article, **2023**. https://doi.org/10.21203/rs.3.rs-3682641/v1 (accessed 2024-06-07).
(27) Neubauer, S.; Haberhauer-Troyer, C.; Klavins, K.; Russmayer, H.; Steiger, M. G.; Gasser, B.; Sauer, M.; Mattanovich, D.; Hann, S.; Koellensperger, G. U13C cell extract of Pichia pastoris–a powerful tool for evaluation of sample preparation in metabolomics. *J. Sep. Sci.* **2012**, *35* (22), 3091−3105.
(28) Campos-M, M.; Campos-C, R. Applications of quartering method in soils and foods. *Int. J. Eng. Res. Ind. Appl.* **2017**, *7* (1), 35−39.
(29) Rødland, E. S.; Samanipour, S.; Rauert, C.; Okoffo, E. D.; Reid, M. J.; Heier, L. S.; Lind, O. C.; Thomas, K. V.; Meland, S. A novel method for the quantification of tire and polymer-modified bitumen particles in environmental samples by pyrolysis gas chromatography mass spectroscopy. *J. Hazard. Mater.* **2022**, *423* (Pt A), No. 127092.
(30) Duemichen, E.; Braun, U.; Senz, R.; Fabian, G.; Sturm, H. Assessment of a new method for the analysis of decomposition gases of polymers by a combining thermogravimetric solid-phase extraction and thermal desorption gas chromatography mass spectrometry. *J. Chromatogr. A* **2014**, *1354*, 117−128.
(31) David, J.; Steinmetz, Z.; Kučerík, J.; Schaumann, G. E. Quantitative Analysis of Poly(ethylene terephthalate) Microplastics in Soil via Thermogravimetry-Mass Spectrometry. *Anal. Chem.* **2018**, *90* (15), 8793−8799.
(32) Eisentraut, P.; Dümichen, E.; Ruhl, A. S.; Jekel, M.; Albrecht, M.; Gehde, M.; Braun, U. Two Birds with One Stone—Fast and Simultaneous Analysis of Microplastics: Microparticles Derived from Thermoplastics and Tire Wear. *Environ. Sci. Technol. Lett.* **2018**, *5* (10), 608−613.
(33) Laermanns, H.; Reifferscheid, G.; Kruse, J.; Földi, C.; Dierkes, G.; Schaefer, D.; Scherer, C.; Bogner, C.; Stock, F. Microplastic in Water and Sediments at the Confluence of the Elbe and Mulde Rivers in Germany. *Front. Environ. Sci.* **2021**, *9*, No. 19, DOI: 10.3389/fenvs.2021.794895.
(34) Linstrom, P. *NIST Chemistry WebBook, NIST Standard Reference Database 69*.
(35) Kittner, M.; Kerndorff, A.; Ricking, M.; Bednarz, M.; Obermaier, N.; Lukas, M.; Asenova, M.; Bordós, G.; Eisentraut, P.; Hohenblum, P.; Hudcova, H.; Humer, F.; István, T. G.; Kirchner, M.; Marushevska, O.; Nemejcová, D.; Oswald, P.; Paunovic, M.; Sengl, M.; Slobodnik, J.; Spanowsky, K.; Tudorache, M.; Wagensonner, H.; Liska, I.; Braun, U.; Bannick, C. G. Microplastics in the Danube River Basin: A First Comprehensive Screening with a Harmonized Analytical Approach. *ACS EST Water* **2022**, *2* (7), 1174−1181.
(36) Schott, M.; Wehrenfennig, C.; Gasch, T.; Düring, R.-A.; Vilcinskas, A. A portable gas chromatograph with simultaneous detection by mass spectrometry and electroantennography for the highly sensitive in situ measurement of volatiles. *Anal. Bioanal. Chem.* **2013**, *405* (23), 7457−7467.
(37) Kopecký, M.; Kolář, L.; Perná, K.; Váchalová, R.; Mráz, P.; Konvalina, P.; Murindangabo, Y. T.; Ghorbani, M.; Menšík, L.; Dumbrovský, M. Fractionation of Soil Organic Matter into Labile and Stable Fractions. *Agronomy* **2022**, *12* (1), No. 73, DOI: 10.3390/agronomy12010073.
(38) Jakobs, A.; Gürkal, E.; Möller, J. N.; Löder, M. G. J.; Laforsch, C.; Lueders, T. A novel approach to extract, purify, and fractionate microplastics from environmental matrices by isopycnic ultra-centrifugation. *Sci. Total Environ.* **2022**, *857* (Pt 3), No. 159610.
(39) Klöckner, P.; Seiwert, B.; Wagner, S.; Reemtsma, T. Organic Markers of Tire and Road Wear Particles in Sediments and Soils: Transformation Products of Major Antiozonants as Promising Candidates. *Environ. Sci. Technol.* **2021**, *55* (17), 11723−11732.
(40) Steinmann, T.; Welp, G.; Wolf, A.; Holbeck, B.; Große-Rüschkamp, T.; Amelung, W. Repeated monitoring of organic carbon stocks after eight years reveals carbon losses from intensively managed agricultural soils in Western Germany. *J. Plant Nutr. Soil Sci.* **2016**, *179* (3), 355−366.

Plastic Quantification and Polyethylene Overestimation in Agricultural Soil Using Large-Volume Pyrolysis and TD-GC-MS/MS

Ryan Bartnick[*1], Andrei Rodionov[1], Simon David Jakob Oster[2], Martin G. J. Löder[2], Eva Lehndorff[1]

[1]Soil Ecology, University of Bayreuth, Dr.-Hans-Frisch-Str. 1-3, 95448 Bayreuth, Germany

[2]Animal Ecology I, University of Bayreuth, Universitätsstraße 30, 95447 Bayreuth, Germany

[*]Corresponding author: Email: ryan.bartnick@uni-bayreuth.de

This supporting information file includes:

Supporting Information

The SI contains soil information, calibration slopes and equations, organic contributions, additional TD-GC-MS/MS analysis of plastic polymers (PLA, PA, PMMA, PP, PBAT), and example calculations. The data that support the findings of this study are public and openly available within the CRC 1357 Microplastics community on Zenodo at doi.org/10.5281/zenodo.6563563

Table S1. Basic measured parameters of soil investigated (triplicates)

	sand	silt
classification (WRB)[a]	sandy loam (SL)	silt loam (SiL)
sand (%)[b]	78.5	22.5
silt (%)[b]	9.7	63.7
clay (%)[b]	11.8	13.8
pH value	6.7	6.5
total C [g kg^{-1}][c]	10.92	15.54
$C_{organic}$ [g kg^{-1}][d]	10.71	15.44
$C_{inorganic}$ [g kg^{-1}]	0.21	0.10
total N [g kg^{-1}][c]	0.95	1.57

[a]*World reference base for soil resources 2014: International soil classification system for naming soils and creating legends for soil maps [3. ed.]. (2014). World soil resources reports: Vol. 106. FAO.*

[b]*Particle size analyzed from PARIO (Meter Group, Munich, Germany) automated soil particle size analysis.*

[c]*C and N measurements analyzed from elemental analyzer Vario Max CN (Elementar, Langenselbold, Germany).*

[d]*Organic C derived from loss on ignition (combustion at 550 °C for 12 h) and total C analysis.*

Table S2. Pure plastic polymers calibrated limit of quantification (LOQ), slope, response (x = polymer concentration in μg), coefficient of determination (R^2), and tested range[a]

polymer label	LOQ [µg]	y = slope*x + (blank offset)	R^2	log(y) = slope*log(x) + log(b)	R^2	tested range [μg]
PET1	–	–	–	2.10 * log(x) – 2.28	0.92	0.50 - 850
PET2[b]	0.50	1569470 * x + (74615)	0.93	–	–	0.50 - 850
PE2[b]	0.96	281851 * x + (1869706)	0.98	0.69 * log(x) + 3.91	0.94	0.96 - 850
PE3	0.96	222838 * x + (997975)	0.96	0.87 * log(x) + 2.80	0.91	0.96 - 850
PS2[b]	0.31	22986388 * x + (24570)	0.92	0.90 * log(x) + 4.59	0.97	0.31 - 850

[a]*Double log(x,y) combining low and high concentration calibrations in a power curve to a linear function to account for multiple levels of magnitude.*

[b]*Used for determining LOQ.*

Table S3. Plastic quantification compound interferences from different organic materials[a]

polymer label	compound (pyrolysis product)	wood	yeast	leonardite (HT)	humic acid (HT)	humic acid (SA)	PE overestimation (average)[b]
PET2	ethyl benzoate [μg mg^{-1}]	< 0.50	< 0.50	< 0.50	< 0.50	< 0.50	-
PE2	1,13-tetra-decadiene [μg mg^{-1}]	< 0.96	< 0.96	12.0 ± 1.4	10.6 ± 0.4	2.1 ± 0.3	8.2 ± 4.7
PE3	1,14-penta-decadiene [μg mg^{-1}]	< 0.96	< 0.96	15.3 ± 2.5	38.2 ± 2.8	10.5 ± 1.0	21.3 ± 13.0
PS2	2,4-diphenyl-1-butene [μg mg^{-1}]	< 0.31	< 0.31	< 0.31	< 0.31	< 0.31	-

[a]*Humic materials were provided by Humintech (HT) and Sigma-Aldrich (SA).*

[b]*"PE overestimation" mean and standard deviation in µg plastic signal per mg organic substance (20 mg, n = 3).*

Table S4. Additional plastic polymer compounds from pyrolysis products of plastics polypropylene (PP), polyamide 66 (PA66), polymethyl methacrylate (PMMA), and biodegradable polymers polylactic acid (PLA) and polybutylene adipate terephthalate (PBAT)[a]

polymer label	compound (pyrolysis product)	t_R (min)	molecular formula	molar mass	SRM (*m/z*)	
					Q1	Q3
PLA	lactide	12.0 – 12.9	$C_6H_8O_4$	144	56	28
PA66	caprolactam	14.6	$C_6H_{11}NO$	113	113	85
PMMA	methyl methacrylate	14.9	$C_5H_8O_2$	100	69	41
PP	2,4,6,8-tetramethyl-10-undecene	15.9 - 16.3	$C_{15}H_{30}$	210	111	69
PBAT	terephthalic acid dibut-3-enyl-ester	27.6	$C_{16}H_{18}O_4$	274	203	149

[a]*Compounds identified by specific retention time (t_R) and selected reaction monitoring (SRM) ions of interest (m/z) at quadrupole 1 (Q1) and quadrupole 3 (Q3) of MS/MS.*

Additional polymers: Using the same deductive method development (SIM to PIS to SRM), we additionally analyzed more plastic polymer types to provide a foundation for MS/MS application for plastics analysis. These results are the first analysis of biodegradable polymers analyzed by MS/MS and, by using our method, can be used as starting point to simultaneously detect many plastic types in soil and environmental matrices which are of interest to researchers. All these plastic pyrolysis products can be separated by retention time in the chromatographic column with minimal overlap to allow simultaneous detection.

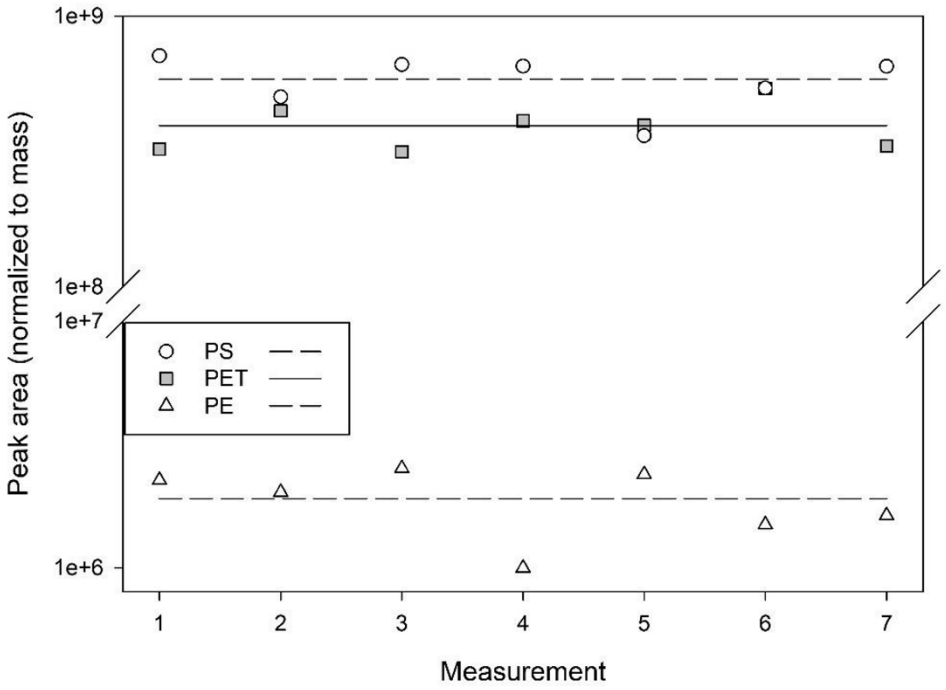

Figure S1. Deviation in area of mass fragment peaks for calibration compounds (7 replicates) of polystyrene (PS2; relative standard deviation, RSD, 19%), polyethylene terephthalate (PET1, RSD 19%), and polyethylene (PE2, RSD 27%), with averages (straight lines). Mix of pure polymers: 200 μg each, normalized to the sample mass.

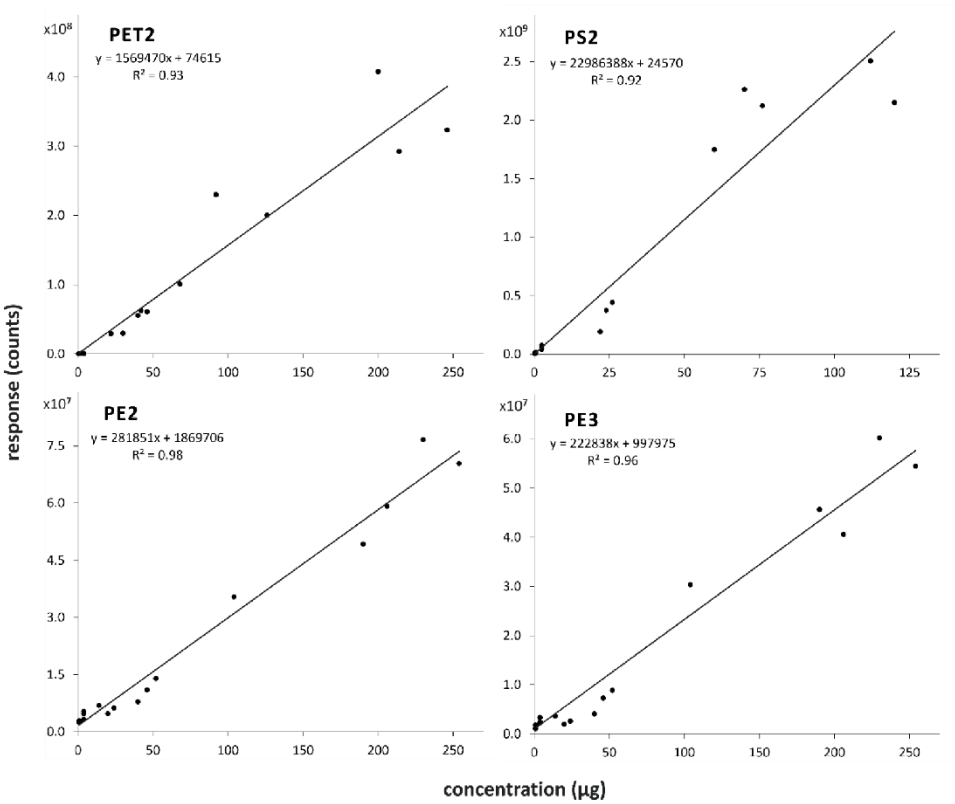

Figure S2. Calibration curves of lower plastic concentrations (n = 20, each plastic mixed) for determining limit of quantification; showing concentration vs. response for a mix of polyethylene (PE), polyethylene terephthalate (PET), and polystyrene (PS) with standards in the concentration range approx. 0.5 to 250 μg.

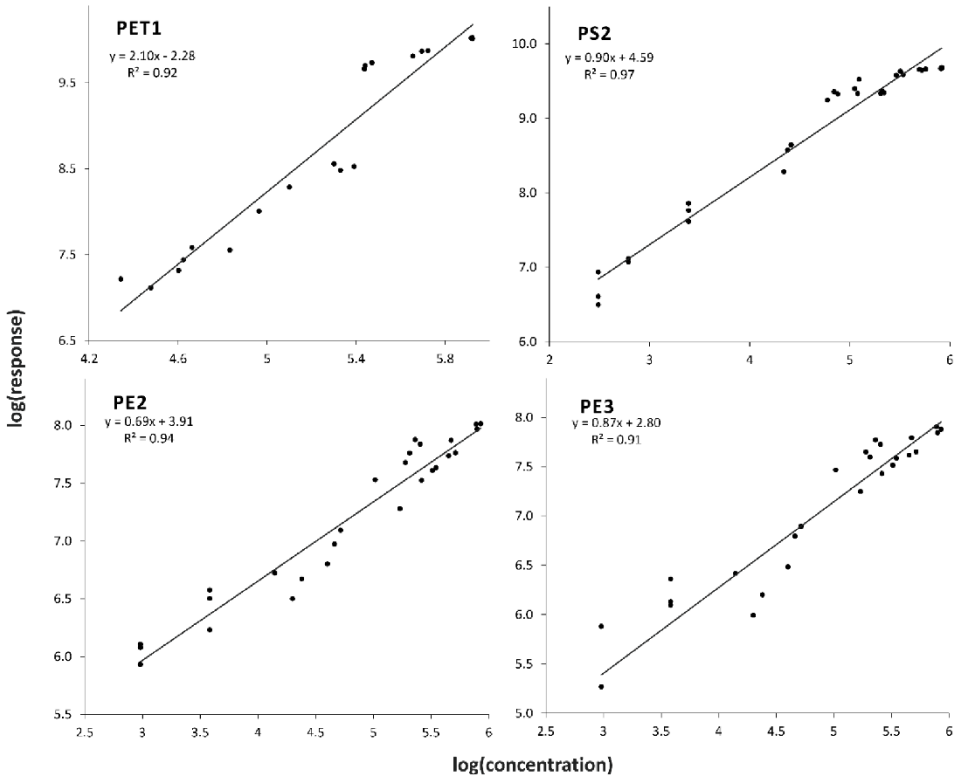

Figure S3. Double log plot of plastic concentrations vs. response over multiple levels of magnitude, approx. 0.5 to 850 μg (n = 30, each plastic mixed), to calibrate a linear function from a power curve (calibration for a large concentration range of plastic, e.g. for samples with yet unknown plastic contents). Note that calibration depends on actual system performance and must be checked regularly.

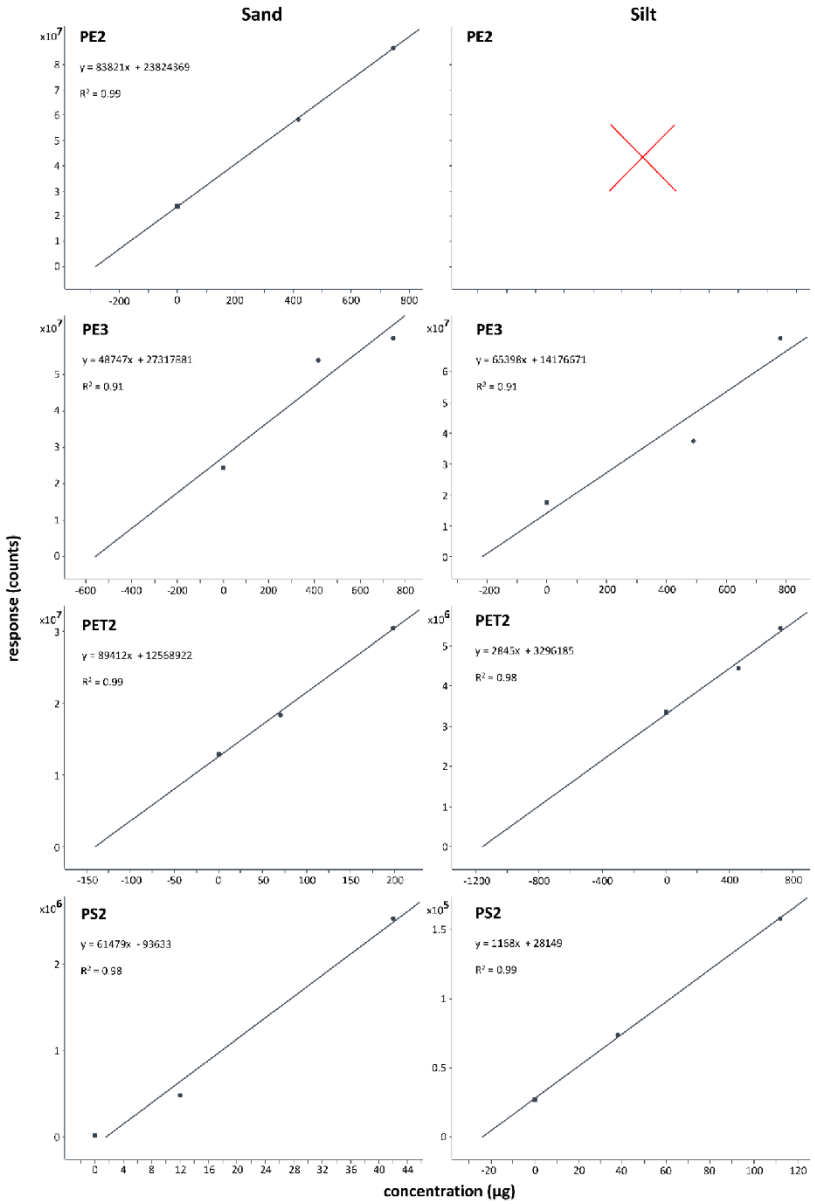

Figure S4. Standard addition three-point calibration for quantification of microplastic in sand and silt agricultural soils. As the magnitude of plastic concentration in soil is unknowable before testing, "spiked" standard additions should first be made in the magnitude of expected quantification, then adjusted until additions are within the sample analyte concentration range for each polymer tested. PE2 in silt soil was not distinguishable from peak separation in sample.

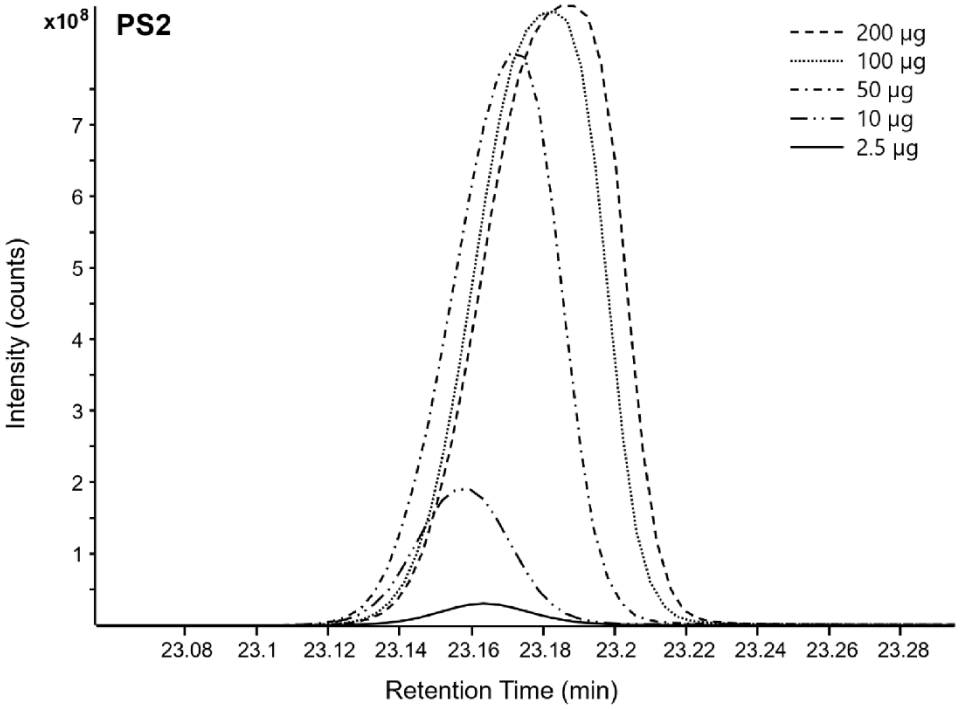

Figure S5. MS/MS chromatogram of PS dimer peak broadening at higher concentrations.

Calculation examples for PE quantification accounting for OM contribution:

(soil PE concentrations in manuscript were calculated from analysis of 5 replicates)

From averaged OM signals (Table S3, µg mg^{-1} converted to *w/w*):

$$PE_{overestimation\ factor} = \frac{(\text{alkadiene}_{\text{OM}}\ [\text{AU}] \times \text{OM}\ [\text{SI}])}{(\text{alkadiene}_{\text{PE}}\ [\text{AU}] \times \text{PE}\ [\text{SI}])} \quad \text{[Eq. 1]}$$

1,13-tetradecadiene: $PE_{overestimation\ factor}$ = 0.00824

1,14-pentadecadiene: $PE_{overestimation\ factor}$ = 0.02134

$$\text{PE}_{\text{corrected}}\ [\text{mg g}^{-1}] = \text{PE}_{\text{soil}}\ [\text{mg g}^{-1}] - \left(\text{sample}\ [\text{g}] \times 2\left(\text{OC}_{\text{sample}}\ [\text{mg g}^{-1}]\right) \times PE_{overestimation\ factor}\right) \quad \text{[Eq. 2]}$$

Sandy:

1,13-tetradecadiene:

$PE_{corrected}$ = 0.2453 [mg g^{-1}] – (1.006 [g] * 2(10.71 [mg g^{-1}]) * 0.00824 [factor])

= 0.2453 – (0.1776) = 0.0677 [mg g^{-1}] = **67.7 [µg g^{-1}]**

$PE_{overestimation}$ = 0.1776 [mg g^{-1}] = **177.6 [µg g^{-1}]**

1,14-pentadecadiene:

$PE_{corrected}$ = 0.3893 [mg g^{-1}] – (1.006 [g] * 2(10.71 [mg g^{-1}]) * 0.02134 [factor])

= 0.3893 – (0.4599) = -0.0706 [mg g^{-1}] = **-70.6 [µg g^{-1}] negative, potential contribution by OM higher than signal intensity**

$PE_{overestimation}$ = 0.4599 [mg g^{-1}] = **459.9 [µg g^{-1}]**

Silty:

1,13-tetradecadiene: Too much interference from OM (OC >1.5%), no clear peak separation

1,14-pentadecadiene:

$PE_{corrected}$ = 0.6053 [mg g^{-1}] – (0.504 [g] * 2(15.44 [mg g^{-1}]) * 0.02134 [factor])

= 0.6053 – (0.3321) = 0.2732 [mg g^{-1}] = **273.2 [µg g^{-1}]**

$PE_{overestimation}$ = 0.3321 [mg g^{-1}] = **332.1 [µg g^{-1}]**

Red color: overestimation by organic materials

5. Manuscript 5: From Sea to Land: Setting the Size Definition of Plastics for Soil Studies

Ryan Bartnick & Eva Lehndorff

Soil Ecology, University of Bayreuth, Dr.-Hans-Frisch-Str. 1-3, 95448 Bayreuth, Germany

Journal of Plant Nutrition and Soil Science, *188*(3), 373–375, 2025. https://doi.org/10.1002/jpln.12006

Journal of Plant Nutrition and Soil Science

WILEY-VCH

VIEWPOINT OPEN ACCESS

From Sea to Land: Setting a Size Definition of Plastics for Soil Ecosystem Studies

Ryan Bartnick | Eva Lehndorff

Soil Ecology, University of Bayreuth, Bayreuth, Germany

Correspondence: Ryan Bartnick (ryan.bartnick@uni-bayreuth.de)

Received: 27 February 2025 | **Accepted:** 5 April 2025

Academic Editor: Hermann Jungkunst

Funding: This study was funded by the Deutsche Forschungsgemeinschaft (DFG, German Research Foundation)–SFB 1357–391977956.

Keywords: biochemical processes | microplastics | nanoplastics | pore system | soil health

ABSTRACT

In soil studies, the current definition of microplastics as particles <5 mm was adopted directly from marine research. To our opinion, a more precise and differentiated size definition is needed to focus studies on specific challenges plastics cause for soil ecosystems. As relevant soil functions such as water, carbon, and nutrient retention and provision are mainly controlled by soil structure, biota, and chemical processes dominantly appearing in the micro- to nanoscale, we suggest adapting size ranges of plastics to the respective process scales in soil ecosystem studies. Even more, we expect that larger particles will not be incorporated into soil until they reach a size threshold compatible to soil structure (<1000 μm, depending on soil properties). Redefining plastic sizes in accordance with soil processes and the International System of Units (SI) should be implemented to focus research. A unified definition of microplastics (1–1000 μm) and nanoplastics (1–1000 nm) will set a standard to further allow relating plastic sizes across research disciplines.

1 | Opinion

The initial concern and popularization of the term "microplastics" originated from ocean and marine research; however, there is now an increasing focus on soils as potential accumulators of plastic pollution. Consequently, the transition of microplastics research from sea to land has brought practices not relatable to soil-specific research questions, and the current accepted definition of microplastics (<5 mm) is misleading when designing studies evaluating effects on soil life and processes. Even the first mentions of "microplastics" in 2004 were in reference to fibers ≈20 μm in diameter (Thompson et al. 2004), which is much smaller than the current broad definition. The current size definition originated from the first proceeding of the National Ocean and Atmospheric Association, which aimed to choose a unified size definition of "microplastics" debris and provided a practical solution to include the larger mesh size of marine nets (Arthur et al. 2009). This proceeding itself suggests a redefinition to microscopic polymer fragments with future scientific advancement, which is now needed, as the current definition is outside the scope for soil research. Here, we aim to improve the definition of environmentally relevant plastic particle sizes that may potentially harm soil quality and suggest a reclassification of plastic sizes used in soil studies.

Plastic research in soil has focused on its effects on biota, as well as physical and chemical processes (Pérez-Reverón et al. 2023). Before entering the soil, plastics must fit within the pore system of soils or be incorporated by mixing animals (Figure 1; macroplastics range). This explains why researchers do not

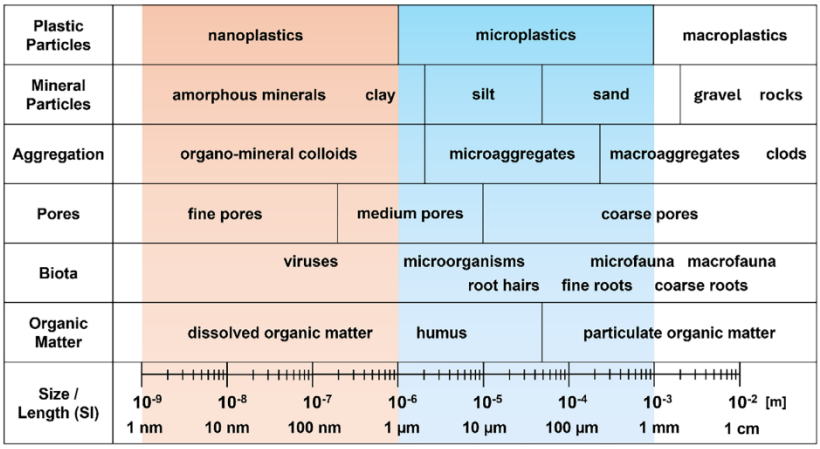

FIGURE 1 | Plastic sizes are displayed on a scale with soil components to highlight their relevance to soil materials and biota. The range where most interactions between soil fauna and roots appear is highlighted in blue (1–1000 µm), whereas most chemical and physical processes occur in red (1–1000 nm). We suggest matching the process scale to the plastic size in soil ecosystem studies.

find large concentrations of millimeter-scale plastics in soils (Jia et al. 2024). As most soil particles and functions occur below 1 mm, a larger definition inclusive of microplastics up to 5 mm is inappropriate for most soil studies. For plastic particles to affect soil biota, they must be within a size range capable of interacting with the respective organism or their environment. Only for macrofauna, such as earthworms, 5-mm particles might cause physical injuries. Organism health is most likely affected by plastics at the micrometer- to nanometer-scale, where sorption behavior and uptake to cells occur (Arthur et al. 2009; Pérez-Reverón et al. 2023). Therefore, it is recommended to fit the scale of an experiment on soil fauna to the relevant size range of plastics (Figure 1).

Research on soil quality involves soil processes that occur below the millimeter-scale, such as water retention, soil aggregation, chemical interactions between organic and inorganic matter, pollutant interactions, and microbial processes (Totsche et al. 2018). Within the micrometer-scale, plastic incorporation into biopores, other pore spaces, and stable soil aggregates is likely to occur first (Figure 1; blue microplastics range) (Totsche et al. 2018). Then, physicochemical degradation and biological changes result in transformed nanoplastics with largely unknown surface characteristics, transport, accumulation, and implications for complex interactions in soil (Figure 1; red nanoplastics range), for example, the uptake into plant cells (Pérez-Reverón et al. 2023). Hence, defining and utilizing plastics across an overly broad size range can misrepresent their effects and reduce the robustness of reviews and compiled data.

Although it is important to consider input of "macroplastics," these will not incorporate and interact in soil systems until degrading into microplastics and nanoplastics (Jia et al. 2024; Pérez-Reverón et al. 2023). A more efficient approach for plastic research in soil science would be to adopt size definitions already established for understanding soil processes and functions (Figure 1). All processes related to soil formation involve the formation of and reaction with particles <2 mm (Totsche et al. 2018). The size definitions common in soil research of mineral particles (sand, silt, and clay) and physical aspects (soil aggregation and pore size) utilize the established International System of Units (SI) and could be directly used to define plastics in soils. A standard classification of plastics by particle diameter length can unify various fields studying "macroplastics" (>1 mm, $>10^{-3}$ m), "microplastics" to the micrometer-scale (1–1000 µm, 10^{-3}–10^{-6} m), and "nanoplastics" to the nanometer-scale (1–1000 nm, 10^{-6}–10^{-9} m). In practice, the size definition of plastics will be the minimum length of the plastic particle that can freely pass through a sieve or defined mesh, meaning that if fibers are longer than they are wide, they will be classified reflective of their width and not their length. Therefore, for soils, the size classification of plastics will remain as the smallest dimension possible for plastic particles to fit through a sieve due to their oblong, non-uniform shapes.

As plastics transport and accumulate across air, water, and soil, they fragment and fractionate into a smaller size, leading to yet unknown complex mixtures and effects in all environmental compartments. With these definitions, we want to support the two main goals of plastic research in soil science: to relate plastic sizes to soil processes and functions relevant to soil quality and to enable bridging gaps between research disciplines such as hydrology and atmospheric science. When studies are comprehensively reviewed, the size definition of microplastics needs to be unified as to not falsely relate studies where experimental microplastics differ magnitudes in size. We defined here microplastics (1–1000 µm) as being most relevant for soil functions such as physical stabilization of soil (aggregation), water, carbon, and nutrient retention; and nanoplastics (1–1000 nm) as most relevant for soil processes, such as organic and inorganic matter interaction, including pollutants and toxic effects. For soil biota, the relevant size of plastic particles would be those that interact directly or indirectly with the respective biota of interest. For macroplastics of greater size (>1 mm), transportation away from soil is more likely than incorporation until specific soil processes are met (Jia et al. 2024). Therefore, this refocus

and redefinition of microplastics and nanoplastics will emphasize effects at the environmentally relevant size range of soil life and processes.

Acknowledgments

This study was funded by the *Deutsche Forschungsgemeinschaft (DFG, German Research Foundation)–SFB 1357–391977956*.

Open access funding enabled and organized by Projekt DEAL.

References

Arthur, C., J. Baker, and H. Bamford (eds). 2009. *Proceedings of the International Research Workshop on the Occurrence, Effects, and Fate of Microplastic Marine Debris*. Sept 9–11, 2008. NOAA Technical Memorandum NOS-OR&R-30.

Jia, Z., W. Wei, Y. Wang, Y. Chang, R. Lei, and Y. Che. 2024. "Occurrence Characteristics and Risk Assessment of Microplastics in Agricultural Soils in the Loess Hilly Gully Area of Yan'an, China." *Science of the Total Environment* 912: 169627. https://doi.org/10.1016/j.scitotenv.2023.169627.

Pérez-Reverón, R., S. J. Álvarez-Méndez, J. González-Sálamo, et al. 2023. "Nanoplastics in the Soil Environment: Analytical Methods, Occurrence, Fate and Ecological Implications." *Environmental Pollution* 317: 120788. https://doi.org/10.1016/j.envpol.2022.120788.

Thompson, R. C., Y. Olsen, R. P. Mitchell, et al. 2004. "Lost at Sea: Where Is all the Plastic?" *Science* 304, no. 5672: 838–838. https://doi.org/10.1126/science.109455.

Totsche, K. U., W. Amelung, M. H. Gerzabek, et al. 2018. "Microaggregates in Soils." *Journal of Plant Nutrition and Soil Science* 181, no. 1: 104–136. https://doi.org/10.1002/jpln.201600451.

(Eidesstattliche) Versicherungen und Erklärungen

(§ 8 Satz 2 Nr. 3 PromO Fakultät)

Hiermit versichere ich eidesstattlich, dass ich die Arbeit selbstständig verfasst und keine anderen als die von mir angegebenen Quellen und Hilfsmittel benutzt habe (vgl. Art. 97 Abs. 1 Satz 8 BayHIG).

(§ 8 Satz 2 Nr. 3 PromO Fakultät)

Hiermit erkläre ich, dass ich die Dissertation nicht bereits zur Erlangung eines akademischen Grades eingereicht habe und dass ich nicht bereits diese oder eine gleichartige Doktorprüfung endgültig nicht bestanden habe.

(§ 8 Satz 2 Nr. 4 PromO Fakultat)

Hiermit erkläre ich, dass ich Hilfe von gewerblichen Promotionsberatern bzw. – vermittlern oder ähnlichen Dienstleisten weder bisher in Anspruch genommen habe noch künftig in Anspruch nehmen werde.

(§ 8 Satz 2 Nr. 7 PromO Fakultät)

Hiermit erkläre ich mein Einverständnis, dass die elektronische Fassung der Dissertation unter Wahrung meiner Urheberrechte und des Datenschutzes einer gesonderten Überprüfung unterzogen werden kann.

(§ 8 Satz 2 Nr. 8 PromO Fakultät)

Hiermit erkläre ich mein Einverständnis, dass bei Verdacht wissenschaftlichen Fehlverhaltens Ermittlungen durch universitätsinterne Organe der wissenschaftlichen Selbstkontrolle stattfinden können.

Bayreuth, 10.11.2025

……

Ort, Datum, Unterschrift